Regime Change in Aggregate Structures of Magnetic Particles in a Time-Dependent Applied Magnetic Field and the Heating Effect due to the Brownian Relaxation Mechanism (Brownian Dynamics Simulations)

時間依存型磁場中での凝集形態転移および ブラウン緩和メカニズムによる発熱効果 (ブラウン動力学シミュレーション)

September 2023

Akita Prefectural University

Seiya Suzuki

鈴木　聖弥

This page intentionally left blank.

Contents

Nomenclature

b	:	thickness of a disk-like particle
d	:	diameter of a particle
D^T, D^R	:	translational and rotational diffusion coefficients
$\boldsymbol{e}$	:	unit vector of direction of a particle
$\boldsymbol{e}_{\perp 1}(t)$, $\boldsymbol{e}_{\perp 2}(t)$	:	orthogonal unit vectors normal to the magnetic moment of a cubic particle
$\boldsymbol{F}^P$	:	force acting on a particle
$\boldsymbol{F}_{ij}^{(m)}$	:	magnetic force due to the magnetic particle-particle interaction
$\boldsymbol{F}^{(V)}$, $\boldsymbol{F}_{ij}^{(V)}$	:	repulsive force due to the overlap of steric layers
$g(r)$	:	radial distribution function
$\boldsymbol{h}_{\mathbf{x}}$	:	component of a magnetic field in x-direction
$\boldsymbol{H}$	:	external magnetic field
H_0	:	magnitude of magnetic field
$\boldsymbol{H}_{alt}$	:	alternating magnetic field
$\boldsymbol{H}_{mod}$	:	modified alternating magnetic field
$\boldsymbol{H}_{rot}$	:	rotating magnetic field
H_{sin}	:	magnitude of sinusoidal magnetic field
$\boldsymbol{H}_{sin}$	:	conventional alternating magnetic field
H_{tri}	:	magnitude of triangular magnetic field
$\boldsymbol{i}_x$, $\boldsymbol{i}_y$	:	unit vector in each axis direction
k_B	:	Boltzmann's constant
l	:	length of a rod-like particle

L_x, L_y, L_z	:	size of a simulation region in each axis direction
$\boldsymbol{m}$	:	magnetic moment of a particle
m		magnitude of a magnetic moment
$\boldsymbol{M}$		magnetization
$\boldsymbol{n}$	:	unit vector of a magnetic moment $\boldsymbol{m}$
n_s		number of surfactant molecules per unit surface of magnetic particles
N	:	total number of particles
N_s	:	number of clusters for describing a cluster size distribution
r	:	radial distance for a radial distribution function $g(r)$
r_{coff}	:	cutoff distance
$\boldsymbol{r}_i$	:	position vector of particle i
$\boldsymbol{r}_{ij}$	:	relative position vector from particle j to particle i
r_p	:	aspect ratio
R_B	:	non-dimensional parameter representing the thermal energy to the random force strength
R_{mod}	:	ratio of the modified magnetic field
t	:	time
$\boldsymbol{t}_{ij}$	:	unit vector of vector $\boldsymbol{r}_{ij}$
t_{total}		total simulation time
T	:	absolute temperature of a liquid
$\boldsymbol{T}$	:	torque acting on the ambient fluid by a particle
$\boldsymbol{T}^P$	:	torque acting on a particle

$\boldsymbol{T}_i^{(H)}$	:	magnetic torque due to the magnetic particle-field interaction
$\boldsymbol{T}_{ij}^{(m)}$	:	magnetic torque due to the magnetic particle-particle interaction
$\boldsymbol{T}^{(V)}$	:	torque due to the overlap of steric layers
V	:	volume of a system
W_{cycl}^{total}	:	work per period an applied magnetic field
W_{cycl}	:	work per particle in one cycle of a magnetic field
δ	:	thickness of a uniform steric layer
$\Delta \boldsymbol{r}^B$	:	random displacement inducing translational Brownian motion
Δt	:	time interval
$\Delta \boldsymbol{\phi}^B$	:	random displacement inducing rotational Brownian motion
η	:	liquid viscosity
λ	:	non-dimensional parameter representing the strength of the magnetic particle-particle interaction
λ_V	:	non-dimensional parameter representing the strength of the repulsive interaction relative to the thermal energy
μ_0	:	permeability of free space
ξ	:	non-dimensional parameter representing the strength of the magnetic particle-field interaction
ϕ_V	:	volumetric fraction of particles
ω_H	:	frequency of an applied magnetic field
$\langle - \rangle$	:	ensemble average

Chapter 1 Introductory remarks

Magnetic particle suspensions have a great possibility as applications in a variety of engineering fields such as magnetically-controlled fluid devices [1], high-density recording materials in magnetic recording engineering field [2], optical units in the magnetic material engineering field [3], magnetic drug delivery systems (magnetically-targeted drug delivery) [4] and magnetic hyperthermia treatments [5] in the biomedical engineering field, and the recovering technology for specific substances such as hazardous heavy metal molecules from water in the environmental resources engineering field [6].

In the field of fluid engineering, the main applications may be mechanical dampers and actuators that employ the functional characteristics of the magnetorheological effect. The functional fluids may be generally classified as exhibiting their functional properties in the presence of either a magnetic or an electric field. Typical functional fluids that respond to an external magnetic field are ferrofluids [7] and magnetorheological (MR) suspensions [1]. Recently, magnetic particle suspensions have been energetically investigated by a variety of researchers with respect to the above-mentioned applications in the field of biomedical engineering since successful applications in this field are able to have a significantly great contribution to human health and happiness. The present doctorial thesis treats the research subject with respect to magnetic hyperthermia using magnetic particles with various geometrical shapes, which will be described later in detail.

Magnetic particles that are used in the above-mentioned application fields have a variety of geometrical shapes such as spherical [8, 9], rod-like (spindle-like) [10, 11], disk-like (oblate or platelet) [12, 13] and cubic particles [14]. For all these particles, it is required to analyze physical characteristics of magnetic particles in the situation of thermodynamic equilibrium and non-equilibrium in a flow field and also for a two-dimensional and a three-dimensional system. The research subjects of magnetic particle suspensions may be aggregation phenomena, regime changes in the internal structure, orientational characteristics, magnetorheological properties, heat generation features in a time-dependent magnetic field, and so forth. Although there are a large number of studies for a three-dimensional system [1, 7], we here briefly describe the studies only for a two-dimensional or a quasi-two-dimensional system since the development of surface-modifying technology is indispensable for obtaining highly functionalized magnetic particles that exhibit their characteristic features required in the application in the biomedical engineering field.

Particle-based simulations may be indispensable for the analysis of the above-mentioned physical phenomena at a microscopic level. When we consider the state of a magnetic particle suspension in thermodynamic equilibrium, the Monte Carlo method is the most straightforward tool for a microscopic analysis of suspensions [15]. When considering the dynamic properties of a magnetic particle suspension, a common simulation approach is to employ molecular dynamics and

Brownian dynamics methods [15]. The standard Brownian dynamics only addresses the particle motion and the ambient flow field is not solved simultaneously. In order to treat flow problems where the multi-body hydrodynamic interactions between particles should be taken into account, a hopeful simulation approach is the lattice Boltzmann [16] and the dissipative particle dynamics [17, 18] and the multi-particle collision dynamics (MPCD or stochastic rotation dynamics) [19]. These methods are based on the concept of virtual fluid particles and are able to give rise to the solution of a flow field where the multi-body hydrodynamic interactions between the dispersed particles are reproduced [17, 18].

As already described in the above, typical applications of magnetic particle suspensions in biomedical engineering field are magnetically-controlled (guided) drug delivery systems and magnetic hyperthermia therapy. Before proceeding to these topics, we briefly describe multi-functionalized magnetic particles that are used in the biomedical engineering field such as drug delivery systems and magnetic hyperthermia therapy.

Multi-functional particles are basically synthesized by coating the base non-magnetic particle with other material such as magnetic materials, or by coating magnetic core particle by polymeric materials [19-25]. Hellenthal et al. synthesized gold nanorods coated by nickels in a design-engineering-like manner and investigated the magnetic characteristics of these functionalized particles [26]. Erb et al. generated multi-functionalized magnetic particles that are applicable to various application fields, not limited to the biomedical engineering field [27]. Patra et al. widely described valuable multi-functionalized magnetic particles that are used in the drug delivery and hyperthermia and their synthesis technologies [28]. Meijer and Rossi described a variety of magnetic hematite particles such as spherical, spindle-like, plate-like, cube-like and star-like particles including chemical physics characteristics, material properties and magnetic features [29]. Richert et al. developed a magnetic capsule that may be used as a drug release system [30]. Zhang et al. synthesized core-shell magnetite particles coated by smart stimuli-responsive polymers [31]. Liu et al. generated thermal-sensitive ferrofluids that may be used as a drug delivery application [32].

In the magnetically-controlled drug delivery system, magnetic composite materials including drugs are captured and transported to the target site such as tumor or cancer cells by a non-uniform applied magnetic field. In this concept, one of key techniques to be developed for a successful application, on the physical side, is the generation of an effective non-uniform magnetic field by using an arrangement of a combination of magnets in order to transport the drugs to the target tissue in a variety of complex circumstances. There are studies with respect to the development of an analytical model for the magnetic particle motion in a pipe flow [33], the guidance and trap of magnetic particles using a non-uniform applied magnetic field [34, 35], the trapping technology of charged rod-like particles by an electric field [36], the aggregation phenomena in a non-uniform applied magnetic field [37], and so forth.

We now describe in detail the background of the studies with respect to magnetic hyperthermia mainly from a physics and engineering point of view. Magnetic particles in a dispersion give rise to heat generation in a time-dependent magnetic field such as an alternating or a rotating magnetic field. A pioneering work by Rosensweig [38] theoretically discussed the relationship between the heat generation effect and an alternating applied magnetic field, where the mechanism for heat generation is dependent on the size of the magnetic particles. That is, the heat generation in a magnetic particle suspension arises due to the relaxation of the magnetic moment of the magnetic particles in such a time-changing field and there are two mechanics for the heat generation, i.e., Néel relaxation mode and Brownian relaxation mode [38, 39]. In the Néel mechanism the motion of a magnetic moment in the particle body induces heating effect. On the other hand, in the Brownian mechanism, the magnetic moment is fixed to the particle body and the particle itself rotates to follow the change in an applied magnetic field, which gives rise to the heating effect due to friction torques or forces. Tumor and cancer cells are much weaker to heat than usual healthy cells, and therefore the heat generation effect obtained in a time-dependent magnetic field is used in order to kill tumor or cancel cells without damages to ordinary cells [40, 41]. The Néel mechanism is the main factor for magnetic particle smaller than around 10nm and the Brownian mechanism is more dominant for those larger than this size [38]. There are a variety of studies regarding magnetic hyperthermia from a physics point of view as well as from a medical therapy point of view [5]. In the following, several representative studies are addressed in order to make the motivation of the present doctorial studies more evident. Bekovic addressed the heating effect in the situation of a rotating applied magnetic field in addition to the more usual alternating magnetic field [42]. The influence of the formation of particle aggregates on the heating effect was investigated [43]. Similarly, the effect of the volumetric fraction was addressed [44, 45] and this study showed that there is an appropriate volumetric fraction which gives rise to a maximum heat generation performance. Moreover, the influence of the isotropic characteristics of magnetic moments was discussed [46]. In addition, there are a variety of experimental studies including the visualization of a magnetic suspension and the measurement of the temperature in a time-dependent magnetic field. Mehdaoui et al. visualized the system and verified the behavior of chain-like clusters, which leads to the understanding of the contribution of magnetic particle-particle interactions to the heating effect in an indirect manner [47]. Similarly, Guibert et al. clarified from a visualization experiment that larger aggregates give rise to lower heat generation performance [48]. Serantes et al. experimentally discussed the strength of magnetic particle-particle interactions and concluded that larger magnetic interactions lead to a decrease in heating effect [49]. Conde-Leboran et al. discussed the influence of the orientational characteristics on the heating effect [50]. From these typical experimental results, it is seen that it is significantly difficult to experimentally clarify the internal structure of particle aggregates in detail in a time-dependent applied magnetic field, and therefore,

particle-based simulation approaches may be desirable to investigate the behavior of magnetic particles and clusters in a time-changing field and the influence of the formation of clusters on the heat generation characteristics. In the above mentioned studies, the magnetic particles of interest are generally smaller than ten nano-meters and therefore the heat generation arises due to the Néel relaxation mechanism. Recently, larger particles draw researchers' attention, where the Brownian relaxation mechanism is the main factor for the heat generation, and thus we briefly describe typical studies treating larger magnetic particles in the following.

Alphandéry et al. performed an experiment of a suspension of bacteria in an alternating magnetic field [51]. Lahiri et al. addressed magnetic nanoemulsions with size of around 20 nm in order to discuss the effects of polydispersity, particle concentration and medium viscosity [52]. Gudoshnikov et al. experimentally studied the characteristics of the hysteresis loop in a suspension of magnetite with size of around 25nm [53] and similarly Guardia et al. addressed a suspension of magnetic cubic particles with size of around 13-40 nm [54], where the effects of the size of the particles and the field strength were discussed. Rousseau et al. experimentally discussed the influence of the viscosity of a base liquid on the heating effect [55]. Yao et al. pointed out a possibility of the mechanical damage to cells by rod-like particles in an alternating magnetic field, although discussing the characteristics of the hysteresis loops [56]. Tomitaka et al. generated larger magnetic particles with size of around 20-30nm and showed the contribution of the Brownian relaxation mechanism and the viscosity of a base liquid on the heat generation [57]. Steinke et al. treated magnetic macrospheres with size of around 5 mm, and showed that this suspension give rise to a sufficient heating effect for remotely releasing drugs from the capsules [58].

From the above-mentioned background, it is seen that there are a quite few studies regarding the magnetic hyperthermia in terms of particle-based simulation techniques, by which the internal structure of particle aggregates and the behavior of these clusters in the situation of an alternating and a rotating applied magnetic field are able to be clarified in detail and also the relationship between the cluster formation and the heat generation characteristics may be clarified. Hence, we have performed Brownian dynamics simulations in order to investigate the behavior of magnetic particles, the aggregation phenomena, the regime change in the internal structure of particle aggregates, the heat generation effect, the relationship between the cluster formation and the heat generation effect, and so forth. The magnetic particles of interest are spherical, rod-like and disk-like particles with a point dipole moment at the particle center. In the heating effect, the Brownian relaxation mechanism is focused on for all these magnetic particles.

The present doctorial thesis is composed of 7 chapters as follows:

Chapter 1 is the introduction.

Chapter 2 treats a suspension composed of magnetic spherical particles in an alternating magnetic field.

Chapter 3 focuses on the discussion of the unexpected characteristic that the stable particle cluster formation induces a decrease in the degree of heating effect

Chapter 4 addresses a rotating magnetic field and the results with respect to the behavior of the magnetic particles and the heating effect are compared with those for an alternating magnetic field in Chapters 2 and 3.

Chapter 5 has extended the above mentioned studies to a magnetic rod-like particle suspension, where a better heat generation performance is shown in comparison with a spherical particle system.

Chapter 6 considers a suspension composed of magnetic disk-like particles, where a further better heat generation performance is expected due to more rigid cluster formation in a face-to-face contact manner. Moreover, an applied magnetic field is modified in order to obtain a larger heat generation performance.

Chapter 7 is the summary of the present results and also describes the future works to be conducted mainly with respect to the magnetic hyperthermia.

References

[1] N. M. Wereley, editor, *Magnetorheology: Advances and Applications* (Royal Society of Chemistry, London, 2013).

[2] C. Verdes, R. W. Chantrell, A. Satoh, J. W. Harrell and D. Nikles, Self-organization, orientation and magnetic properties of FePt nanoparticle arrays, J. Magn. Magn. Mater., 304, (2006), 27−31.

[3] S. Furumi and Y. Sakka, Circularly polarized laser emission induced by supramolecular chirality in cholesteric liquid crystals, J. Nanosci. Nanotech., 6, (2006), 1819−1822.

[4] T. Neuberger, B. Schöpf, H. Hofmann, M. Hofmann and B. von Rechenberg, Superparamagnetic nanoparticles for biomedical applications: Possibilities and limitations of a new drug delivery system, J. Magn. Magn. Mater., 293, (2005), 483−496.

[5] A. M. Schmidt, Thermoresponsive magnetic colloids, Colloid Polym. Sci., 285, (2007), 953–966.

[6] K. Dashtian and R. Zare-Dorabei, Synthesis and characterization of functionalized mesoprous SBA-15 decorated with Fe3O4 nanoparticles for removal of Ce(III) ions from aqueous solution: ICP–OES detection and central composite design optimization, J. Colloid Interface Sci., 494, (2017), 114−123.

[7] R. E. Rosensweig, *Ferrohydrodynamics* (Cambridge University Press, Cambridge, 1985).

[8] S. Patra, E. Roy, P. Karfa, S. Kumar, R. Madhuri and P. K. Sharma, Dual-responsive polymer coated superparamagnetic nanoparticle for targeted drug delivery and hyperthermia treatment, ACS Appl. Mater. Interfaces, 7, (2015), 9235–9246.

[9] J. M. Meijer and L. Rossi, Preparation, properties, and applications of magnetic hematite microparticles, Soft Matter, 17, (2021), 2354−2368.

[10] M. Ozaki and E. Matijević, Preparation and magnetic properties of monodispersed spindle-type γ-Fe2O3 particles, J. Colloid Interface Sci., 107, (1985), 199–203.

[11] H. Itoh and T. Sugimoto, Systematic control of size, shape, structure, and magnetic properties of uniform magnetite and maghemite particles, J. Colloid Interface Sci., 265, (2003), 283−295.

[12] D. Primc, D. Makovec, D. Lisjak and M. Drofenik, Hydrothermal synthesis of ultrafine barium hexaferrite nanoparticles and the preparation of their stable suspensions, Nanotech., 20, (2009), 315605.

[13] S. Okada, K. Takagi and K. Ozaki, Synthesis of submicron plate-like hematite without organic additives and reduction to plate-like α-Fe, Mater. Lett., 140, (2015), 135−139.

[14] S. H. Sajjadi and E. K. Goharshadi, Highly monodispersed hematite cubes for removal of ionic dyes, J. Environ. Chem. Eng., 5, (2017), 1096−1106.

[15] M. P. Allen and D. J. Tildesley, *Computer Simulation of Liquids* (Clarendon Press, Oxford, 1987).

[16] S. Succi, *The Lattice Boltzmann Equation for Fluid Dynamics and Beyond* (Clarendon Press, Oxford, 2001).

[17] P. J. Hoogerbrugge and J. M. V. A. Koelman, Simulating microscopic hydrodynamic

phenomena with dissipative particle dynamics, Europhys. Lett., 19, (1992), 155-160.

[18] J. M. V. A. Koelman and P. J. Hoogerbrugge, Dynamic simulations of hard-sphere suspensions under steady shear, Europhys. Lett., 21, (1993), 363-368.

[19] A. Malevanets and R. Kapral, Mesoscopic model for solvent dynamics, J. Chem. Phys., 110, (1999), 8605-8613.

[20] J. Weingart, P. Vabbilisetty and X. Sun, Membrane mimetic surface functionalization of nanoparticles: Methods and applications, Adv. Colloid Interface Sci., 197-198, (2013), 68−84.

[21] S. Balakrishnan, M. J. Bonder and G. C. Hadjipanayis, Particle size effect on phase and magnetic properties of polymer-coated magnetic nanoparticles, J. Magn. Magn. Mater., 321, (2009), 117−122.

[22] A. Tomitaka, K. Ueda, T. Yamada and Y. Takemura, Heat dissipation and magnetic properties of surface-coated Fe3O4 nanoparticles for biomedical applications, J. Magn. Magn. Mater., 324, (2012), 3437−3442.

[23] A. Tomitaka, T. Koshi, S. Hatsugai, T. Yamada and Y. Takemura, Magnetic characterization of surface-coated magnetic nanoparticles for biomedical application, J. Magn. Magn. Mater., 323, (2011), 1398−1403.

[24] B. J. Jankiewicz, D. Jamiola, J. Choma and M. Jaroniec, Silica–metal core–shell nanostructures, Adv. J. Colloid Interface Sci., 170, (2012), 28−47.

[25] M. W. Ambrogio, M. Frasconi, M. D. Yilmaz and X. Chen, New methods for improved characterization of silica nanoparticle-based drug delivery systems, Langmuir, 29, (2013), 15386−15393.

[26] C. Hellenthal, W. Ahmed, E. S. Kooij, A. Van Silfhout, B. Poelsema and H. J. W. Zandvliet, Tuning the dipole-directed assembly of core-shell nickel-coated gold nanorods, J. Nanoparticle Research, 14, (2012), 1–14.

[27] R. M. Erb, H. S. Son, B. Samanta, V. M. Rotello and B. B. Yellen, Magnetic assembly of colloidal superstructures with multipole symmetry, Nature Lett., 457, (2009), 999−1002.

[28] S. Patra, E. Roy, P. Karfa, S. Kumar, R. Madhuri and P. K. Sharma, Dual-responsive polymer coated superparamagnetic nanoparticle for targeted drug delivery and hyperthermia treatment, ACS Appl. Mater. Interfaces, 7, (2015), 9235–9246.

[29] J. M. Meijer and L. Rossi, Preparation, properties, and applications of magnetic hematite microparticles, Soft Matter, 17, (2021), 2354−2368.

[30] H. Richert, O. Surzhenko, S. Wangemann, J. Heinrich and P. Gömert, Development of a magnetic capsule as a drug release system for future applications in the human GI tract, J. Magn. Magn. Mater., 293, (2005), 497−500.

[31] J. L. Zhang, R. S. Srivastava and R. D. K. Misra, Core-shell magnetite nanoparticles surface encapsulated with smart stimuli-responsive polymer: Synthesis, characterization, and LCST of viable drug-targeting delivery system, Langmuir, 23, (2007) 6342−6351.

[32] T. Liu, S. Hu, S. Hu, S. Tsai and S. Chen, Preparation and characterization of thermal-sensitive

ferrofluids for drug delivery application, J. Magn. Magn. Mater., 310, (2007), 2850−2852.

[33] S. Sharma, V. K. Katiyar and U. Singh., Mathematical modelling for trajectories of magnetic nanoparticles in a blood vessel under magnetic field, J. Magn. Magn. Mater., 379, (2015), 102−107.

[34] S. H. Dubina and L. E. Wedgewood, Application of nonuniform magnetic fields in a Brownian dynamics model of ferrofluids with an iterative constraint scheme to fulfill Maxwell's equations, Phys. Fluids, 29, (2017), 092001.

[35] L. Qiao and G. W. Slater, Capture of rod-like molecules by a nanopore: Defining an "orientational capture radius", J. Chem. Phys., 152, (2020), 144902.

[36] R. Waszkiewicz and M. Lisicki, Hydrodynamic effects in the capture of rod-like molecules by a nanopore, J. Phys.: Condensed Matter, 33, (2021), 104005.

[37] J. B. Tracy and T. M. Crawford, Magnetic field-directed self-assembly of magnetic nanoparticles, MRS Bulletin, 38, (2013), 915–920.

[38] R.E. Rosensweig, Heating magnetic fluid with alternating magnetic field, J. Magn. Magn. Mater., 252, (2002), 370−374.

[39] A. E. Deatsch and B. A. Evans, Heating efficiency in magnetic nanoparticle hyperthermia, J. Magn. Magn. Mater., 354, (2014), 163–172.

[40] Y. L. Golovin, S. L. Gribanovsky, D. Y. Golovin, N. L. Klyachko, A. G. Majouga, A. M. Master, S. Marina and A. V. Kabanov, Towards nanomedicines of the future: Remote magneto-mechanical actuation of nanomedicines by alternating magnetic fields, J. Control. Release, 219, (2015), 43–60.

[41] A. Ito, M. Shinkai, H. Honda, T. Kobayashi, Medical application of functionalized magnetic nanoparticles, J. Biosci. Bioeng., 100, (2005), 1−11.

[42] M. Bekovic, M. Trbusic, M. Trlep, M. Jesenik and A. Malter, Magnetic Fluids' Heating Power Exposed to a High-Frequency Rotating Magnetic Field, Adv. Mater. Sci. Eng., 2018 (2018), ID 6143607.

[43] S. L. Saville, B. Qi, J. Baker, R. Stone, R. E. Camley, K. L. Livesey, L. Ye, T. M. Crawford and O. T. Mefford, The formation of linear aggregates in magnetic hyperthermia: Implications on specific absorption rate and magnetic anisotropy, J. Colloid Interface Sci., 424, (2014), 141−151.

[44] C. Haase and U. Nowak, Role of dipole-dipole interactions for hyperthermia heating of magnetic nanoparticle ensembles, Phys. Rev. B, 85, (2012), 045435.

[45] I. Conde-Leboran, D. Baldomir, C. Martinez-Boubeta, O. Chubykalo-Fesenko, D. del Puerto Morales, G. Salas, D. Cabrera, J. Camarero, F. J. Teran and D. Serantes, A single picture explains diversity of hyperthermia response of magnetic nanoparticles, J. Phys. Chem. C, 119, (2015), 15698–15706.

[46] R. P. Tan, J. Carrey and M. Respaud, Magnetic hyperthermia properties of nanoparticles inside lysosomes using kinetic Monte Carlo simulations: Influence of key parameters and dipolar

interactions, and evidence for strong spatial variation of heating power, Phys. Rev. B, 90, (2014), 214421.

[47] B. Mehdaoui, R. P. Tan, A. Meffre, J. Carrey, S. Lachaize, B. Chaudret and M. Respaud, Increase of magnetic hyperthermia efficiency due to dipolar interactions in low anisotropy magnetic nanoparticles: theoretical and experimental results, Phys. Rev. B, 87, (2013), 174419.

[48] C. Guibert, V. Dupuis, V. Peyre and J. Fresnais, Hyperthermia of magnetic nanoparticles: Experimental study of the role of aggregation, J. Phys. Chem. C, 119, (2015), 28148–28154.

[49] D. Serantes, D. Baldomir, C. Martinez-Boubeta, K. Simeonidis, M. Angelakeris, E. Natividad, M. Castro, A. Mediano, D. X. Chen, A. Sanchez, L. I. Balcells and B. Martínez, Influence of dipolar interactions on hyperthermia properties of ferromagnetic particles, J. Appl. Phys., 108, (2010), 073918.

[50] I. Conde-Leborán, D. Serantes and D. Baldomir, Orientation of the magnetization easy axes of interacting nanoparticles: Influence on the hyperthermia properties, J. Magn. Magn. Mater., 380, (2015), 321−324.

[51] E. Alphandéry, S. Faure, L. Raison, E. Duguet, P. A. Howse and D. A. Bazylinski, Heat production by bacterial magnetosomes exposed to an oscillating magnetic field, J. Phys. Chem. C, 115, (2011), 18–22.

[52] B. B. Lahiri, S. Ranoo, A. W. Zaibudeen and J. Philip, Magnetic hyperthermia in magnetic nanoemulsions: Effects of polydispersity, particle concentration and medium viscosity, J. Magn. Magn. Mater., 441, (2017), 310−327.

[53] S. A. Gudoshnikov, B. Y. Liubimov and N. A. Usov, Hysteresis losses in a dense superparamagnetic nanoparticle assembly, AIP Advances, 2, (2012), 012143.

[54] P. Guardia, R. D. Corato, L. Lartigue, C. Wilhelm, A. Espinosa, M. Garcia-Hernandez, F. Gazeau, L. Manna, and T. Pellegrino, Water-Soluble Iron Oxide Nanocubes with High Values of Specific Absorption Rate for Cancer Cell Hyperthermia Treatment, ACS Nano, 6, (2012), 3080–3091.

[55] A. Rousseau, M. Tellier, L. Marin, M. Garrow, C. Madelaine, N. Hallali and J. Carrey, Influence of medium viscosity on the heating power and the high-frequency magnetic properties of nanobeads containing magnetic nanoparticles, J. Magn. Magn., 518, (2021), 167403.

[56] X. Yao, K. Sabyrov, T. Klein, R. L. Penn and T. S. Wiedmann, Evaluation of magnetic heating of asymmetric magnetite particles, J. Magn. Magn. Mater., 381, (2015), 21−27.

[57] A. Tomitaka, T. Koshi, S. Hatsugai, T. Yamada and Y. Takemura, Magnetic characterization of surface-coated magnetic nanoparticles for biomedical application, J. Magn. Magn. Mater., 323, (2011), 1398−1403.

[58] F. Steinkea, W. Andrä, R. Heide, C. Werner and M. E. Bellemann, Rotating magnetic macrospheres as heating mechanism for remote controlled drug release, J. Magn. Magn. Mater., 311, (2007), 216−218.

Chapter 2 The behavior and heating effects of spherical magnetic particles in an alternating magnetic field

2.1 Introduction

In the field of biomedical engineering, many researchers have been energetically investigating the application to magnetically-guided drug delivery system [1] and magnetic particle hyperthermia treatment [2-5]. Multi-functional magnetic particles [6] exhibit a high heating performance in hyperthermia and an effective loading performance of anti-cancer drugs in drug delivery system.

The Néel relaxation mechanism is the governing factor for the heat production of magnetic particles smaller than approximately 10 nano-meters and, on the other hand, the Brownian relaxation mechanism governs the heat generation phenomena for particles larger than this order.

Although the Néel relaxation mode has been largely focused on for heat production up to the present, recently some researchers have been searching for a possibility of larger magnetic particles where the heat generation arises mainly from the Brownian relaxation mechanism. Studies in respect to the characteristics of heat production of these larger particles from the Brownian relaxation mechanism seem to be significantly important even from an academic point of view in order to further expand the application of magnetic particles in the fields of magnetically drug delivery system and magnetic particle hyperthermia.

From this background, in the present study, we elucidate aggregation phenomena in a suspension composed of magnetic spherical particles in an alternating magnetic field in order to clarify the relationship between the particle aggregates and the heating effect due to Brownian relaxation mechanism.

2.2 Model of magnetic particles

We consider aggregation phenomena in a suspension composed of magnetic spherical particles in an alternating magnetic field and their influence on heat production due to Brownian relaxation mechanism. To do so, the following particle model is employed for Brownian dynamics simulations. If it is necessary to distinguish quantities of each particle, the subscripts i and j will be attached to the quantities of particle i and j, respectively. A magnetic particle i with diameter d is covered by a uniform steric layer with thickness δ and has a magnetic moment $\boldsymbol{m}_i$ at the particle center. Employing this particle model, an magnetic dipole-dipole interaction energy $U_{ij}^{(m)}$ and an repulsive interaction energy due to an overlap of steric layers $U_{ij}^{(V)}$ act on particle i exerted by particle j, and also a magnetic dipole-field interaction energy $U_i^{(H)}$ acts on particle i by an external magnetic field [7, 8].

The forces and torques are straightforwardly derived in a mathematical expression, that is, the force $\boldsymbol{F}_{ij}^{(m)}$ and torque $\boldsymbol{T}_{ij}^{(m)}$ are derived from $U_{ij}^{(m)}$, and the repulsive force $\boldsymbol{F}_{ij}^{(V)}$ from $U_{ij}^{(V)}$.

Moreover, the torque $\boldsymbol{T}_i^{(H)}$ due to the particle-field interaction is derived from $U_i^{(H)}$ [7, 8].

2.3 External alternating magnetic field

We address a flow problem of a suspension in the situation of an alternating magnetic field that has a time-dependent magnitude of a magnetic field applied along a certain direction. If a magnetic field is assumed to be applied along the *x*-direction, a time-dependent magnetic field $\boldsymbol{H}$ is expressed as

$$\boldsymbol{H}(t) = (H_0 \sin(\omega_H t))\boldsymbol{i}_x \tag{2.1}$$

in which $\boldsymbol{i}_x$ is the unit vector denoting the *x*-direction, expressed as $\boldsymbol{i}_x$=(1,0,0), H_0 is the maximum of its magnitude and the cycle period T_{cycl} is expressed as $T_{cycl}=2\pi/\omega_H$.

2.4 Brownian dynamics method

In order to induce the Brownian motion of magnetic particles, an appropriate simulation method has to be used and we here employ the Brownian dynamics method [7, 9, 10]. The particle motion that performs the Brownian motion in an alternating magnetic field is simulated by the usual equations of the translational and rotational motion [11, 12]. It is noted that the direction of the magnetic moment of magnetic particles is obtained from the basic equation for the rotational motion. The translational Brownian motion is characterized by the translational diffusion coefficient $D^T = k_B T / (3\pi\eta d)$ where η is the viscosity of a base liquid, k_B is Boltzmann's constant, T is the absolute temperature of the liquid and d is the diameter of magnetic particles. The random displacements Δr_1^B, Δr_2^B and Δr_3^B in each axis direction are required to satisfy the following stochastic characteristics [11, 12]:

$$\left.\begin{aligned} &\langle \Delta r_1^B \rangle = \langle \Delta r_2^B \rangle = \langle \Delta r_3^B \rangle = 0 \\ &\langle (\Delta r_1^B)^2 \rangle = \langle (\Delta r_2^B)^2 \rangle = \langle (\Delta r_3^B)^2 \rangle = 2D^T \Delta t \end{aligned}\right\} \tag{2.2}$$

Similarly, the rotational Brownian motion is characterized by the rotational diffusion coefficient $D^R = k_B T / (\pi\eta d^3)$. The random displacements $\Delta\phi_1^B$, $\Delta\phi_2^B$ and $\Delta\phi_3^B$ about each axis line satisfy the following stochastic characteristics [11, 12]:

$$\left.\begin{aligned} &\langle \Delta\phi_1^B \rangle = \langle \Delta\phi_2^B \rangle = \langle \Delta\phi_3^B \rangle = 0 \\ &\langle (\Delta\phi_1^B)^2 \rangle = \langle (\Delta\phi_2^B)^2 \rangle = \langle (\Delta\phi_3^B)^2 \rangle = 2D^R \Delta t \end{aligned}\right\} \tag{2.3}$$

It is noted that in the above expressions, subscript *i* denoting particle name is dropped for simplicity.

2.5 Heating effect due to the relaxation phenomenon of magnetic moment

In a magnetic particle suspension, the work per unit volume exerted on the system, W_{cycl}, during one cycle of an alternating magnetic field, which induces the magnetization $\boldsymbol{M}$, is expressed using the alternating magnetic field $\boldsymbol{H}$ as [13]

$$W_{cycl}^{total} = \mu_0 \oint \boldsymbol{H} \cdot d\boldsymbol{M} \tag{2.4}$$

This is equivalent to the area of the hysteresis loop of the field-magnetization (H-M) curve, and thus Eq. (2.4) is rewritten as

$$\begin{aligned} W_{cycl}^{total} &= -\mu_0 \oint \boldsymbol{M} \cdot d\boldsymbol{H} = -\mu_0 m H_0 N \oint \langle n_x \rangle d(H/H_0) \\ &= -\mu_0 m H_0 N \oint (\langle n_x \rangle + 1) d(H/H_0) \end{aligned} \tag{2.5}$$

in which H is the magnitude of the magnetic field shown in Fig. 2.1, expressed as $H/H_0 = \sin(\omega_H t)$. We here address the work per particle, W_{cycl}, expressed as

$$W_{cycl} = -\mu_0 m H_0 \oint (\langle n_x \rangle + 1) d(H/H_0) \tag{2.6}$$

In this equation, $\langle n_x \rangle$ is the mean value of the x-component n_x of the unit vector $\boldsymbol{n}$ denoting the magnetic field direction. This work W_{cycl} corresponds to the heat production that is used for magnetic hyperthermia treatment.

2.6 Non-dimensionalization of expressions

In simulations, the non-dimensionalized equations and quantities are generally used [11, 12]. In a non-dimensionalization procedure, the following representative quantities are adopted. The diameter of solid sphere, d, is used for lengths, the period of an alternating field, $2\pi/\omega_H$, for time, $\omega_H d/(2\pi)$ for velocities, ω_H for angular velocities, the viscous friction force $(3/2)\eta\omega_H d^2$ for forces, similarly $\pi\eta\omega_H d^3$ for torques and $k_B T$ for energies.

Through the non-dimensionalization procedure, the following non-dimensional parameters appear the non-dimensional equations:

$$\begin{aligned} &R_B = \frac{k_B T}{3\pi\eta d^3} \cdot \frac{2\pi}{\omega_H}, \quad R_m = \frac{\mu_0 m^2}{2\pi\eta d^6 \omega_H} = 3R_B\lambda, \quad R_V = \frac{\pi n_s k_B T}{3\eta d\omega_H} = R_B\lambda_V, \\ &R_H = \frac{\mu_0 m H_0}{\pi\eta d^3 \omega_H} = \frac{3}{2\pi} R_B \xi \end{aligned} \tag{2.7}$$

In these expressions, the quantity R_B, R_m, R_V and R_H are the non-dimensional parameters describing the strength of the random force, the magnetic particle-particle interaction, the repulsive interaction due to the overlap of steric layers and the magnetic torque due to the external field

relative to the viscous force or torque, respectively.

The quantities λ, ξ and λ_V appearing in Eq. (2.7) are the non-dimensional parameters relative to the thermal motion, that is, imply the strength of magnetic particle-particle, particle-field and steric repulsive interactions, respectively. These are defined as [8]

$$\lambda = \frac{\mu_0 m^2}{4\pi d^3 k_B T}, \qquad \xi = \frac{\mu_0 m H_0}{k_B T}, \qquad \lambda_V = \frac{\pi n_s d^2}{k_B T} \tag{2.8}$$

These parameters λ, ξ and λ_V are quite useful in comparison to the aggregation results that were obtained in a uniform (time-independent) applied magnetic field.

2.7 Simulation parameters for Brownian dynamics simulations

Unless specifically noted, we used the following values for performing the present simulations. The number of particles N is set as N=125 (=5^3), the volumetric fraction ϕ_V (=$N(\pi/6)d^3/V$) as ϕ_V= 0.02 (where V is the volume of the simulation region), the side length l_x^*(=l_x/d) of a cubic simulation region as l_x^*=l_y^*=l_z^*=14.85, the time interval Δt^* as Δt^* =0.0005, and the total simulation time t_{total}^* as t_{total}^*=20 (i.e., 20 cycles). The averaging procedure was conducted using the data that were obtained during the later half part of the total simulation time. Moreover, the thickness of the steric layer, δ^*, was taken as δ^*=0.15, and the repulsive interaction strength λ_V as λ_V=150. The non-dimensional parameters λ, ξ and R_B were taken in a variety of cases such as λ=1, 5 and 10, ξ=1, 5 and 10, and R_B=0.1, 1, 5, 10 and 15.

2.8 Results and discussion

2.8.1 Time change in aggregate structures of particles in an alternating magnetic field

We first discuss a change in particle aggregates as a function of time in the situation of an alternating magnetic field. Before discussion, it is noted that if the frequency of an alternating magnetic field is sufficiently large, that is, if the value of the non-dimensional parameter R_B is much smaller than unity, the viscous force will dominate the phenomenon more strongly. This implies that the cluster formation and internal structure of particle aggregates will be significantly influenced by the viscous force.

Figure 2.1 shows the time change in the aggregate structures of magnetic particles for R_B=5 and ξ=5, where three cases of the magnetic interaction strength are addressed, i.e., (a) λ=1, (b) λ=5 and (c) λ=10. Each figure has snapshots at the three angles of the alternating magnetic field, θ_{time} (=$\omega_H t^*$, defined for 0~2π)=π/2, π and 3π/2. Since the magnetic interaction is significantly strong in the case of λ=10, shown in Fig. 2.1(c), it is seen that large aggregate structures are stably formed. However, since the magnetic field strength is not so strong in comparison with the magnetic interaction between particles, these clusters are not restricted to the field direction in orientation. A noteworthy point is that these chain-like clusters are not dissociated due to a change in the direction of the magnetic field at around θ_{time}=π, where the field direction is switched from the positive to the negative *x*-direction. This is because the magnetic interaction is much more dominant than both the viscous force and the magnetic particle-field interaction.

For the case of λ=5, long chain-like clusters are not significantly formed but short clusters are formed. These chain-like clusters seem to tend to be slightly formed in thick chain formation along the field direction. This is partly because the influence of the magnetic field become more significant in comparison with the previous case, and therefore the magnetic moment is more strongly restricted to the field direction, which enhances the tendency of the thick formation along the field direction. As in the previous case, these weak chain-like clusters are not disturbed by a change in the alternating magnetic field for a weak viscous force case R_B=5.

For the case of λ=1, since the magnetic interaction is much weaker than the thermal motion, particles do not aggregate to form any clusters at any phase angles. In this situation, the magnetic moment of each particle responds to a change in the magnetic field in orientation separately.

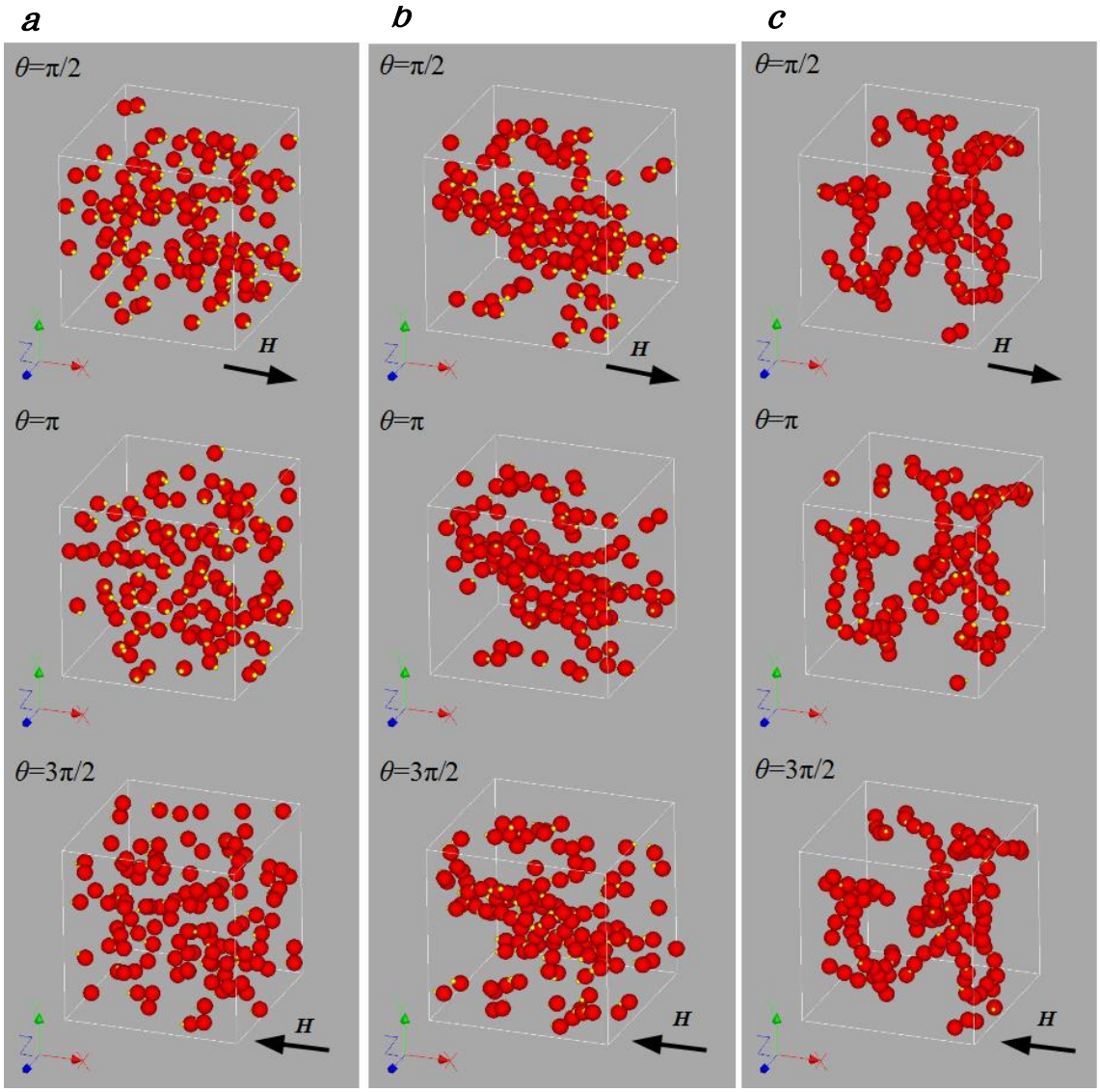

Fig. 2.1 Time change in the aggregate structures of magnetic particles for R_B=5 and ξ=5: (a) for λ=1, (b) for λ=5 and (c) for λ=10. Each figure has snapshots at the three angles of the alternating magnetic field, θ_{time} (=$\omega_H t^*$, defined for 0~2π) =π/2, π and 3π/2. The magnetic moment of each particle is reoriented toward the magnetic field direction with a delay without dissociation of the chain-like clusters for the case of λ=10.

2.8.2 Hysteresis loops on the field-magnetization curves

In this section, we discuss the relationship between particle aggregate structures and characteristics of heat production. It is noted that a larger area of the hysteresis loop of field-magnetization curves gives rise to a larger heating effect that is produced by the Brownian relaxation of the magnetic moments.

Figure 2.2(a) shows results of the hysteresis loop of the normalized magnetization $\langle n_x \rangle$ as a function of the normalized magnetic field strength H_x^*: results for R_B=0.1, 1, 5, 10 and 15 were shown in the case of a strong particle-particle and particle-field interaction, $\lambda=\xi=10$. Similar results are shown in Fig. 2.2(b) for the case of $\lambda=1$ and $\xi=10$.

In the case of R_B=0.1, the maximum of $\langle n_x \rangle$ is approximately $\langle n_x \rangle \simeq 0.3$, not attains to around unity, so that the area of the hysteresis loop give rise to a small value, yielding a poor heating production performance. In this case, although small and large clusters are formed in the system, these clusters do not contribute to an improvement of the heating production; the frequency of the magnetic field seems to be high for the appearance of Brownian relaxation effect. This characteristic clearly exemplifies that if the magnetic moments do not sufficiently respond to the magnetic field change in a high frequency area, then the area of the hysteresis loop is small and thus a large heating effect cannot be obtained. This dependence on the frequency of the field is similar to that for a smaller particle system where the heating production is obtained by Néel relaxation phenomenon [14]. As the value of R_B is increased, a stronger magnetic field is necessary for the magnetic moments inclining in the opposite direction to rotate in the field direction. For instance, in the case of R_B=10, the quantity $\langle n_x \rangle$ maintains a value of -1 until the field strength $H_x^* \simeq 0.5$, and then steeply increases with increasing magnetic field strength. From these characteristics, it is evident that strong magnetic interactions between particles function to delay the response of the particle rotational motion toward the magnetic field direction. Hence, this delay of the orientation gives rise to a large area of the hysteresis loops or a large heat production performance.

Since particle aggregates are not sufficiently formed in the system in Fig. 2.2(b), the characteristics of the hysteresis loops will be mainly determined by two factors, i.e., the magnetic particle-field interaction and the viscous friction force. One of characteristic points is that the magnetic field strength at which the value of $\langle n_x \rangle$ arrives at nearly $\langle n_x \rangle \simeq 1$ is much smaller than that for the previous case in Fig. 2.2(a); for instance, in the case of R_B =15, this situation is almost attained at $H_x^* \simeq 0.5$. This characteristic comes to appear more clearly for a larger value of R_B, because a low viscous friction force leads to a larger influence of the magnetic field and thus the magnetic torque acting on particles relatively becomes lager, whereby the magnetic moments can incline in the magnetic field direction more promptly.

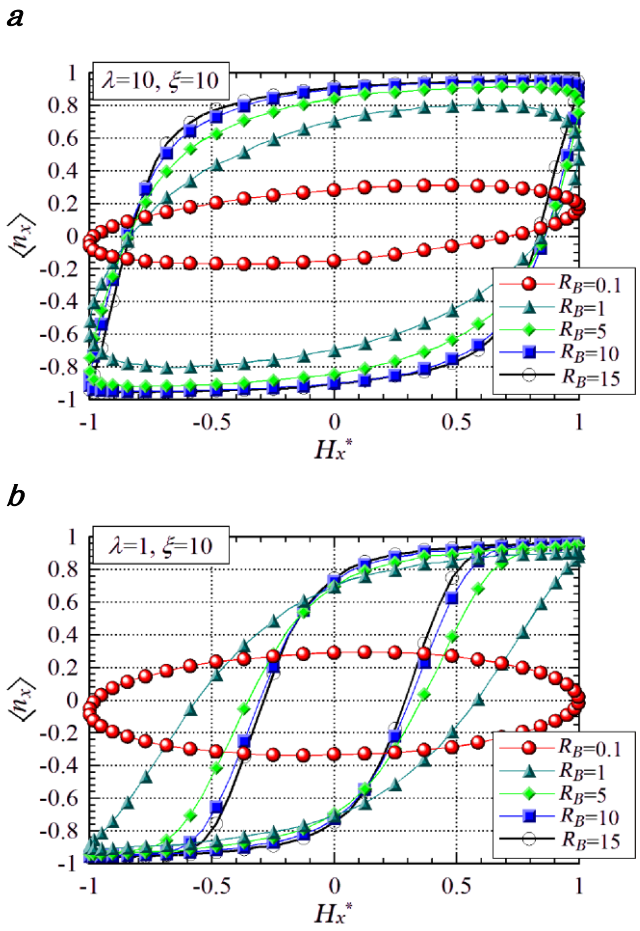

Fig. 2.2 Hysteresis loop of the magnetic field-magnetization curves: (a) λ=10 and ξ=10, and (b) λ=1 and ξ=10. In the case of the viscous force being dominant (R_B=0.1), the magnetic moments of particles do not sufficiently reorient toward the magnetic field direction, which leads to a smaller area of the hysteresis loop.

2.8.3 Heat production effect due to Brownian relaxation mechanism

Finally, we consider the work per particle W_{cycl}^* that is equivalent to the heat production generated from the Brownian relaxation of the rotational motion of the magnetic moments.

Figure 2.3 shows the dependence of the heat production W_{cycl}^* ($=W_{cycl}/k_BT$) on the magnetic particle-particle interaction strength λ for the case of the viscous force being relatively weak: results are obtained for the field strength, ξ=1, 5 and 10. From Eq. (2.6), it is straightforwardly predicted that the heating effect is quite small for a weak magnetic field such as ξ=1.

In the case of ξ =10, a larger heating effect is obtained with increased values of λ. This is because the area of the hysteresis loop becomes larger with increasing magnetic interactions (i.e.,

with increasing values of λ), shown in Fig. 2.2. As already pointed out, in the circumstance where chain-like clusters are formed and incline in the field direction, a larger heat production performance is achieved.

In the case of ξ=5, the value of W_{cycl}^{*} slightly increases until $\lambda \simeq 5$ and then turns to significantly decrease with increased values of λ. This characteristic is evident from the behavior of the characteristics of the chain-like clusters in the alternating magnetic field. That is, chain-like clusters are formed in the field direction and their length becomes larger until $\lambda \simeq 5$ with increasing values of λ. Similar to the case of λ=10, these chain-like clusters formed in the field direction function to delay the orientation of the magnetic moments along the field direction. This tendency of the rotational motion of particles results into a hysteresis loop with a larger area, i.e., a larger heating effect is attained. In contrast, in the area larger than $\lambda \simeq 5$, since the magnetic particle-particle interaction becomes more dominant than the influence of the applied magnetic field with increasing values of λ, the chain-like clusters are not restricted to the field direction in orientation, which yields the convergence of the quantity $\langle n_x \rangle$ to $\langle n_x \rangle \simeq 0$. This implies that the hysteresis loop become significantly small and thus the heating effect approaches approximately zero. This characteristic can be recognized also for a suspension composed of small magnetic particles where the heat production is generated due to the Néel relaxation mechanism [15].

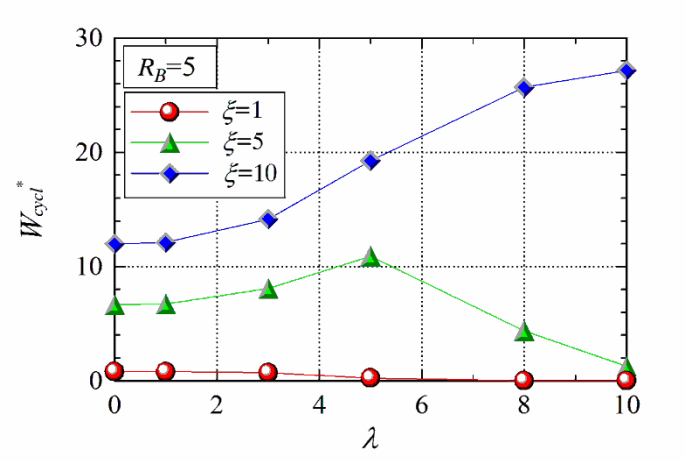

Fig. 2.3 Dependence of the heating effect on the magnetic particle-particle interaction strength. A decrease after $\lambda \simeq 5$ with increasing values of λ in the case of ξ=5 implies that larger clusters do not significantly respond to the change in the magnetic field strength.

2.9 Conclusion

We have investigated the aggregate structures in a suspension of magnetic particles in an alternating magnetic field and their influence on the heat production effect. In the present study, we address the Brownian relaxation mode that generates the heat production due to the rotational motion of magnetic particles in an ambient viscous medium with experience of the friction force (or torque). The main factors characterizing the present phenomenon are the viscous friction force arising from an alternating external magnetic field, the applied magnetic field strength and the particle-particle interaction strength. In the situation where chain-like clusters are stably formed in the magnetic field direction, the magnetic particle-particle interaction considerably delays the response of the magnetic moment reorienting in the field direction to a change in the alternating magnetic field. In the situation where particle aggregates are not significantly formed due to an insufficient magnetic interaction, the viscous friction force alone is the main factor for delaying the orientation of the magnetic moments in the field direction and therefore the response of the orientation of particles becomes more prompt in comparison with the other situations. A large heat production performance can be achieved in the situation where large chain-like clusters are formed and inclined in the applied alternating magnetic field that is more dominant than the magnetic interaction between particles. On the other hand, if these chain-like clusters are not sufficiently restricted to the field direction in orientation, a large heat production cannot be obtained.

References

[1] U. Häfeli, W. Schütt, J. Teller and M. Zborowski, (Eds.), *Scientific and Clinical Applications of Magnetic Carriers* (Springer, Berlin, 1997).

[2] A. M. Schmidt, Thermoresponsive magnetic colloids, Colloid Polym. Sci., 285, (2007), 953-966.

[3] C. S. S. R. Kumar and F. Mohammad, Magnetic nanomaterials for hyperthermia-based therapy and controlled drug delivery, Advan. Drug Delivery Rev., 63, (2011), 789-808.

[4] I. M. Obaidat, B. Issa and Y. Haik, Magnetic properties of magnetic nanoparticles for efficient hyperthermia, Nanomaterials., 5, (2015),63-89.

[5] Y. I. Golovin, S. L. Gribanovsky, D. Y. Golovin, N. L. Klyachko, A. G. Majouga, A. M. Master, S. Marina and A. V. Kabanov, Towards nanomedicines of the future: Remote magneto-mechanical actuation of nanomedicines by alternating magnetic fields, J. Controll. Release., 219, (2015), 43-60.

[6] S. Patra, E. Roy, P. Karfa, S. Kumar, R. Madhuri and P. K. Sharma, Dual-responsive polymer coated superparamagnetic nanoparticle for targeted drug delivery and hyperthermia treatment, ACS Appl. Mater. Inter., 7, (2015), 9235-9246.

[7] A. Satoh, *Introduction to Molecular-Microsimulation of Colloidal Dispersions* (Elsevier, Amsterdam, 2013).

[8] A. Satoh, *Modeling of Magnetic Particle Suspensions for Simulations* (CRC Press, Boca Laton, FLm 2017).

[9] M. P. Allen and D. J. Tildesley, *Computer Simulation of Liquids* (Clarendon Press, Oxford, 1987).

[10] A. Satoh, *Introduction to Practice of Molecular Simulation: Molecular Dynamics, Monte Carlo, Brownian Dynamics, Lattice Boltzmann and Dissipative Particle Dynamics* (Elsevier, Amsterdam, 2010).

[11] A. Satoh, Brownian dynamics simulations with spin Brownian motion on the negative magneto-rheological effect of a rod-like hematite particle suspension, Mol. Phys., 113, (20105), 656-670.

[12] A. Satoh, Brownian dynamics simulation of a dispersion composed of disk-like hematite particles regarding aggregation phenomena, Colloid Surf. A, 483, (2015), 328-340.

[13] R. E. Rosensweig, Heating magnetic fluid with alternating magnetic field, J. Magn. Magn. Mater., 252, (2002), 370-374.

[14] S. A. Gudoshnikov, B. Y. Liubimov and N. A. Usov, Hysteresis losses in a dense superparamagnetic nanoparticle assembly, AIP Advan., 2, (2012), 012143.

[15] R. P. Tan, J. Carrey and M. Respaud, Magnetic hyperthermia properties of nanoparticles inside lysosomes using kinetic Monte Carlo simulations: Influence of key parameters and dipolar interactions, and evidence for strong spatial variation of heating power, Phys. Rev. B, 90, (2014), 214421.

Chapter 3 Unexpected characteristics of spherical particles in an alternating magnetic field

3.1 Introduction

In the present chapter we focus on the discussion of the unexpected characteristic that the stable particle cluster formation induces a decrease in the degree of heating effect, which has been shown in Chapter 2 [1].

A macroscopic theory regarding the heating of a magnetic particle suspension in an alternating magnetic field has been developed without consideration of particle aggregate formation by Rosensweig's pioneering work [2]. The dependence of the heating effect on the cluster formation was indirectly clarified in a suspension with a high volumetric fraction of particles and therefore large clusters are to be expected in the system and the interaction between magnetic moments is expected to have a significant contribution to the heating effect. Therefore we understand that it may be of importance to clarify the effect of the cluster formation of magnetic particles on the degree of heat production.

Recently, Zhao and Rinaldi [3] have performed Brownian dynamics simulations in order to investigate the relationship between the aggregate structure of magnetic particles and the heat production characteristics at a microscopic level. Our Brownian dynamics approach is quite similar to that of Zhao and Rinaldi, but in the present report, as described above, we focus on the discussion of the unexpected characteristic that the stable particle cluster formation induces a decrease in the degree of heating effect, which has not sufficiently been discussed in their paper.

3.2 Model of magnetic particles and an external alternating magnetic field

We consider aggregation phenomena in a suspension composed of magnetic spherical particles in an alternating magnetic field and their influence on heat production due to a Brownian relaxation mechanism. Magnetic particles are required to perform translation and rotational Brownian motion in an applied alternating magnetic field. In order to induce Brownian motion, an appropriate simulation method has to be used and here we employ the Brownian dynamics method [4-6]. The magnetic forces and torques acting on magnetic particles and the repulsive force due to the overlap of steric layers covering each particle are straightforwardly derived from the corresponding interaction energies. These expressions may be found from references [7, 8] and so not written here. The present physical phenomenon is characterized by the four non-dimensional parameters λ, ξ, λ_V and R_B. The former three parameters are expressed relative to the thermal motion, and imply the strength of magnetic particle-particle, particle-field and steric repulsive interactions, respectively. These are defined as [8]

$$\lambda = \frac{\mu_0 m^2}{4\pi d^3 k_B T}, \qquad \xi = \frac{\mu_0 m H_0}{k_B T}, \qquad \lambda_V = \frac{\pi n_s d^2}{2} \tag{3.1}$$

The last parameter R_B describes the strength of the random force relative to the viscous force, expressed as

$$R_B = \frac{k_B T}{3\pi\eta d^3} \cdot \frac{2\pi}{\omega_H} \tag{3.2}$$

In these equations, d is the particle diameter, m is the magnitude of the magnetic moment $\boldsymbol{m}_i$ (=$m\boldsymbol{n}_i$) of an arbitrary particle i, η is the viscosity of a base liquid, μ_0 is the permeability of free space, n_s is the number of surfactant molecules on the unit surface of a magnetic particle, k_B is Boltzmann's constant, and T is the absolute temperature of the system.

The time-dependent magnetic field $\boldsymbol{H}$ is applied along the x-direction and expressed as

$$\boldsymbol{H}(t) = (H_0 \sin(\omega_H t))\boldsymbol{i}_x \tag{3.3}$$

in which $\boldsymbol{i}_x$ is the unit vector denoting the x-direction, expressed as $\boldsymbol{i}_x$ =(1,0,0), H_0 is the magnitude of an alternating magnetic field, and ω_H is the angular velocity.

3.3 Heating effect due to the relaxation phenomenon of magnetic moments

In a magnetic particle suspension, the work per unit volume exerted on the system, W_{cycl}^{total}, during one cycle of an alternating magnetic field in order to induce the magnetization $\boldsymbol{M}$ is expressed using the alternating magnetic field $\boldsymbol{H}$ as [2]

$$W_{cycl}^{total} = -\mu_0 \oint \boldsymbol{M} \cdot d\boldsymbol{H} = -\mu_0 m H_0 \hat{N} \oint \langle n_x \rangle d(H / H_0) \tag{3.4}$$

This is equivalent to the area of the hysteresis loop of the field-magnetization (H-M) curve. In this equation, $\hat{N}$ is the number density of particles, and $\langle n_x \rangle$ is the mean value of the x-component n_x of the unit vector $\boldsymbol{n}$ denoting the magnetic moment orientation. We here address the work per particle, W_{cycl}= $W_{cycl}^{total} / \hat{N}$.

3.4 Results and discussion

As already described in the introduction, we here restrict our discussion to the influence of the cluster formation of magnetic particles on the degree of heating effect. Unless specifically noted, we used the following values for performing the present simulations. The number of particles N is set as N=512 (=8^3), the volumetric fraction ϕ_V (=$N(\pi/6)d^3/V$) as ϕ_V= 0.02 where V is the volume of the simulation region, the side length l_x^*(=l_x/d) of the cubic simulation region as l_x^*=l_y^*=l_z^*=23.75. Moreover, the thickness of the steric layer, δ^* (=δ/d), was taken as δ^*=0.15, and the repulsive interaction strength λ_V was taken as λ_V=150.

Figure 3.1 shows the dependence of the heat production W_{cycl}^* (=W_{cycl}/k_BT) on the magnetic particle-particle interaction strength λ for the case of a relatively weak viscous force (R_B=5). Results are shown for the field strengths ξ=5 and 10. It is seen that in both the cases a larger heating effect is obtained with increasing values of λ until each certain criterion value of λ. That is, the value of W_{cycl}^* tends to increase until $\lambda\simeq$5 and 10 for ξ=5 and 10, respectively, and thereafter decreases and approaches zero with increasing values of λ. Moreover, a larger value of the magnetic field strength ξ leads to a larger effect of the heat production. This decrease tendency after each certain criterion value of the magnetic interaction strength is a significantly unexpected characteristic of the heating effect, and therefore in the following discussion we concentrate on the mechanism for this decrease with increasing values of λ in conjunction with the formation of particle aggregates.

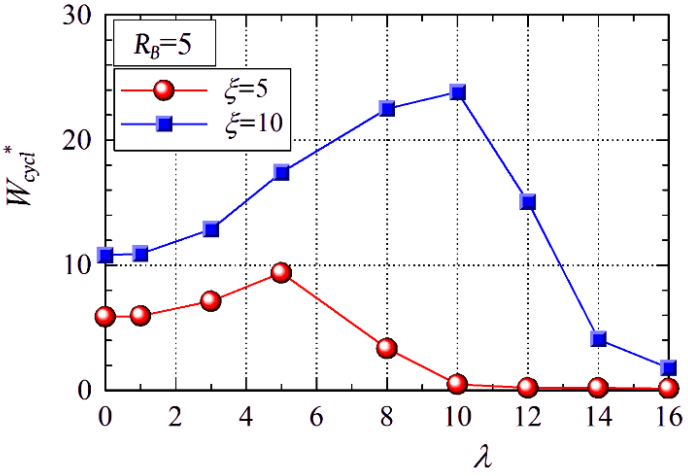

Fig. 3.1 Dependence of the heating effect on the magnetic particle-particle interaction strength. It is seen that the value of W_{cycl}^* tends to increase until $\lambda\simeq$5 and 10 for ξ=5 and 10, respectively, and thereafter decreases and approaches zero with increasing values of λ.

Figure 3.2 shows snapshots for two difference cases of the magnetic interaction strength, (a) λ=10 and (b) λ=16, for the same condition of the particle-field interaction strength ξ=10 and the strength of the random force relative to the viscous force, R_B=5. In these figures, only the snapshot at the phase angle of θ_{time}=45° is shown since in this case the response characteristics are more straightforwardly recognized with respect to the chain-like clusters and the orientation of the magnetic moments. Moreover, a relatively small system of N=125 is intentionally addressed for a clear understanding of the structure of particle aggregates.

From Fig. 3.2(a), it is seen that large aggregate structures are stably formed since the magnetic particle-particle interaction λ=10 is sufficiently strong for the cluster formation. In addition, the effect of the magnetic field strength is also sufficiently larger than thermal energy and therefore these clusters tend to form a linear thick chain-like formation inclined along the magnetic field direction (x-direction). The strong magnetic interactions (λ=10) between particles function to maintain the linear cluster formation without a large distortion, whereby the magnetic moments exhibit a resistance to rotate toward the magnetic field direction; even at the angle of θ_{time}=45° the magnetic moments do not significantly incline in the field direction. This tendency does not simply leads to the characteristic that more stable chain-like clusters give rise to a better heat production, which will be clarified later. It is a noteworthy point that even if the magnetic field switches in the positive x-direction, the chain-like clusters do not collapse but remain whilst rotating the particle body itself in order for the magnetic moment to incline toward the magnetic field direction. The reason for exhibiting this characteristic behavior of the chain-like clusters may be explained in the following manner. As the magnetic field strength is increased after switching from the negative to the positive x-direction, the chain-like clusters gradually become unstable and tend to make the magnetic moments of the constituent particles reorient in the field direction. This reorientation of each magnetic moment may be accomplished by the two mechanisms, i.e. the rotation of each particle or the rotation of chain-like clusters as a whole. It may be reasonably expected that the rotational motion of each particle can be performed more quickly than the rotational motion of chain-like clusters as a whole. Hence, as shown in Fig. 3.2(a), chain-like clusters can be maintained to a certain degree in reorientating the magnetic moments of the constituent particles toward the field direction, although this reorientation of the magnetic moments is achieved through a temporal transition of unstable chain-like clusters during a short period.

From Fig. 3.2(b), it is seen that long chain-like clusters are not restricted to the field direction but orient in various directions, which is a significant contrast to the previous snapshot in Fig. 3.2(a). Moreover, it is observed that each magnetic moment of the particles is not restricted to the field direction to a considerable level. This characteristic of not inclining in the field direction does not vary during one period of the alternating magnetic field for the case of λ=16. Furthermore, it is recognized that the magnetic moments of the particles constituting several chain-like clusters approximately incline in each cluster direction; the direction of some clusters is roughly opposite to the magnetic field direction. We may understand that these orientational characteristics arise due to

the situation where the influence of the magnetic interaction between particles is sufficiently stronger than that of the external magnetic field, which leads to a poor Brownian relaxation effect, i.e. a poor degree of heating effect. This expectation will be discussed in more detail in a quantitative manner in the following.

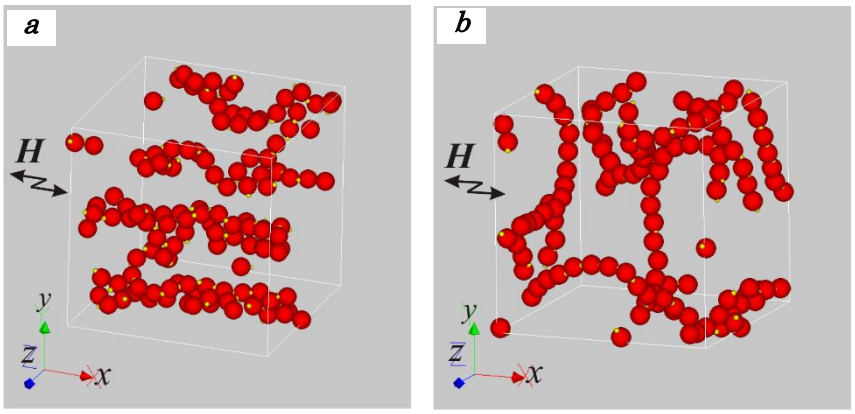

Fig. 3.2 Aggregate structures of magnetic particles at θ_{time}= 45° for R_B=5 and ξ=10: (a) λ=10 and (b) λ=16. A stronger magnetic interaction strength (λ=16) leads to a weaker tendency of the reorientation of the magnetic moments toward the field direction and also a weaker tendency of the formation of chain-like clusters along the field direction.

Figure 3.3 shows results of the response of the averaged quantity $\langle n_x \rangle$ to a change in the alternating magnetic field $H/H_0=|\boldsymbol{H}|/H_0=\sin(2\pi t^*)$ for R_B=5 and ξ=10 where two cases of λ=10 and λ=16 are addressed. It is noted that the non-dimensional time of t^*=1 corresponds to the phase angle of θ_{time} =360°. In the case of λ=10, it is seen that the curve has a trapezoidal change with a maximum value of $\langle n_x \rangle \simeq 0.85$ at $t^* \simeq 0.34$ and a plateau area between $t^* \simeq 0.3$ and $t^* \simeq 0.5$. The maximum value of around unity implies that the magnetic particles can sufficiently follow a change in the magnetic field during one period, although a large delay is observed in the response. These characteristics should give rise to a larger area of the hysteresis loop of the field-magnetization curve, which will be shown later, and therefore as a result lead to a larger heating effect at λ=10 in the curve shown in Fig. 3.1. The reason why the delay in the response is significant is that particles belonging to the same cluster which have not already oriented in the field direction show a resistance to change their orientation to follow the switched direction of the alternating magnetic field due to the magnetic interactions between the particles in a cluster. That is, the particles constituting a cluster are strongly bound with each other, and this gives rise to a large resistance to the rotation of the magnetic moment toward the magnetic field direction, which leads to a large delay in the response. A steep

increase toward the maximum value from $t^* \simeq 0.1$ is due to the characteristic that the magnetic particles which have already oriented in the field direction accelerate other particles in the cluster to rotate in the field direction through the influence of the magnetic particle-particle interactions. The curve for λ=16 exhibits a completely different response in comparison to the former case of λ=10. The most different feature is that the maximum value is much lower than unity around $\langle n_x \rangle \simeq 0.3$ at $t^* \simeq 0.3$, which implies that numerous magnetic particles do not follow the field direction, as already pointed out in the discussion of the snapshots. Since the magnetic interaction is the dominant effect in the case of λ=16, R_B=5 and ξ=10, the magnetic moments cannot rotate sufficiently during the period of the alternating magnetic field. It is this characteristic that is the cause for the heating effect decreasing and approaching zero with increasing values of λ after each criterion value in the curves of ξ=5 and 10 shown in Fig. 3.1. The reason why the curve for λ=16 does not vary around zero but is shifted toward the y-axis direction by a certain small positive value is that the system of N=512 is not sufficiently large for the case of a strong magnetic interaction strength λ=16, where stable chain-like clusters are significantly formed in the whole simulation region. However, from simulations for various sizes of the simulation region, we understand that the essential features regarding the response of the magnetic moments are able to be obtained even for the present system size of N=512.

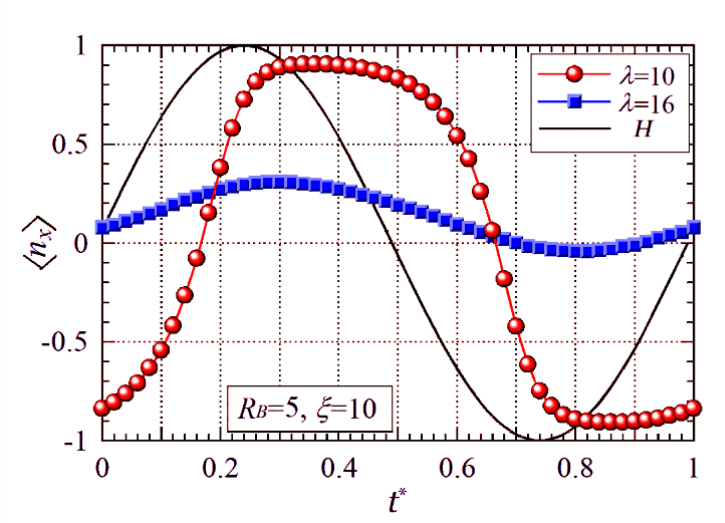

Fig. 3.3 Response of the reorientation of the magnetic particles to the change in the magnetic field strength for the case of R_B=5 and ξ=10, where two curves for λ=10 and λ=16 are shown. For the case of λ=10 chain-like clusters sufficiently response to the change in the magnetic field strength with a larger delay. In contrast, for the case of λ=16 the magnetic moments do not significantly reorient in the magnetic field direction.

Finally we show results of the hysteresis loops of the field-magnetization curves in Fig. 3.4, where two cases of λ=10 and λ=16 are addressed for the case of R_B=5 and ξ=10. As already mentioned, a larger area of the hysteresis loop gives rise to a larger heating effect which is produced by the Brownian relaxation of the magnetic moments. As already expected from the response curves shown in Fig. 3.3, the hysteresis loop is significantly larger in the case of λ=10, which gives rise to a more significant heating effect shown in Fig. 3.1. That is, a strong magnetic interaction between the particles will function to delay the response of the particle rotational motion toward the magnetic field direction, and therefore this significant delay in the orientation gives rise to a larger area of the hysteresis loop indicating a higher degree of heat production. In contrast, for the case of λ=16, the area of the hysteresis loop is significantly smaller in comparison to the previous case of λ=10, which leads to a significantly poor heating effect. This poor performance is mainly due to the tendency that the magnetic moment of each constituent particle in a cluster tends to resist to the reorientation toward the field direction, which cannot give rise to a larger maximum value of $\langle n_x \rangle$ in the case of the magnetic particle-particle interaction being significantly more dominant. The reason why the curve for λ=16 is shifted toward the y-axis direction by a certain small positive value has already been described in the above discussion regarding the response of the magnetic moments.

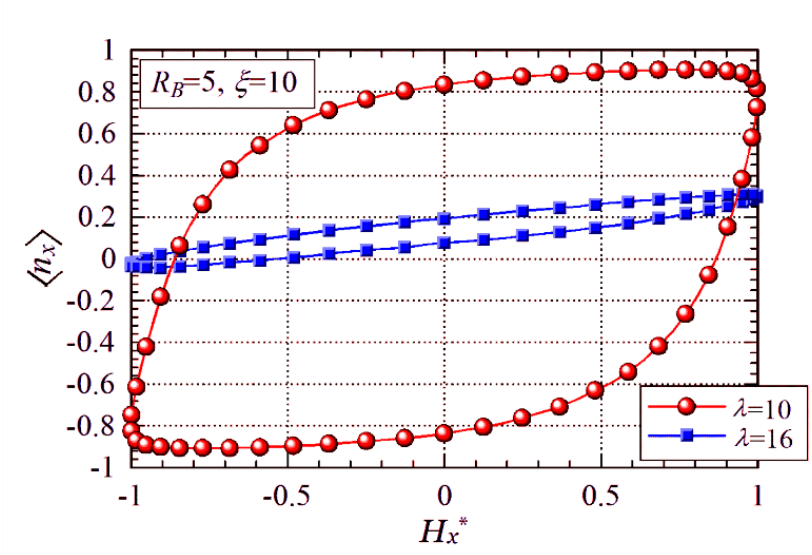

Fig. 3.4 Hysteresis loop of the magnetic field-magnetization curves for the case of R_B=5 and ξ=10, where two curves for λ=10 and λ=16 are shown. In the case of the magnetic interaction being dominant (λ=16), the magnetic moments of particles do not sufficiently reorient toward the magnetic field direction, which leads to a smaller area of the hysteresis loop.

3.5 Conclusion

We have investigated the relationship between the aggregate structures in a suspension of magnetic particles and the heating effect in an alternating magnetic field. In the present study, we address the Brownian relaxation mode that generates heat due to the rotational motion of magnetic particles that experience a frictional force or torque in an ambient viscous medium. The main factors characterizing the present phenomenon are the viscous friction force arising from an alternating external magnetic field, the applied magnetic field strength and the particle-particle interaction strength. The magnitude correlation of these factors will the characteristics of the aggregate structures and the heat production effect. In the present study we focus on the results of the unexpected characteristic that the stable particle cluster formation induces a decrease in the degree of heating effect, which has not sufficiently been discussed in other papers. That is, the heating effect tends to increase until a criterion value and thereafter decreases and approaches zero with increasing magnetic interaction strengths. From the present results, we may conclude the cause for the decrease in the degree of heating effect after criterion values in a following manner. If chain-like clusters are stably formed in the system, whether or not a large heating effect is obtained is dependent on the magnitude relationship between the magnetic particle-particle and the magnetic particle-field interaction strengths. As the magnetic particle-particle interaction strength increases and becomes more dominant than the influence of the magnetic field, the area of hysteresis loops of the field-magnetization curves become smaller and so the heating effect comes to vanish. In the opposite case where the magnetic particle-field interaction is significantly more dominant, the magnetic moment of each constituent particle is able to sufficiently respond to the change in the magnetic field, which leads to a larger area of the hysteresis loop or a better heat production performance. We therefore understand that significant heat production can be achieved in the situation where large chain-like clusters are formed and inclined in the applied alternating magnetic field. On the other hand, if these chain-like clusters are not sufficiently restricted in orientation to the field direction, a significant heat production cannot be obtained.

References

[1] S. Suzuki, A. Satoh and M. Futamura, Brownian Dynamics Simulations of Aggregation Phenomena in a Magnetic Particle Suspension with an Alternating Magnetic Field (Relationship between the Aggregate Structure and the Heat Production), International Mechanical Engineering Congress & Exposition 2018, ASME proceedings, (2018), IMECE2018-86544, V007T09A037.

[2] R. E. Rosensweig, Heating magnetic fluid with alternating magnetic field, J. Magn. Magn. Mater., 252, (2002), 370-374.

[3] Z. Zhao and C. Rinaldi, Magnetization dynamics and energy dissipation of interacting magnetic nanoparticles in alternating magnetic fields with and without a static bias field, J. Phys. Chem. C, 122, (2018), 21018-2130.

[4] A. Satoh, *Introduction to Molecular-Microsimulation of Colloidal Dispersions* (Elsevier, Amsterdam, 2003).

[5] M. P. Allen and D. J. Tildesley, *Computer Simulation of Liquids* (Clarendon Press, Oxford, 1987).

[6] A. Satoh, *Introduction to Practice of Molecular Simulation: Molecular Dynamics, Monte Carlo, Brownian Dynamics, Lattice Boltzmann and Dissipative Particle Dynamics* (Elsevier, Amsterdam, 2010).

[7] A. Satoh, *Modeling of Magnetic Particle Suspensions for Simulations* (CRC Press, Boca Laton, FL, 2017).

Chapter 4 The behavior and heating effects of spherical magnetic particles in a rotating magnetic field

4.1 Introduction

There are a variety of studies regarding the heat generation phenomena of magnetic particles in an alternating magnetic field. Yao et al. [1] have treated a suspension composed of magnetic spheroidal particles with the size larger than 100nm and have investigated a heating effect of this suspension, whilst Lahiri et al. [2] have addressed magnetic emulsion droplets. In addition, Zhao and Rinaldi have clarified the heat production characteristics of magnetic spherical particles in an alternating magnetic field [3]. Our research group has focused on the internal structure of the particle aggregates found in a spherical particle suspension, and have elucidated the relationship between the performance of heat generation and the particle aggregate structures in an alternating magnetic field [4]. We now advance this simulation study to the aggregation phenomena and the heating effect in the situation of a rotating magnetic field.

There are several experimental studies that have been conducted in regard to the behavior of magnetic particles in a rotating magnetic field. Cantillon-Murphy et al. [5] have elucidated the mechanism of heat generation in a magnetic fluid under a rotating magnetic field and in the study of Bekovic et al. [6], it has been experimentally clarified that the heating performance of magnetic particles in a rotating magnetic field may be more enhanced than in an oscillating magnetic field. Furthermore, Abu-Bakr and Zubarev [7] have clarified that the interaction between magnetic particles is expected to contribute to the performance of the heating effect. However, at the present time, there are no experimental or simulation studies elucidating the relationship between the internal structure of particle aggregates and the heating characteristics.

In a previous study [4], we investigated the relationship between the heating effect and the particle aggregates for the case of a spherical particle suspension in an alternating magnetic field. From this study it was suggested that the aggregation phenomena may be expected to have an effective contribution to the heating effect under the certain conditions. In other words, the cluster formation does not necessarily contribute to better performance of the heat generation.

From this background, in the present study, we address the behavior of magnetic spherical particles in the situation of an applied rotating magnetic field. From Brownian dynamics simulations, we attempt to clarify the internal structure of the particle aggregates and the relationship between the particle aggregates and the heating effect due to the mechanism of Brownian relaxation. Moreover, we compare the heating effect in a rotating and an alternating magnetic field in order to clarify a difference in the characteristics of the heat generation for the two different applied magnetic fields.

4.2 Particle model and a rotating magnetic field

A spherical magnetic particle with diameter d is coated with a uniform steric layer of thickness δ and has a point magnetic moment $\boldsymbol{m}$ at the particle center.

As described above, here we intend to discuss the heating effect of a magnetic particle suspension in a time-dependent magnetic field. Therefore, a rotating magnetic field $\boldsymbol{H}$ is applied along the xy-plane and expressed as

$$\boldsymbol{H}(t) = H_0 \left\{ \cos(\omega_H t)\boldsymbol{i}_x + \sin(\omega_H t)\boldsymbol{i}_y \right\} \tag{4.1}$$

in which, H_0 is the magnitude of the magnetic field, ω_H is the angular velocity and $\boldsymbol{i}_x$ and $\boldsymbol{i}_y$ are the unit vectors in the x- and y- direction, respectively.

The response of the magnetic particles is affected by the five factors, i.e., (1) the strength of the magnetic particle-particle interaction, (2) the magnetic particle-field interaction, (3) the repulsive force due to the overlap of steric layers, (4) the strength of the viscous force related to the frequency of the rotating field and (5) the thermal motion of magnetic particles, which are denoted by the non-dimensional parameters, λ, ξ, λ_V and R_B, respectively, relative to the effect of the thermal motion. The expressions for these quantities are shown in the previous study [4]. If the quantities of λ, ξ and λ_V are significantly larger than unity, then it is implied that each factor is much more dominant than the thermal motion. If the quantity R_B is much smaller than unity, then the frequency of the rotating magnetic field is significantly large and thus the viscous friction force is much more dominant than the thermal motion. Hence, the behavior of magnetic particles will be determined in a complex manner by these five factors inducing the effect of the thermal motion.

4.3 Heating effect

The heat production in a time-dependent magnetic field arises from the relaxation of the magnetic moments of the suspended particles. In general, there are two different modes for this relaxation phenomenon [8]. The Néel relaxation mode is a mechanism for magnetic particles with a diameter smaller than approximately 10 nm, where the magnetic moment can rotate within the particle body, and there are a numerous number of studies [9-12] regarding the heat production due to this mechanism. The Brownian relaxation mode [8] is another mechanism that is for larger particles, where the magnetic moment is locked to the particle body, and thus the particle itself rotates to incline in the field direction, which leads to the heat generation [1-3]. In the present study, we focus on heat generation based on the Brownian relaxation mode. The heating effect of a magnetic particle suspension in a rotating magnetic field is obtained from the work during one cycle of the magnetic field. As in the previous study [4], we here treat the heating effect generated by one particle, W_{cycl}, which is evaluated from the same equation shown in the previous study.

4.4 Parameters for simulations

Unless specifically noted, the present results were obtained by adopting the following parameter values. The number of particles N=125=5^3, time step $\Delta t^*=\Delta t / (2\pi/\omega_H)$=0.0001, and total simulation time $t_{total}^*= t_{total} / (2\pi/\omega_H)$=5000 where data from the last 50% of the simulation time was used for the averaging procedure. The diameter of a particle is d^*=1.0, the thickness of the steric layer $\delta^*=\delta/d$=0.15, and the cutoff radius $r_{coff}^*=r_{coff}/d$=8.0.

The main reason why we adopted a relatively small system of N=125 is that it is more straightforward to graphically grasp a change in the formation of clusters in a rotating field, especially the breaking-up and recombination of the chain-like clusters, shown in Fig. 4.3 in addition to Figs. 4.1 and 4.4. We assessed the dependence of the results on the size of a simulation region (i.e., the number of magnetic particles in a system), and obtained a conclusion that the results for the case of N=125 are not essentially dependent on the system size even in a quantitative meaning.

Moreover, in contrast to the previous study [4] where the volumetric fraction was taken as ϕ_V=0.02, we focus on a significantly dilute suspension such as ϕ_V=0.001 in the present rotating magnetic field. This is because in a dense system the rotation of magnetic particles in the situation of a rotating magnetic field is expected to have a significant tendency to induce the rotating flow field of a dispersion medium. Since the Brownian dynamics method is not able to solve the flow field together with the particle motion, it is quite reasonable that we restrict our attention to a dilute suspension system of ϕ_V=0.001 in the first change of the present phenomenon for a rotating magnetic field.

Furthermore, it is certainly desirable to employ the Ewald sum [13] for taking into account long-range magnetic interactions. However, since we here address a significantly dilute particle suspension of ϕ_V=0.001, the employment of a sufficiently longer cutoff distance such as r_{coff} =8d may be sufficient as a first approximation [11]. Other researchers [15] also have a conclusion that the minimum image convention is a reasonable technique as a first approximation even for a dipolar system. Similar treatment without the employment of the Ewald sum was sufficient for the case of a monolayer of magnetic spherical particles with the volumetric fraction ϕ_V=0.05 to 0.5 [16]. From this background, we have here used a sufficiently long cutoff distance of r_{coff}=8d without the employment of the Ewald sum [14]. It is noted that the present results were not substantially dependent on the value of the cutoff radius unless a small value such as r_{coff}=3d and 5d is used.

Using the above-mentioned parameters we evaluate the dimensions of the simulation cell as $l_x^*=l_x/d=l_y^*=l_z^*\approx$40.3. The non-dimensional parameters λ, ξ, λ_V and R_B are set within the wide ranges of λ=1～15, ξ=1～10, λ_V=150 and R_B=1～20. In this study, one of the parameters on which we focus is the frequency of the rotating magnetic field that is represented by the non-dimensional parameter R_B. It is noted that as the frequency is decreased the value of R_B will increase. We now consider the actual values of the physical parameters in order to assess the range of the

non-dimensional parameters. If we set the physical diameter of a magnetic particle as d=1.8×10^{-8} nm, the viscosity of liquid η=1×10^{-3} Pa·s, the magnitude of the rotating magnetic field H_0=1×10^4 A/m, the saturation magnetization M=4.46×10^5 A/m, the frequency of field ω_H=20×10^3 Hz and the temperature T=293 K, then the non-dimensional parameters are then evaluated as λ=7.86, ξ=4.23 and R_B=3.68. The ranges of the non-dimensional parameters used in the simulations are set around these typical values. The Brownian dynamics method for a spherical particle system is adequately described in textbooks [13, 17].

4.5 Results and discussion

First, we discuss the dependence of the aggregate structures on the magnetic particle-particle interaction strength λ. Although the simulations were performed on a 3D system, it is relatively difficult to discern the characteristics of the aggregate structures from 3D snapshots, therefore in order to grasp the behavior of the aggregates more clearly we use snapshots of an *xy*-plane, viewed along the *z*-axis. Figure 4.1 shows the aggregate structures for the magnetic particle-field strength ξ=5, the relative viscous force R_B =20 and the magnetic particle-particle interaction strengths of λ=1, λ=7 and λ=12. It is noted that the yellow dot of each particle implies the direction of the magnetic moment. In the case of the weak magnetic particle-particle interaction strength λ=1 shown in Fig.4.1(a), the particles do not tend to aggregate to form clusters and tend to move as single particles. The magnetic moment of each particle quickly inclines in the field direction due to the influence of the relatively strong magnetic particle-field interaction strength ξ=5. In the case of the relatively large magnetic particle-particle interaction strength λ=7 shown in Fig.4.1(b), it is seen that short linear chain-like clusters are formed in the system that tend to be restricted to motion in the *xy*-plane. This is because the magnetic moment of each particle is restricted to the magnetic field direction due to the influence of the magnetic field being more dominant. Moreover, it is seen that the short chain-like clusters tend to incline in the field direction to a greater degree than the long chain-like clusters. This is because long chain-like clusters are significantly influenced by the viscous friction force, which leads to a larger resistance when the particle motion is tending to incline them in the field direction. That is, these long chain-like clusters function to delay the magnetic moments of the constituent particles to align toward the magnetic field direction. In the case of the relatively strong magnetic particle-particle interaction strength λ=12 shown in Fig.4.1(c), both chain-like and ring-like clusters are formed in the system. The direction of the magnetic moments of the particles constituting the ring-like clusters is not significantly restricted to the magnetic field direction because the influence of the magnetic particle-particle interaction tends to dominate over the effect of the magnetic field. In the situation where the frequency of the magnetic field is sufficiently low, the orientation of the magnetic moment of each particle is primarily determined by the influence of magnetic particle-particle interaction.

Figure 4.2 shows the radial distribution function for the three cases of the magnetic particle-particle interaction strength λ=1, λ=7 and λ=12. For the case of the weak magnetic particle-particle interaction strength λ=1, the curve exhibits a typical gas-like distribution. For the case of the relatively strong magnetic particle-particle interaction strength λ=7, several sharp peaks are seen that clearly imply the formation of the linear chain-like clusters where the second, third and fourth neighboring particles in a linear cluster would be located at $r^* \simeq 1.3$, $r^* \simeq 2.6$ and $r^* \simeq 3.9$. For the case of the stronger magnetic particle-particle interaction strength λ=12, although similar peaks appear at $r^* = 1.3$, $r^* \simeq 2.6$ and $r^* \simeq 3.9$, they exhibit duller characteristics that quantitatively suggest that ring-like clusters have formed in the system. The distance between the constituent particles in a ring-like cluster is dependent on the number of constituent particles, giving rise to the duller characteristics of the radial distribution function.

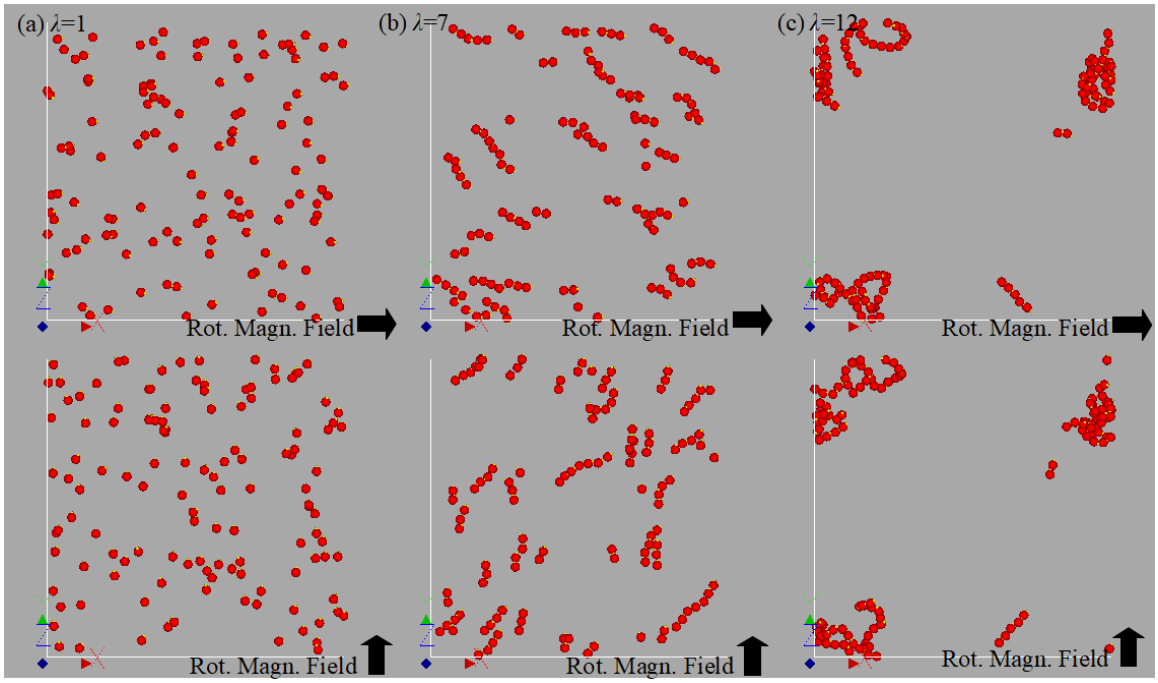

Fig. 4.1 Aggregate structures for ξ=5 and R_B=20: (a) λ=1, (b) λ=7 and (c) λ=12. A stronger magnetic particle-particle interaction induces the formation of larger and more stable clusters.

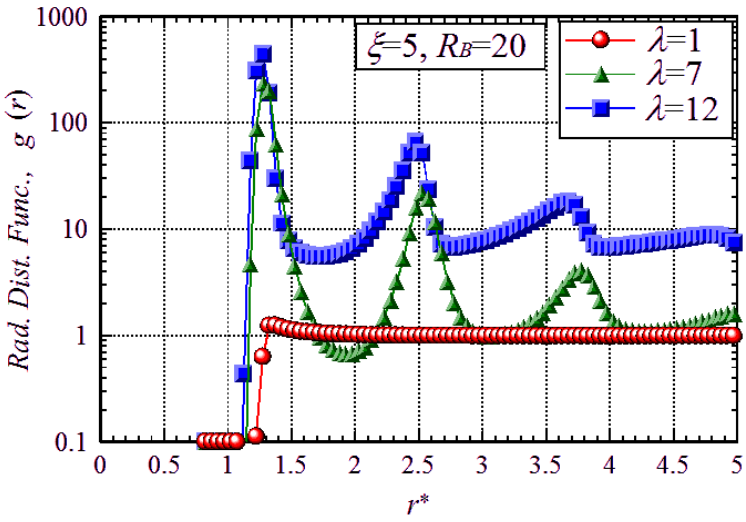

Fig. 4.2 Radial distribution function for ξ=5 and R_B=20. For the case of λ=7 and 12, the curves exhibit pronounced peaks. For the case of a relatively strong magnetic particle-particle interaction strength λ=7, it is seen that several sharp peaks appear, which clearly implies the formation of the linear chain-like clusters.

We now focus on the rotational behavior of a linear chain-like cluster. Figure 4.3 shows the transition of the aggregate structures for the case of the magnetic particle-particle interaction strength λ=10, the magnetic particle-field interaction strength ξ=10 and the relative viscous force R_B=20. The linear chain-like cluster shown in Fig.4.3(a) transforms to the distorted chain-like cluster shown in Fig.4.3(b) since the frequency of the magnetic field is not low enough to maintain the linear chain-like configuration. The constituent particles located at both the ends of the chain-like cluster exhibit a relative freedom in their motion over the particles in the center area of the cluster, so they are able to exhibit a significant tendency to follow the rotating magnetic field. When the distortion exceeds a certain degree, the long chain-like cluster cannot maintain the linear configuration and then dissociate into two chain-like clusters as shown in Fig 4.3(c). In the process of following the magnetic field, these short chain-like clusters then tend to reassemble and reform a long chain-like cluster. In this manner, the long linear chain-like clusters repeat this dissociation and association behavior while following the applied rotational magnetic field.

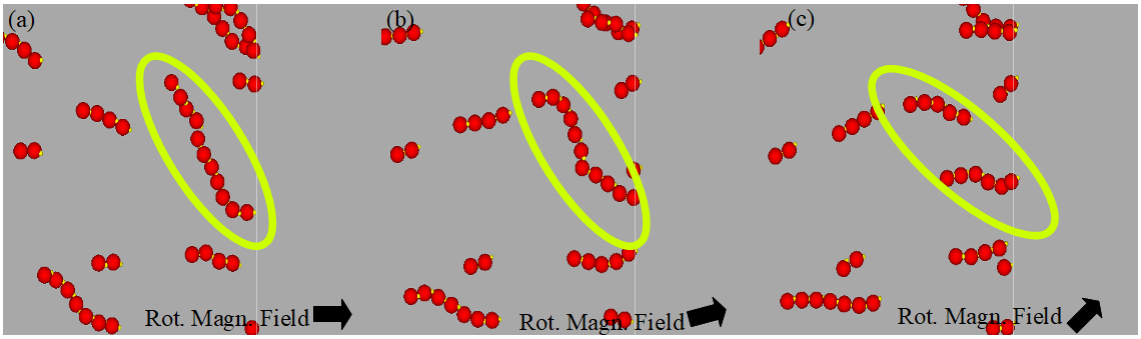

Fig. 4.3 Transition of the aggregate structures for R_B =20, λ=10 and ξ=10. When the distortion exceeds allowance, the long chain-like cluster cannot keep the linear formation. Then, the cluster dissociates into two chain-like clusters shown in Fig 4.3(c).

Next, we discuss the dependence of the aggregate structures on the frequency of the rotating magnetic field. Figure 4.4 shows the aggregate structures for the case of the magnetic particle-particle interaction strength λ=12, and the magnetic particle-field strength ξ=5 for the relative frequency of a rotating field with values R_B=1, R_B=5 and R_B=10. It is noted that a larger value of R_B implies a lower frequency of the rotating magnetic field. In the case of the relatively low frequency R_B=10 shown in Fig. 4.4(c), the more complex chain-like and ring-like clusters are formed. The orientation of the magnetic moments tends to follow the field more significantly than for the case of R_B =20 shown in Fig. 4.1(c). This is because the ring-like clusters are unstable in the case of R_B=10 since the viscous force is more dominant than the magnetic particle-particle force. From a change in the internal structure of the clusters, we observe that these clusters alternate between a chain-like and a ring-like formation as the time advances. In contrast, in the case of a high frequency R_B =1 shown in Fig. 4.4(a), many single particles move without forming clusters, although several clusters composed of a configuration of two or three particles are formed. This is because, in the situation of a dilute system with a small volumetric fraction ϕ_V=0.001, the influence of the large viscous force of R_B =1 does not provide an opportunity for particles to approach each other and therefore, only single particles and small clusters will be observed. In the case of the intermediate frequency R_B =5 shown in Fig. 4.4(b), ring-like clusters tend not to be formed and only distorted chain-like clusters and single particles are observed in the system. This is because the influence of the viscous force is of the same order as the magnetic particle-particle interaction, and thus the particles are able to form chain-like clusters but are not able to form ring-like clusters. From these results, we may understand that the frequency of the rotating magnetic field is able to control the regime of the internal configuration of the clusters.

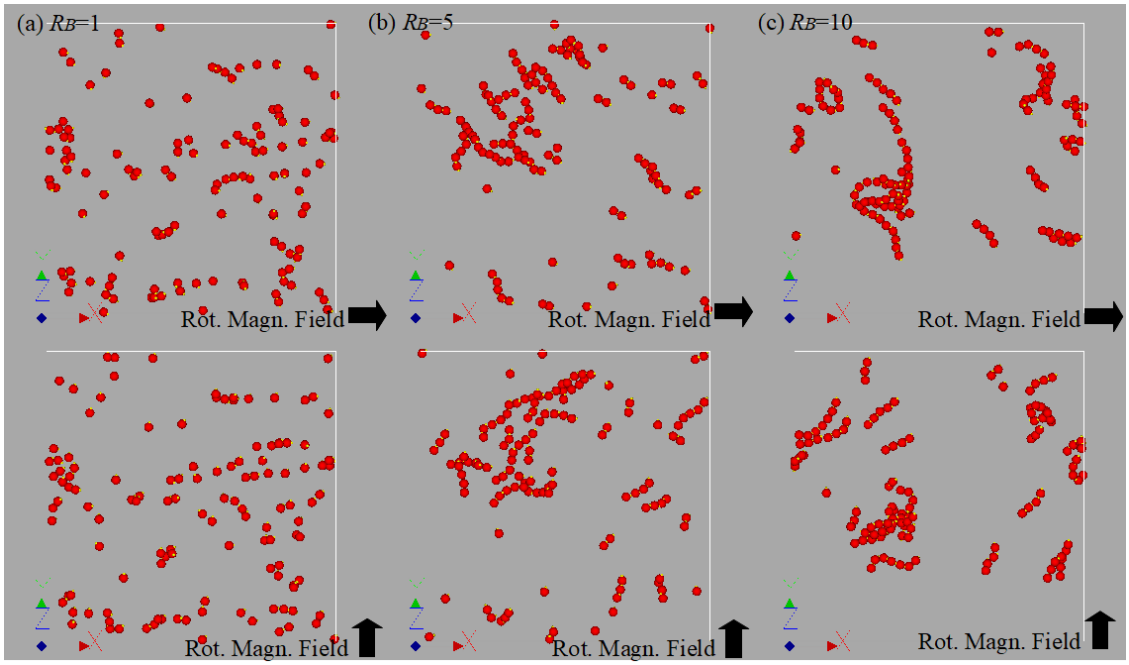

Fig. 4.4 Aggregate structures in a rotating field with the relative frequency (a) R_B =1, (b) R_B =5 and (c) R_B =10 for a system with parameter values λ=12 and ξ=5. In the case of a low frequency R_B=10 shown in Fig. 4.4(c), the complex chain-like and ring-like clusters are formed. The orientation of the magnetic moments tends to follow more significantly than for the case of R_B =20 shown in Fig. 4.1(c).

Figure 4.5 shows the cluster size distribution for the three cases of the relative viscous force R_B=1, R_B=5 and R_B=10, where N_s is the number of the clusters composed of s constituent particles. For the case of a rotating field with the relatively high frequency R_B =1, the curve exhibits a high peak value at s=1 that steeply decreases with increasing values of s. This characteristic quantitatively suggests that the particles predominately move as single particles as shown in Fig. 4.4(a). For the case of the intermediate frequency R_B =5, a peak still evident at s=1, but the height is much lower than for the previous case and a cluster composed of around 7 particles is observed in the system. For the case of the further lower frequency R_B =10, since the frequency is sufficiently low, particles are able to form longer clusters and thus a more flat region of the curve appears in the range of $s \lesssim 5$, and also a larger 9 particle cluster is evident. These characteristics quantitatively indicate that even with the influence of viscous forces, stable clusters have formed with 2 to 9 constituent particles.

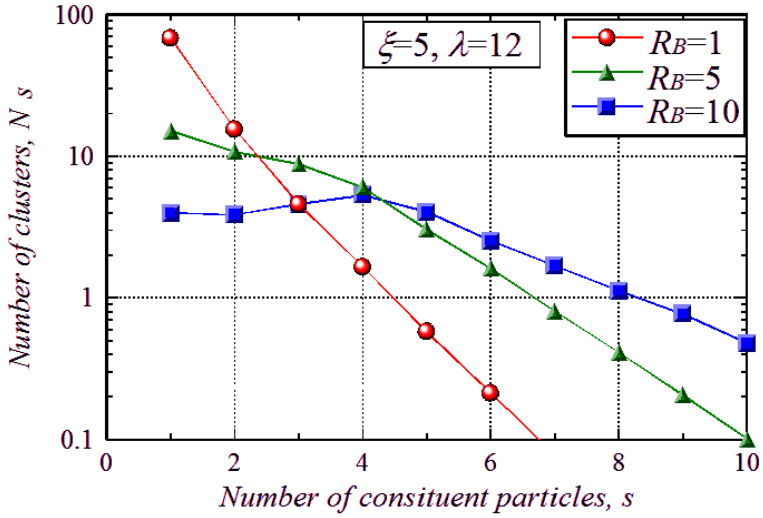

Fig. 4.5 Cluster size distribution for λ=12 and ξ=5. For the case of R_B =10, since the frequency is sufficiently low, particles are able to form longer clusters and thus a more flat region of the curve appears in the range of $s \lesssim 5$, and a larger cluster composed of 9 particles is evident in the system.

We now proceed to the discussion regarding the characteristics of the heating effect. First, we consider the dependence of the heating effect on the magnetic particle-particle interaction strength. Figure 4.6 shows the dependence of the heating effect on the magnetic particle-particle interaction strength for the case of the relatively low viscous force R_B =20 and the magnetic particle-field interaction strengths ξ=1, ξ=5 and ξ=10. In the figure, W_{cycl}^{*} is the quantity non-dimensionalized by the thermal energy kT, where k is Boltzmann's constant and T is the absolute temperature of the system. For the case of the relatively weak magnetic particle-field strength ξ=1, as is to be expected, the heating effect is significantly small. This is simply because the applied magnetic field strength is too weak for generating a heat production by means of magnetic particle-field interactions. In contrast, for the case of the higher magnetic field strength ξ=10, the heating effect exhibits a monotonic increase with increasing values of λ. This is because chain-like clusters that offer a larger resistance to the particle rotation are formed in the system, which leads to a larger value of the heating effect. Therefore in this situation, there is no significant formation of ring-like clusters in the system. In contrast, the curve for ξ=5 exhibits a pronounced change in the heating effect as a function of the magnetic particle-particle interaction strength. That is, the heating effect increases in a similar way to the case of ξ=10 in the region below $\lambda \simeq 6$ but then deviates and attains to a maximum value at $\lambda \simeq 10$ and then finally with increasing values of λ monotonically decreases to zero. In the range of $3 \lesssim \lambda \lesssim 10$, the chain-like clusters are predominately formed in the system and these increase in length with increasing values of λ. Within this range the magnetic

moments of the particles are able to sufficiently follow the changing magnetic field direction by the motion of a delayed rotation of the whole chain-like cluster. The rotational motion of a longer chain-like cluster exhibits a larger viscous resistance, which leads to a more significant heating effect. The decrease in the heating effect in the region with a magnetic particle-particle interaction strength greater than λ=10 is due to an increase in the formation of ring-like clusters together with a decrease in the number of chain-like clusters. Ring-like clusters tend to be much more stable than chain-like clusters in the situation of the magnetic particle-particle interaction of $\lambda \gtrsim 10$ being more dominant than the magnetic particle-field interaction of ξ=5. Hence, the magnetic moment of each constituent particle in a ring-like cluster does not respond sufficiently to the rotating magnetic field, and therefore the more stable ring-like cluster gives rise to a smaller heating effect with increasing values of λ.

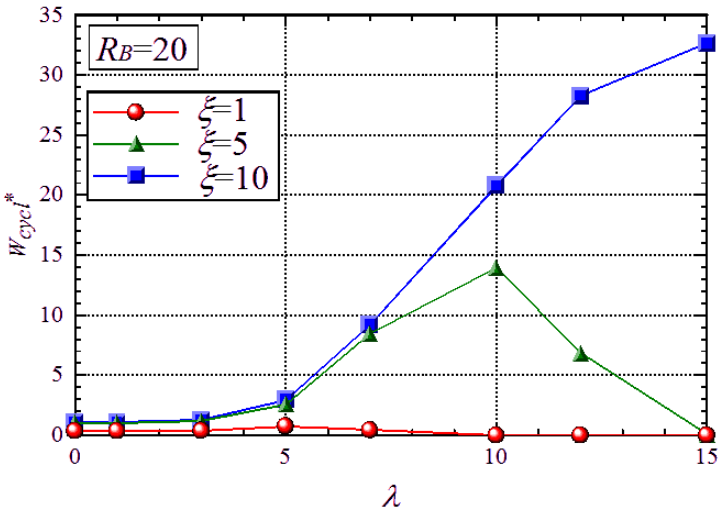

Fig. 4.6 Dependence of the heating effect on the magnetic particle-particle interaction strength. Since ring-like clusters are much more stable than chain-like clusters in the situation of the magnetic particle-particle interaction being more dominant than the magnetic particle-field interaction, thus giving rise to a smaller heating effect in the range of $\lambda \gtrsim 10$ for ξ=5.

Next, we discuss the influence of the frequency of the rotating magnetic field on the heating characteristics, where the average size of clusters is shown for references. Figure 4.7 shows this influence to the heating effect and the average size of the aggregate structures for the case of the magnetic particle-particle interaction strength λ=1, λ=5 and λ=10 and the magnetic particle-field strength ξ=5. For the cases of a weak λ=1 and a relatively weak λ=5 magnetic particle-particle interaction strength, the heating effect decreases with increasing values of R_B or with decreasing values of the relative frequency. Since a larger value of R_B also implies a lower viscous friction force, the magnetic moment of single particles and the shorter clusters can easily follow a change in the orientation of the rotating magnetic field, which gives rise to the monotonic decrease in the heating effect with decreasing values of the frequency. On the other hand, for the case of λ=5, it is seen that a deviation from the curve of λ=1 becomes evident around $R_B \simeq 10$ and shows a slight increases with increasing values of R_B that may be explained in the following. For the case of λ=5, many short clusters are expected to be formed if the viscous friction force is not a dominant factor in relation to the magnetic particle-particle interaction, or, if R_B has a sufficiently large value such as R_B=20. However, short clusters are not formed in the region of a large viscous force such as R_B=5, and this accounts for the monotonic decrease in the range of $R_B \lesssim 10$. For values greater than $R_B \simeq 10$, the effect of the magnetic interaction gradually surpasses the viscous force and thus with increasing values of R_B an increasing number of short clusters are formed. Short chain-like clusters give rise to a larger resistance to their orientation than the single particles following a change in the frequency of the rotating magnetic field. This yields a slight increase in the heating effect in the range of $R_B \gtrsim 10$. The curve for λ=10 exhibits a significantly different characteristic in contrast to the former two curves. That is, the heating effect decreases until around R_B =3, then exhibits a significant increase that finally approaches a constant value in the region of $R_B \simeq 14$. The decrease in the region before R_B=3 can be explained by the same reasoning as for the previous two cases. As the value of R_B exceeds a value around $R_B \simeq 3$, the effect of the magnetic particle-particle interaction surpasses the effect of the viscous friction forces and so particles are able to approach each other. This results in the formation of chain-like clusters that induce a larger resistance to the rotational motion, leading to a larger heating effect. The reason for the asymptotic approach of R_B to the value around $R_B \gtrsim 14$ is that the chain-like clusters have tended to maximum growth and therefore a larger resistance cannot be obtained even if the frequency of the rotating magnetic field decreases.

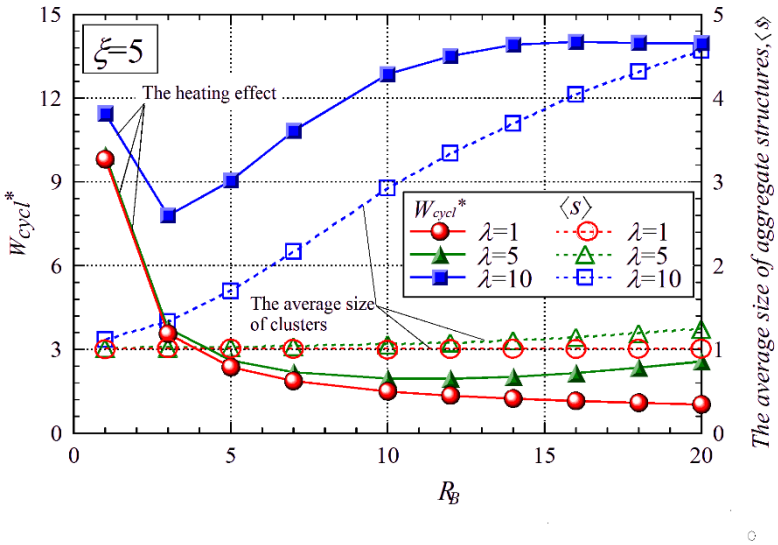

Fig. 4.7 Dependence of the heating effect and the average size of clusters on the frequency of the magnetic field. The solid line and the broken line indicate the degree of the heating effect W_{cycl}^{*} and the average size of the aggregate structures <s>, respectively. The curve for λ=10 exhibits a steep increase since around R_B =3 in contrast to the other cases. As the value of R_B exceeds around $R_B \simeq 3$, the magnetic particle-particle interaction surpasses the viscous friction forces for particles to approach each other and to form chain-like clusters, which induces a larger heating effect.

Finally, we make a comparison of the present results with those for the previous alternating magnetic field [4], which were obtained by re-performing the simulations for the same condition of the present prescribed parameters. Figure 4.8 shows the dependence of the heating effect on the magnetic particle-particle interaction strength λ for the case of R_B=20 and ξ=10. In the region of weak magnetic particle-particle interaction strengths, $\lambda \lesssim 7$, the alternating magnetic field gives rise to a higher heating effect than the rotating magnetic field. This is because magnetic particles rotate with larger angular velocities in order to follow the change in the direction of an alternating magnetic field, whereas in the rotating magnetic field magnetic particles almost constantly rotate with smaller angular velocities. A larger angular velocity yields a larger friction force, and therefore a more significant heating effect is obtained for an alternating magnetic field. As the magnetic particle-particle interaction strength is increased from $\lambda \simeq 4$, both the magnetic fields more significantly enhance the heat production and afterwards exhibit characteristic differences in the dependence on the magnetic particle-particle interaction strength. That is, the heating effect

continuously increases with values of λ for the rotating magnetic field, whereas the curve arrives at a maximum value at $\lambda \simeq 12$ and then significantly decreases for the case of the alternating magnetic field. These different heating characteristics are evidently due to the completely different behaviors of the chain-like clusters in a rotating and an alternating magnetic field. As sufficiently clarified in the previous study [4], longer chain-like clusters have a stronger tendency to maintain their configuration without rotation as the magnetic particle-particle ingeneration becomes more dominant than the magnetic particle-filed interaction, i.e., in the region of $\lambda \gtrsim \xi$, giving rise to a sharp decrease after the value of $\lambda \simeq 12$. In significant contrast, for the case of a rotating magnetic field, linear chain-like clusters are able to rotate to a certain degree without a large resistance to the rotation in order to follow the change in the orientation of an rotating magnetic field, which gives rise to a constant increase in the range of $\lambda \gtrsim 5$, although there is a repeat of breaking-up and recombination of linear chain-like clusters, as already pointed out in Fig. 4.3. From these characteristics, we understand that a rotating magnetic filed is more superior in order to obtain a more significant heating effect if we make use of a magnetic particle suspension where chain-like clusters are significantly expected to be formed.

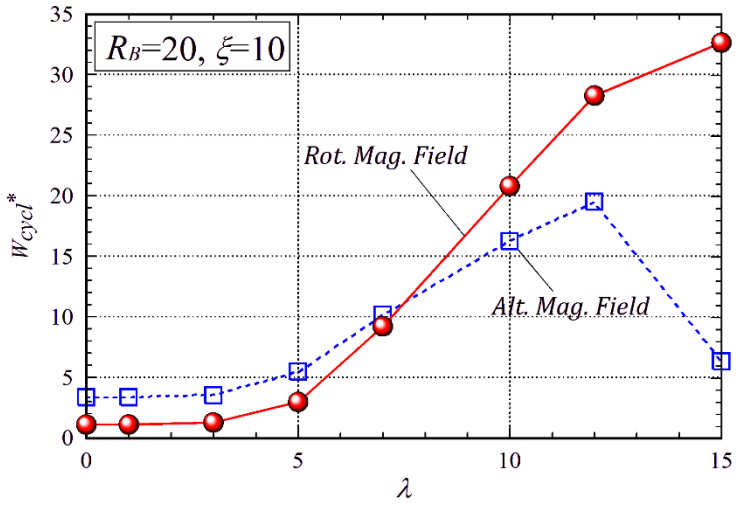

Fig. 4.8 Comparison of the results for a roating and an alternating magnetic field with respect to the dependence of the heating effect on the magnetic particle-particle interaction strength. A characteristic difference in the heating effect in the region of $\lambda \gtrsim 12$ is due to the completely different behaviors of chain-like clusters in a rotating and an alternating magnetic field. In the case of the alternating magnetic field, the heating effect is decreased with a smaller magnetic particle-particle interaction than the case of the rotating magnetic field.

Figure 4.9 shows the comparison of the results of a rotating and an alternating magnetic field with respect to the dependence of the heating effect on the frequency of the applied magnetic field, where a relatively weak magnetic field of ξ=5 is addressed. In the case of λ=1, magnetic particles solely move or rotate without the formation of clusters, and thus similar characteristics are exhibited for these two different applied magnetic fields. Since long linear chain-like clusters are expected to be formed for the case of λ=10, a rotating and an alternating magnetic field certainly yield completely different characteristics regarding the dependence on the value of R_B, i.e., on the frequency of the magnetic field. That is, the heating effect monotonically increases after $R_B \simeq 3$ with increased values of R_B for a rotating magnetic field, whereas in the case of an alternating magnetic field the heating effect comes to decrease after the attainment to an maximum value at $R_B \simeq 10$. Moreover, it is a noticeable point that the former field gives rise to a significantly larger heat performance than the latter magnetic field. A much poorer heat generation performance for an alternating magnetic field is due to the characteristic feature of chain-like clusters that the magnetic interactions of the magnetic particles constituting a chain-like cluster play a governing role to maintain the configuration of linear chain-like clusters without the rotation as a whole of clusters. This feature becomes more significant as the value of R_B is increased, i.e., as the frequency of the magnetic field is decreased. In contrast, for the case of a rotating field, chain-like clusters are able to rotate as a whole without a significant resistance resulting from the magnetic interactions among the particles forming a cluster, as already pointed out in Fig. 4.8, which leads to a monotonic increase after $R_B \simeq 3$. The reason why the heating effect is decreased for the both cases with increased values of R_B in the region of $R_B \lesssim 3$ is that the frequency of the magnetic field is too large for chain-like clusters to follow the change in the direction of the magnetic field, where large viscous resistances arise for the chain-like clusters to rotate in this situation, giving rise to less active rotational motion of chain-like clusters. From these characteristics, as in Fig. 4.8, we also make a conclusion that a rotating magnetic field is significantly more suitable for producing the heat generation in a strongly interaction system of magnetic particles.

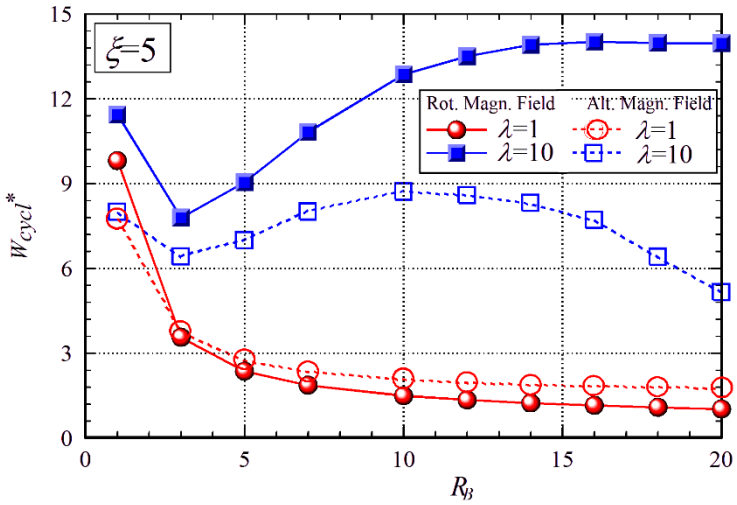

Fig. 4.9 Comparison of the results for a rotating and an alternating magnetic field with respect to the dependence of the heating effect on the frequency of the magnetic field for the case of the magnetic field strength ξ=5. For the case of a rotating field, chain-like clusters are able to rotate as a whole without a significant resistance resulting from the magnetic interactions among the particles forming a cluster, which leads to a large and monotonic increase after $R_B \simeq 3$.

4.6 Conclusion

In the present study, we have investigated the relationship between the aggregate structures and the heating effect in a rotating magnetic field by means of Brownian dynamics simulations. The main factors characterizing the present phenomenon are the viscous friction force arising from the strength of a rotating magnetic field, the strength of the magnetic particle-particle interaction and the random Brownian force. The main results obtained are summarized in the following. In the situation of a weak magnetic particle-particle interaction, magnetic particles do not aggregate to form significant clusters, and the single particles do not give rise to a sufficiently large heating effect. In the situation where chain-like clusters are predominantly formed in the system and where the aggregates exhibit a larger viscous resistance during their rotation, a significantly large heating effect may be obtained as a result. If the magnetic particle-particle interaction is sufficiently strong then particles may form ring-like clusters. The magnetic moments of the constituent particles in a ring-like cluster are not able to respond sufficiently to a change in the field direction due to the strong attractive forces between the constituent particles. This implies that stable ring-like clusters are not able to provide a

large heating effect in a rotating magnetic field. From these characteristics, we may conclude that if the effect of the applied magnetic field is relatively more dominant than the magnetic particle-particle interaction in the situation where the magnetic interaction surpasses the effect of the thermal motion, then linear chain-like clusters are predominately formed in the system that give rise to a significantly larger heating effect than single particles. From the comparison of the present results with the previous ones for an alternating magnetic field, we have obtained a significant difference in the heat generation performance. In the case of a rotating magnetic field, chain-like clusters are able to rotate as a whole without a significant resistance resulting from the magnetic interactions among the particles forming a cluster, which yields a sufficiently large heating effect even in the situation of the magnetic particle-particle interaction being more dominant than the magnetic particle-field interaction. We therefore make a conclusion that a rotating magnetic field is significantly more suitable for producing the heat generation in a strongly interaction system of magnetic particles than an alternating magnetic field.

References

[1] X. Yao, K. Sabyrov, T. Klein, R. L. Penn and T. S. Wiedmann, Evaluation of magnetic heating of asymmetric magnetite particles J. Magn. Magn. Mater., 381, (2015), 21-27.

[2] B. B. Lahiri, S. Ranoo, A. W. Zaibudeen and J. Philip, Magnetic hyperthermia in magnetic nanoemulsions: Effects of polydispersity, particle concentration and medium viscosity, J. Magn. Magn. Mater., 441, (2017), 310-327.

[3] Z. Zhao and C. Rinaldi, Magnetization dynamics and energy dissipation of interacting magnetic nanoparticles in alternating magnetic fields with and without a static bias field, J. Phys. Chem. C, 122, (2018), 21018-2130.

[4] S. Suzuki and A. Satoh, Influence of the cluster formation in a magnetic particle suspension on heat production effect in an alternating magnetic field, Colloid Poly. Sci., 297, (2019), 1265-1273.

[5] P. Cantillon-Murphy, L. L. Wald, E. Adalsteinsson and M. Zahn, Heating in the MRI environment due to superparamagnetic fluid suspensions in a rotating magnetic field, J. Magn. Magn. Mater., 322, (2010), 727-733.

[6] M. Bekovic, M. Trbusic, M. Trlep, M. Jesenik and A. Malter, Magnetic Fluids' Heating Power Exposed to a High-Frequency Rotating Magnetic Field, Adv. Mater. Sci. Eng., 2018, (2018), DOI:10.1155/2018/6143607.

[7] A. F. Abu-Bakr and A. Yu. Zubarev, Hyperthermia in a system of interacting ferromagnetic particles under rotating magnetic field, J. Magn. Magn. Mater., 477, (2019), 404-407.

[8] R. E. Rosensweig, Heating magnetic fluid with alternating magnetic field, J. Magn. Magn. Mater., 252, (2002), 370-374.

[9] I. M. Obaidat, B. Issa and Y. Haik, Magnetic properties of magnetic nanoparticles for efficient hyperthermia, Nanomaterials, 5, (2015), 63-89.

[10] C. S. S. R. Kumar and F. Mohammad, Magnetic nanomaterials for hyperthermia-based therapy and controlled drug delivery, Advan. Drug Delivery Rev., 63, (2011), 789-808.

[11] C. Guibert, V. Dupuis, V. Peyre and J. Fresnais, Hyperthermia of magnetic nanoparticles: Experimental study of the role of aggregation, J. Phys. Chem. C, 119, (2015), 28148–28154.

[12] D. Serantes, D. Baldomir, C. Martinez-Boubeta, K. Simeonidis, M. Angelakeris, E. Natividad, M. Castro, A. Mediano, D.-X. Chen, A. Sanchez, L. I. Balcells and B. Martínez, Influence of dipolar interactions on hyperthermia properties of ferromagnetic particles, J. Appl. Phys., 108, (2010), 073918.

[13] M. P. Allen and D. J. Tildesley, *Computer Simulation of Liquids* (Clarendon Press, Oxford, 1987).

[14] A. Satoh, A., R. W. Chantrell, S. Kamiyama and G. N. Coverdale, Potential curves and orientational distributions of magnetic moments of chainlike clusters composed of secondary particles, J. Magn. Magn., Mater. 154, (1996), 183-192.

[15] D. J. Adams, E. M. Adams and G. J. Hills, The computer simulation of polar liquids, Mol. Phys., 38, (1979), 387-400.

[16] P. D. Duncan and P. J. Camp, Structure and dynamics in a monolayer of dipolar spheres, J. Chem. Phys., 121, (2004), 11322-11331.

[17] A. Satoh, *Modeling of Magnetic Particle Suspensions for Simulations* (CRC Press, Boca Raton, 2017).

Chapter 5 The behavior and heating effects of rod-like magnetic particles in an alternating and a rotating magnetic field

5.1 Introduction

Magnetic hyperthermia is one of the medical therapies for killing tumor or cancer cells by means of a heating effect that is generated by the interactions between magnetic particles and an applied magnetic field [1-3]. To this end, an alternating or a rotating applied magnetic field is ordinarily employed instead of a typical uniform time-independent magnetic field.

In a previous study [4], we have addressed the behavior of a magnetic spherical particle suspension in response to an alternating magnetic field, and clarified that chain-like clusters effectively function to give rise to a significant heat generation effect under certain situations. Subsequently we expanded this study to the case of a rotating magnetic field in order to clarify the dependence of the aggregate structure and the heat generation effect on the type of a time-dependent applied magnetic field [5]. From this study, we clearly understand that a higher heating effect is obtained by means of a rotating magnetic field rather than an alternating magnetic field in the situation where stable aggregate structures are formed in the system.

In the Brownian relaxation mode, a larger viscous friction may be expected to give rise to a larger heat generation performance, and thus as a simulation study at the next stage it is naturally required to address a suspension of magnetic particles with a more general geometrical shape such as rod-like, disk-like and cube-like shape. Modern synthesis technology enables the generation of these magnetic particles, for example, rod-like particles [6-8], disk-like particles [9,10] and cubic particles [11-14].

From this background, in the present study we address a suspension composed of magnetic rod-like particles in order to elucidate the behavior of the aggregate structure and the heat generation effect in the two cases of an applied magnetic field, an alternating and a rotating applied magnetic field. To this end, as in the previous studies, we have employed the Brownian dynamics method as a particle-based simulation technique, which enables us to discuss the influence of the dynamic behavior of the aggregate structure of the particles on the heat generation effect.

5.2 Modelling of magnetic rod-like particles and time-dependent applied magnetic fields

We employ a spherocylinder particle shown in Fig. 5.1 as a model of rod-like particles. The rod-like particle has a magnetic moment $\boldsymbol{m}$ oriented in the major axis direction at the particle centre. The diameter and length of the rod-like particle are denoted by d and l, which give rise to the particle aspect ratio $r_p(=l/d)$. In order to recognize the magnetic moment direction in snapshots, the hemisphere in the magnetic moment direction is colored by red (dark) and the opposite hemisphere is colored by blue (light), as shown in Fig. 5.1. Moreover, it is assumed that the surface of each particle is covered by a uniform steric layer with thickness δ for generating a steric repulsion in order to prevent them from a physically unreasonable overlap.

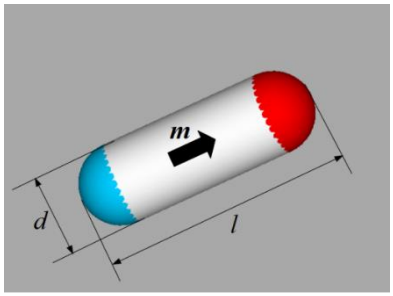

Fig. 5.1 Particle model of a magnetic rod-like particle. It is idealized as a spherocylinder with a magnetic dipole moment in the major axis direction at the particle centre.

As already mentioned, in the present study we employ two types of time-dependent applied magnetic fields, specifically, an alternating magnetic field and a rotating magnetic field. An alternating magnetic field $\boldsymbol{H}_{alt}(t)$ is applied in the x-direction, expressed as

$$\boldsymbol{H}_{alt}(t) = H_0 \sin(\omega_H t)\, \boldsymbol{i}_x \tag{5.1}$$

Similarly, a rotating magnetic field $\boldsymbol{H}_{rot}(t)$ is applied in the xy-plane, expressed as

$$\boldsymbol{H}_{rot}(t) = H_0 \left\{ \cos(\omega_H t)\, \boldsymbol{i}_x + \sin(\omega_H t)\, \boldsymbol{i}_y \right\} \tag{5.2}$$

In these expressions, H_0 and ω_H are the magnitude and the angular velocity of the applied magnetic field, respectively, and $\boldsymbol{i}_x$ and $\boldsymbol{i}_y$ are the unit vectors in the x- and y- direction, respectively.

5.3 Brownian dynamics

The Brownian dynamics simulation method for axisymmetric particles such as rod-like and disk-like particles has already been described sufficiently in previous papers and textbook [15-17], and therefore we here merely describe only the key expressions relevant for the current investigation.

In the case of the axisymmetric particle, the equation of motion can be decomposed into the translational motion in the particle axis direction and in the direction normal to the particle axis. The particle position $\boldsymbol{r}(t)$ at time t is described as

$$\boldsymbol{r}_{\parallel}(t+\Delta t)=\boldsymbol{r}_{\parallel}(t)+\frac{1}{k_BT}D_{\parallel}^{T}\boldsymbol{F}_{\parallel}^{P}(t)\Delta t+\Delta r_{\parallel}^{B}\boldsymbol{e}(t) \tag{5.3}$$

$$\boldsymbol{r}_{\perp}(t+\Delta t)=\boldsymbol{r}_{\perp}(t)+\frac{1}{k_BT}D_{\perp}^{T}\boldsymbol{F}_{\perp}^{P}(t)\Delta t+\Delta r_{\perp 1}^{B}\boldsymbol{e}_{\perp 1}(t)+\Delta r_{\perp 2}^{B}\boldsymbol{e}_{\perp 2}(t) \tag{5.4}$$

The particle direction $\boldsymbol{n}$ (=$\boldsymbol{m}/m=\boldsymbol{m}/|\boldsymbol{m}|$) obeys the following equation of motion

$$\boldsymbol{n}(t+\Delta t)=\boldsymbol{n}(t)+\frac{1}{k_BT}D_{\perp}^{R}\boldsymbol{T}_{\perp}^{P}(t)\times\boldsymbol{n}\Delta t+\Delta\phi_{\perp 1}^{B}\boldsymbol{e}_{\perp 1}(t)+\Delta\phi_{\perp 2}^{B}\boldsymbol{e}_{\perp 2}(t) \tag{5.5}$$

In these equations the notations have the following meanings. The quantities with subscripts $\perp$ and $||$ represent components normal and parallel to the particle axis, respectively, $\boldsymbol{F}^{p}$ and $\boldsymbol{T}^{p}$ are the forces and torques acting on the particle of interest, Δt is the time interval, D^{T} and D^{R} are the diffusion coefficients of the spherocylinder particle for the translational and rotational motion [16,17], respectively, $\boldsymbol{e}_{\perp 1}$ and $\boldsymbol{e}_{\perp 2}$ are the unit vectors normal to each other in the plane normal to the particle axis, T is the liquid temperature, and k_B is Boltzmann's constant. It is noted that the force $\boldsymbol{F}^{p}$ and torque $\boldsymbol{T}^{p}$ are evaluated from sum of the magnetic and steric repulsive forces and torques exerted by the other particles and an applied magnetic field. Moreover, $\Delta r_{||}^{B}$, $\Delta r_{\perp 1}^{B}$ and $\Delta r_{\perp 2}^{B}$ are the random displacements inducing the translational Brownian motion and have the stochastic characteristics that imply a relationship with the translational diffusion coefficients [16,17]. Similarly, $\Delta\phi_{\perp 1}^{B}$ and $\Delta\phi_{\perp 2}^{B}$ are the random displacements inducing the rotational Brownian motion and have the stochastic characteristics that imply a relationship with the rotational diffusion coefficients [31,32]. For reference, the diffusion coefficients will be expressed in Appendix, where the non-dimensional expressions are shown to be dependent on the particle aspect ratio r_p.

5.4 Heating effect

As already mentioned, magnetic particles sufficiently larger than around 10 nm tend to give rise to a heat generation due to the Brownian relaxation mechanism. From the thermodynamic theory, it is seen that the work dW done on the system by an increase in the magnetic flux density, $d\boldsymbol{B}$, in a magnetic field $\boldsymbol{H}$ gives rise to an increase in the internal energy of the system, dU, that is, dW=

$\boldsymbol{H}\cdot d\boldsymbol{B}=dU$, where an adiabatic process has been assumed. By taking into account the expression of $\boldsymbol{B}=\mu_0(\boldsymbol{H}+\boldsymbol{M})$, where $\boldsymbol{M}$ is the magnetization and μ_0 is the permeability of free space, the work per period of an applied magnetic field is expressed as

$$\begin{aligned} W_{cycl}^{total} &= \oint \boldsymbol{H}\cdot d\boldsymbol{B} = \mu_0 \oint \boldsymbol{H}\cdot d(\boldsymbol{H}+\boldsymbol{M}) = \left[\mu_0 \boldsymbol{H}\cdot(\boldsymbol{H}+\boldsymbol{M})\right]_{cycl} - \mu_0 \oint (\boldsymbol{H}+\boldsymbol{M})\cdot d\boldsymbol{H} \\ &= -\mu_0\left[(1/2)\boldsymbol{H}\cdot\boldsymbol{H}\right]_{cycl} - \mu_0 \oint \boldsymbol{M}\cdot d\boldsymbol{H} = -\mu_0 \oint \boldsymbol{M}\cdot d\boldsymbol{H} \end{aligned} \tag{5.6}$$

This relationship has already been shown and formalized in a pioneer work by R. E. Rosensweig [13]. In Eq. (5.6) the magnetic field $\boldsymbol{H}$ is the time-dependent magnetic field, $\boldsymbol{H}=\boldsymbol{H}_{alt}$ or $\boldsymbol{H}=\boldsymbol{H}_{rot}$ in the present study. The magnetization $\boldsymbol{M}$ is a quantity per unit volume and therefore this quantity corresponds to $\boldsymbol{m}=m\boldsymbol{n}$ per particle. Hence, the heat generation per particle in one cycle is expressed as

$$W_{cycl} = -\mu_0 m H_0 \oint \left(\boldsymbol{n}\cdot d\left(\boldsymbol{H}/H_0\right)\right) \tag{5.7}$$

Equation (5.7) is normalized by thermal energy k_BT, expressed as

$$W_{cycl}^{\ *} = -\xi \oint \left(\boldsymbol{n}\cdot d\left(\boldsymbol{H}/H_0\right)\right) \tag{5.8}$$

In Eqs. (5.7) and (5.8), H_0 is the maximum value of a time dependent magnetic field $\boldsymbol{H}$, as already defined, and ξ is a non-dimensional parameter that implies the strength of the magnetic particle-field interaction, which will be shown in Eq. (5.9).

5.5 Parameters for simulations

Unless specifically noted, the present results were obtained by adoption of the following parameter values. The number of particles $N=216=6^3$, the volumetric function $\phi_V=0.001$, the time step $\Delta t^*(=\Delta t/(2\pi/\omega_H))=0.00001$, and the total simulation time $t_{total}^{\ *}(=t_{total}/(2\pi/\omega_H))=3000$, where data from the last 30% of the simulation time were used for the averaging procedure. The diameter of the particles $d^*=1.0$, the thickness of the steric layer $\delta^*(=\delta/d)=0.15$, the particle aspect ratio $r_p=3$, and the cutoff radius $r_{coff}^{\ *}(=r_{coff}/d)=8.0$ for evaluation of magnetic forces and torques. Using these parameters, we evaluate the dimensions of the simulation cell as $l_x^*=l^*_y=l_z^*=76.77$, where $l^*_x=l_x/d$, and so forth.

The present phenomenon is characterized by the four non-dimensional parameters, λ, ξ, λ_V and R_B as [31,32]

$$\lambda=\frac{\mu_0 m^2}{4\pi d^3 k_B T},\qquad \xi=\frac{\mu_0 m H_0}{k_B T},\qquad \lambda_V=\frac{\pi n_s d^2}{2},\qquad R_B=\frac{k_B T}{3\pi\eta d^3}\cdot\frac{2\pi}{\omega_H} \tag{5.9}$$

in which λ is the strength of the magnetic particle-particle interaction, ξ is the strength of the magnetic particle-field interaction and λ_V is the strength of the repulsive force due to the overlap of

the steric layers relative to thermal motion. Moreover, R_B is the strength of the random force relative to the viscous force. In these expressions, η is the viscosity of the base liquid, and n_s is the number of surfactant molecules per unit surface of magnetic particles.

If R_B is much smaller than unity, i.e., if the frequency is significantly high, then viscous friction forces become the dominant factor for governing the particle motion, and therefore the magnetic rod-like particles may not be able to follow a change in the magnetic field direction due to large viscous forces. On the other hand, if R_B is much smaller than unity, the random force, i.e. Brownian motion, becomes dominant over the viscous forces, and thus the magnetic rod-like particles may change their direction in response to the applied magnetic field in the case of sufficiently strong interactions between the magnetic moment and the applied magnetic field. In the latter case, the relationship between the magnitudes of λ and ξ determines the behavior of the magnetic rod-like particles in a time-dependent applied magnetic field. In the present study, these non-dimensional parameters λ, ξ, R_B and λ_V are set within the wide range of λ=1~100, ξ=0~100, R_B =0.1~3 and λ_V=150.

5.6 Results and discussion

5.6.1 For the case of the alternating magnetic field

5.6.1.1 Time variation change in aggregate structures of particles

In Section 5.6.1 we discuss results for the case of an alternating magnetic field and firstly consider the characteristics of aggregate structures of rod-like particles. It is noted that, although the present simulations were performed for a 3D system, snapshots that are viewed from the *z*-axis direction will be shown in order to illustrate aggregate structures more straightforwardly.

Before proceeding to a discussion regarding the time change in aggregate structures, we show the influence of magnetic particle-particle interactions on the cluster formation for the case of a low frequency region of R_B=3, where an alternating magnetic field is applied along the *x*-axis direction. Figure 5.2 shows snapshots for three different cases of the magnetic particle-particle interaction strength, λ=1, 60 and 100, which were obtained at the time of maximum field strength in the *x*-axis direction, i.e., $|\boldsymbol{H}|=H_0$ with the particle-field interaction strength ξ=80.

In the case of a weak magnetic particle-particle interaction strength λ=1, shown in Fig. 5.2 (a), the particles do not aggregate to form clusters and thus move as single particles. This is because the magnetic interaction strength is not sufficient for the formation of clusters for λ=1. Moreover, since viscous forces are sufficiently low for the rotational motion of the particles in the low frequency R_B=3, the rod-like particles are able to respond to a change in the field direction. This is clearly shown in the snapshot where all the rod-like particles strongly tend to incline in the magnetic field direction (or *x*-axis direction). In the case of λ=60, it is evidently seen that relatively thick chain-like clusters are formed along the magnetic field direction and each constituent particle of the rod-like clusters inclines along the field direction. In contrast, in the case of a further increase in interaction strength λ=100, the rod-like particles exhibit completely different clusters, that is, densely-packed clusters are formed, rather than chain-like clusters, and the neighboring rod-like particles constituting a cluster orient in the opposite directions to each other, which gives rise to a lower magnetic interaction energy. Although the values of λ=60 and λ=100 are sufficiently strong for the cluster formation, why do these completely different aggregate structures appear? It is the magnetic field strength that mainly governs the behavior of the rod-like particles, that is, these different structures arise due to the relative magnitudes between the magnetic particle-particle (λ) and particle-field (ξ) interaction strengths. In the case of λ=60, the field strength is still one of the governing factors for the particle motion in the situation of ξ=80, and therefore the rod-like particles are able to form clusters and each particle strongly tends to incline in the field direction, which leads to linear thick chain-like clusters with the constituting particles aligning to the field direction, shown in Fig. 5.2(b). In contrast, in the case of λ=100, the magnetic particle-particle interaction is significantly stronger than the magnetic particle-field interaction, and thus in this situation the former factor has a main influence on the cluster formation. If the rod-like particles have a dipole

moment along the major axis direction at the particle centre, in the case of a sufficiently strong interaction, two particles aggregate to form a raft-like cluster along the minor axis direction. This cluster unit is repeated and expanded in the 3D system to form the densely-compacted aggregate structures shown in Fig. 5.2(c). From now on, we focus on results for the case of λ=60 unless specifically noted.

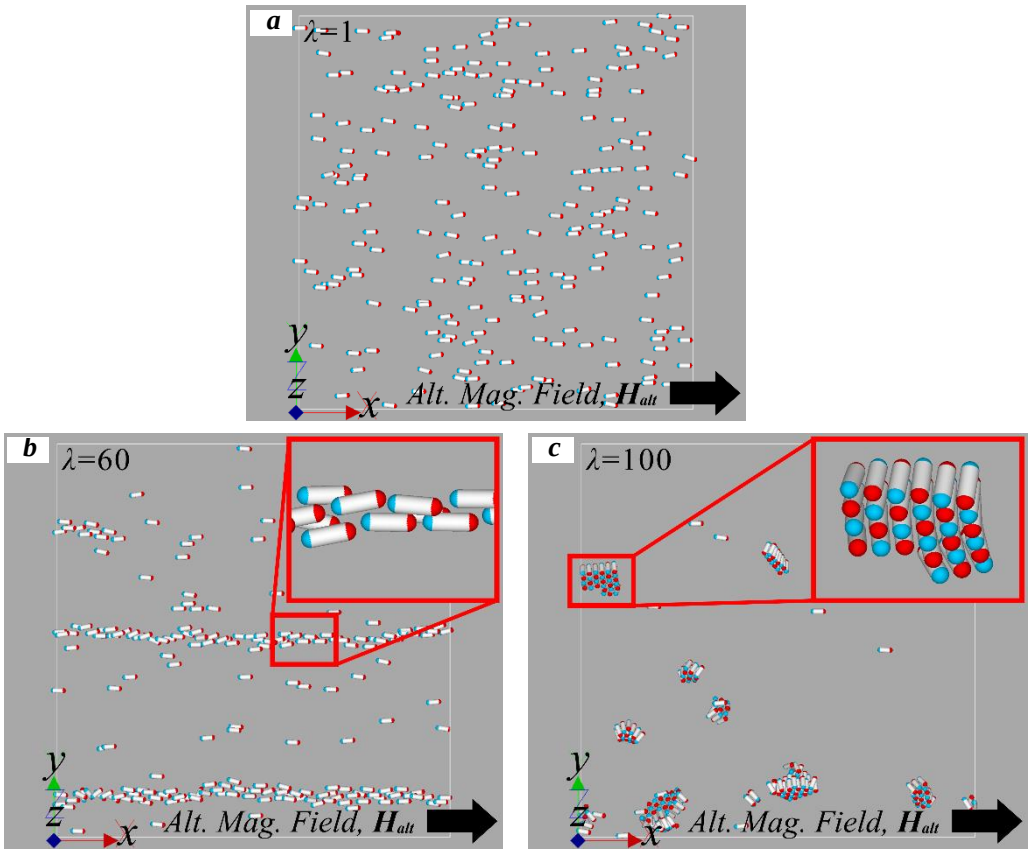

Fig. 5.2 Aggregate structures for ξ=80 and R_B =3: (a) for λ=1, (b) for λ=60 and (c) for λ=100. In the case of an intermediate magnetic particle-particle interaction strength λ=60, relatively thick chain-like clusters are formed along the magnetic field direction and each rod-like particle inclines along the field direction.

Figure 5.3 shows the time variation in the chain-like clusters for the case of a strong magnetic field ξ=80 with a low frequency of R_B=3, where three different snapshots are shown at the phase angles, (a) $\theta=\pi$, (b) $\theta=6\pi/5$ and (c) $\theta=4\pi/3$. The snapshot in Fig. 5.2(b) should be referred to for the case of $\theta=\pi/2$. As already shown above, since rod-like particles form relatively thick chain-like clusters, as shown in Fig. 5.2(b), we here focus on the behavior of the thick chain-like clusters mainly at the phase angle around $\theta=\pi$, where the alternating magnetic field switches direction from the positive toward the negative x-axis direction. At the phase angle of $\theta=\pi/2$, shown Fig. 5.2(b), the magnetic field strength attains the maximum value, and thus the thick chain-like clusters strongly tend to align to the field direction (x-direction). At the larger phase angle of $\theta=\pi$, the thick chain-like cluster starts to become unstable since the mechanism for keeping linear chain-like cluster formation disappears in the absence of an external magnetic field. At a later phase of $\theta=6\pi/5$, it seems that the raft-like cluster is largely formed and at the phase angle of $\theta=4\pi/3$ each particle has completed the reversal motion to align to the field direction (the negative x-direction). It is reasonable that raft-like clusters shown in Fig. 5.3(b) are preferred as intermediate cluster formation from an energy point of view. Since viscous friction forces are not sufficiently strong in the case of R_B=3, each particle promptly changes the orientation in order to follow the change in the magnetic field direction, which leads to the reformation of stable thick chain-like cluster inclining in the reverse direction, shown in Fig. 5.3(c).

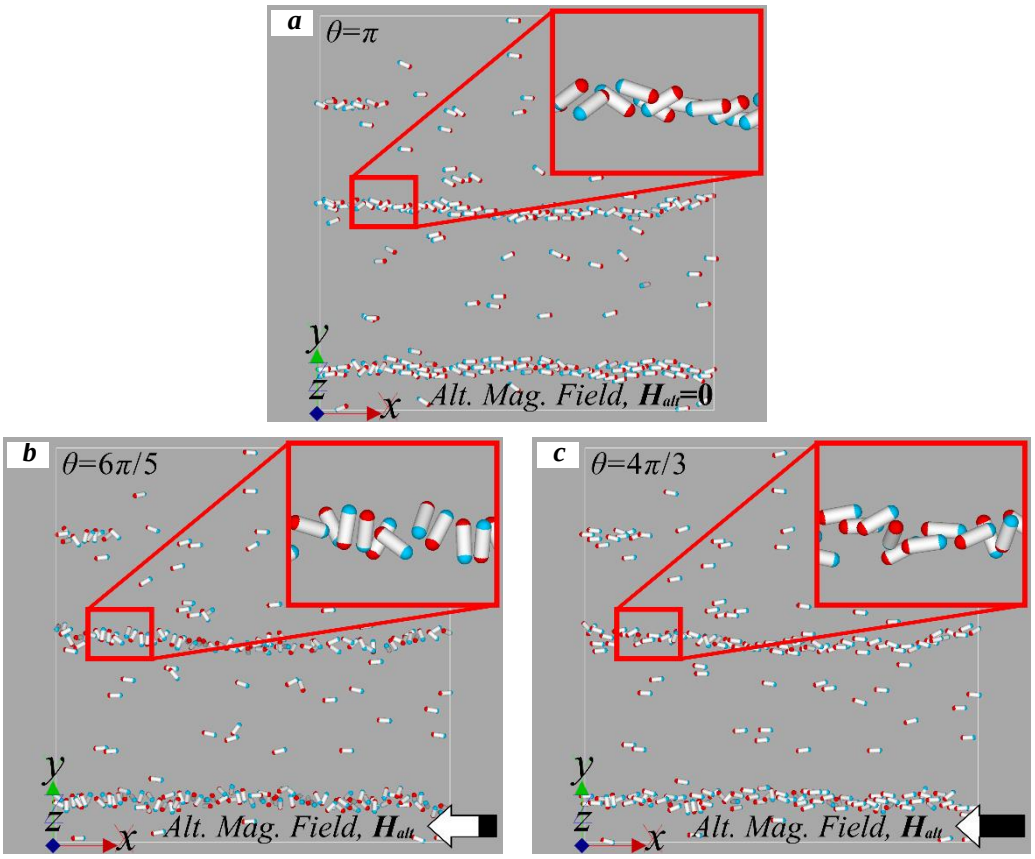

Fig. 5.3 Variation in the aggregate structures for ξ=80, R_B =3 and λ=60: (a) at $\theta=\pi$, (b) at $\theta=6\pi/5$ and (c) at $\theta=4\pi/3$. The snapshot in Fig. 5.2(b) should be referred to for the case of $\theta=\pi/2$. Since the viscous friction forces are not sufficiently strong in the case of R_B=3, each particle promptly changes the orientation in order to follow the change in the magnetic field direction, through the intermediate formation of raft-like clusters.

Figure 5.4 shows the influence of the frequency of the magnetic field, R_B, on the behavior of the rod-like particles for the case of λ=60 and ξ=80, where two different snapshots are shown for R_B=0.1 and R_B=0.5. The snapshot in Fig. 5.2(b) should be referred to for the case of R_B=3. It is noted that all the snapshots were obtained at the phase angle of $\theta=\pi/2$ and also that a smaller value of R_B corresponds to a larger frequency of the alternating magnetic field. In the case of a larger frequency of R_B=0.1, shown in Fig. 5.4(a), many short raft-like clusters are observed to be formed and these clusters do not follow the change in the magnetic field direction, rather tend to incline in various directions. The reason why only short raft-like clusters are formed but do not grow to form densely-packed clusters as in Fig. 5.2(c) is that the viscous friction forces are significantly large for the translational and rotational motion of rod-like particles, and therefore they are not able to

perform the translational motion to join the other raft-like clusters: a requirement for significant growth of structures, which results in the formation of many small raft-like clusters located separately from each other. Moreover, in the case of large viscous friction forces, they are not restricted to the field direction and exhibit a preference for the formation of small raft-like clusters, where the neighboring particles internal to a cluster incline in the opposite directions to each other, giving rise to a lower magnetic interaction energy. In contrast, for the case of an intermediate frequency of R_B=0.5, short raft-like cluster are not formed, but instead rod-like particles tend to individually rotate in order to follow the change in the magnetic field direction. This may be explained as follows. In the case of R_B=0.5, viscous friction forces are small enough that the particles are able to follow the change in the field direction, but sufficiently large to inhibit the translational motion required to join the other clusters. Hence, the rod-like particles tend to rotate due to the interaction with the applied magnetic field while remaining essentially fixed at their original position. Since the rod-like particles orientate in the field direction, in this situation, the neighboring particles are exerted by a repulsive magnetic interaction, which leads to the independent rotational motion of the rod-like particles, as shown in Fig. 5.4(b). For the case of a lower frequency of R_B=3, shown in Fig. 5.2(b), rod-like particles have sufficient time for the translational motion and thus aggregate to form linear thick chain-like clusters. As already pointed out, in this situation, the constituent particles are able to respond to the change in the field direction while remaining at their specific site within a cluster, with the linear chain-like cluster formation maintained during the process.

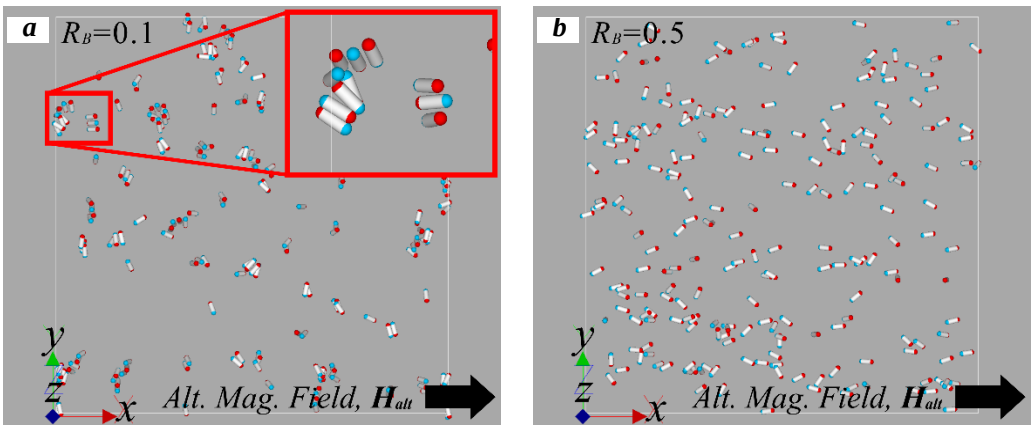

Fig. 5.4 Influence of the frequency of the magnetic field, R_B, on the aggregate structures for the case of λ=60 and ξ=80: (a) R_B=0.1 and (b) R_B=0.5. Magnetic rod-like particles tend to aggregate to form linear thick chain-like clusters from short raft-like clusters with increasing values of R_B or with smaller values of the frequency of the alternating magnetic field.

5.6.1.2 Hysteresis loops

In the previous section we have qualitatively discussed the behavior of the rod-like particles in the alternating magnetic field, including the different regimes of the aggregate structures. In this section, we focus on hysteresis loops that arise from a delay of the magnetic moment (rod-like particle) relative to the change in the strength and direction of the applied magnetic field. The hysteresis loops are directly used for discussing a heat generation effect.

Figure 5.5 shows the dependence of hysteresis curves (or loops) on the frequency of the magnetic field for the case of λ=60 and ξ=80, where results for three cases of the frequency, R_B＝0.1, 0.5 and 3 are shown for comparison. The ordinate is the mean value of the *x*-components of the magnetic moments which were obtained by averaging the magnetic moments of the particle in the system at each phase angle. It is noted that a larger area enclosed by a loop gives rise to a more significant heat generation effect, which will be discussed in Section 5.6.3.

In the case of R_B＝0.1, the hysteresis loop is significantly different from those for the cases of R_B＝0.5 and R_B＝3. That is, the maximum value of $\langle n_x \rangle$ does not reach unity, which implies that the rod-like particles are not able to significantly follow the change in the magnetic field strength and direction. This is quite understandable because in this case, as shown in Fig. 5.4(a), short raft-like clusters incline in various directions and do not incline in the magnetic field direction. The appearance of the maximum value $\langle n_x \rangle \simeq 0.33$ at around $h_x^* \simeq 0.4$ during the path from h_x^*=1 to h_x^*=0 is due to a large delay of the relaxation of the magnetic moment (rod-like particle) under a significant influence of large viscous friction forces.

In the case of R_B =0.5, the hysteresis loop becomes significantly larger than that for the previous case of R_B=0.1. One characteristic point is that the rod-like particles remain inclining in the opposite direction even at the time when the applied magnetic field changes direction toward the positive *x*-axis direction and they promptly start to rotate since around h_x^*=0.7, approaching $\langle n_x \rangle$ =1 at h_x^*=1. This may be explained as follows. In this case, relatively large viscous friction forces act on the rod-like particles, and therefore a sufficiently large magnetic field strength is required in order to trigger the rotational motion of rod-like particles. In other words, we understand that this threshold magnetic field strength is around $h_x^* \simeq 0.7$. Another characteristic point is that the maximum value $\langle n_x \rangle$ =1 appears at around $h_x^* \simeq 0.6$ during the path from h_x^*=1 to h_x^*=0. This delay is due to the same mechanism that has already been described for the previous case of R_B =0.1.

In contrast, for the case of R_B=3, the hysteresis loop gives rise to a significantly smaller enclosed area in comparison with that for R_B=0.5, although we initially expected that a large hysteresis area could be obtained due to the linear chain-like cluster formation, which may lead to a large delay in the response to the time-varying applied magnetic field. The reason for this smaller enclosed area may be explained as follows. The formation of linear chain-like clusters certainly tends to delay the reorientation of the constituent particles in the alternating magnetic field, which

should provide a large hysteresis loop. However, the value of R_B=3 corresponds to a low frequency region of the alternating magnetic field, and therefore the constituting particles are able to follow the change in the magnetic field more promptly in the case of lower viscous friction forces, even in the case where the magnetic interactions acting between constituent particles function to suppress the reorientation of each particle. This consideration may be reinforced by the characteristic of the hysteresis loop that the curve starts to steeply increase since $h_x^* \simeq 0$ when the magnetic field is switched to the positive x-direction, which is significantly in contrast to the curve for R_B=0.5.

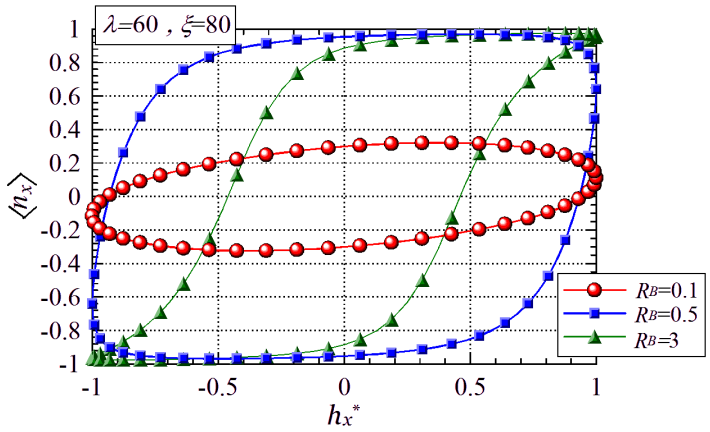

Fig. 5.5 Dependence of hysteresis loops on the frequency of the magnetic field for the case of λ=60 and ξ=80, where results for three cases of the frequency, R_B＝0.1, 0.5 and 3 are shown for comparison. In the case of R_B =0.5, the hysteresis loop becomes significantly larger than that for the other cases of R_B =0.1 and R_B =3. This is because relatively large viscous friction forces act on the rod-like particles, and therefore a sufficiently large magnetic field strength is required in order to trigger the rotational motion of rod-like particles.

We next discuss the dependence of the hysteresis loops on the magnetic particle-particle interaction strength λ. Figure 5.6 show results for the hysteresis loops for the case of R_B=3 and ξ=80, where the two cases of λ=1 and 60 are shown for comparison. It is noted that the value of λ=60 is sufficient for cluster formation, as shown in Fig. 5.2(b), whereas no clusters appear for the case of λ=1, as shown in Fig. 5.2(a). It is seen that the cluster formation in the case of λ=60 gives rise to a larger loop than the weakly interacting case of λ=1 where no clusters are formed. As already pointed out above, the rod-like particles can rapidly respond to the change in the alternating magnetic field in the case of smaller viscous friction forces for R_B=3. A significant differently characteristic between these two loops appears in the relaxation motion of the rod-like particles in the path from h_x^*=0 to 1 (or from h_x^*=0 to −1). That is, the curve for λ=1 increases more steeply than that for λ=60, in other words, the rod-like particles reorient more rapidly to follow the change in the magnetic field in the case of λ=1. This may be explained as follows. After the magnetic field moves into the positive x-direction at h_x^*=0, the rod-like particles rapidly start to incline in the field direction, which leads to a steep increase since h_x^*=0 in the path toward h_x^*=1 for both the cases of λ=1 and 60. However, the magnetic interactions between the constituent particles forming a chain-like cluster significantly inhibits the rotation of each constituent particle following the magnetic field change, which leads to a gentler slope than for λ=1 as shown in Fig. 5.6.

From the results shown in Figs. 5.5 and 5.6, we understand that the rapid rotational motion of rod-like particles is mainly dependent on the frequency of the alternating applied magnetic field, and the second governing factors are the magnetic particle-particle interaction strength and the magnetic field strength.

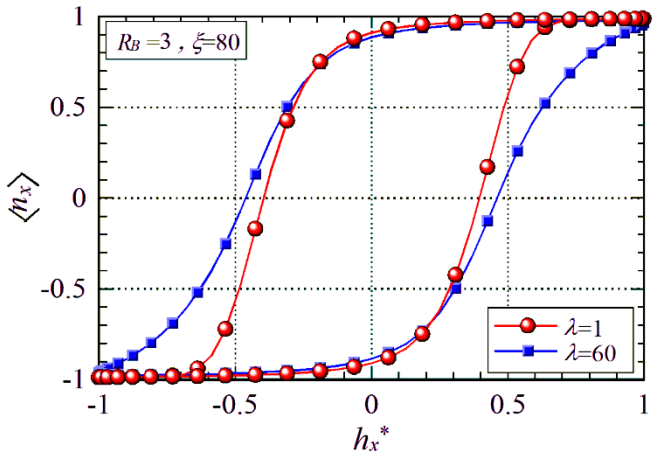

Fig. 5.6 Hysteresis loops for the case of R_B=3 and ξ=80, where the two cases of λ=1 and 60 are shown for comparison. It is seen that the cluster formation in the case of λ=60 gives rise to a larger loop than no cluster formation in the case of λ=1.

5.6.2 Time variation in aggregate structures for the case of the rotating magnetic field

In this section, we investigate the effects of a rotating magnetic field on the behavior of magnetic rod-like particles. As already described, a magnetic field is rotated about the *z*-axis in the anticlockwise direction.

Figure 5.7 shows the effect of magnetic particle-particle interactions on the cluster formation for the case of a low frequency of R_B=3 and a strong applied magnetic field of ξ=80, where three cases of the magnetic interactions λ=1, 60 and 100 are shown for comparison. These snapshots were obtained at the phase angle of θ=0, when the rotating magnetic field aligns to the *x*-axis direction. In the case of λ=1, since the magnetic particle-particle interaction strength is sufficiently weak, the rod-like particles perform rotational motion individually without the cluster formation and are able to follow the change in the field direction, thus inclining in the *x*-axis direction (or the magnetic field direction). In the case of λ=60, only several small clusters comprising three or four particles are observed to be formed, which is significantly in contrast to the case of the alternating magnetic field, where linear thick chain-like clusters are formed along the field direction and keep these linear formation during the change in the direction and strength of the alternating magnetic field. The above-mentioned small clusters have the following characteristics regarding the aggregate internal structure. If the two magnetic rod-like particles or the two magnetic moments approximately incline in the same direction, a staggered configuration is preferred as a cluster, where the neighboring particle is located at an off-set position by around half the particle length along the major axis direction, leading to a lower magnetic interaction energy or an attractive force between the two particles. This cluster unit is repeated and expanded to form the linear thick chain-like clusters in Fig. 5.2(b). However, in the case of the rotating magnetic field, the rotational motion of the constituent particles functions to prevent this linear cluster formation following the field direction. We describe this situation in more detail in the following. As recognized in Fig. 5.7(b), the upper rod-like particle is necessarily located at an offset position along the major axis in the direction opposite to the magnetic field direction. In this configuration, even if the two rod-like particles rotate in the anticlockwise direction (the direction of rotation), the integrity of this cluster unit is maintained without dissociation during the rotational motion of each constituent particle. In the case of an increased magnetic interaction strength λ=100, shown in Fig. 5.7(c), this cluster unit is repeated and expanded in an oblique direction (or in the upper-left direction in Fig. 5.7(c)). This large linear cluster formation is expected to be maintained and will rotate to follow the rotation of the applied magnetic field in the low frequency region. Hence these linear clusters with offset internal structure will rotate as a whole body with a large phase delay to the rotating magnetic field, which can be clearly seen in Fig. 5.7(c). At relatively large frequencies, these linear clusters might be expected to repeatedly dissociate into several long clusters and re-associate into longer clusters, as shown in the previous study [17] for a magnetic spherical particle suspension. Another characteristic

point recognized from Fig. 5.7(c) is that the constituent rod-like particles exhibit a larger rotational delay for a longer cluster. The reason for this delay may be similar to that of the observed slow increase of the hysteresis loop for λ=60 in Fig. 5.6. That is, a longer and larger cluster is more significantly influenced by viscous friction forces in the rotational motion, which leads to a larger phase delay to the magnetic field in comparison with the rotational motion of single rod-like particles. Hence, the magnetic particle-particle interactions function to delay the rotational motion of each constituent particle in a linear cluster. Moreover, a noticeable point is that a larger magnetic field strength is required for the formation of stable larger clusters in a rotating magnetic field than in the alternating magnetic field, which becomes clearer by comparing Fig. 5.7(b) with Fig. 5.2(b) for the same case of λ=60. This may be due to the difference in the strength of steric repulsive forces; that is, in the rotational field case, steric repulsive forces more significantly appear through the overlap of the steric layer arising from the rotational motion of the constituent rod-like particles in a long cluster. In contrast, in the alternating magnetic field situation, significant steric repulsive forces appear only in a short period during the change in their direction from the negative to the positive *x*-direction or in the reverse case, which leads to the stability of the thick chain-like clusters for a smaller magnetic particle-particle interaction strength in comparison with the case of a rotating magnetic field.

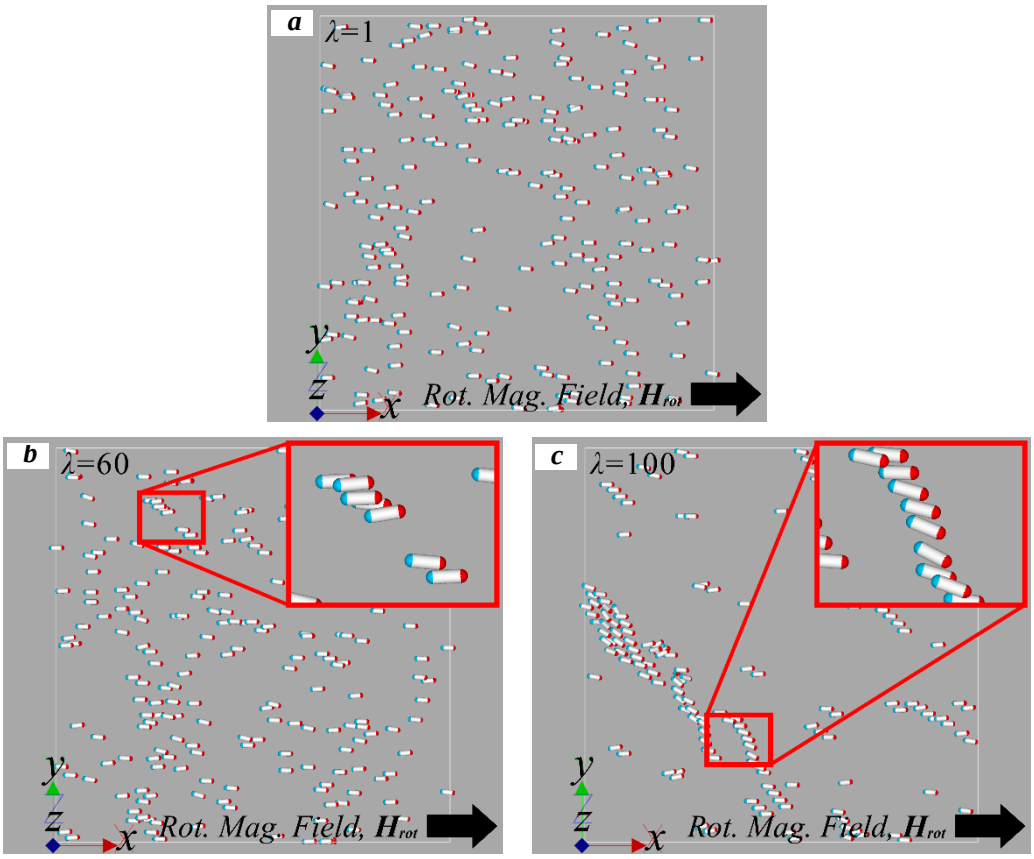

Fig. 5.7 Dependence of magnetic particle-particle interactions on the cluster formation for the case of a low frequency region of R_B=3 and a strong applied magnetic field of ξ=80, where three cases of the magnetic interactions λ=1, 60 and 100 are shown for comparison. As recognized in Fig. 5.7(c), linear and large clusters rotate as a whole body with a large delay to the rotating magnetic field.

We next discuss the dependence of the behavior of rod-like particles on the frequency of the rotating magnetic field, shown in Fig. 5.8 for the case of λ=100 and ξ=80, where two different snapshots are shown for R_B=0.1 and R_B=0.5. The snapshot shown in Fig. 5.7(c) should be referred to for the case of R_B=3. It is noted that all the snapshots were obtained at the phase angle of θ=0.

In the case of a high frequency region of R_B=0.1, shown in Fig. 5.8(a), several short raft-like clusters are formed and these clusters do not significantly respond to the rotation of the magnetic field, as in Fig. 5.4(a). This is because significantly larger viscous friction forces will act on the particles during the rotational motion, and therefore these short raft-like clusters are unable to rotate sufficiently rapidly to follow the rotation of the applied magnetic field. Even single particles incline in various directions and, do not align to the field direction. In the case of an intermediate

frequency of R_B=0.5, shown in Fig. 5.8(b), viscous friction forces are still large with respect to the rotational motion, and thus the single particles are able to rotate to follow the rotation of the magnetic field with a large delay, that is, the rod-like particles incline in the bottom-right direction. In the case of a low frequency of R_B=3, as already described above, viscous friction forces are not large for the rotational motion, and also magnetic particle-particle interaction forces are sufficiently strong for the cluster formation. Hence, the particles aggregate to form long clusters and these clusters rotate as a whole body to follow the rotation of the field with a large delay.

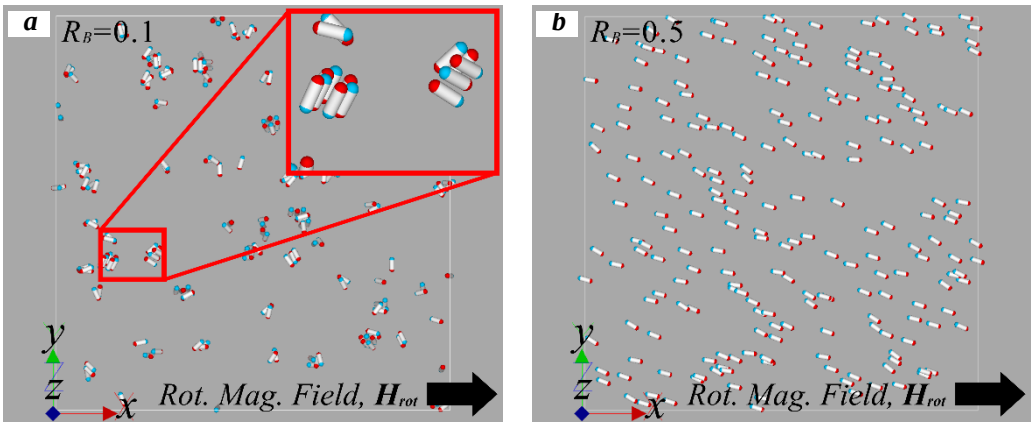

Fig. 5.8 Influence of the frequency of the magnetic field, R_m, on the aggregate structures for the case of λ=100 and ξ=80: (a) for R_B=0.1 and for (b) R_B=0.5. The snapshot shown in Fig. 5.7(c) should be referred to for the case of R_B=3. In the case of an intermediate frequency of R_B=0.5, shown in Fig. 5.8(b), viscous friction forces are still large with respect to the rotational motion, but the single particles are able to rotate to follow the rotation of the magnetic field with a large delay.

5.6.3 Comparison of results between the alternating and rotating magnetic fields

Finally we discuss the characteristics of the heat generation effect by comparing results between the alternating and rotating magnetic fields.

We first address the influence of the frequency of the magnetic field on the characteristics of the heating effect. Figure 5.9 shows these characteristics for the case of a weak magnetic interaction strength λ=1, where the results for both the magnetic fields are shown for ξ=40 and 80. It is noted that the value of λ=1 is too small for the formation of clusters and this is common for the alternating and the rotating applied magnetic field, that is, linear and raft-like clusters are not formed in the system. Moreover, a smaller value of R_B corresponds to a lower frequency of the time-dependent applied magnetic fields. The ordinate W_{cycl}^* in Fig. 5.9 is a quantity that is evaluated by integrating over one cycle of the alternating and the rotating magnetic field.

Several common characteristics of both the applied magnetic fields are recognized and are described as follows. In the limits of large and small of R_B, the heating effect tends to decrease and eventually disappear for both cases of the applied magnetic field. This is because large viscous forces act on rod-like particles and thus they cannot rotate for small R_B. For large R_B, rod-like particles can perform rotational motion with a slower rotational velocity for the case of significantly lower viscous friction forces. This slower rotational motion of rod-like particle gives a smaller contribution to the heat generation effect. We summarize the dependence of the heat generation effect on the frequency as follows. As the value of R_B increases from zero, i.e., as the frequency of the applied magnetic fields is decreased, rod-like particles begin to perform rotational motion to follow the magnetic fields, and this tendency becomes more significant with decreasing values of frequency (or increasing R_B values), giving rise to a larger heating effect. As the value of R_B further increases, the rod-like particles are able to follow the change in the magnetic field with slower speeds due to lower viscous friction forces, which leads to a decrease in the heating effect. The contrasting relationship between the magnetic torques and the viscous friction torques gives rise to maximum values of the heating effect in the intermediate region of the values of R_B for all the curves in Fig. 5.9.

For both alternating and rotational magnetic fields, the peak position yielding a maximum value is shifted toward to a larger value of R_B, with decreasing field, specifically, the peak position is shifted from $R_B \simeq 0.2$ for ξ=80 to $R_B \simeq 0.4$ for ξ=40 in the case of the rotating field and from $R_B \simeq 0.5$ for ξ=80 to $R_B \simeq 0.8$ for ξ=40 in the case of the alternating magnetic field. The reason for the shifting of the peak position may be explained as follows, for example, by focusing on the results for the alternating magnetic field. The threshold value of R_B, after which the rod-like particles can respond to a more slowly rotating magnetic field for smaller viscous friction forces, should determine the position yielding the maximum value. If the magnetic torque is larger or if the magnetic field is stronger, the rod-like particles can respond to the magnetic field from a larger frequency in the

intermediate region. This characteristic is certainly the reason for the shifting of the peak position. A similar argument is also valid for the rotating magnetic field case.

From Eq. (5.8), it is seen to be quite reasonable that a larger magnetic field gives rise to a larger heat generation effect for both the magnetic field variations, since the heat generation effect arises from the relaxation phenomenon through the magnetic interactions between rod-like particles and a time-dependent external magnetic field. An interesting observation is that the dependence on the frequency after R_B=0.4 is approximately the same for ξ=40 and 80 in the case of the rotating magnetic field, whereas it is completely different in the case of the alternating field. This is certainly due to the different characteristics in the motion of the rod-like particle in a time-varying applied magnetic field. In the region of $R_B \gtrsim 0.4$ for the rotating field, rod-like particles are able to follow the rotation of the magnetic field, albeit with a delay. Even if the applied magnetic field strength is different, the rod-like particles rotate with the approximately same rotational velocity with a different phase delay for the case of the same frequency, which gives rise to essentially the same heating as the case without cluster formation. In contrast, for the case of the alternating magnetic field, large viscous friction forces arise only during the short time when the rod-like particles switch their direction to follow the change in the magnetic field direction (i.e., at the phase angle θ =0 and π). In this switching motion, the rotational speed of rod-like particles is larger for a larger magnetic field strength. Moreover, continuous rotational motion of rod-like particles under the friction forces (torques) in the rotating field in the early stage of the intermediate region, $R_B \lesssim 0.2$, is able to contribute to the heat generation performance more significantly during a longer period than in the alternating field where heat generation arises during a much shorter period when rod-like particles switch their direction.

From these characteristics, we may understand that for the case of rod-like particles capable of responding rapidly to the field changes, a rotating magnetic field is significantly superior to an alternating field for obtaining a larger heat generation effect, whereas in the situation of rod-like particles rotating with a slower speed, which corresponds to a low frequency region, the alternating magnetic field is desirable for heat generation. The critical value of R_B for decision regarding which magnetic field should be employed is of course dependent on the magnetic field strength, as suggested in Fig. 5.9 as one example.

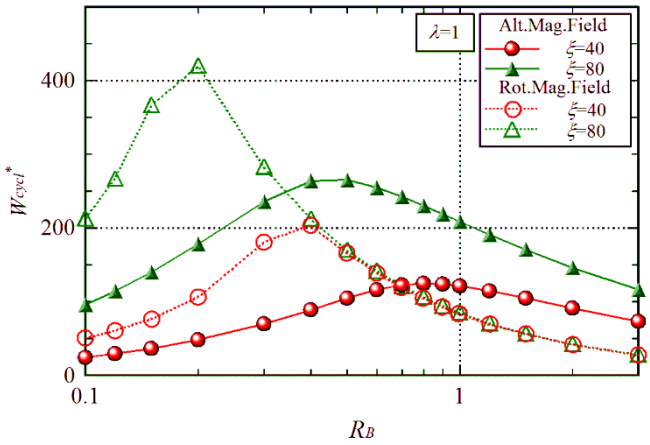

Fig. 5.9 Influence of the frequency of the magnetic field on the characteristics of the heating effect for the case of a weak magnetic interaction strength λ=1, where the results for two cases of the field strength are shown for ξ=40 and 80. As the value of R_B increases form zero, i.e., as the frequency of the applied magnetic fields is decreased, rod-like particles starts to perform the rotational motion to follow the change in the magnetic fields, and this tendency becomes more significant with decreasing values of the frequency (or, increasing R_B values), giving rise to a larger heating effect.

We next discuss how the cluster formation influences the heat generation effect. To this end, the case of a large applied magnetic field strength ξ=80 is focused on for investigating the characteristics of the heat generation. Figure 5.10 shows the influence of the magnetic particle-particle interaction strength λ on the heat generation, where results for the three different cases of magnetic interaction strengths are shown for λ=1, λ=60 and λ=100 for each applied magnetic field. The results for λ=1 are just for reference, since this value is not sufficient for the formation of clusters.

We first consider the results for the alternating magnetic field. It is seen that the curves for λ=1 and λ=60 exhibit the almost same characteristics but the curve for λ=100 is significantly different from those for the former two cases. As shown in Fig. 5.2(c), this is due to the formation of densely-packed clusters that are notably stable even in the situation of the time-changing applied magnetic field. These clusters do not respond to the varying magnetic field, and tend to orient in various directions rather than that of the magnetic field. Hence this limited motion of each constituent particle in a densely-packed cluster cannot yield a significant relaxation effect, resulting in a weak heating effect as shown in Fig. 5.10. A slight improvement of the heat generation in the

region of $R_B \gtrsim 1$ for the case of $\lambda=60$ is due to the magnetic particle-particle interactions that function to suppress the rotational motion of the consituent particles in a cluster, which results in faster rotational motion of the rod-like particles, giving a response to the alternating magnetic field. This consideration has already been made with respect to the hysteresis loop shown in Fig. 5.6. On the other hand, in the range of $R_B \lesssim 0.3$, the heat generation effect for $\lambda=60$ is slightly smaller than for $\lambda=1$. This is simply because the constituent particles in the stable short clusters shown in Fig. 5.4(a) cannot sufficiently rotate in the alternating magnetic field with a larger frequency. That is, the magnetic interactions between rod-like particles function to add a more significant restriction to the rotational motion than single particles.

Next we consider the results for the rotating magnetic field. The most different characteristic between the two applied magnetic fields appears in the result for the case of $\lambda=100$. The heat generation effect for the rotating field exhibits characteristics similar to those for $\lambda=1$ and $\lambda=60$, not shows significantly smaller values. This is simply because the rod-like particles rotate to follow the rotation of the field irrespective of whether particles aggregate to form linear clusters. This characteristic regarding the relaxation motion of rod-like particles will give rise to approximately similar characteristics of the heat generation effect, which is clearly shown in Fig. 5.10. Smaller values for $\lambda=100$ than those for $\lambda=1$ and $\lambda=60$ in the range of $R_B \lesssim 0.15$ is due to the same reason for the characteristics of the curve for $\lambda=100$ in the range of $R_B \lesssim 0.3$ for the case of the alternating field, as described above. Another characteristic feature is observed in the region of $R_B \gtrsim 0.5$ in the curve for $\lambda=100$. That is, the larger magnetic interaction strength $\lambda=100$ yields larger values of the heat generation effect, which can be understood by considering the characteristics of the cluster formation, shown in Fig. 5.7(c). Similar to thick chain-like clusters shown in Fig. 5.2(b) for the case of the alternating field, the long linear clusters, observed in Fig. 5.7(c), function to suppress the rotational motion of the constituent particles through the magnetic particle-particle interactions, although in the range of sufficiently low frequencies, these particles will finally rotate to follow the rotation of the field. Hence, the constituent particles of a long linear cluster will rotate with a larger rotational velocity than single particles, which results in larger friction forces (torques) and therefore leads to a larger heating effect.

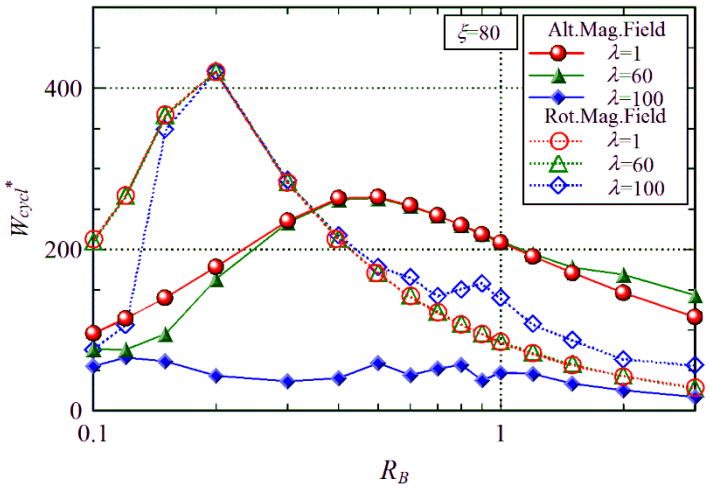

Fig. 5.10 Influence of the magnetic particle-particle interaction strength λ on the heat generation effect, where results for three different cases of magnetic interaction strengths are shown for λ=1, λ=60 and λ=100 for each applied magnetic field. Larger magnetic interaction λ=100 yields larger values of the heat generation effect in the region of $R_B \gtrsim 0.5$ for the case of the rotating field, whereas a rather weak heating effect is predicted for λ=100 in the case of the alternating field.

Finally we discuss the influence of the magnetic particle-particle interaction strength on the heat generation effect. Figure 5.11 shows the heat generation effect as a function of the magnetic particle-particle interaction strength for the intermediate frequency R_B=1. From these results we observe a common feature that the variation with interaction strength changes dramatically at the threshold it which clusters are formed. This is valid for both the applied magnetic field variation types. Specifically, this threshold can be seen to occur at $\lambda \simeq 50$ and $\lambda \simeq 65$ for ξ=40 and ξ=80, respectively, in the case of the alternating field, and $\lambda \simeq 75$ for both the cases of ξ=40 and ξ=80 in the case of the rotating field. Prior to reaching these threshold values, the heat generation effect is due to the motion of single particles and is thus approximately constant, that is independent of the values of λ. In the following, we discuss the dependence on the magnetic interaction strength for the two types of magnetic field variations separately in more detail.

In the case of the alternating magnetic field, the heat generation steeply decreases to approach zero above each threshold value of ξ= 40 and 80. Above these threshold values, the densely-packed aggregates shown in Fig. 5.2(c) are formed in increasing numbers and density. As a result, the constituent particles are not able to change their orientation due to the stronger magnetic

interactions between neighboring particles. This is quite understandable because the densely-packed aggregates shown in Fig. 5.2(c) are extremely stable from an interaction energy point of view. The reason why the threshold value for ξ=80 is much larger than for ξ=40 is that, for a larger applied field strength, a larger magnetic interaction strength is required in order for the magnetic interaction to overcome the influence of the applied magnetic field.

In the case of the rotating magnetic field, the dependence on the magnetic interaction strength exhibits divergent behavior for the two applied field values. Specifically, in the case of ξ=40, the situation of λ=75 ensures that the magnetic interaction is the dominant factor for the behavior of the constituent particles, and therefore these particles cannot respond to the change in the rotating field due to strong magnetic interactions. This leads to a diminishing effect with increasing magnetic interaction strength. In contrast, for the case of ξ=80, in the region of $75 \lesssim \lambda \lesssim 100$, the magnetic field retains significant influence on the particle behavior, and consequently the constituent particles are able to rotate to follow the rotation of the field, albeit with a phase lag. As already described before with respect to the hysteresis loops for the alternating field in Fig. 5.6, the magnetic interaction between the constituent particles tend to suppress the rotational motion of the individual particles. As a result, the rod-like particles finally rotate with a larger speed, which leads to a larger heating effect, as shown in Fig. 5.11.

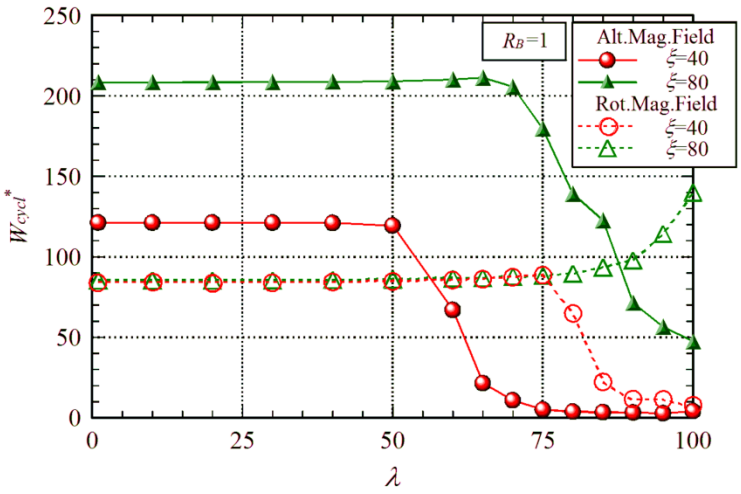

Fig. 5.11 Heat generation effect as a function of the magnetic particle-particle interaction strength for the intermediate frequency R_B=1. The magnetic interactions between constituent particles in a cluster tend to function to suppress the rotational motion of the particles. As a result, the rod-like particles finally rotate with a larger speed, which leads to a larger heating effect in the region of $\lambda \gtrsim 75$ for ξ=80 in the case of the rotating magnetic field.

Finally, we summarize the characteristic features with respect to the aggregate structure and the heat generation effect using tables by focusing on several typical situations of the magnetic particle-particle and particle field interaction strengths. It is noted that in each situation these features are dependent on the frequency of the time-dependent applied magnetic field, that is, on the inverse of the non-dimensional parameter R_B. The cluster formation is mainly governed by the magnetic interaction strength λ and the internal structure is influenced by both the magnetic field strength ξ and the frequency of the applied magnetic field, $1/R_B$. Hence, the criterion value of the magnetic interaction strength for the formation of clusters is employed for specifying typical cases or situations in order to describe the characteristic features regarding the aggregate structure and the heating effect.

Tables 5.1 and 5.2 show the characteristic features regarding the aggregate structure and the heat generation effect for the cases of alternating and rotating magnetic fields, respectively. A noticeable point is that in Situation (5) the rotational magnetic field gives rise to a significantly high heating effect, whereas the alternating field yields a simply low heating effect. This is mainly due to the difference in the behavior of chain-like clusters in these two time-dependent magnetic fields. In the rotating magnetic field, if the chain-like clusters stably formed in the system are able to follow the rotation of the field, this motion induces a significantly larger viscous friction force, which leads to a larger heat generation effect. In contrast, for the case of the alternating magnetic field, each constituting particle of a chain-like cluster strongly tends to rotate to follow the alternating magnetic field, which clearly gives rise to a significantly smaller viscous friction force, resulting in a much smaller heat generation effect in comparison with the former applied magnetic field.

Table 5.1 Summary of the situation and results in the alternating magnetic field

Situations		Reasults	
Magnetic particle-particle interaciton strength λ	Magnetic field strength ξ	Aggregate structure	Heating effect
(1) $\lambda \ll 60$ (weak)	$\xi \ll \lambda$	No cluster formation (any R_B)	significantly Low for any R_B
(2) $\lambda \ll 60$ (weak)	$\xi \gg \lambda$	No cluster formation (any R_B)	significantly High for $0.3 \lesssim R_B \lesssim 1.0$ Higher with increasing ξ
(3) $\lambda \ll 60$ (weak)	$\xi \gg \lambda$	No cluster formation (any R_B)	High for $1.0 \lesssim R_B \lesssim 3.0$ Higher with increasing ξ
(4) $\lambda \gg 60$ (strong)	$\xi \ll \lambda$	Densely-packed clusters ($R_B \gtrsim 1$)	significantly Low for any R_B
(5) $\lambda \gg 60$ (strong)	$\xi \simeq \lambda$	Chain-like and raft-like clusters ($R_B \gtrsim 1$)	Low for $R_B \gtrsim 1$
(6) $\lambda \gg 60$ (strong)	$\xi \gg \lambda$	No cluster formation ($R_B \lesssim 1$)	significantly Low for $R_B \lesssim 1$

Table 5.2 Summary of the situation and results in the rotating magnetic field

Situations		Reasults	
Magnetic particle-particle interaciton strength λ	Magnetic field strength ξ	Aggregate structure	Heating effect
(1) $\lambda \ll 75$ (weak)	$\xi \ll \lambda$	No cluster formation (any R_B)	significantly Low for any R_B
(2) $\lambda \ll 75$ (weak)	$\xi \gg \lambda$	No cluster formation (any R_B)	significantly High for $0.1 \lesssim R_B \lesssim 0.5$ Higher with increasing ξ
(3) $\lambda \ll 75$ (weak)	$\xi \gg \lambda$	No cluster formation (any R_B)	High for $0.5 \lesssim R_B \lesssim 3.0$
(4) $\lambda \gg 75$ (strong)	$\xi \ll \lambda$	Densely-packed clusters ($R_B \gtrsim 1$)	significantly Low for any R_B
(5) $\lambda \gg 75$ (strong)	$\xi \gg \lambda$	Chain-like clusters ($R_B \gtrsim 1$)	significantly High for $0.1 \lesssim R_B \lesssim 0.5$ significanlty Higher with increasing ξ
(6) $\lambda \gg 75$ (strong)	$\xi \gg \lambda$	No cluster formation ($R_B \lesssim 1$)	significantly Low for $R_B \lesssim 1$

5.7 Conclusion

In the present study, we have investigated the behavior of rod-like magnetic particles and their relationship with the heat generation effect for two kinds of applied magnetic field variations, i.e., alternating and rotating magnetic fields, by means of Brownian dynamics simulations. The governing factors for characterizing the present phenomenon are viscous friction forces (torques), the strength and directional characteristics of each applied magnetic field variations and magnetic particle-particle interactions. The relative magnitudes of these factors govern the characteristics of the aggregate structures and the heating effect. The main results obtained here are summarized as follows. As a common feature for both the magnetic field variations, in the case of significantly strong particle-particle interaction strengths, rod-like particles exhibit densely-packed clusters are formed, rather than chain-like clusters, and the neighboring rod-like particles constituting a cluster incline in opposite directions to each other. For the case of an alternating magnetic field, in the intermediate frequency range, linear thick chain-like clusters are formed along the field direction and the constituent rod-like particles themselves tend to rotate to follow the change in the alternating magnetic field during a short period. In contrast, for the case of the rotating field, linear clusters rotate as a whole body to respond to the rotation of the magnetic field. In both the applied magnetic field variations, the magnetic interactions between the constituent particles in a cluster tend to function to suppress the relaxation motion of the rod-like particles, which, as a result, leads to improvement in the heat generation effect in certain situations. In a relatively large frequency region, the rotating applied magnetic field gives rise to a larger heat generation effect, whereas in a

relatively lower frequency region the alternating magnetic field is superior to the former applied magnetic field for a heat generation point of view.

References

[1] A. E. Deatsch and B. A. Evans, Heating efficiency in magnetic nanoparticle hyperthermia J. Magn. Magn. Mater., 354, (2014), 163–172.

[2] I. M. Obaidat, B. Issa and Y. Haik, Magnetic Properties of Magnetic Nanoparticles for Efficient Hyperthermia, Nanomater., 5, (2015), 63–89.

[3] C. S. S. R. Kumar and F. Mohammad, Magnetic nanomaterials for hyperthermia-based therapy and controlled drug delivery, Advan. Drug Delivery Rev., 63, (2011), 789-808.

[4] S. Suzuki and A. Satoh, Influence of the cluster formation in a magnetic particle suspension on heat production effect in an alternating magnetic field, Colloid Poly. Sci., 297, (2019), 1265-1273.

[5] S. Suzuki, A. Satoh and M. Futamura, The behaviour of magnetic spherical particles and the heating effect in a rotating magnetic field via Brownian dynamics simulations, Mol. Phys., 119, (2021), e1892225.

[6] L. C. Varanda, M. Jafelicci Jr. and G. F. Goya, Magnetic properties of spindle-type iron fine particles obtained from hematite, J. Magn. Magn. Mater., 226-230, (2001), 1933-1935.

[7] T. P. Raming, A. J. A. Winnubst, C. M. Van Kats and A. P. Philipse, The Synthesis and Magnetic Properties of Nanosized Hematite (α-Fe2O3) Particles, J. Colloid Interface Sci., 249, (2002), 346-350.

[8] K. Slyusarenko, D. Constantin and P. Davidson, A two-dimensional nematic phase of magnetic nanorods, J. Chem. Phys., 140, (2014), 104904.

[9] K. Kandori, Y. Yamotoa and T. Ishikawa, Effects of vinyl series polymers on the formation of hematite particles in a forced hydrolysis reaction, J. Colloid Interface Sci., 283, (2005), 432-439.

[10] D. Van der Beek, H. Reich, P. Van der Schoot, M. Dijkstra, T. Schilling, R. Vink, M. Schmidt, R. Van Roij and H. Lekkerkerker, Isotropic-Nematic Interface and Wetting in Suspensions of Colloidal Platelets, Phys. Rev. Lett., 97, (2006), 087801.

[11] J. M. Meijer, F. Hagemans, L. Rossi, D. Byelov, S. I. R. Castillo, I. Snigireva, A. P. Philipse and A. V. Petukhov, Self-Assembly of Colloidal Cubes via Vertical Deposition, Langmuir, 28, (2012), 7631-7638.

[12] J. M. Meijer, D. Byelov, L. Rossi, A. Snigirev, I. Snigireva, A. P. Philipse and A. V. Petukhov, Self-assembly of colloidal hematite cubes: a microradian X-ray diffraction exploration of sedimentary crystals, Soft matter., 9, (2013), 10729-10738.

[13] M. Aoshima, M. Ozaki and A. Satoh, Structural Analysis of Self-Assembled Lattice Structures Composed of Cubic Hematite Particles, J. Phys. Chem. C, 116, (2012), 17862-17871.

[14] E. Wetterskog, M. Agthe, A. Mayence, J. Grins, D. Wang, S. Rana, A. Ahniyaz, G. Salazar-Alvarez and L. Bergström, Precise control over shape and size of iron oxide nanocrystals suitable for assembly into ordered particle arrays, Sci. Technol. Adv. Mater., 15, (2014), 055010.

[15] A. Satoh, *Introduction to Practice of Molecular Simulation: Molecular Dynamics, Monte Carlo, Brownian Dynamics, Lattice Boltzmann and Dissipative Particle Dynamics* (Elsevier, Amsterdam, 2010).

[16] A. Satoh, Application of the Brownian dynamics method to a rod-like hematite particle dispersion, Mol. Phys., 112, (2014), 1002–1011.

[17] A. Satoh, On aggregate structures in a rod-like haematite particle suspension by means of Brownian dynamics simulations, Mol. Phys., 112, (2014), 2122–2137.

Chapter 6 The behavior and heating effect of disk-like magnetic particles in an alternating magnetic field (Sine and modified magnetic field)

6.1 Introduction

Recent studies have addressed the relatively coarse particles with various geometric shapes in order to investigate the behavior of particles and the heating effect that arises due to Brownian relaxation. Two studies that have investigated heat generation and particle behavior based on Brownian relaxation are the experimental study by S. A. Gudoshnikov et al. on the relationship between the frequency of alternating magnetic fields and hysteresis loops for magnetite particles of around 25 nm in diameter [1], and the study by P. Guardia et al. on the relationship between the magnetic field strength and the hysteresis loop for cubic particles of around 13-40 nm [2]. Moreover, H. Richert et al. examined the possibility of drug release by the heating effect of relatively coarse particles for the preparation of particles for application to drug delivery systems [3].

In the preceding section, we examined the correlation between the internal structure of the aggregate and the heating effect by using rod-like magnetic particles in alternating and rotating magnetic fields, expecting that the heating effect would be enhanced by increasing the friction between the particles and the mother liquid. The change of particle shape from rod-like to disk-like particles with a plane surface is expected to increase friction with the mother liquid, which is expected to improve the heat generation effect.

From the above background, the objective of the present study is to investigate the heating effect based on the aggregation and Brownian relaxation of magnetic disk-like particles in an alternating magnetic field using Brownian dynamics. By conducting a detailed comparison with the characteristics of the heating effect observed in the previous chapter involving rod-like particles, we focus on an applied magnetic field and attempt to improve the heating effect by modifying the magnetic field.

6.2 Particle model and alternating magnetic field

In this study, a disk-like particle with diameter d and thickness b is adopted as the particle model. The magnetic moment $\boldsymbol{m}$ is located at the center of the particle and is oriented along the disk plane. The particle is coated with a surfactant layer of uniform thickness δ to prevent excessive aggregation. The direction of the magnetic moment $\boldsymbol{n}$ (=$\boldsymbol{m}$/|$\boldsymbol{m}$|) is represented by a blue pebble on the particle surface.

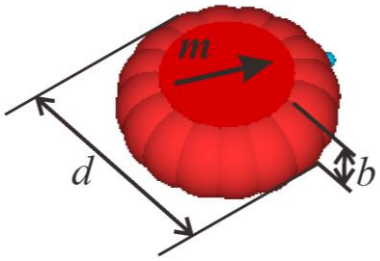

Fig. 6.1 Particle model

Furthermore, it is necessary to apply a time-dependent magnetic field to investigate the heat generation effect of the particles. The magnetic field commonly used previously is a sinusoidal wave applied in one arbitrary axis. If an external magnetic field is applied in the x-direction as a conventional magnetic field, it is expressed as in Eq. (6.1).

$$\boldsymbol{H}_{alt}(t) = H_0 \sin(\omega_H t)\boldsymbol{i}_x \tag{6.1}$$

where H_0 is the magnitude of the magnetic field, ω_H is the angular velocity, and $\boldsymbol{i}_x$ is the unit vector in the x-direction.

In addition, it aims to improve the heat generation effect by modifying the magnetic field. The modified magnetic field is obtained by combining a sinusoidal wave with a triangular wave that is a quarter of a period faster than the sinusoidal wave. If the modified magnetic field is applied in the x-axis direction, it is expressed as

$$\begin{cases} \boldsymbol{H}_{mod} = \left\{ H_{sin}\sin(\omega_H t) + H_{tri}\left(-\dfrac{2\pi}{\omega_H} t + 1 \right) \right\} \boldsymbol{i}_x & for\ 0 \le t < \pi/\omega_H \\ \boldsymbol{H}_{mod} = \left[H_{sin}\sin(\omega_H t) + H_{tri}\left\{ \dfrac{2\pi}{\omega_H}\left(t - \dfrac{\pi}{\omega_H} \right) - 1 \right\} \right] \boldsymbol{i}_x & for\ \pi/\omega_H \le t < 2\pi/\omega_H \end{cases} \tag{6.2}$$

where H_{tri} is the magnitude of the triangular wave and H_{sin} is the magnitude of the sinusoidal wave. The present study suggests that the ratio R_{modH} ($=H_{tri}/H_{sin}$) of the modified magnetic field to the sinusoidal field is $R_{modH}=2$. When comparing the conventional magnetic field with the modified magnetic field, the amplitude is adjusted so that the amplitude is the same as the conventional magnetic field.

Figure 6.2 shows the time variation of both the conventional magnetic field and the modified magnetic field with their amplitude set to 1 and their peaks adjusted to be at the same time. There is no difference in the period wave between the conventional and modified magnetic fields. The modified magnetic field switches direction later in time compared to the conventional magnetic field after reaching its peak. In other words, the time from $h_x=0$, when the direction of the magnetic field switches, to the maximum value $h_x=1$ is shorter than that of the conventional magnetic field.

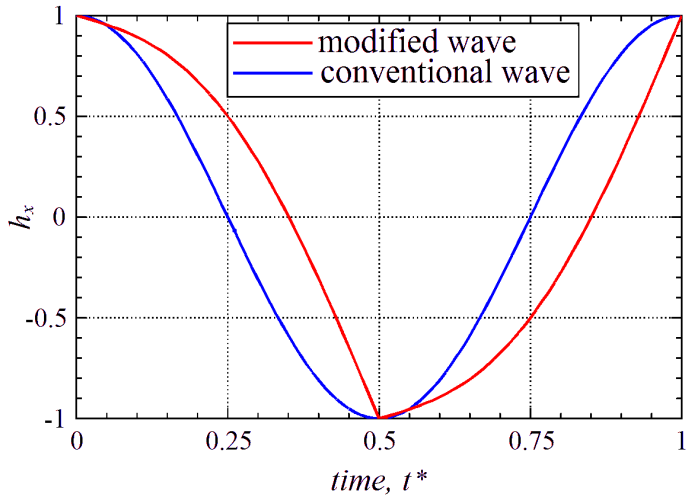

Fig. 6.2 Comparison between conventional and modified magnetic fields

6.3 Brownian dynamics method

Brownian dynamics methods for axisymmetric particles are described in typical books and previous papers. Therefore, only the main parts are presented here. The motion of an axisymmetric particle is treated separately in the direction along the particle axis and the direction perpendicular to the particle axis. The axial component is denoted by ∥ and the perpendicular component is denoted by ⊥. The position $\boldsymbol{r}$ of the disk-like particle at time t is written as in Eq.s (6.3) and (6.4).

$$\boldsymbol{r}_{\parallel}(t+\Delta t)=\boldsymbol{r}_{\parallel}(t)+\frac{1}{k_BT}D_{\parallel}^{T}\boldsymbol{F}_{\parallel}^{P}(t)\Delta t+\Delta r_{\parallel}^{B}\boldsymbol{e}(t) \tag{6.3}$$

$$\boldsymbol{r}_{\perp}(t+\Delta t)=\boldsymbol{r}_{\perp}(t)+\frac{1}{k_BT}D_{\perp}^{T}\boldsymbol{F}_{\perp}^{P}(t)\Delta t+\Delta r_{\perp 1}^{B}\boldsymbol{e}_{\perp 1}(t)+\Delta r_{\perp 2}^{B}\boldsymbol{e}_{\perp 2}(t) \tag{6.4}$$

where k_B is Boltzmann's constant, T is the absolute temperature, D^T is the diffusion coefficient of translation, $\boldsymbol{F}^P$ is the sum of forces acting on the particle, and $\Delta\boldsymbol{r}^B$ is the random displacement.

A similar expression is given for the direction $\boldsymbol{e}$ of the particle axis and the direction $\boldsymbol{n}$ of the magnetic moment of the particle.

6.4 Heat generation effect

Heat generation in magnetic particle suspensions is caused by the relaxation of magnetic moments. As mentioned, when the particle size is sufficiently larger than 10 nm, the magnetic moment of the particle rotates due to Brownian relaxation. A theoretical study on the heating effect of magnetic particles in a time-dependent magnetic field was performed by Rosensweig [4], and the heating value $W_{cycl}^{\ total}$ per magnetic field period is

$$W_{cycl}^{total} = \mu_0 \oint \boldsymbol{H} \cdot d\boldsymbol{M} \tag{6.5}$$

where μ_0 is the magnetic permeability of the vacuum, $\boldsymbol{H}$ is the magnetic field, and $\boldsymbol{M}$ is the magnetization.

The heat generation per particle W_{cycl} is

$$W_{cycl} = -\mu_0 m H_0 \oint \left(\boldsymbol{n} \cdot d\left(\boldsymbol{H} / H_0\right)\right) \tag{6.6}$$

where $\boldsymbol{m}$ is the magnitude of the magnetic moment and H_0 is the magnitude of the magnetic field.

When nondimensionalized with the representative value k_BT

$$W_{cycl}^{*} = -\xi \oint \left(\boldsymbol{n} \cdot d\left(\boldsymbol{H} / H_0\right)\right) \tag{6.7}$$

where ξ is a dimensionless parameter that represents the strength of the magnetic field.

6.5 Parameters for simulations

The following parameters were used in the simulations. Non-dimensional values are indicated by an asterisk (*). The number of particles N=27 (=3^3), diameter d^*=1.0, surfactant layer thickness δ^*(=δ/d)=0.15, aspect ratio r_p(=d/b)=3, volumetric fraction ϕ_V=0.02, time interval Δt^*=0.00001 and total simulation time $t_{total}{}^*$=100. The phenomena treated in this study are governed by the four dimensionless parameters as expressed in Equation (6.8).

$$\lambda = \frac{\mu_0 m^2}{4\pi d^3 k_B T}, \qquad \xi = \frac{\mu_0 m H_0}{k_B T}, \qquad \lambda_V = \frac{\pi n_s d^2}{2}, \qquad R_B = \frac{k_B T}{3\pi\eta d^3} \cdot \frac{2\pi}{\omega_H} \tag{6.8}$$

λ is the strength of the magnetic interaction between particles, ξ is the strength of the interaction with the magnetic field, and λ_V is the strength of the repulsion force due to the overlap between surfactant layers. R_B is the ratio of the random force to the viscous force. If R_B is greater than 1, the random force dominates, and if R_B is less than 1, the viscous force dominates. R_B also contains a term related to the frequency of the alternating magnetic field; the smaller R_B is, the higher the frequency is. These dimensionless parameters were set to λ = 1 to 120, ξ = 1 to 100, λ_V = 150, and R_B = 0.1 to 10.

6.6 Results and discussion

6.6.1 Influence of the frequency of the magnetic field on the heat generation effect

First, the effect of the frequency of the magnetic field on the heat generation effect is discussed. Figure 6.3 shows the dependence of the heating effect on the frequency of the magnetic field for rod-like and disk-like particles in a conventional magnetic field and disk-like particles in a modified magnetic field. In the case of λ=1, the magnetic force between particles is so small that no cohesive structure is produced, and friction with the mother liquid is the main factor preventing particle motion.

In all cases, the heat generation effect increases with increasing R_B, reaches a peak, and then decreases. In the small R_B region, the heat generation effect is small because the magnetic moment of the particles cannot be sufficiently oriented in the magnetic field direction due to high friction with the mother liquid. As R_B increases, i.e., the viscous effect of the mother liquid decreases, the magnetic moments of the particles improve their ability to follow the magnetic field, and the heat generation effect increases. As R_B increases further, the heat generation effect decreases. This is because the decrease in the viscous effect of the mother liquid no longer provides sufficient friction.

By comparing the heating effect of rod-like particles with that of disk-like particles, it is shown that the heating effect of rod-like particles is higher than that of disk-like particles for R_B < 0.7. This results from the difference in friction with the mother liquid, i.e., the difference in the particle shape. These rod-like particles, which have relatively low friction with the mother liquid, respond to and follow the magnetic field better than disk-like particles, even when the R_B is small,

i.e., when the viscous effect of the mother liquid is high. Therefore, rod-like particles generate more heat than disk-like particles in the low-frequency range. On the other hand, in the low-frequency region where R_B is large, disk-like particles with greater friction with the mother liquid are more advantageous.

A comparison of the conventional magnetic field with the modified magnetic field reveals that the heat generation effect in the high-frequency region is slightly lower for the modified magnetic field than for the conventional magnetic field. However, the heating effect in the low-frequency range is higher. The magnetic moment of a particle rotates significantly after the direction of the applied magnetic field is switched, and tries to follow it. In the case of the modified magnetic field, the time between the switch in the direction of the magnetic field and the maximum magnitude of the applied magnetic field is shorter than the conventional magnetic field. Therefore, for the magnetic moment of the particle to follow the magnetic field, it must rotate in a shorter time than when a conventional magnetic field is applied. Hence, when the modified magnetic field is applied, for the same R_B, the magnetic moment cannot be oriented sufficiently in the direction of the magnetic field, and the heat generation effect becomes small. When the magnetic field is very slow (R_B = 10), there is almost no difference in the heating effect between the conventional and modified magnetic fields. This is because the magnetic field is so slow and as a result, even the modified magnetic field can no longer generate a large frictional resistance.

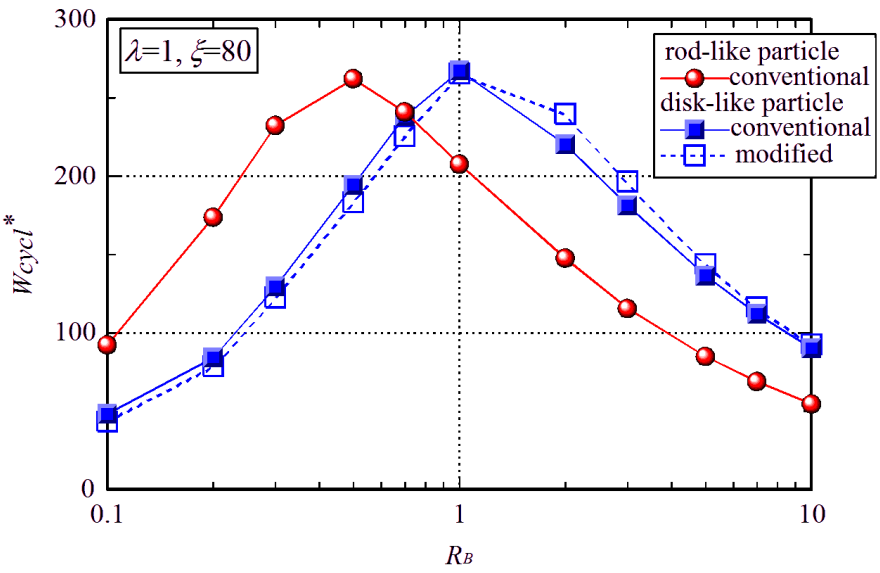

Fig. 6.3 Dependence of the heating effect on the frequency of the magnetic field (λ=1, ξ=80). In the low-frequency range, a high heating effect is obtained for disk-like particles in the modified magnetic field, where a large heating effect occurs.

6.6.2 Effect of the frequency of the magnetic field on the formation of aggregates and heat generation under conditions where aggregates are formed

We here consider the effect of the frequency of the magnetic field on the heating effect of the disk-like particles and the aggregates. Figure 6.4 shows snapshots obtained by varying the frequency of the magnetic field, R_B = 0.3, 0.7 and 3 in the modified magnetic field with a very strong inter-particle magnetic force λ = 120 and a strong magnetic field ξ = 80. For the case of R_B =0.3 in Figure 6.4(a), the particles form column-like clusters with magnetic moments inclining in the opposite direction to each other. In this situation, the magnetic moments of the particles cannot be oriented in the direction of the magnetic field because the frequency of the magnetic field is too high. In contrast, the inter-particle magnetic force is strong enough to form aggregates, so that the cluster formation is column-like. At the intermediate value of R_B = 0.7, the particles do not form aggregates and move independently, as shown in Figure 6.4(b). The magnetic moment of the particles follows the magnetic field as the field slows down to R_B = 0.7. However, despite the magnetic field being reduced at R_B = 0.7, the direction of the magnetic field switches before the particles approach each other, causing them to rotate. At R_B = 3, the particles form chain-like clusters along the magnetic field direction. This phenomenon occurs because the magnetic field is sufficiently slowed down so that the magnetic moments of the particles are oriented in the magnetic field direction, and the magnetic forces between the particles allow them to form aggregates. The particles that form clusters are not aligned in a straight line but tend to shift in the direction of the particle axis and contact each other in a face-to-face contact manner.

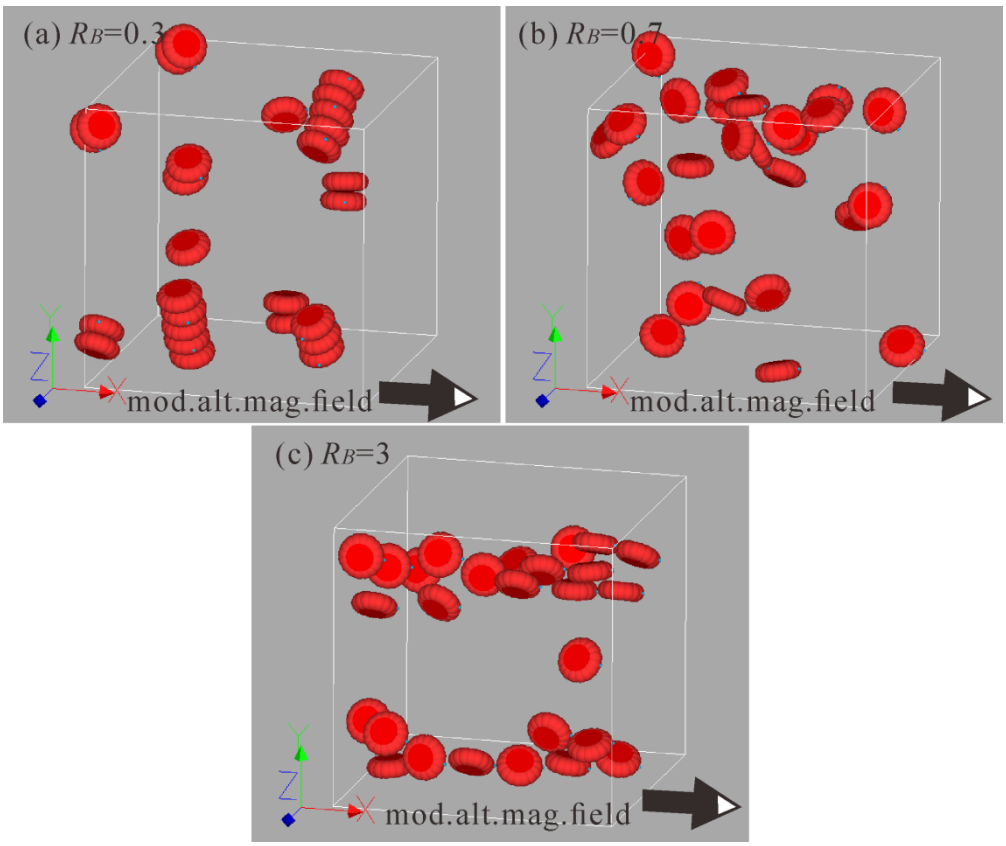

Fig. 6.4 Effect of magnetic field frequency on aggregates (λ = 120, ξ = 80, t^* = 0.1, modified magnetic field: (a)R_B = 0.3, (b)R_B = 0.7 and (c)R_B = 3). At R_B =0.3 shown in Fig. 6.4(a), the particles are dominated by the influence of magnetic particle-particle interaction and form column-like clusters. On the contrary, for R_B = 3 shown in Fig. 6.4(c), the clusters are influenced by the magnetic field and form chain-like clusters oriented in the field direction.

Furthermore, we discuss the effect of the frequency of the magnetic field and the strength of the magnetic force between particles on the heat generation effect. Figure 6.5 shows the dependence of the heating effect of disk-like particles in a modified magnetic field on the frequency of the magnetic field. In the case of R_B = 0.3, the heating effect is observed to be greater in the decreasing order of inter-particle magnetic forces. In this situation, as mentioned earlier, for the case of λ = 100 or λ = 120, when the magnetic force between particles is strong, the particles form column-like clusters due to the effect of the magnetic interaction between the particles. The magnetic moment of the particles is strongly affected by the interactions with nearby particles and shows little response to the magnetic field. Therefore, the heating effect is small. In contrast, when λ = 1, the particle-particle interaction is so weak that no aggregates are produced, and the only factor

preventing particle motion is friction with the mother liquid. For the case of R_B = 0.5, there is almost no difference in the heating effect between λ = 1 and λ = 100. This arises because the magnetic field is reduced in the case of R_B = 0.5, so that the magnetic moment of the particle is affected mainly by the magnetic field and thus follows the magnetic field. Under these circumstances, there is sufficient time for the magnetic moment of the particles to reorient and follow the magnetic field, but insufficient time to form aggregates. Consequently, the absence of aggregate formation causes the particles to behave as if they were individually in motion, resulting in a similar heating effect in the case of λ = 1, where no aggregates are formed. In the case of λ = 120, alternatively, the particles continue to aggregate and form column-like clusters due to very strong particle-particle interactions. When the magnetic field is further slowed down to R_B = 0.7, for the same reason as for λ = 100, the aggregate formation does not occur even for λ = 120, and the heating effect is almost the same as for λ = 1 and 100. For the case of R_B = 3, the heating effect increases in the order of the strength of the magnetic force between the particles. In this range, particles form chain-like clusters since the inter-particle magnetic force is sufficiently strong. Particles forming chain clusters repeatedly collapse and re-aggregate as the magnetic field changes. The collapsing and re-aggregation of the chain clusters act as significant resistance to the magnetic field, thus improving the heat generation effect.

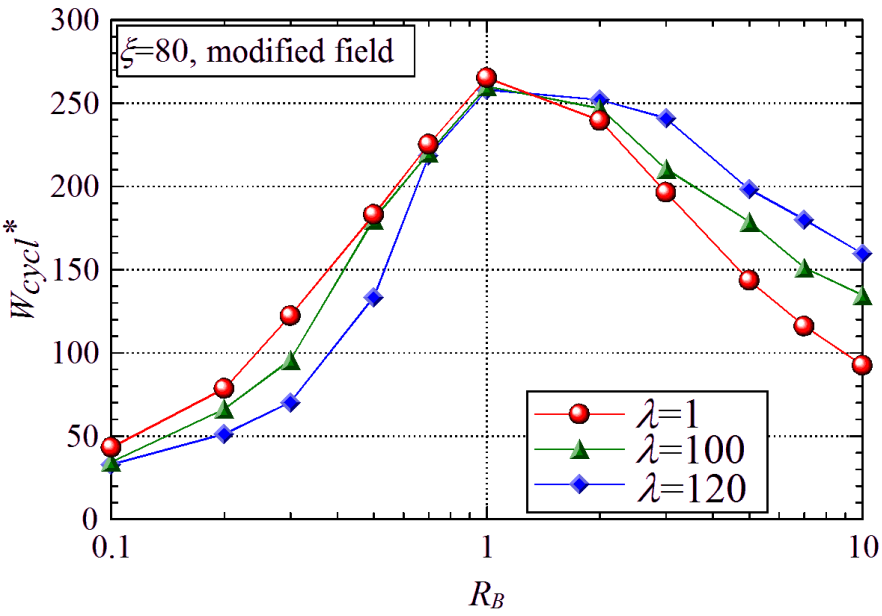

Fig. 6.5 Dependence of the heat generation effect on the inter-particle magnetic force and the frequency of the magnetic field (modified magnetic field ξ = 80). In the high-frequency area, the aggregate structures restrict the motion of the particles and thus reducing the heating effect. In the low-frequency range, the clusters have a significant effect on the heating effect.

6.6.3 Effect of inter-particle magnetic force on the heating effect

Figure 6.6 shows the dependence of the heat generation effect of disk-like particles in a modified magnetic field at R_B =3 on the strength of the inter-particle magnetic force. At R_B =3, the magnetic field is slow enough that the magnetic moments of the particles adequately follow the magnetic field if the inter-particle magnetic force is weak. However, if the inter-particle magnetic force is sufficiently large, aggregates are formed.

For the case of λ=1, where the inter-particle magnetic force is very weak, the magnitude of the magnetic field strength ξ determines the heating effect. This is evident from the dimensionless heat generation equation (6.7), where the heating effect is highly dependent on the strength of the magnetic field, provided that the particles are well-tracked with little influence other than that of the frictional force. At around λ = 80, when the inter-particle magnetic forces become slightly stronger, the particles begin to form aggregates due to the influence of the inter-particle magnetic forces, and a significant change in the heating effect occurs. In the case of a relatively weak magnetic field ξ = 40, the heating effect decreases rapidly as the strength of the inter-particle magnetic force λ increases. This is because the influence of the inter-particle magnetic force becomes dominant and the particles form stable column-like clusters. The magnetic moment of the particles is strongly affected by the interactions between the particles in the vicinity so that they do not respond to the magnetic field and the heating effect decreases. In the case of a strong magnetic field ξ = 80, on the other hand, the heat generation effect increases as the inter-particle magnetic force increases. For the case of λ = 120, unlike the case of ξ = 40, the particles form chain-like clusters that extend in the direction of the magnetic field due to the strong magnetic field, even when the inter-particle magnetic force is very strong. The chain clusters formed undergo repeated collapse and reformation as the magnetic field changes. The magnetic moment of the particles is significantly delayed by the magnetic field because the chain cluster collapses after the magnetic field becomes somewhat stronger in the opposite direction. In addition to the frictional force, the aggregates also retard the rotation of the magnetic moment of the particles, resulting in a higher heating effect than in the absence of aggregates. For the intermediate value of ξ = 60, there is a slight increase in the heating effect from λ = 60 to λ = 100, and for λ = 120, there are signs of a decrease in the heating effect. This is due to the influence of inter-particle magnetic forces becoming dominant and the formation of column-like clusters begins. However, the effect of the inter-particle magnetic forces is not strong enough to counter the effect of the magnetic field, so the particles are unable to maintain the column-like clusters and collapse, and the magnetic moment of the particles responds to the magnetic field only in a certain degree. In this situation, the heating effect for ξ = 60 is less variable than in the other cases, as the aggregates cannot have enough influence on the heating effect.

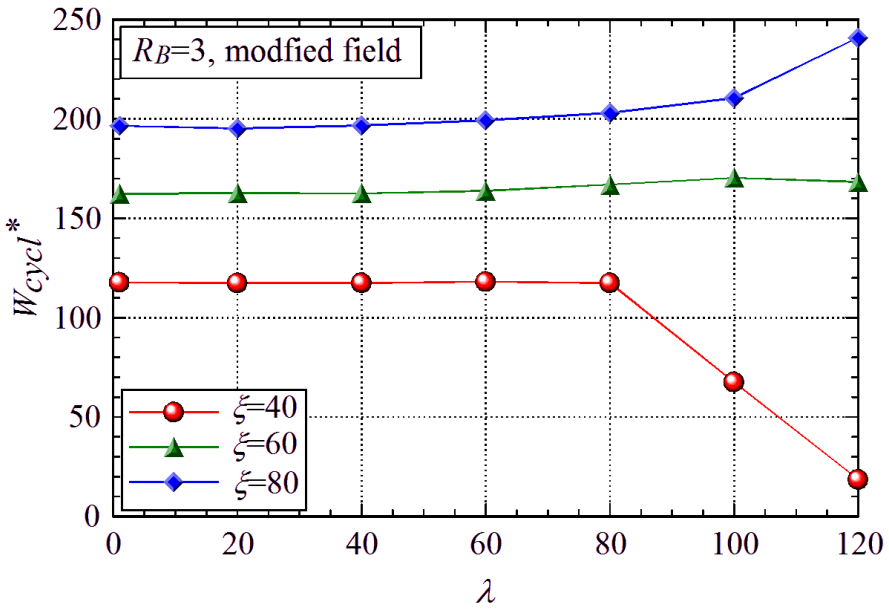

Fig. 6.6 Dependence of the heating effect on the magnetic force between particles (modified magnetic field, R_B =3). From λ = 80, the particles begin to form clusters due to the influence of the magnetic particle-particle interaction, causing a significant change in the heating effect. The heating effect decreases rapidly when the magnetic field is weak. Under a strong magnetic field, the heating effect increases with increasing values of λ.

6.7 Conclusion

The present study has examined the behavior of disk-like particles in an alternating magnetic field and the heat generation effect through Brownian dynamics. Moreover, the heating effect was improved by modifying the applied magnetic field. The main factors that characterize the aggregation and heat generation phenomena are the strength of the magnetic interaction between the particles, the strength of the interaction between the particles and the applied magnetic field, and the frictional resistance between the particles and the mother liquid. The main results obtained in this study are summarized in the following.

Under relatively high-frequency magnetic fields applied to a suspension of rod-like or disk-like particles, where weak inter-particle magnetic forces act on the particle, the use of rod-like particles is expected to have a higher heat-generating effect than disk-like particles. At lower frequencies of the magnetic field, the disk-like particles are more effective in generating heat. This is due to the effect of the particle shape, that is, the disk-like particles have greater friction with the mother liquid than the rod-like particles.

Disk-like particles with sufficiently strong inter-particle magnetic forces form column-like clusters at high magnetic field frequencies and do not respond to the change in the magnetic field. At lower frequencies, the particles move independently and behave in the same way as when the inter-particle magnetic force is weak. At even lower frequencies, the particles form chain-like clusters. In this case, these clusters act as resistance to the rotational motion of the particles, and thus the heat generation effect is higher than when the magnetic force between the particles is weak and they move independently.

We also proposed a modified magnetic field in which a triangular wave is added to a sinusoidal wave. The characteristic feature of this magnetic field is that the time between the switch in the direction of the magnetic field and its maximum value is shortened. When this modified magnetic field is applied, the heat generation effect is reduced in the high-frequency region where the magnetic moment of the particles does not sufficiently follow the change in the magnetic field, thereby deteriorating their ability to follow the magnetic field. On the contrary, in regions where the magnetic field is sufficiently slow, the magnetic moment of the particles must rotate in a shorter time than in conventional magnetic fields, resulting in a larger frictional force and thus an improved heat generation.

References

[1] S. A. Gudoshnikov, B. Y. Liubimov, and N. A. Usov, Hysteresis losses in a dense superparamagnetic nanoparticle assembly, AIP Advances, 2, (2012), 012143.

[2] T. L. Nguyen, T. R. Nizamov, M. A. Abakumov, I. V. Shchetinin, A. G. Majouga, and A. G. Savchenko, Hyperthermal Effect of Cubic Magnetic Nanoparticles, Bull. Russ. Acad. Sci.: Phys., 83, (2019), 1294–1299.

[3] H. Richert, O. Surzhenko, S. Wangemann, J. Heinrich and P. Gömert, Development of a magnetic capsule as a drug release system for future applications in the human GI tract, J. Magn. Magn. Mater., 293, (2005), 497−500.

[4] R. E. Rosensweig, Heating magnetic fluid with alternating magnetic field, J. Magn. Magn. Mater., 252, (2002), 370−374.

Chapter 7 Summary and concluding remarks

7.1 Summary of the present paper

In the present paper, we addressed a magnetic particle suspension in a time-dependent magnetic field and elucidate the dependence of particle aggregation and the heating effect on the strength of the magnetic particle-particle interaction, the strength of the magnetic particle-field interaction, and the frequency of the magnetic field, using Brownian dynamics simulations. We focused on Brownian relaxation for relatively large particles, rather than Néel relaxation by small particles, which has usually been treated in previous studies. The main appealing points of the present paper are as follows:

1. We have elucidated the formation and time change of particle aggregates in a time-dependent magnetic field.
2. We have clarified the influence of the particle shapes on the heating effect.
3. We have examined and established the influence of aggregate structures on the heat generation effect.
4. We have shown the possibility of the modified magnetic field to obtain a more effective heating effect.

7.1.1 Summary of Chapter 2

We elucidated the relationship between aggregate structures and heat effects for spherical magnetic particles in an alternating magnetic field, which are relatively straightforward to handle. Regarding chain-like clusters that are formed and restricted to the magnetic field direction, the magnetic moment of the particles is slowed down by the magnetic particle-particle interaction. The hysteresis loop becomes large, which leads to a large heat generation effect. In this case of weak magnetic particle-particle interactions, the only factor that delays the response of the magnetic moment of the particles to the magnetic field is friction between the particles and the mother liquid, so that the particles follow the change in the magnetic field well and the heat generation effect becomes small.

7.1.2 Summary of Chapter 3

We investigated the outcomes of an unexpected characteristic, whereby the formation of a stable particle cluster induces a decrease in the degree of heating effect. If chain-like clusters are stably formed in the system, whether or not a large heating effect is obtained is dependent on the magnitude relationship between the magnetic particle-particle and the magnetic particle-field interaction strengths. In situations where the magnetic particle-particle interaction is significantly strong, stable chain-like clusters are formed that are not restricted to the field direction, This leads to a smaller area of the hysteresis loop and therefore the stable cluster formation induces a significant decrease in the

heating effect.

7.1.3 Summary of Chapter 4

We extended the previous studies to investigate the behavior of spherical particles in a rotating magnetic field. In the case of rotating magnetic fields, the chain-like clusters tend to rotate as a whole body to follow the magnetic field. In the case of long chain-like clusters being formed, a section of the cluster collapses leading to the formation of a small chain-like cluster and undergoes rotational motion. Then, the short chain-like clusters reassemble in the process of rotation. When these chain-like clusters are formed, the heating effect becomes large. In the case of significantly strong magnetic particle-particle interaction, the particles form ring-like clusters and the magnetic moments of the particles do not respond to the field direction, which leads to a decrease in the heat generation effect. Comparing alternating and rotating magnetic fields, the rotating magnetic field provides a higher heating effect even in situations where magnetic particle-particle interaction is stronger. In the case of weak magnetic particle-particle interaction, the rotating magnetic field is more advantageous at relatively high frequencies, but at lower frequencies, the oscillating magnetic field has a higher heating effect.

7.1.4 Summary of Chapter 5

We addressed rod-like particles and elucidate the particle aggregate and heating effects in an alternating or rotating magnetic field. If the magnetic particle-particle interaction is significantly strong, the particles aggregate to form densely-pack clusters and do not respond to the magnetic field. When the influence of the magnetic field is strong, the particles tend to form chain-like clusters. In the situation of an alternating magnetic field, the particles tend to rotate in response to the change in the magnetic field. On the other hand, in the case of a rotating magnetic field, the cluster tends to rotate as a whole body. Comparing the heating effect, the rotating magnetic field has a greater heating effect in the relatively high-frequency range, while the alternating magnetic field has a higher heating effect in the relatively low-frequency range.

7.1.5 Summary of Chapter 6

We considered disk-like particles to clarify the behavior of the particles in an alternating magnetic field and the heating effect via Brownian dynamics, with the expectation that changing the particle shape will improve the frictional force. In the situation where the influence of magnetic particle-particle interaction is dominant, the particles aggregate to form column-like clusters and do not respond to the magnetic field. On the contrary, in the situation where particles aggregate to form chain-like clusters, the heating effect becomes large because the clusters act as a significant resistance. In comparison to the heating effect of rod-like particles, at relatively low frequencies,

disk-like particles have a higher heating effect than rod-like particles because of the larger friction between the particles and the mother liquid. Moreover, we proposed a modified magnetic field that is generated by the combination of sinusoidal and triangular waves. In the situation that a modified magnetic field with a high frequency is applied, the heating effect is reduced by worsening the following property of the magnetic field. In the case that a low-frequency modified magnetic field is applied, the particles are subjected to a larger frictional force than in a conventional magnetic field, and as a result, the heating effect is improved.

7.2 Topics for future research

7.2.1 Magnetic cubic particle suspensions

Magnetic cubic particles aggregate to form more stable clusters than other particles such as spherical and rod-like particles via cluster formation in the manner of face-to-face contact [1, 2]. Hence these particles are expected to exhibit significantly different dependence on a variety of factors. For instance, the particle aggregates may be able to survive in a much stronger shear flow or a much stronger applied magnetic field. The cluster formation has significant influences on the behavior of the magnetic particles and as a result, the heat generation performance is strongly dependent on the internal structure of the particle aggregates in an alternating or a rotating magnetic field. From this background, it may be necessary to investigate the dependence of the motion of magnetic cubic particles on the formation of particle aggregates, the regime change in the internal structure of the aggregates, and the heating effect in the situation of a time-dependent applied magnetic field.

7.2.2 Particle-based simulation methods for multi-body hydrodynamic interactions

In a dense suspension system, both the magnetic particle-particle interactions and the multi-body hydrodynamic interactions among dispersed particles play important roles in determining the physical quantities of interest such as magnetorheological effects and heat generation characteristics. The Brownian dynamic method is a straightforward simulation technique for investigating the dynamic properties of particle dispersions [3]. However, in this simulation method, it is significantly difficult to take into consideration multi-body hydrodynamic interactions and to solve the particle motion and the flow field simultaneously. There are several simulation techniques for this purpose, i.e., dissipative particle dynamics (DPD) [4], lattice Boltzmann (LB) [5] and multi-particle collision dynamics (MPCD) methods [6-8]. Among these simulation methods, the MPCD method may be the most desirable simulation technique in that a special technique is not necessary for inducing the Brownian motion of dispersed particles and also CPU time is much shorter than DPD and LB methods. From this background, it may be significantly desirable to apply the MPCD simulation method to the heat generation phenomenon in the situation of a time-dependent applied magnetic field.

7.2.3 Motion of the magnetic moment inside the particle body

In a heat-generation phenomenon, the Néel relaxation mechanism or Brownian mechanism is the main factor for the heat-generating effect for a suspension composed of magnetic particles smaller or larger than 10nm size, respectively [9]. In the present paper, we have concentrated on the heat generation phenomenon due to the latter mechanism. In the former mechanism, it is required to simulate the motion of the magnetic moment in the particle body, where the precession motion will be treated in determining the orientation of the magnetic moment of interest. There are several models for governing the precession motion, i.e., the Landau-Lifshits equation, Gilbert equation and Bloch equation, where the second modeling is usually employed for describing the precession motion with a damping effect. In the field of magnetic hyperthermia, a stochastic Landau-Lifshits-Gilbert modeling may be employed in simulations [10, 11], In an intermediate region of the particle size, both the heat generation mechanisms will govern the heat generation process, that is, we have to develop a simulation technique that simulates both the particle motion in a viscous friction circumstance and the motion of the magnetic moment in the particle body in the situation of a fluctuation effect. From this background, in order to investigate the heat generation phenomenon of magnetic particles with an intermediate size, it is significantly desirable to develop a new particle-based simulation method that effectively simulates both the particle motion and the magnetic motion simultaneously.

7.2.4 Heat generation phenomenon at a boundary surface

In actual hyperthermia therapy, magnetic particles loading drugs are guided into a tumor or cancer cell and the application of a time-dependent magnetic field induces heat generation due to the Néel or Brownian relaxation mechanism of the magnetic moments. In this situation, magnetic particles may be charged and aggregate to form linear or densely-packed clusters in the vicinity area of the cell boundary. This kind of phenomenon has already been observed at a laboratory level in basic studies [12]. From this background, from a simulation point of view, we may have to treat the behavior of charged magnetic particles in a vicinity area to a material surface in a time-dependent applied magnetic field. In this approach, it is required to investigate the effect of the electric interactions between magnetic particles and the material surface on the aggregation phenomenon and their effect on the heat generation characteristics. It may be expected that the formation of clusters of magnetic particles is significantly influenced by the existence of the boundary surface of cells due to the geometrical restriction of the particle shape. That is, the internal structure of particle aggregates is determined by both the shapes of the cell boundary and magnetic particles.

References

[1] K. Okada, and A. Satoh, Brownian dynamics simulations of a cubic hematite particle suspension with a more effective treatment of steric layer interactions, Mol. Phys., 118, 17, (2020), e1740806.

[2] K. Okada, and A. Satoh, Elucidation of the relationship between aggregate structures and magnetorheological properties of a magnetic cubic particle suspension by means of Brownian dynamics simulations, Mol. Phys., 120, 3, (2022), e1988168,.

[3] M. P. Allen and D. J. Tildesley, *Computer Simulation of Liquids*, (Clarendon Press, Oxford, 1989).

[4] P. J. Hoogerbrugge, J. M. V. A. Koelman, Simulating microscopic hydrodynamic phenomena with dissipative particle dynamics, Europhys. Lett., 19, (1992), 155–160.

[5] S. Succi, *The Lattice Boltzmann Equation for Fluid Dynamics and Beyond*, (Oxford, Clarendon Press, 2001).

[6] A. Malevanets, R. Kapral, Mesoscopic model for solvent dynamics, J. Chem. Phys., 110, (1999), 8605–8613.

[7] A. Malevanets, R. Kapral, Solute molecular dynamics in a mesoscale solvent, J. Chem. Phys., 112, (2000), 7260–7269.

[8] G. Gompper, T. Ihle, D. M. Kroll and R. G. Winkler, Multi-particle collision dynamics: a particle-based mesoscale simulation approach to the hydrodynamics of complex fluids, Adv. Polym. Sci., 221, (2009), 1–91.

[9] R. E. Rosensweig, Heating magnetic fluid with alternating magnetic field, J. Magn. Magn. Mater., 252, (2002), 370−374.

[10] A. A. Kuznetsov, Force acting on a cluster of magnetic nanoparticles in a gradient field: A Langevin dynamics study, J. Magn. Magn. Mater., 475, (2019), 415-420.

[11] N. A. Usov and B.Y. Liubimov, Dynamics of magnetic nanoparticle in a viscous liquid: Application to magnetic nanoparticle hyperthermia, J. Appl. Phys, 112, (2012), 023901.

[12] T. Pellegrino, Magnetic hyperthermia-meditated drug deliver: the challenges met from the synthesis of magnetic nanocubes with stimuli responsive coatings to the preclinical efficacy studied, 3rd Workshop on Magnetic Nanoparticles for Hyperthermia Anisotropy and Other Adventures, Universidade de Santiago de Compostela, Spain, April 19-21, 2023.

Research performances regarding the present study

Journal papers

1. S. Suzuki, A. Satoh and M. Futamura, Brownian Dynamics Simulations of Aggregation Phenomena in a Magnetic Particle Suspension with an Alternating Magnetic Field (Relationship between the Aggregate Structure and the Heat Production), International Mechanical Engineering Congress & Exposition 2018, ASME proceedings, (2018), IMECE2018-86544, V007T09A037.
2. S. Suzuki and A. Satoh, Influence of the cluster formation in a magnetic particle suspension on heat production effect in an alternating magnetic field, Colloid Polym. Sci., 297, (2019), 1265-1273. (IF=1.906)
3. S. Suzuki, A. Satoh and S. Wada, Monte Carlo simulations of magnetic particle suspensions with a simple assessment method for the particle overlap between magnetic spheroids, Mol. Phys., 118, 3, (2020), e1607915. (IF=1.704)
4. S. Suzuki, A. Satoh, M. Futamura, The behavior of magnetic spherical particles and the heating effect in a rotating magnetic field via Brownian dynamics simulations, Mol. Phys., 119, 9, (2021), e189222. (IF=1.962)
5. S. Suzuki and A. Satoh, The behavior and heat generation effect of a magnetic rod-like particle suspension in an alternating and a rotating magnetic field, Mol. Phys., 121, 1, (2023), e2151523.

International conference (Oral presentation in English)

1) S. Suzuki, A. Satoh and M. Futamura, “Brownian Dynamics Simulations of the Motion of Spherical Particles in a Rotating Magnetic Field”, ASME International Mechanical Engineering Congress & Exposition 2019, IMECE2019-10550, Salt Lake City, America, November, 2019.
2) S. Suzuki, S. Wada, A. Satoh and M. Futamura, “Simple Assessment Method for Particle Overlap of Spheroidal Particles and Its Application to Monte Carlo Simulations”, ASME International Mechanical Engineering Congress & Exposition 2019, IMECE2019-10552, Salt Lake City, America, November 2019.
3) S. Suzuki, A. Satoh and M. Futamura, “The Behavior of the magnetic rod-like particles in an alternating magnetic field: Brownian dynamics simulations”, ASME International Mechanical Engineering Congress & Exposition 2021, IMECE2021-72971, Online, November 2021.
4) S. Suzuki and A. Satoh, “Comparison of the Heating Effect of Rod-Like Particles in an Alternating and a Rotating Magnetic Field”, ASME International Mechanical Engineering Congress & Exposition 2022, IMECE2022- 99174, Online, November 2022.

Transactions of the JSME (in Japanese)

1. S. Suzuki, A. Satoh and M. Futamura, Aggregation phenomena of a magnetic particle suspension in an alternating magnetic field and the influence on the heat generation effect (Brownian dynamics simulations), Transactions of the JSME (in Japanese), 84, 860, (2018).

Internal conference (Oral presentation in Japanese)

1) S. Suzuki, A. Satoh and M. Futamura, “Elucidation of the Behavior of Magnetic Particles in an Alternating Magnetic Field for Application to Magnetic Hyperthermia (Brownian Dynamics Simulations)”, the 53th congress and meeting on Tohoku affiliate, Miyagi, (Japan), March, 2018.
2) S. Suzuki, A. Satoh and M. Futamura, “Elucidation of Spherical Magnetic Particle in a Rotating Magnetic Field (Brownian Dynamics Simulations)”, the 54th congress and meeting on Tohoku affiliate, Miyagi, (Japan), March, 2019.
3) S. Suzuki, A. Satoh and M. Futamura, “Brownian Dynamics Simulations of Magnetic Rod-like Particles in an Alternating Magnetic Field”, Mechanical Engineering Congress, 2021 Japan, online, September, 2021.

Internal conference (Poster presentation in Japanese)

1) S. Suzuki, A. Satoh and M. Futamura, “Brownian Dynamics for Magnetic Particle in a Rotating Magnetic Field”, Mechanical Engineering Congress, 2019 Japan, Akita September, 2021.

Acknowledgement

The present study was conducted under the supervision of Professor Akira Satoh at Akita Prefectural University. This research would not have been possible without the support and encouragement of many people. The author of the present paper would like to acknowledge them.

First of all, I would like to express my deepest gratitude to my supervisor, Professor Akira Satoh of Akita Prefectural University. I had been directly instructed by Professor Satoh for a total of seven years in undergraduate, masters and doctoral courses since I was assigned to Prof. Satoh's laboratory. He gave me the opportunity to participate in international conferences and supported me during my presentations. In addition, I learned many important things for continuing my research, such as my attitude toward research.

Secondary, I am grateful to Principal Researcher Dr. Noriyuki Hirota of National Institute for Materials Science (NIMS), Prof. Tsutomu Ando of Nihon University, and Associate Professor Satoshi Ogata of Tokyo Metropolitan University. They have helped me with the preparation of present paper as sub-reviewers. They gave me a lot of advice, sometimes harshly, mainly from the viewpoint of experimental research. I would like to express my gratitude again.

Thirdly, I would like to express my gratitude to Dr. Muneo Futamura, Assistant Professor at Akita Prefectural University. He gave me a lot of advice about my research and future. Moreover, he has provided me with a lot of support in terms of research, including attendance at internal conferences. I would like to express my deep gratitude to them.

I would like to thank Dr. Kazuya Okada, a lecturer at Saitama Institute of Technology. He gave me a lot of advice on my research and attitude toward it from my third year as an undergraduate to my first year as a doctoral student. From my second grade Ph.D student, he was an assistant professor and lecturer at the Saitama Institute of Technology, where he gave advice. I would also like to thank Mr. Shohei Wada. I received a lot of support and advice on the fundamentals of my research from my third year as an undergraduate to my first year as a master's student. I also thank Mr. Takeru Yamanouchi, second grade Ph.D student. He supported me in laboratory in areas where I lacked support.

I would like to acknowledge the financial support from Grant-in-Aid for JSPS Fellows (20J22468). I also received financial supports from the Honjo Yuri Foundation for Industry and the Marubun Research Promotion Foundation in order to attend some international conferences.

Finally, I would like to be grateful to everyone who assisted in this study.

Published papers

Bulletin of the JSME
日本機械学会論文集
Transactions of the JSME (in Japanese)
Vol.84, No.860, 2018

球状磁性粒子サスペンションの振動磁場下での凝集現象とその発熱効果への影響
（ブラウン動力学シミュレーション）

鈴木 聖弥[*1]，佐藤 明[*2]，二村 宗男[*2]

Aggregation phenomena of a magnetic particle suspension in an alternating magnetic field and the influence on the heat generation effect (Brownian dynamics simulations)

Seiya SUZUKI[*1], Akira SATOH[*2] and Muneo FUTAMURA[*2]
[*1,*2] Faculty of System Science and Technology, Akita Prefectural University
84-4 Ebinokuchi, Tsuchiya-aza, Yuri-honjo-shi, Akita 015-0055, Japan

Received: 16 January 2018; Revised: 13 March 2018; Accepted: 18 March 2018

Abstract
We have elucidated the aggregation phenomena in a suspension composed of spherical magnetic particles in an alternating magnetic field by means of Brownian dynamics method. The relationship between aggregate structures and heating phenomena has been discussed using the hysteresis loops of the magnetic field-magnetization curves, which were obtained from Brownian dynamics simulations. A large heating effect is inevitably necessary in applying a magnetic particle suspension to magnetic hyperthermia treatment in the medical engineering field. We here focus on the Brownian relaxation mode of magnetic moments of particles as the factor inducing the heating effect. The main results obtained here are summarized as follows. In the situation where stable chain-like clusters are formed in the field direction, the magnetic particle-particle interaction induces a significant delay for the magnetic moments inclining in the alternating magnetic field direction. These chain-like clusters respond to a change in the magnetic field without collapse and reformation of the clusters, by the magnetic moment of each constituent particle rotating to incline in the field direction. These behaviors of chain-like clusters in an alternating magnetic field exhibit a hysteresis loop with large area in the magnetic filed-magnetization curve, which gives rise to a significantly large heating effect. On the other hand, in the situation where large clusters are formed but these clusters do not strongly tend to incline in the field direction, the area of the hysteresis loop becomes small and therefore a large heating effect cannot be obtained.

Keywords : Magnetic particle suspension, Aggregation phenomenon, Magnetic hyperthermia, Brownian dynamics, Alternating magnetic field, Heating effect, Hysteresis loop

1. 緒　　言

磁性粒子サスペンションは非常に可能性のある機能性流体であり，その基礎および応用研究は，流体工学，磁気材料工学，医用工学，環境資源工学など，種々の分野で活発に研究が成されるに至っている．流体工学の分野では，印加磁場によって見かけ粘度が変化する磁気粘性効果を利用したダンパーやアクチュエータへの応用が主として考えられている（Rosensweig, 1987, Bullough, 1996, Wereley, 2013）．このような応用の場合，印加磁場や流れ場によって所望の磁気粘性効果を発揮するような機能性サスペンションを創成することが重要となる．磁気材料工学では，サスペンションという中間的な状態を経て，最終的な高密度の新規な磁気記録材料を創成することが試みられている（Harrell et al., 2005, Verdes et al., 2006）．この場合，種々の磁化特性ならびに形状の磁性粒子を創成し，粒子を材料表面上などに配向制御することで所望の機能性を発揮させるようにすることが重要となる．近年，磁性サスペンションの応用展開が急激に拡大し

No.18-00030 [DOI:10.1299/transjsme.18-00030], J-STAGE Advance Publication date : 28 March, 2018
[*1] 学生員，秋田県立大学 システム科学技術学部（〒015-0055　秋田県由利本荘市土谷字海老ノ口 84-4）
[*2] 正員，秋田県立大学 システム科学技術学部
E-mail of corresponding author: asatoh@akita-pu.ac.jp

[DOI: 10.1299/transjsme.18-00030]

た分野が医用工学である．この分野での応用は，薬剤を包含する高次機能性磁性粒子の開発（Patra et al., 2015），ならびに drug delivery システム（Hafeli et al., 1997）や磁気温熱療法（Schmidt, 2007, Kumar and Mohammad, 2011, Obaidat et al., 2015, Golovin et al., 2015）などへの応用を目指した研究が非常に精力的に成されている．環境資源工学の分野では，海水などに溶けた貴金属を収集する技術や有害物質を回収する技術を構築するに際して，機能性磁性粒子を利用しようとする応用展開が活発に試みられている（Bruce and Sen, 2005, Girginova et al., 2010）．以上の応用展開では，所望の機能性を発揮するような磁性粒子の創成と，必要となる物理特性を効果的に引き出せる制御技術等に関する基礎および応用研究が展開されている．

本研究では，医用工学の分野における磁性粒子サスペンションの磁気温熱療法への応用を念頭にした研究を推進する．磁気温熱療法は，磁性サスペンションに振動磁場を印加することで，磁性粒子の磁気モーメントの振動磁場方向への緩和現象により発生する発熱効果により，ガン細胞を死滅させる方法である（Schmidt, 2007）．この発熱効果を発生させるメカニズムとして，磁性粒子の内部で磁気モーメントが磁場方向に動くことにより発熱効果が得られるネール緩和と，磁気モーメントは粒子内部に固定されるが粒子全体が回転することで磁場方向に向こうとするブラウン緩和の二つのメカニズムが考えられる（Rosensweig, 2002）．前者は概略 10nm 程度より小さい磁性粒子に対して発生するメカニズムであり，後者はそれよりも大きな磁性粒子の場合に支配的となるメカニズムである．現在応用に際して注目され，広範囲に研究されているのが比較的小さな磁性粒子を対象としたネール緩和に基づく発熱効果の研究である（Schmidt, 2007, Kumar and Mohammad, 2011, Obaidat et al., 2015, Golovin et al., 2015）．振動磁場中での磁性粒子の磁気モーメントの磁場方向への緩和現象による発熱効果に関する理論は，先駆的な研究によりすでに構築されている（Rosensweig, 2002）．磁性サスペンションを用いたネール緩和に基づく磁気温熱療法の研究は非常に多く成されているので，ここでは，本研究に関連する研究例を簡単に概説するに止める．発熱効果への粒子径や粒子分布の影響（Munoz-Menendez, et al., 2015），磁性粒子間の相互作用の影響（Burrows et al., 2010, Haase and Nowak, 2012, Martinez-Boubeta et al., 2012, Branquinho et al., 2013, Tan et al., 2014, Conde-Leboran et al., 2015a），磁性粒子の配向が及ぼす影響（Conde-Leboran et al., 2015b），振動磁場下で生じる磁性粒子の凝集体形成による発熱効果の実験的研究（Serantes et al., 2010, Lima et al., 2013, Mehdaoui et al., 2013, Saville et al., 2014, Guibert et al., 2015）などの種々のアプローチがなされている．最後の凝集体形成の影響に関する研究では，磁性粒子の体積分率を増加させることで，凝集体を形成させ，その状態で発熱量を測定することで，磁気モーメント間の相互作用の発熱効果への影響を明らかにしようとするものである．ただし，従来の研究ではナノオーダーの磁性粒子を対象としているので，発熱効果はネール緩和に基づいたメカニズムによるものである．従って，凝集構造自体を解明した上での粒子間相互作用の発熱効果への影響を検討した研究までには至っていない．さらには，球状以外の形状を有する磁性粒子を用いたサスペンションや，ある凝集構造を仮定した上での発熱効果の研究も進展しつつある．例えば，強磁性回転楕円体粒子を対象とした研究（Abbas and Bossos, 2017），バクテリアのような磁性球状粒子が連結した鎖状粒子やリング状凝集体を対象とした研究（Alphandery et al., 2011, Serantes et al., 2014），などが遂行されている．

最近では，ブラウン緩和現象に基づいた磁気温熱療法への応用の可能性も模索されつつある．磁性粒子は 10nm より大きくなると，磁気モーメントの磁場方向への配向に際して，粒子自体が回転することで磁場の変化に追随しようとする．このような比較的大きな磁性粒子の発熱効果を解明することは，学術的な観点からはもちろんのこと，磁気温熱療法や drug delivery システムへの応用のさらなる可能性を広げる上でも，非常に重要であるものと思われる．このような方向に沿って，大きさが 100nm 程度以上の大きさの磁性回転楕円体粒子を用いた発熱効果の研究（Yao et al., 2015）や，大きさが 200nm 程度の磁性エマルジョン液滴を対象とした研究（Lahiri et al., 2017）などがある．注目すべきことは，棒状磁性粒子の振動磁場中での回転運動（振り子運動）がガン細胞に力学的なダメージを与えて死滅させる作用の可能性があることである（Yao et al., 2015）．従って，新たなる医用工学分野での応用の可能性を提起する上でも，磁性粒子サスペンションの振動磁場や回転磁場での力学的な特性を詳細に解明することは非常に重要であるものと考えられる．このような方向に沿っていくつかの研究がすでに成されている．例えば，磁性回転楕円体の 2 粒子系を対象とした振動磁場中での挙動（Abba and Bossis, 2017），回転磁場中でのミクロンオーダーの磁性球状粒子の凝集現象と磁気特性（De Las Cuevas et al., 2008, Llera et al., 2015），回転磁場中での磁気モーメントの緩和現象（Coughlan and Bevan, 2016），回転磁場中での磁性扁平粒子の配向特性（Tan et al., 2016），振動および回転磁場中での磁気粘性特性（Sanchez and Rinaldi, 2010）などの研究が推進されている．

[DOI: 10.1299/transjsme.18-00030]

以上のような背景により，本研究では，現在までほとんど行われていなかった，振動磁場中での磁性粒子の凝集構造の解明と，その凝集構造とブラウン緩和に基づく発熱特性との関係を，ブラウン動力学法を用いたミクロな解析法により，詳細に解明することを試みる．本現象を特徴づける主たる要因は，振動磁場に起因する流体粘性力，印加磁場の強さ，粒子間に作用する磁気的な相互作用であるので，具体的には，これらの要因を種々に変えたシミュレーションを行うことにより，上述の特性を詳細に解明することを試みることになる．

2. 磁性粒子のモデル

本研究では球状磁性粒子サスペンションを対象に，振動磁場中での磁性粒子の凝集現象の解明を試みる．その際，次のような磁性粒子のモデルを用いる．ただし，粒子を区別する必要がある場合，諸量に下付き添字 i もしくは j を付すことにする．粒子は直径 d の球状剛体粒子まわりを一様な厚さ δ の界面活性剤で被覆され，粒子中心に磁気双極子 $\boldsymbol{m}_i$ を有するものとする．このような磁性粒子 i, j 間に作用する磁気的な粒子間相互作用のエネルギー $U_{ij}^{(m)}$ および界面活性剤層の重畳による相互作用のエネルギー $U_{ij}^{(V)}$，さらに磁場 $\boldsymbol{H}$ と磁気モーメント $\boldsymbol{m}_i$ との相互作用のエネルギー $U_i^{(H)}$ は次のように表される（Satoh, 2003, 2017）．

$$U_{ij}^{(m)} = \frac{\mu_0 m^2}{4\pi r_{ij}^3}\left\{\boldsymbol{n}_i\cdot\boldsymbol{n}_j - 3(\boldsymbol{n}_i\cdot\boldsymbol{t}_{ij})(\boldsymbol{n}_j\cdot\boldsymbol{t}_{ij})\right\},\quad U_{ij}^{(V)} = \frac{n_s k_B T\pi d^2}{2}\left\{2 - \frac{r_{ij}}{\delta}\ln\frac{d+2\delta}{r_{ij}} - \frac{r_{ij}-d}{\delta}\right\},\quad U_i^{(H)} = -\mu_0\boldsymbol{m}_i\cdot\boldsymbol{H} \tag{1}$$

ここに，$\boldsymbol{n}_i$ は磁気モーメント $\boldsymbol{m}_i$ の方向を表す単位ベクトルで，$\boldsymbol{n}_i=\boldsymbol{m}_i/m$（$m=|\boldsymbol{m}_i|$），$\boldsymbol{t}_{ij}$ は粒子 i,j 間を結ぶベクトル $\boldsymbol{r}_{ij}(=\boldsymbol{r}_i-\boldsymbol{r}_j)$ の単位ベクトル表現で，$\boldsymbol{t}_{ij}=\boldsymbol{r}_{ij}/r_{ij}$, $r_{ij}=|\boldsymbol{r}_{ij}|$, μ_0 は真空の透磁率，n_s は粒子表面の単位面積当たりの界面活性剤分子の数，k_B はボルツマン定数，T は液温である．

粒子に作用する力およびトルクは式(1)よりベクトル演算より容易に得られる．すなわち，式(1)の第 1 式より，粒子 j が粒子 i に作用する磁気力 $\boldsymbol{F}_{ij}^{(m)}$ と磁気トルク $\boldsymbol{T}_{ij}^{(m)}$ が導出でき，式（1）の第 2 式より界面活性剤層の重畳による斥力 $\boldsymbol{F}_{ij}^{(V)}$ が得られ，さらに，印加磁場との相互作用により生じるトルク $\boldsymbol{T}_p^{(H)}$ が式（1）の第 3 式より表すことができる．詳細は文献（Satoh, 2003, 2017）に載っているので，ここでは表式を示すことはしない．

3. 振動磁場

磁気粘性効果に及ぼす磁性粒子の凝集現象を検討する場合には，通常一様印加磁場下での単純せん断流を対象とする．一方，本研究のように，粒子の磁気モーメントの緩和現象に基づいた発熱効果を検討する場合には，磁場の方向が一方向で変化する振動磁場下での現象を問題にすることになる．

印加磁場方向を x 軸に沿った方向とすると，印加磁場 $\boldsymbol{H}$ は時間に依存した量となり，次のように表される．

$$\boldsymbol{H}(t) = (H_0\sin(\omega_H t))\boldsymbol{h} \tag{2}$$

ここに $\boldsymbol{h}$ は x 軸方向の単位ベクトルで $\boldsymbol{h}=(1, 0, 0)$ であり，H_0 は印加磁場の最大値である．周期の時間 T_{cycl} $(=2\pi/\omega_H)$ の前半は x 軸の正方向に磁場が作用し，後半は x 軸の負の方向に作用することになる．

4. ブラウン動力学

磁性粒子は振動磁場の環境下でブラウン運動しながら並進および回転運動を行う．このような運動をシミュレートする場合には，粒子のブラウン運動を的確に誘起させるシミュレーション法を用いる必要があるが，本研究ではシミュレーション法としてブラウン動力学法（Allen and Tildesley, 1987, Satoh, 2003, 2010）を採用する．

球状粒子のブラウン運動を含めた並進運動をシミュレートする方程式は，粒子の位置ベクトルを $\boldsymbol{r}(t)$ とすれば，次のように表される．

$$\boldsymbol{r}(t+\Delta t) = \boldsymbol{r}(t) + \frac{1}{k_B T}D^T\boldsymbol{F}(t)\Delta t + \Delta r_1^B\boldsymbol{\delta}_1 + \Delta r_2^B\boldsymbol{\delta}_2 + \Delta r_3^B\boldsymbol{\delta}_3 \tag{3}$$

[DOI: 10.1299/transjsme.18-00030]

なお，表記の簡略化のために，粒子の区別を表す下付き添字 i を省略している．式（3）において，D^T は並進の拡散係数で，η を母液の粘度とすると，$D^T = k_B T/(3\pi\eta d)$ で表される．$\boldsymbol{F}(t)$ は前述の粒子に作用する磁気力および界面活性剤による斥力の和で，$(\boldsymbol{\delta}_1, \boldsymbol{\delta}_2, \boldsymbol{\delta}_3)$ は各軸方向を表す単位ベクトルである．また，$\Delta r_1^B, \Delta r_2^B, \Delta r_3^B$ は粒子の並進のブラウン運動を誘起させるランダム変位で，次のような確率特性を有する．

$$\langle \Delta r_1^B \rangle = \langle \Delta r_2^B \rangle = \langle \Delta r_3^B \rangle = 0, \qquad \langle (\Delta r_1^B)^2 \rangle = \langle (\Delta r_2^B)^2 \rangle = \langle (\Delta r_3^B)^2 \rangle = 2D^T \Delta t \tag{4}$$

粒子の回転運動の方程式より，磁気モーメントの方向 $\boldsymbol{e}$ を与える式が次のように得られる（Satoh, 2015a, 2015b）．

$$\boldsymbol{e}(t+\Delta t) = \boldsymbol{e}(t) + \frac{1}{kT} D^R \boldsymbol{T}(t) \times \boldsymbol{e}\Delta t + \Delta\phi_1^B \boldsymbol{\delta}_1 + \Delta\phi_2^B \boldsymbol{\delta}_2 + \Delta\phi_3^B \boldsymbol{\delta}_3 \tag{5}$$

ここに，D^R は回転の拡散係数で $D^R = k_B T/(\pi\eta d^3)$，$\Delta\phi_1^B, \Delta\phi_2^B, \Delta\phi_3^B$ は粒子の回転のブラウン運動を誘起させるランダム変位で，次のような確率特性を有する．

$$\langle \Delta\phi_1^B \rangle = \langle \Delta\phi_2^B \rangle = \langle \Delta\phi_3^B \rangle = 0, \qquad \langle (\Delta\phi_1^B)^2 \rangle = \langle (\Delta\phi_2^B)^2 \rangle = \langle (\Delta\phi_3^B)^2 \rangle = 2D^R \Delta t \tag{6}$$

5. 磁気モーメントの緩和現象による発熱効果

振動磁場中での磁性粒子の発熱現象は，磁性粒子の磁気モーメントの緩和現象から生じ，主にネール緩和とブラウン緩和の二つのメカニズムから生じる．ネール緩和での発熱現象の場合，磁気モーメントが磁場に追随しようとするために，粒子内で方向を変えることによる，磁気モーメントの緩和現象から発熱効果が得られる．一方，ブラウン緩和による発熱現象は，磁気モーメントが粒子内で固定され，粒子自体がまわりの流体中で回転することによる摩擦熱より発熱効果が得られるものである．概略的に言えば，磁性粒子が 10 nm オーダーより小さくなるとネール緩和が支配的となり，それよりも大きくなるとブラウン緩和が発熱効果として支配的となる．現在多く行われているのはネール緩和を用いた磁気温熱療法への応用である．しかしながら，ブラウン緩和による発熱効果の応用も可能性としては研究するべき対象であり，実際に大きな磁性粒子と見なせる磁性エマルジョン液滴によるブラウン運動緩和による発熱効果の研究も行われるに至っている（Lahiri et al., 2017）．磁性粒子の磁化特性を設計工学的に調製する技術（Erb et al., 2009）も大きく進展してきていることを鑑みると，ブラウン緩和が主たる寄与をする磁性粒子サスペンションの緩和現象を詳細に解明することは，物理現象の解明という学術的な観点に加えて，応用上の観点においても，非常に重要である．なぜなら，磁性粒子の振動磁場中での凝集現象は磁気モーメントの緩和現象すなわち発熱効果に非常に大きな影響与えると予期されるからである．このような粒子の凝集を考慮したミクロな立場から解明するには，本研究で採用するブラウン動力学法などの粒子シミュレーション法を採用することで，初めて可能となる．

磁性粒子サスペンションにおいて，磁化の強さ $\boldsymbol{M}$ を誘起させるために，振動磁場の 1 周期の間に系になされた単位体積当たりの仕事量 W_{cycl} は，振動磁場 $\boldsymbol{H}$ を用いて次のように表される（Rosensweig, 2002）．

$$W_{cycl}^{total} = \mu_0 \oint \boldsymbol{H} \cdot d\boldsymbol{M} \tag{7}$$

この式が図 1 に示すような，H–M 曲線が描くヒステリシス・ループの囲む面積であることを考慮すると，式（7）は次のようにも書ける．

$$W_{cycl}^{total} = -\mu_0 \oint \boldsymbol{M} \cdot d\boldsymbol{H} = -\mu_0 m H_0 \hat{N} \oint \langle nx \rangle d(H/H_0) = -\mu_0 m H_0 \hat{N} \oint (\langle nx \rangle + 1) d(H/H_0) \tag{8}$$

ここに，$\hat{N}$ は単位体積当たりの磁性粒子の数，H は磁場の強さで式（2）より $H/H_0 = \sin(\omega_H t)$ である．本研究では，粒子 1 個当たりの仕事量 W_{cycl} を対象とすることにする．すなわち，

[DOI: 10.1299/transjsme.18-00030]

$$W_{cycl} = -\mu_0 m H_0 \oint (\langle n_x \rangle + 1) d(H / H_0) \tag{9}$$

以上の式において$\langle n_x \rangle$は，磁気モーメントの方向を表す単位ベクトル$\boldsymbol{n}$のx方向成分n_xの粒子平均で，時間の関数となる．この仕事量W_{cycl}が磁気温熱療法に用いられる発熱量に相当する．

式（9）で表された仕事量をシミュレーションで求めるためには，図1に示したように，1周期を4つの部分に分割した積分を評価して求める．例えば，最初の第 1 の積分区間の積分値を$E^{(1)}_{hyste}$とすると，次のような線積分で表すことができる．

$$E^{(1)}_{hyste} = -\mu_0 m H_0 \int_{H^{(1)}_{st}}^{H^{(1)}_{ed}} (\langle n_x \rangle + 1) d(H / H_0) \tag{10}$$

同様にして，他の積分区間での値$E^{(2)}_{hyste}$，$E^{(3)}_{hyste}$，$E^{(4)}_{hyste}$を求めると，仕事量W_{cycl}が$W_{cycl} = E^{(1)}_{hyste} + E^{(2)}_{hyste} + E^{(3)}_{hyste} + E^{(4)}_{hyste}$として得られる．

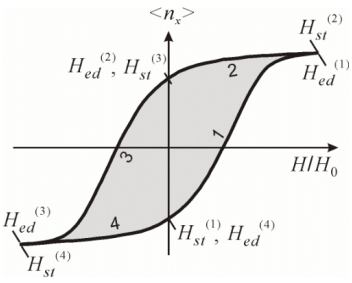

Fig. 1 Hysteresis loop of a magnetic field-magnetization curve. The area of the hysteresis loop is evaluated from the four linear integrals. A large area leads to a stronger effect of heat generation.

6. 表式の無次元化

本現象を支配する主たる要因は，粒子間磁気力，印加磁場，流体粘性力，ランダム力である．基礎方程式を無次元化するとこれらの要因が無次元パラメータとして明確に現れるようになる．諸量の無次元化に際して，次のような代表値を用いる．距離を粒子の固体部の直径d，時間を印加磁場の周期$2\pi/\omega_H$，速度を$\omega_H d/(2\pi)$，角速度をω_H，力は球の粘性摩擦力に取り$(3/2)\eta\omega_H d^2$，トルクを同様に$\pi\eta\omega_H d^3$，エネルギーをkTの代表値を採用する．以下においては，無次元化した式の最終結果のみを示すとともに（Satoh, 2015a, 2015b），無次元化の過程で生じた無次元パラメータの意味するところも併せて示す．なお，無次元化された物理量は上付き添字*を付して表すことにする．

並進運動の運動方程式：

$$\boldsymbol{r}^*(t^* + \Delta t^*) = \boldsymbol{r}^*(t^*) + \boldsymbol{F}^*(t^*)\Delta t^* + \Delta r_1^{B*}\boldsymbol{\delta}_1 + \Delta r_2^{B*}\boldsymbol{\delta}_2 + \Delta r_3^{B*}\boldsymbol{\delta}_3 \tag{11}$$

$$\langle \Delta r_1^{B*} \rangle = \langle \Delta r_2^{B*} \rangle = \langle \Delta r_3^{B*} \rangle = 0, \qquad \langle (\Delta r_1^{B*})^2 \rangle = \langle (\Delta r_2^{B*})^2 \rangle = \langle (\Delta r_3^{B*})^2 \rangle = 2R_B \Delta t^* \tag{12}$$

式（12）に現れたR_Bは粘性力に対するランダム力の大きさを表す無次元パラメータで，次のように定義される．

$$R_B = \frac{k_B T}{3\pi\eta d^3} \cdot \frac{2\pi}{\omega_H} \tag{13}$$

[DOI: 10.1299/transjsme.18-00030]

粒子の方向を与える方程式：

$$\boldsymbol{e}(t^*+\Delta t^*)=\boldsymbol{e}(t^*)+2\pi\boldsymbol{T}^*(t^*)\times\boldsymbol{e}\Delta t^*+\Delta\phi_1^B\boldsymbol{\delta}_1+\Delta\phi_2^B\boldsymbol{\delta}_2+\Delta\phi_3^B\boldsymbol{\delta}_3 \tag{14}$$

$$\langle\Delta\phi_1^B\rangle=\langle\Delta\phi_2^B\rangle=\langle\Delta\phi_3^B\rangle=0,\qquad\langle(\Delta\phi_1^B)^2\rangle=\langle(\Delta\phi_2^B)^2\rangle=\langle(\Delta\phi_3^B)^2\rangle=2(3R_B)\Delta t^* \tag{15}$$

粒子間相互作用による力とトルク（Satoh, 2015a, 2015b）：

$$\boldsymbol{F}_{ij}^{(m)*}=-R_m\frac{1}{r_{ij}^{*4}}\left[-(\boldsymbol{n}_i\cdot\boldsymbol{n}_j)\boldsymbol{t}_{ij}+5(\boldsymbol{n}_i\cdot\boldsymbol{t}_{ij})(\boldsymbol{n}_j\cdot\boldsymbol{t}_{ij})\boldsymbol{t}_{ij}-\{(\boldsymbol{n}_j\cdot\boldsymbol{t}_{ij})\boldsymbol{n}_i+(\boldsymbol{n}_i\cdot\boldsymbol{t}_{ij})\boldsymbol{n}_j\}\right] \tag{16}$$

$$\boldsymbol{T}_{ij}^{(m)*}=-R_m\frac{1}{2\pi r_{ij}^{*3}}\left\{(\boldsymbol{n}_i\times\boldsymbol{n}_j)-3(\boldsymbol{n}_j\cdot\boldsymbol{t}_{ij})\boldsymbol{n}_i\times\boldsymbol{t}_{ij}\right\} \tag{17}$$

$$\boldsymbol{F}_{ij}^{(V)*}=R_V\frac{1}{\delta^*}\boldsymbol{t}_{ij}\ln\frac{1+2\delta^*}{r_{ij}^*}\qquad(1\le r_{ij}^*\le 1+2\delta^*) \tag{18}$$

式（16），（17）に現れた R_m は粘性力に対する粒子間磁気力の大きさを表す無次元パラメータ，式（18）に現れた R_V は粘性力に対する界面活性剤による斥力の大きさを表す無次元パラメータであり，次のように定義される．

$$R_m=\frac{\mu_0 m^2}{2\pi\eta d^6\omega_H}=3R_B\lambda,\qquad R_V=\frac{\pi n_s kT}{3\eta d\omega_H}=R_B\lambda_V \tag{19}$$

粒子と磁場との相互作用によるトルク：

$$\boldsymbol{T}_i^{(H)*}=R_H\sin(2\pi t^*)\boldsymbol{n}_i\times\boldsymbol{h} \tag{20}$$

ここに，R_H は粘性力によるトルクに対する磁場による磁気トルクの大きさを表す無次元パラメータで，次のように表される．

$$R_H=\frac{\mu_0 mH_0}{\pi\eta d^3\omega_H}=\frac{3}{2\pi}R_B\xi \tag{21}$$

式（19），（21）に現れた λ,ξ,λ_V は熱運動に対する粒子間磁気力の相互作用，磁場の強さ，界面活性剤による相互作用の大きさを表す無次元パラメータで，次のように定義される．

$$\lambda=\frac{\mu_0 m^2}{4\pi d^3 k_B T},\qquad\xi=\frac{\mu_0 mH_0}{k_B T},\qquad\lambda_V=\frac{\pi n_s d^2}{k_B T} \tag{22}$$

これらの無次元パラメータ λ,ξ,λ_V は一様磁場中における凝集現象の結果（Satoh, 2010）と比較するときに有用である．

シミュレーションに際しては，λ,ξ,λ_V の値を過去の一様磁場中でのシミュレーションを参考に設定し，R_B の値を種々に設定してシミュレーションを行うことで，粘性力の影響，すなわち，振動磁場の振動数の影響を検討することになる．なお，R_B の値が 1 より十分小さいとき，すなわち，高振動数の振動磁場のときには粘性力が支配的となり，反対に，R_B の値が 1 より十分大きいとき，すなわち，低振動数のときには，粘性力に対してブラウン運動が支配的となる．後者の場合，さらに λ,ξ の大小関係で，凝集構造や粒子の磁場方向への配向特性が大きく異なるようになる．

粒子 1 個当たりの仕事量すなわち発熱量：

[DOI: 10.1299/transjsme.18-00030]

$$W^*_{cycl} = -\xi \oint (\langle nx \rangle + 1) d(H / H_0) \tag{23}$$

$$E^{(1)*}_{hyste} = -\xi \int_{H^{(1)}_{sat}}^{H^{(1)}_{sat}} (\langle n_x \rangle + 1) d(H / H_0) \tag{24}$$

7. シミュレーションのための諸量の設定

特に断らない限り，シミュレーションに際して次のようなパラメータの値を設定した．磁性粒子の粒子数 N を N=125 (=5^3)，体積分率 ϕ_V (=$N(\pi/6)d^3/V$ （V：シミュレーション領域の体積）を ϕ_V=0.02，立方体のシミュレーション領域の一辺の長さは l_x^*(=l_x/d)=l_y^*=l_z^*=14.85，時間きざみ Δt^* を Δt^*=0.0005，シミュレーションのトータルな無次元時間 t_{total}^*は 20 周期分の時間である t_{total}^*=20，その内 t_{total}^*=10 以後（トータルな無次元時間の 50% ）で得られた値を用いて平均操作を行って着目する量を求めている．また，界面活性剤の厚さ δ^*を δ^*=0.15，粒子間斥力による相互作用の大きさを λ_V=150 とした．磁気的な粒子間相互作用の無次元パラメータ λ は λ=1, 5, 10，磁場の強さ ξは ξ=1, 5, 10，流体粘性力に対するランダム力の大きさを表す無次元パラメータ R_B は R_B=0.1, 1, 5, 10, 15 と設定している．参考までに，マグネタイト粒子の物性値を用いて無次元パラメータの値を求めた結果を示す．Rosensweig の論文（Rosensweig, 2002）を参考にすると，磁化の強さを M=4.46×10^5A/m，粒子直径を d=1.8×10^{-8}m，磁気モーメントを m=$M\pi d^3/6$=1.36×10^{-18}A·m^2，粘度を η=1×10^{-3}Pa·s，磁場の強さを H_0=1×10^4A/m，温度を T=293K，磁場の振動数を 20×10^3Hz とすれば，無次元パラメータの値は，λ=7.86，ξ=4.23，R_B=3.68 となる．シミュレーションはこれらの値を含んだ広い領域の値を設定して行っている．

なお，今回の研究では比較的小さな系 N=125 を取り扱ったが，N=512 (=8^3)と大きな系にしても，凝集構造やヒステリシス・ループ曲線に関しては本質的に変化ない．ただし，ヒステリシス・ループの面積から算出される発熱量に関して，N=125 の系の本結果は，顕著な鎖状クラスタが磁場方向に配向する場合には，約 10 パーセント程度大きな値を与える傾向があるが，定性的な結論は全く変わらないことを確認している．

8. 結果と考察

8・1 凝集構造の時間変化

まず，磁性粒子の凝集構造が，振動磁場下において，時間とともにどのように変化するかを検討する．従来の熱力学的平衡状態のシミュレーションの結果より，λ≈4 程度の粒子間相互作用の大きさから顕著なクラスタを形成するようになることがわかっている（Satoh, 2017）．さらに，ξ≈5 程度以上大きくなると印加磁場の影響が顕著に現れるようになる．本研究の場合，このような凝集構造が，R_B の値によって，振動磁場の変化で受ける影響の度合いが異なることになる．先に指摘したように，R_B の値が大きいということは，振動磁場の振動数が小さいことを意味し，凝集構造に及ぼす流体粘性力の影響が小さくなることになる．

図 2 は，λ=10, ξ=10, R_B=10 の場合に対して，振動磁場の変化に関して粒子の凝集構造がどのように変化するかを見るために，振動磁場の変位角度 θ_{time} （=$\omega_H t^*$, 0°~360°で定義）を θ_{time} =0°, 45°, 90° とした凝集構造のスナップショットを示したものである．粒子間の磁気的な相互作用が λ=10 と非常に大きいので，顕著な鎖状クラスタを形成し，さらに（最大）印加磁場が ξ=10 と非常に大きいので，鎖状クラスタは印加磁場方向（x 軸方向）に顕著に配向していることが確認できる．図 2（a）の θ_{time} =0°の場合，振動磁場の方向が x 軸の負の方向から正の方向に切り替わる点でのスナップショットであるが，粒子の磁気モーメントは依然としてほとんどが x 軸の負の方向に配向していることがわかる．これは粒子間の磁気力が非常に大きいので，磁場の強さがある程度大きくなるまで，安定な鎖状クラスタを維持することによるものである．従って，図 2（b）の θ_{time} =45°の場合には，磁場の強さがかなり上昇するので，かなりの磁性粒子の磁気モーメントが磁場方向に配向しようとする傾向が見て取れる．さらに磁場が大きい図 2（c）の θ_{time} =90°の場合には，ほとんどの磁性粒子の磁気モーメントが磁場方向（x 軸方向）に配向していることが確認できる．従って，後に考察するように，粒子の磁気モーメントの配向は振動磁場の変化に対してかなり位相が遅れることがわかる．このような位相の遅れは流体の粘性力が大きいほど粒子の回転運動が緩慢となることに起因するが，さらに，磁性粒子間の磁気力がより一層このような傾向を強める．すなわち，より安定した鎖状クラスタは，振動磁場の時間変化に追随しにくくなる特徴が，より顕著に現れることを意味し

[DOI: 10.1299/transjsme.18-00030]

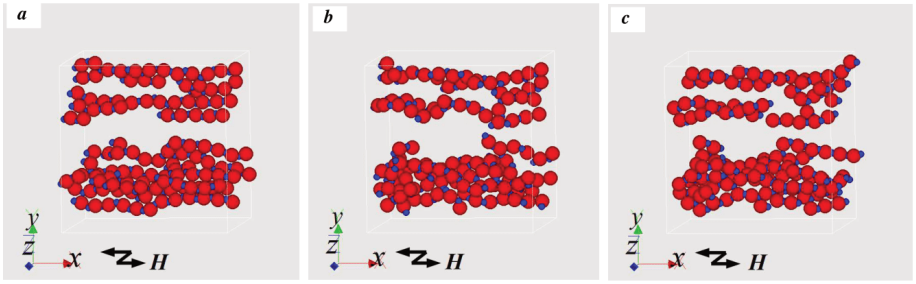

Fig. 2 Time change in the aggregate structures of magnetic particles for R_B=10, λ=10 and ξ=10: (a) θ_{time}= 0°, (b) θ_{time}= 45° and (c) θ_{time}= 90°. The direction of the magnetic moment is recognized by a blue (dark) small dot on each sphere. The magnetic moment of each particle is reoriented toward the magnetic field direction with a delay without dissociation of the chain-like clusters.

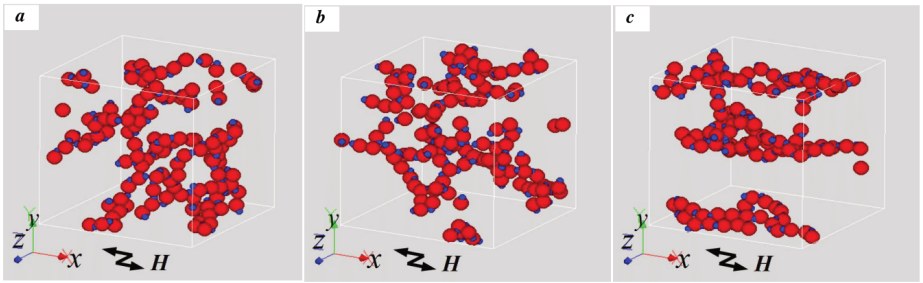

Fig. 3 Aggregate structures of magnetic particles at θ_{time}= 45° for λ=10 and ξ=10: (a) R_B=0.1, (b) R_B=1 and (c) R_B=5. A stronger viscous force (R_B=0.1) leads to a weaker tendency of the reorientation of the magnetic moments toward the field direction.

ている．ここで注目すべき点は，鎖状クラスタは印加磁場の方向が逆転しても崩壊することはなく，鎖状クラスタを形成する各粒子の磁気モーメントが磁場方向に変化することで，鎖状クラスタの形成を維持しながら，振動磁場の変化に追随している点である．ただし，後に明らかになるように，このような状況は流体の粘性力がブラウン運動に対して支配的でない R_B =10 の場合に生じるものであり，R_B =0.1 のような粘性力が支配的な場合は異なる状況（応答特性）が生じるようになる．

8・2 凝集構造の磁場の振動数への依存性

前節では，凝集構造が振動磁場の変化に対して，どのように凝集構造が応答するかを，粘性力があまり支配的でない場合に焦点を絞って議論した．本節では，ランダム力に対して粘性力の影響を変化させた場合，鎖状クラスタの応答がどのように変化するかを議論する．

図 3 は，λ=10, ξ=10 の場合に対して，粘性力の影響を R_B =0.1, 1, 5 の 3 通りに取って得たスナップショット結果である．なお，鎖状クラスタおよび磁気モーメントの方向の応答の状況が，より明確に確認できる θ_{time} =45°の時点でのスナップショットが示してある．さらに，考察に際しては，R_B =10 の場合である図 2（b）の結果も考慮に入れる．図 3（a）の R_B =0.1 の場合はランダム力に対して粘性力が非常に支配的となるので，鎖状クラスタは磁場方向に配向する強い傾向を有さず，かなりばらけた鎖状クラスタや小さなクラスタを形成していることがわかる．各粒子の磁気モーメントの方向も，図 2（b）の結果と比較して，磁場方向（x 方向）に配向する傾向がかなり弱い．すなわち，磁気モーメントの振動磁場への応答は非常に緩慢であることが理解できる．これは，粒子が

[DOI: 10.1299/transjsme.18-00030]

回転して磁場方向を向こうとしても，粘性力が大きいので，摩擦力によりそのような状況が生じにくいことによるものである．粘性力の影響を R_B =1, 5, 10 と小さくしていくと，より顕著な鎖状クラスタが，磁場方向により顕著に配向するようになることがわかる．さらに，鎖状クラスタを構成する粒子の磁気モーメントも，より顕著に磁場方向に配向するようになることが確認できる．このように，R_B の値が小さくなるほど，すなわち，振動磁場の振動数が大きくなるほど，粘性力が現象をより大きく支配するようになり，磁性粒子のクラスタの構造が粘性力によって著しい影響を受けるようになる．さらに，磁気モーメントの磁場方向への配向の応答が著しく遅れることになる．このことはもちろん，粘性力が磁気力に対して大きくなると，磁性粒子の並進や回転運動の特性時間が振動磁場の特性時間と比較して長くなるので，そのような磁性粒子の運動が振動磁場の周期内において十分成されないことになる．

8・3 磁化–磁場曲線のヒステリシス曲線

前節までで，振動磁場に対する磁性粒子の凝集構造と磁気モーメントの応答を，種々の条件下で得たスナップショットの結果を用いて詳細に明らかにした．本節から，これらの解析結果を受けて，磁性粒子の磁気粒子温熱療法への応用に際して重要な，発熱効果の特性を考察する．なお，先に言及したように，磁場–磁化曲線のヒステリシス・ループの描く曲線の面積が大きいほど，磁気モーメントのブラウン緩和に基づく発熱効果が大きくなることに注意されたい．

図 4（a）は式（23）で表された発熱効果を現す仕事量を評価するために必要な，正規化された磁場 H_x^* と正規化された磁化 $\langle n_x \rangle$ に関するヒステリシス曲線を調べた結果であり，λ=ξ=10 の場合に対して R_B=0.1, 1, 5, 10, 15 の 5 通りの結果が示してある．図 4（b）は λ=1, ξ=10 の場合に対する同様の結果である．

まず，図 4（a）の粒子間磁気力がランダム力より十分大きな場合を考察する．粘性力が支配的となる磁場の振動数が大きい R_B=0.1 の場合，$\langle n_x \rangle$ の値は最大でも $\langle n_x \rangle \approx 0.3$ 程度なので，ヒステリシス・ループが与える面積は非常に小さなものとなってしまう．このように，磁気モーメントが振動磁場の変化に十分応答しない場合には，面積が小さくなり大きな発熱効果が得られないことがわかる．この磁場の振動数への依存性は，小さな磁性粒子を対象としたネール緩和現象による結果と同様である（Gudoshnikov et al., 2012）．R_B の値が大きくなるほど，すなわち，振動磁場の振動数が小さくなるに従って，反対方向を向いた鎖状クラスタの磁気モーメントは磁場方向に配向するようになるのに大きな磁場の強さを必要とするようなる．例えば，R_B=10 の場合には，$H_x^* \approx 0.5$ 付近まで $\langle n_x \rangle$ は–1 に近い値を維持し，それから，磁場の強さの増加に従って急激に磁気モーメントが磁場方向に向きを反転するようになることがわかる．このように強く結合した鎖状クラスタ内の粒子同士の磁気的な相互作用は，磁気モーメントの磁場方向への配向を非常に遅らせる働きをする．その結果大きな面積のヒステリシス・ループを描くようになる．すなわち，大きな発熱効果が得られることになる．

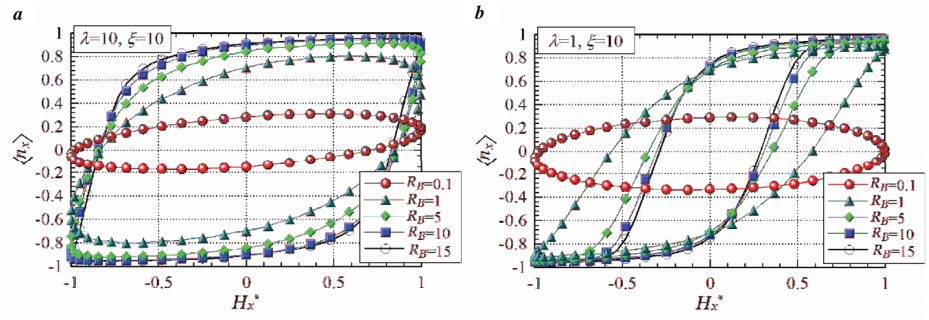

Fig. 4 Hysteresis loop of the magnetic field-magnetization curves: (a) λ=10 and ξ=10, and (b) λ=1 and ξ=10. In the case of the viscous force being dominant (R_B=0.1), the magnetic moments of particles do not sufficiently reorient toward the magnetic field direction, which leads to a smaller area of the hysteresis loop.

[DOI: 10.1299/transjsme.18-00030]

次に，図 4（b）の粒子間磁気力がランダム力に対して十分小さく，系内に顕著なクラスタが生じない場合の結果を考察する．系内に顕著なクラスタが形成されないので，ヒステリシス曲線の形状は粒子の磁気モーメントと印加磁場の相互作用ならびに粘性力でほぼ決定されることになる．以下においては，前述の図 4（a）に示した結果との相違点について主に考察する．まず，特徴的な点は，R_B=0.1 の粘性力が支配的な場合には，図 4（a）に示した同じ場合のループと比較して，かなり面積が拡大している．すなわち，より大きな発熱効果が得られることがわかる．これは，クラスタを形成することがないので，各粒子の磁気モーメントが磁場の変化に追随することを妨げる粒子間磁気力が作用しないことから生じるものである．このような粒子間磁気力による磁気モーメントの追随を妨げる要因がないことから，R_B≳1 では，各磁気モーメントは，磁場が x 軸の正方向へ反転した H_x^*≃0 の点から，磁場方向に配向しようとする傾向が顕著に現れるようになる．このことは，先の図 4（a）の場合の H_x^*≃0.5 付近からの配向の顕在化と非常に対照的である．さらに特徴的なことは，R_B の値が大きくなるほど，$\langle n_x \rangle$ ≃ 1 にほぼ到達する磁場の強さが，図 4（a）の場合と比較して非常に小さいことである．例えば，R_B =10 の場合，ほぼ H_x^*≃0.5 でこのような状態が達成されている．この傾向は R_B の値が大きくなるほど顕著となっていることが見て取れる．R_B の値が大きくなるほど，すなわち，粘性力が小さくなるほど，磁場の影響が顕著になり，粒子に作用する磁気トルクの影響が相対的に大きくなる．このことにより，より短い時間で磁気モーメントは磁場方向に配向することが可能となる．以上のことから，磁性粒子が凝集を生じないような，粒子間磁気力が小さい場合には，ブラウン緩和に基づく発熱効果を最大にする，振動数の最適値が存在するものと推察される．

8・4 磁気モーメントの緩和現象による発熱効果

最後に，粒子 1 個当たりの仕事量 W_{cycl}^*，すなわち，磁気モーメントの配向によるブラウン緩和現象に基づいた発熱量の結果を考察する．なお，磁性粒子サスペンションを磁気温熱療法に応用する場合には，この発熱効果が十分大きいことが求められる．

図 5 は発熱量の印加磁場の強さ ξ への依存性を調べた結果であり，流体粘性力がある程度弱い場合である R_B=5 と取り，粒子間磁気力の大きさは λ=1, 5, 10 の 3 通りに取って得た結果が載せてある．λ=1 の場合，ξ の値の増加とともに単調に増加するのは，式（23）からわかるように，磁気モーメントと磁場との相互作用の大きさ ξ が大きいほど大きな発熱効果が得られることになるからである．λ=10 の場合，ξ≲5 領域では λ=1 の値と比較して非常に小さな値となること，すなわち，非常に小さな発熱効果しか得られないことは，図 4 の R_B=0.1 のヒステリシス・ループ曲線および図 3(a)のスナップショットの結果から次のように推測される．粒子間磁気力が十分大きく，磁場が十分弱い場合には，鎖状クラスタは，磁場方向に配向する傾向が非常に弱く，さらに，クラスタ内の粒子の磁気モーメントは粒子間磁気力により振動磁場の変化に追随する傾向があまり大きくない．このことが，図 4 の R_B=0.1 のヒステリシス・ループ曲線よりも一

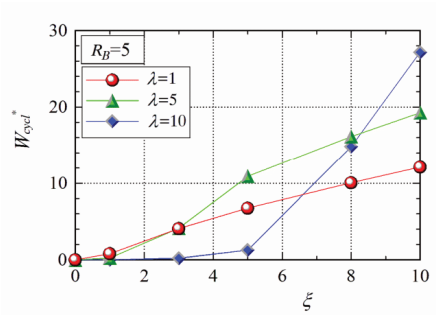

Fig. 5 Dependence of the heating effect on the applied magnetic field strength. For the case of λ=10, a large increase from ξ≃5 arises due to the inclination of the chain-like clusters in the magnetic field direction.

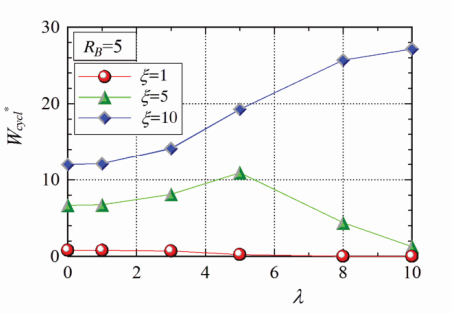

Fig. 6 Dependence of the heating effect on the magnetic particle-particle interaction strength. A decrease after λ≃ 5 with increasing values of λ in the case of ξ=5 implies that larger clusters do not significantly respond to the change in the magnetic field strength.

[DOI: 10.1299/transjsme.18-00030]

層面積が小さな(楕円体の短軸の長さが長軸の長さより非常に小さくなる)ループ曲線を与えることになり，発熱効果が小さくなってしまうことになる．一方，$\xi \gtrsim 5$ の領域で急激に発熱効果が増加し，$\xi=10$ では他の場合に比較して非常に大きな発熱効果を与えるようになる．これは先の磁場–磁化曲線のヒステリシス曲線のところで考察したように，強く結合した鎖状クラスタが磁場の強さとともに磁場方向に配向する傾向が強くなり，この状況下では各粒子が磁場の変化に追随することが非常に遅れ，その結果より大きな面積を有するヒステリシス・ループが得られる．すなわち，より大きな発熱効果を与えることになる．$\lambda=5$ の場合，$\xi \gtrsim 3$ 領域での類似の大きな発熱効果が得られるようになるのは，$\lambda=10$ の場合と同様の原理で説明できる．

図 6 は発熱量の粒子間相互作用の強さ λ への依存性を調べた結果であり，流体粘性力がある程度弱い場合である $R_B=5$ と取り，磁場の強さを $\xi=1$, 5, 10 の 3 通りに取って得た結果が示してある．$\xi=1$ のように印加磁場が弱い場合には，発熱効果が小さくなることは，式（23）から容易に想像できる．図 4（a）と（b）に示したヒステリシス・ループの特徴から，$\xi=10$ の場合，λ の値の増加とともに，すなわち，粒子間磁気力が強くなるほど，ループで囲まれた領域の面積が大きくなることから，発熱効果がより顕著に得られることになる．このように，安定した鎖状クラスタを磁場方向に形成するような粒子間磁気力と磁場の強さの場合には，より大きな発熱効果が得られることがわかる．ところが，非常に注目すべき結果は，$\xi=5$ の場合の粒子間相互作用の大きさへの依存性である．すなわち，λ の値とともに増加していた W_{cycl}^{*} の値が $\lambda=5$ 付近から著しく減少に転じる点である．この理由としては次のように考えられる．$\lambda \approx 5$ 付近までは λ の値の増加とともに，磁場方向により長い鎖状クラスタを形成するようになるが，このような鎖状クラスタは，$\xi=10$ の場合と同様に，粒子間相互作用により，振動磁場への追随が非常に遅れるようになる．その結果，ヒステリシス・ループの面積が大きくなり，発熱効果が大きくなる．ところが，$\lambda \approx 5$ 付近を超えた領域では，λ の値の増加とともに粒子間磁気力の影響が印加磁場の影響よりも支配的となるので，形成された鎖状クラスタは磁場方向に拘束されにくくなり，次第に磁場方向に沿った直線的なクラスタから，複雑に曲がりくねった立体的な鎖状クラスタを構成する．この鎖状クラスタを構成する粒子は，非常に強い粒子間磁気力の作用により磁場に対しほとんど追随しないため，$\langle n_x \rangle$ の最大値が 0 に漸近するようになる．これは，ヒステリシス・ループの面積は非常に小さくなることを意味するので，発熱効果がほぼゼロに収束するようになる．これらの傾向がネール緩和が主たるメカニズムである小さな粒子の場合でも生じることがわかる（Tan et al., 2014）．すなわち，粒子の体積分率が増すほど粒子間相互作用が重要となるので，磁場–磁化曲線のヒステリシス・ループの面積が小さくなり，従って発熱効果がゼロに漸近するようになる．

以上からわかることは，より強い印加磁場の環境下で，図 2 に示すような磁場方向に顕著な鎖状クラスタを形成する場合には，より大きな発熱効果が得られる．一方，顕著な鎖状クラスタは形成されるが，このような鎖状クラスタの配向が振動磁場方向に拘束されない環境下では，大きな発熱効果が得られない．

9. 結　　言

ブラウン動力学シミュレーションにより，振動磁場下での磁性粒子サスペンションの凝集現象を明らかにするとともに，磁気温熱療法への応用に際して重要な，磁気モーメントのブラウン緩和現象による発熱効果と凝集現象との関係を明らかにした．本現象を特徴づける主たる要因は，振動磁場に起因する流体粘性力，印加磁場の強さ，粒子間に作用する磁気的な相互作用である．これらの要因の大小関係で，凝集構造ならびに発熱効果が大きく異なる結果を与えることになる．本研究で得られた主な結果を要約すると次のようになる．より安定した鎖状クラスタが磁場方向に形成される状況下では，粒子間の磁気的な相互作用により，粒子の磁気モーメントの配向は振動磁場の変化に対してかなり位相が遅れる．鎖状クラスタは印加磁場の方向が反転しても崩壊することはなく，鎖状クラスタを形成する各粒子の磁気モーメントが磁場方向に変化することで，鎖状クラスタの形成を維持しながら，振動磁場の変化に追随する．振動磁場の振動数が大きくなるほど，粘性力が現象をより大きく支配するようになるので，磁性粒子のクラスタの構造が著しい影響を受けるとともに，磁気モーメントの磁場方向への配向の応答が著しく遅れる．系に顕著なクラスタが形成されないような粒子間磁気力が小さい場合，磁気モーメントの振動磁場への応答を遅らせる要因は流体粘性による摩擦力のみとなるので，振動磁場の変化に対する応答は非常に速やかになる．以上の磁気モーメントの振動磁場の変化への応答特性から，次のような発熱効果の特徴を得る．凝集構造が形成されるに十分な粒子間磁気力($\lambda \gtrsim 5$ 程度)が作用する場合，粒子間磁気力が大きい場合ほどより大きな発熱効果が得られる．磁場の強さを増していくと，強く結合した鎖状クラスタが磁場方向に配向する

[DOI: 10.1299/transjsme.18-00030]

傾向が強くなり，この状況下では各粒子が磁場の変化に追随することが非常に遅れる．これに起因して，大きな面積を有するヒステリシス・ループが得られ，大きな発熱効果が得られる．このときの無次元パラメータの関係は，$\xi \approx \lambda$である．一方，顕著な鎖状クラスタは形成されるが，このような鎖状クラスタの配向が振動磁場方向に拘束されない環境下では，大きな発熱効果が得られない．

今後の課題としては，より効果的な発熱条件を解明するために，棒状やキューブ状などの粒子モデルを用いたシミュレーションによる形状の違いが与える影響の検討，また流体力学的な粒子間作用を含む解析や，従来のネール緩和とブラウン緩和の境界付近での発熱現象の解明などが挙げられる．

References

Abbas, M. and Bossis, G., Separation of two attractive ferromagnetic ellipsoidal particles by hydrodynamic interactions under alternating magnetic field, Physical Review E, Vol. 95 (2017), pp. 062611.

Allen, M. P. andTildesley, D. J., Computer Simulation of Liquids (1987), Clarendon Press.

Alphandéry, E., Faure, S., Raison, L., Duguet, E., Howse, P. A. and Bazylinski, D. A., Heat production by bacterial magnetosomes exposed to an oscillating magnetic field, Journal of Physical Chemistry C, Vol. 115 (2011), pp 18–22.

Branquinho, L.C., Carriao, M. S., Costa, A. S., Zufelato, N., Sousa, M. H., Miotto, R., Ivkov, R. and Bakuzis, A. F., Effect of magnetic dipolar interactions on nanoparticle heating efficiency: Implications for cancer hyperthermia, Scientific Reports, Vol. 3 (2013), pp. 2887.

Bruce, I. J. and Sen, T., Surface modification of magnetic nanoparticles with alkoxysilanes and their application in magnetic bioseparations, Langmuir, Vol. 21 (2005), pp. 7029-7035.

Bullough, W. A., (Ed.), Electro-Rheological Fluids, Magneto-Rheological Suspensions and Associated Technology (1996), World Scientific.

Burrows, F., Parker, C., Evans, R. F. L., Hancock, Y., Hovorka, O. and Chantrell, R. W., Energy losses in interacting fine-particle magnetic composites, Journal of Physics D: Applied Physics, Vol. 43 (2010), pp. 474010.

Conde-Leboran, I., Baldomir, D., Martinez-Boubeta, C., Chubykalo-Fesenko, O., del Puerto Morales, D., Salas, G., Cabrera, D., Camarero, J., Teran, F. J. and Serantes, D., A single picture explains diversity of hyperthermia response of magnetic nanoparticles, Journal of Physical Chemistry C, Vol. 119 (2015a), pp. 15698–15706.

Conde-Leboran, I., Serantes, D. and Baldomir, D., Orientation of the magnetization easy axes of interacting nanoparticles: Influence on the hyperthermia properties, Journal of Magnetism and Magnetic Materials, Vol. 380 (2015b), pp. 321-324.

Coughlan, A. C. H. and Bevan, M. A., Rotating colloids in rotating magnetic fields: Dipolar relaxation and hydrodynamic coupling, Physical Review E, Vol. 94 (2016), pp. 042613.

De Las Cuevas, G., Faraudo, J. and Camacho, J., Low-gradient magnetophoresis through field-induced reversible aggregation, Journal of Physical Chemistry C, Vol. 112 (2008), pp. 945–950.

Erb, R. M., Son, H. S., Samanta, B., Rotello, B. M. and Yellen, B. B., Magnetic assembly of colloidal superstructures with multipole symmetry, Nature, Vol. 457 (2009), pp. 999–1002.

Girginova, P. I., Daniel-da-Silva, A. L., Lopes, C. B., Figueira, P., Otero, M., Amaral, V. S., Pereira, E. and Trindade, T., Silica coated magnetite particles for magnetic removal of Hg2+ from water, Journal of Colloid and Interface Science, Vol. 345 (2010), pp. 234-240.

Golovin, Y. I., Gribanovsky, S. L., Golovin, D. Y., Klyachko, N. L., Majouga, A. G., Master, A. M., Marina, S. and Kabanov, A. V., Towards nanomedicines of the future: Remote magneto-mechanical actuation of nanomedicines by alternating magnetic fields, Journal of Controlled Release, Vol. 219 (2015), pp. 43-60.

Gudoshnikov, S. A., Liubimov, B. Y. and Usov, N. A., Hysteresis losses in a dense superparamagnetic nanoparticle assembly, AIP Advances, Vol. 2 (2012), pp. 012143.

Guibert, C., Dupuis, V., Peyre, V. and Fresnais, J., Hyperthermia of magnetic nanoparticles: Experimental study of the role of aggregation, Journal of Physical Chemistry C, 119 (2015), pp. 28148–28154.

[DOI: 10.1299/transjsme.18-00030]

Haase, C. and Nowak, U., Role of dipole-dipole interactions for hyperthermia heating of magnetic nanoparticle ensembles, Physical Review B, Vol. 85 (2012), pp. 045435.

Häfeli,U., Schütt, W., Teller, J. and Zborowski, M., (Eds.), Scientific and Clinical Applications of Magnetic Carriers (1997), Springer.

Harrell, J. W., Kang, S., Jia, Z., Nikles, D. E., Chantrell, R. W. and Satoh, A., Model for the easy-axis alignment of chemically synthesized L10 FePe nanoparticles, Applied Physics Letters, Vol. 87 (2005), pp. 202-208.

Kumar, C. S. S. R. and Mohammad, F., Magnetic nanomaterials for hyperthermia-based therapy and controlled drug delivery, Advanced Drug Delivery Reviews, Vol. 63 (2011), pp. 789-808.

Lahiri, B. B., Ranoo, S., Zaibudeen, A. W. and Philip, J., Magnetic hyperthermia in magnetic nanoemulsions: Effects of polydispersity, particle concentration and medium viscosity, Journal of Magnetism and Magnetic Materials, Vol. 441 (2017), pp. 310-327.

Lima, E., Biasi, E. D., Mansilla, M. V., Saleta, M. E., Granada, M., Troiani, H. E., Effenberger, F. B., Rossi, L. M., Rechenberg, H. R. and Zysle, R. D., Heat generation in agglomerated ferrite nanoparticles in an alternating magnetic field, Journal of Physics D: Applied Physics, Vol. 46 (2013), pp. 045002.

Llera, M., Codnia, J. and Jorge, G. A., Aggregation dynamics and magnetic properties of magnetic micrometer-sized particles dispersed in a fluid under the action of rotating magnetic fields, Journal of Magnetism and Magnetic Materials, Vol. 384 (2015), pp. 93-100.

Martínez-Boubeta, C., Simeonidis, K., Serantes, D., Conde-Leboran, I., Kazakis, I., Stefanou, G., Pena, L., Galceran, R., Balcells, L., Monty, C., Baldomir, D., Mitrakas, M. and Angelakeris, M., Adjustable hyperthermia response of self-assembled ferromagnetic Fe-MgO core–shell nanoparticles by tuning dipole–dipole interactions, Advanced Functional Materials, Vol. 22 (2012), pp. 3737–3744.

Mehdaoui, B., Tan, R. P., Meffre, A., Carrey, J., Lachaize, S., Chaudret, B. and Respaud, M., Increase of magnetic hyperthermia efficiency due to dipolar interactions in low anisotropy magnetic nanoparticles : Theoretical and experimental results, Physical Review B, 87 (2013), pp.174419.

Munoz-Menendez, C., Conde-Leboran, I., Baldomir, D., Chubykalo-Fesenko, O. and Serantes, D., The role of size polydispersity in magnetic fluid hyperthermia: average vs. local infra/over-heating effects, Physical Chemistry Chemical Physics, Vol. 17 (2015), pp. 27812-27820.

Patra, S., Roy, E., Karfa, P., Kumar, S., Madhuri, R. and Sharma, P. K., Dual-responsive polymer coated superparamagnetic nanoparticle for targeted drug delivery and hyperthermia treatment, ACS Applied Material and Interfaces, Vol. 7 (2015), pp 9235–9246.

Rosensweig, R. E., Magnetic fluid, Annual Review of Fluid Mechanics, Vol. 19 (1987), pp. 437-463.

Rosensweig, R.E., Heating magnetic fluid with alternating magnetic field, Journal of Magnetism and Magnetic Materials, Vol. 252 (2002), pp. 370-374.

Sánchez, J. H. and Rinaldi, C., Magnetoviscosity of dilute magnetic fluids in oscillating and rotating magnetic fields, Physics of Fluids, Vol. 22 (2010), pp. 043304.

Satoh, A., Introduction to Molecular-Microsimulation of Colloidal Dispersions (2003), Elsevier.

Satoh, A., Introduction to Practice of Molecular Simulation: Molecular Dynamics, Monte Carlo, Brownian Dynamics, Lattice Boltzmann and Dissipative Particle Dynamics (2010), Elsevier.

Satoh, A., Brownian dynamics simulations with spin brownian motion on the negative magneto-rheological effect of a rod-like hematite particle suspension, Molecular Physics, Vol. 113 (2015a), pp. 656-670.

Satoh, A., Brownian dynamics simulation of a dispersion composed of disk-like hematite particles regarding aggregation phenomena, Colloid and Surfaces A, Vol.483 (2015b), pp. 328-340.

Satoh, A., Modeling of Magnetic Particle Suspensions for Simulations (2017), CRC Press.

Saville, S. L., Qi, B., Baker, J., Stone, R., Camley, R. E., Livesey, K. L., Ye, L., Crawford, T. M. and Mefford, O. T., The formation of linear aggregates in magnetic hyperthermia: Implications on specific absorption rate and magnetic anisotropy, Journal of Colloid and Interface Science, Vol. 424 (2014), pp. 141-151.

[DOI: 10.1299/transjsme.18-00030]

Schmidt, A. M., Thermoresponsive magnetic colloids, Colloid and Polymer Science, Vol. 285 (2007), pp. 953-966.

Serantes, D., Baldomir, D., Martinez-Boubeta, C., Simeonidis, K., Angelakeris, M., Natividad, E., Castro, M., Mediano, A., Chen, D.-X., Sanchez, A., Balcells, L. I. and Martínez, B., Influence of dipolar interactions on hyperthermia properties of ferromagnetic particles, Journal of Applied Physics, Vol. 108 (2010), pp. 073918.

Serantes, D., Simeonidis, K., Angelakeris, M., Chubykalo-Fesenko, O., Marciello, M., Del Puerto Morales, M., Baldomir, D. and Martinez-Boubeta, C., Multiplying magnetic hyperthermia response by nanoparticle assembling, Journal of Physical Chemistry C, Vol. 118 (2014), pp. 5927–5934.

Tan, M., Song, H., Dhagat, P., Jander, A. and Walker, T. W., Theoretical study of alignment dynamics of magnetic oblate spheroids in rotating magnetic fields, Physics of Fluids, Vol. 28 (2016), pp. 062004.

Tan, R. P., Carrey, J. and Respaud, M., Magnetic hyperthermia properties of nanoparticles inside lysosomes using kinetic Monte Carlo simulations: Influence of key parameters and dipolar interactions, and evidence for strong spatial variation of heating power, Physical Review B, Vol. 90 (2014), pp. 214421.

Verdes, C., Chantrell, R. W., Satoh, A., Harrell, J. W. and Nikles, D., Self-organization, orientation and magnetic properties of FePt nanoparticle arrays, Journal of Magnetism and Magnetic Materials, Vol.304 (2006), pp. 27-31.

Wereley, N. M., (Ed.), Magnetorheology: Advances and Applications (2013), Royal Society of Chemistry.

Yao, X., Sabyrov, K., Klein, T., Penn, R. L. and Wiedmann, T. S., Evaluation of magnetic heating of asymmetric magnetite particles, Journal of Magnetism and Magnetic Materials, Vol. 381 (2015), pp. 21-27.

[DOI: 10.1299/transjsme.18-00030]

Proceedings of the ASME 2018
International Mechanical Engineering Congress and Exposition
IMECE2018
November 9-15, 2018, Pittsburgh, PA, USA

IMECE2018-86544

BROWNIAN DYNAMICS SIMULATIONS OF AGGREGATION PHENOMENA IN A MAGNETIC PARTICLE SUSPENSION WITH AN ALTERNATING MAGNETIC FIELD (RELATIONSHIP BETWEEN THE AGGREGATE STRUCTURE AND THE HEAT PRODUCTION)

Seiya Suzuki
Department of Machine Intelligence and Systems Engineering
Akita Prefectural University
Yuri-honjo, Akita-pref. 015-0055
Japan
m20a014@akita-pu.ac.jp

Akira Satoh
Department of Machine Engineering
Akita Prefectural University
Yuri-honjo, Akita-pref. 015-0055
Japan
asatoh@akita-pu.ac.jp

Muneo Futamura
Department of Machine Engineering
Akita Prefectural University
Yuri-honjo, Akita-pref. 015-0055
Japan
futamura@akita-pu.ac.jp

ABSTRACT

The present study addresses physical phenomena of a suspension composed of magnetic spherical particles in an alternating magnetic field in order to elucidate particle aggregation phenomena and their influence on heat production. For this objective, we have performed Brownian dynamics simulations in a variety of circumstances of the magnetic field strength and frequency of an alternating magnetic field, and the magnetic dipole-dipole interaction strength. As in a time-independent uniform external magnetic field, large aggregates are formed in the case of strong magnetic particle-particle interactions. However, these clusters exhibit completely different behaviors that are dependent on the frequency of an alternating magnetic field. If the frequency is significantly high, then the viscous torque is the dominant factor, so that the formation of the clusters is not significantly influenced by the time-dependent magnetic field. If the frequency is significantly low, the magnetic field have a significant effect on the rotational motion of the particles, so that the formation of the cluster is dependent on which factor dominates the particle motion between the applied magnetic field and the magnetic particle-particle interaction. If the magnetic interaction is more dominant than the external field, stable chain-like clusters are formed in the field direction, and the magnetic particle-particle interaction induces a significant delay for the moments inclining in the alternating magnetic field direction. This behavior gives rise to a hysteresis loop with a larger area and therefore a large heating effect is obtained.

INTRODUCTION

A magnetic particle suspension is a hopeful functional fluid for application, and therefore many researchers have been actively conducting basic and application studies in a variety of fields such as fluid engineering, magnetic material engineering, biomedical engineering and environmental resource engineering. In the field of biomedical engineering, many researchers have been energetically investigating the application to magnetically guided drug delivery system [1] and magnetic particle hyperthermia treatment [2-5]. Multi-functional magnetic particles [6] exhibit a high heating performance in hyperthermia and an effective loading performance of anti-cancer drugs in drug delivery system.

The Neel relaxation mechanism is the governing factor for the heat production of magnetic particles smaller than approximately 10 nano-meters and, on the other hand, the Brownian relaxation mechanism governs the heat generation phenomena for particles larger than this order.

Although the Neel relaxation mode has been largely focused on for heat production up to the present, recently some researchers have been searching for a possibility of larger magnetic particles where the heat generation arises mainly from the Brownian relaxation mechanism. Studies in respect to the characteristics of heat production of these larger particles from the Brownian relaxation mechanism seem to be significantly important even from an academic point of view in order to further expand the application of magnetic particles in the

fields of magnetically drug delivery system and magnetic particle hyperthermia.

From this background, in the present study, we elucidate aggregation phenomena in a suspension composed of magnetic spherical particles in an alternating magnetic field in order to clarify the relationship between the particle aggregates and the heating effect due to Brownian relaxation mechanism.

MODEL OF MAGNETIC PARTICLES

We consider aggregation phenomena in a suspension composed of magnetic spherical particles in an alternating magnetic field and their influence on heat production due to Brownian relaxation mechanism. To do so, the following particle model is employed for Brownian dynamics simulations. If it is necessary to distinguish quantities of each particle, the subscripts i and j will be attached to the quantities of particle i and j, respectively. A magnetic particle i with diameter d is covered by a uniform steric layer with thickness δ and has a magnetic moment $\boldsymbol{m}_i$ at the particle center. Employing this particle model, an magnetic dipole-dipole interaction energy $U_{ij}^{(m)}$ and an repulsive interaction energy due to an overlap of steric layers $U_{ij}^{(V)}$ act on particle i exerted by particle j, and also a magnetic dipole-field interaction energy $U_i^{(H)}$ acts on particle i by an external magnetic field [7, 8].

The forces and torques are straightforwardly derived in a mathematical expression, that is, the force $\boldsymbol{F}_{ij}^{(m)}$ and torque $\boldsymbol{T}_{ij}^{(m)}$ are derived from $U_{ij}^{(m)}$, and the repulsive force $\boldsymbol{F}_{ij}^{(V)}$ from $U_{ij}^{(V)}$. Moreover, the torque $\boldsymbol{T}_i^{(H)}$ due to the particle-field interaction is derived from $U_i^{(H)}$ [7, 8].

EXTERNAL ALTERNATING MAGNETIC FIELD

We address a flow problem of a suspension in the situation of an alternating magnetic field that has a time-dependent magnitude of a magnetic field applied along a certain direction. If a magnetic field is assumed to be applied along the x-direction, a time-dependent magnetic field $\boldsymbol{H}$ is expressed as

$$\boldsymbol{H}(t) = (H_0 \sin(\omega_H t))\boldsymbol{h} \tag{1}$$

in which $\boldsymbol{h}$ is the unit vector denoting the x-direction, expressed as $\boldsymbol{h}$=(1,0,0), H_0 is the maximum of its magnitude and the cycle period T_{cycl} is expressed as $T_{cycl}=2\pi/\omega_H$.

BROWNIAN DYNAMICS METHOD

In order to induce the Brownian motion of magnetic particles, an appropriate simulation method has to be used and we here employ the Brownian dynamics method [7, 9, 10]. The particle motion that performs the Brownian motion in an alternating magnetic field is simulated by the usual equations of the translational and rotational motion [11, 12]. It is noted that the direction of the magnetic moment of magnetic particles is obtained from the basic equation for the rotational motion. The translational Brownian motion is characterized by the translational diffusion coefficient $D^T = k_B T / (3\pi\eta d)$ where η is the viscosity of a base liquid, k_B is Boltzmann's constant, T is the absolute temperature of the liquid and d is the diameter of magnetic particles. The random displacements Δr_1^B, Δr_2^B and Δr_3^B in each axis direction are required to satisfy the following stochastic characteristics [11, 12]:

$$\left.\begin{aligned} &\langle \Delta r_1^B \rangle = \langle \Delta r_2^B \rangle = \langle \Delta r_3^B \rangle = 0 \\ &\langle (\Delta r_1^B)^2 \rangle = \langle (\Delta r_2^B)^2 \rangle = \langle (\Delta r_3^B)^2 \rangle = 2D^T \Delta t \end{aligned}\right\} \tag{2}$$

Similarly, the rotational Brownian motion is characterized by the rotational diffusion coefficient $D^R = k_B T / (\pi\eta d^3)$. The random displacements $\Delta\phi_1^B$, $\Delta\phi_2^B$ and $\Delta\phi_3^B$ about each axis line satisfy the following stochastic characteristics [11, 12]:

$$\left.\begin{aligned} &\langle \Delta\phi_1^B \rangle = \langle \Delta\phi_2^B \rangle = \langle \Delta\phi_3^B \rangle = 0 \\ &\langle (\Delta\phi_1^B)^2 \rangle = \langle (\Delta\phi_2^B)^2 \rangle = \langle (\Delta\phi_3^B)^2 \rangle = 2D^R \Delta t \end{aligned}\right\} \tag{3}$$

It is noted that in the above expressions, subscript i denoting particle name is dropped for simplicity.

HEATING EFFECT DUE TO THE RELAXATION PHENOMENON OF MAGNETIC MOMENT XTERNAL ALTERNATING MAGNETIC FIELD

In a magnetic particle suspension, the work per unit volume exerted on the system, W_{cycl}, during one cycle of an alternating magnetic field, which induces the magnetization $\boldsymbol{M}$, is expressed using the alternating magnetic field $\boldsymbol{H}$ as [13]

$$W_{cycl}^{total} = \mu_0 \oint \boldsymbol{H} \cdot d\boldsymbol{M} \tag{4}$$

This is equivalent to the area of the hysteresis loop of the field-magnetization (H-M) curve, and thus Eq. (4) is rewritten as

$$\begin{aligned} W_{cycl}^{total} &= -\mu_0 \oint \boldsymbol{M} \cdot d\boldsymbol{H} = -\mu_0 m H_0 N \oint \langle nx \rangle d(H / H_0) \\ &= -\mu_0 m H_0 N \oint (\langle nx \rangle + 1) d(H / H_0) \end{aligned} \tag{5}$$

in which H is the magnitude of the magnetic field shown in Fig. (1), expressed as $H/H_0 = \sin(\omega_H t)$. We here address the work per particle, W_{cycl}, expressed as

$$W_{cycl} = -\mu_0 m H_0 \oint (\langle nx \rangle + 1) d(H / H_0) \tag{6}$$

In this equation $\langle n_x \rangle$ is the mean value of the x-component n_x of the unit vector $\boldsymbol{n}$ denoting the magnetic field direction. This work W_{cycl} corresponds to the heat production that is used for magnetic hyperthermia treatment.

NON-DIMENSIONALIZATION OF EXPRESSIONS

In simulations, the non-dimensionalized equations and quantities are generally used [11, 12]. In a non-dimensionalization procedure, the following representative quantities are adopted. The diameter of solid sphere, d, is used for lengths, the period of an alternating field, $2\pi/\omega_H$, for time, $\omega_H d/(2\pi)$ for velocities, ω_H for angular velocities, the viscous friction force $(3/2)\eta\omega_H d^2$ for forces, similarly $\pi\eta\omega_H d^3$ for torques and k_BT for energies.

Through the non-dimensionalization procedure, the following non-dimensional parameters appear the non-dimensional equations:

$$R_B = \frac{k_BT}{3\pi\eta d^3}\cdot\frac{2\pi}{\omega_H},$$
$$R_m = \frac{\mu_0 m^2}{2\pi\eta d^6\omega_H} = 3R_B\lambda, \qquad R_V = \frac{\pi n_s k_B T}{3\eta d\omega_H} = R_B\lambda_V, \qquad (7)$$
$$R_H = \frac{\mu_0 m H_0}{\pi\eta d^3\omega_H} = \frac{3}{2\pi}R_B\xi$$

In these expressions, the quantity R_B, R_m, R_V and R_H are the non-dimensional parameters describing the strength of the random force, the magnetic particle-particle interaction, the repulsive interaction due to the overlap of steric layers and the magnetic torque due to the external field relative to the viscous force or torque, respectively.

The quantities λ, ξ and λ_V appearing in Eq. (7) are the non-dimensional parameters relative to the thermal motion, that is, imply the strength of magnetic particle-particle, particle-field and steric repulsive interactions, respectively. These are defined as [8]

$$\lambda = \frac{\mu_0 m^2}{4\pi d^3 k_B T}, \qquad \xi = \frac{\mu_0 m H_0}{k_B T}, \qquad \lambda_V = \frac{\pi n_s d^2}{k_B T} \qquad (8)$$

These parameters λ, ξ and λ_V are quite useful in comparison to the aggregation results that were obtained in a uniform (time-independent) applied magnetic field.

BROWNIAN DYNAMICS METHOD SIMULATION PARAMETERS FOR BROWNIAN DYNAMICS SIMULATIONS

Unless specifically noted, we used the following values for performing the present simulations. The number of particles N is set as N=125 (=5^3), the volumetric fraction ϕ_V (=$N(\pi/6)d^3/V$) as ϕ_V = 0.02 (where V is the volume of the simulation region), the side length l_x^*(=l_x/d) of a cubic simulation region as l_x^*=l_y^*=l_z^*=14.85, the time interval Δt^* as Δt^*=0.0005, and the total simulation time t_{total}^* as t_{total}^*=20 (i.e., 20 cycles). The averaging procedure was conducted using the data that were obtained during the later half part of the total simulation time. Moreover, the thickness of the steric layer, δ^*, was taken as δ^*=0.15, and the repulsive interaction strength λ_V as λ_V=150. The non-dimensional parameters λ, ξ and R_B were taken in a variety of cases such as λ=1, 5 and 10, ξ=1, 5 and 10, and R_B=0.1, 1, 5, 10 and 15.

RESULTS AND DISCUSSION

Time change in aggregate structures of particles in an alternating magnetic field

We first discuss a change in particle aggregates as a function of time in the situation of an alternating magnetic field. Before discussion, it is noted that if the frequency of an alternating magnetic field is sufficiently large, that is, if the value of the non-dimensional parameter R_B is much smaller than unity, the viscous force will dominate the phenomenon more strongly. This implies that the cluster formation and internal structure of particle aggregates will be significantly influenced by the viscous force.

Figure 1 shows the time change in the aggregate structures of magnetic particles for R_B=5 and ξ=5, where three cases of the magnetic interaction strength are addressed, i.e., (a) λ=1, (b) λ=5 and (c) λ=10. Each figure has snapshots at the three angles of the alternating magnetic field, θ_{time} (=$\omega_H t^*$, defined for 0~2π)=π/2, π and 3π/2. Since the magnetic interaction is significantly strong in the case of λ=10, shown in Fig. 1(c), it is seen that large aggregate structures are stably formed. However, since the magnetic field strength is not so strong in comparison with the magnetic interaction between particles, these clusters are not restricted to the field direction in orientation. A noteworthy point is that these chain-like clusters are not dissociated due to a change in the direction of the magnetic field at around θ_{time}=π, where the field direction is switched from the positive to the negative x-direction. This is because the magnetic interaction is much more dominant than both the viscous force and the magnetic particle-field interaction.

For the case of λ=5, long chain-like clusters are not significantly formed but short clusters are formed. These chain-like clusters seem to tend to be slightly formed in thick chain formation along the field direction. This is partly because the influence of the magnetic field become more significant in comparison with the previous case, and therefore the magnetic moment is more strongly restricted to the field direction, which enhances the tendency of the thick formation along the field direction. As in the previous case, these weak chain-like clusters are not disturbed by a change in the alternating magnetic field for a weak viscous force case R_B=5.

For the case of λ=1, since the magnetic interaction is much weaker than the thermal motion, particles do not aggregate to form any clusters at any phase angles. In this situation, the magnetic moment of each particle responds to a change in the magnetic field in orientation separately.

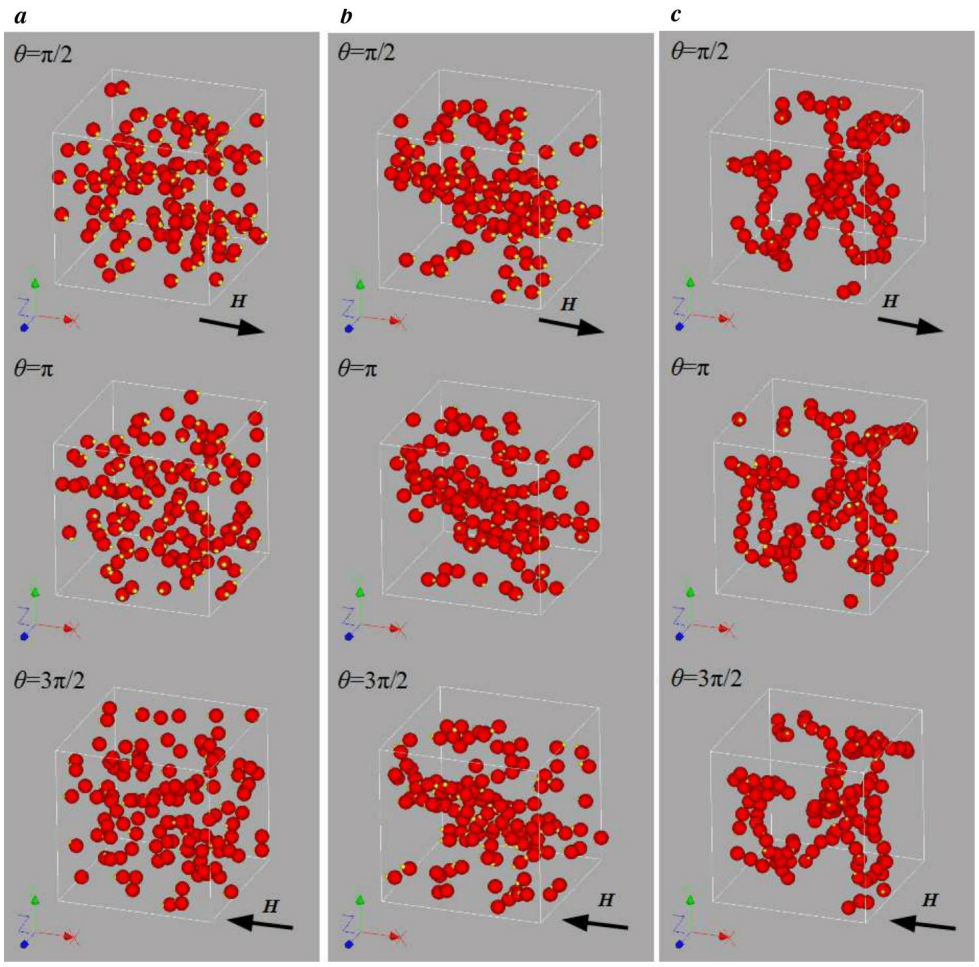

Figure 1. Time change in the aggregate structures of magnetic particles for R_{ij}=5 and ξ=5: (a) for λ=1, (b) for λ=5 and (c) for λ=10. Each figure has snapshots at the three angles of the alternating magnetic field, θ_{time} (=$\omega_H t^*$, defined for 0~2π) =π/2, π and 3π/2. The magnetic moment of each particle is reoriented toward the magnetic field direction with a delay without dissociation of the chain-like clusters for the case of λ=10.

Hysteresis loops of the field-magnetization curves

In this section, we discuss the relationship between particle aggregate structures and characteristics of heat production. It is noted that a larger area of the hysteresis loop of field-magnetization curves gives rise to a larger heating effect that is produced by the Brownian relaxation of the magnetic moments.

Figure 2(a) shows results of the hysteresis loop of the normalized magnetization $\langle n_X \rangle$ as a function of the normalized magnetic field strength H_x^*: results for R_B=0.1, 1, 5, 10 and 15 were shown in the case of a strong particle-particle and particle-field interaction, λ=ξ=10. Similar results are shown in Fig. 2(b) for the case of λ=1 and ξ=10.

In the case of R_B=0.1, the maximum of $\langle n_X \rangle$ is approximately $\langle n_X \rangle \simeq 0.3$, not attains to around unity, so that the area of the hysteresis loop give rise to a small value, yielding a poor heating production performance. In this case, although small and large clusters are formed in the system, these clusters do not contribute to an improvement of the heating production; the frequency of the magnetic field seems to be high for the appearance of Brownian relaxation effect. This characteristic clearly exemplifies that if the magnetic moments do not sufficiently respond to the magnetic field change in a high frequency area, then the area of the hysteresis loop is small and thus a large heating effect cannot be obtained. This dependence on the frequency of the field is similar to that for a smaller particle system where the heating production is obtained by Neel relaxation phenomenon [14]. As the value of R_B is increased, a stronger magnetic field is necessary for the magnetic moments inclining in the opposite direction to rotate in the field direction. For instance, in the case of R_B=10, the quantity $\langle n_X \rangle$ maintains a value of -1 until the field strength $H_x^* \simeq 0.5$, and then steeply increases with increasing magnetic field strength. From these characteristics, it is evident that strong magnetic interactions between particles function to delay the response of the particle rotational motion toward the magnetic field direction. Hence, this delay of the orientation gives rise to a large area of the hysteresis loops or a large heat production performance.

Since particle aggregates are not sufficiently formed in the system in Fig. 2(b), the characteristics of the hysteresis loops will be mainly determined by two factors, i.e., the magnetic particle-field interaction and the viscous friction force. One of characteristic points is that the magnetic field strength at which the value of $\langle n_X \rangle$ arrives at nearly $\langle n_X \rangle \simeq 1$ is much smaller than that for the previous case in Fig. 2(a); for instance, in the case of R_B =15, this situation is almost attained at $H_x^* \simeq 0.5$. This characteristic comes to appear more clearly for a larger value of R_B, because a low viscous friction force leads to a larger influence of the magnetic field and thus the magnetic torque acting on particles relatively becomes lager, whereby the magnetic moments can incline in the magnetic field direction more promptly.

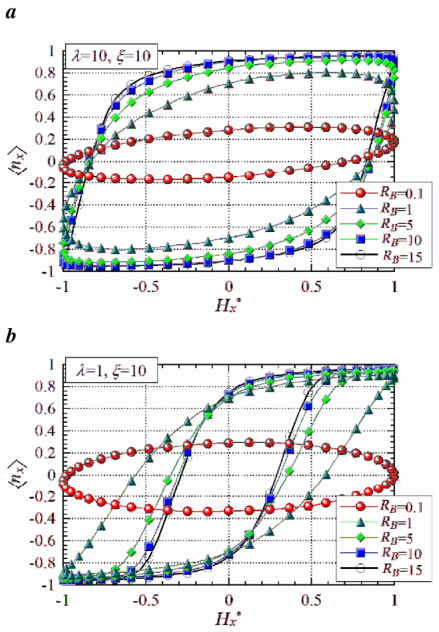

Figure 2. Hysteresis loop of the magnetic field-magnetization curves: (a) λ=10 and ξ=10, and (b) λ=1 and ξ=10. In the case of the viscous force being dominant (R_B=0.1), the magnetic moments of particles do not sufficiently reorient toward the magnetic field direction, which leads to a smaller area of the hysteresis loop.

Heat production effect due to Brownian relaxation mechanism

Finally, we consider the work per particle W_{cycl}^* that is equivalent to the heat production generated from the Brownian relaxation of the rotational motion of the magnetic moments.

Figure 3 shows the dependence of the heat production W_{cycl}^* (=W_{cycl}/k_BT) on the magnetic particle-particle interaction strength λ for the case of the viscous force being relatively weak: results are obtained for the field strength, ξ=1, 5 and 10. From Eq. (6), it is straightforwardly predicted that the heating effect is quite small for a weak magnetic field such as ξ=1.

In the case of ξ =10, a larger heating effect is obtained with increased values of λ. This is because the area of the hysteresis loop becomes larger with increasing magnetic interactions (i.e., with increasing values of λ), shown in Fig. 2. As already pointed out, in the circumstance where chain-like clusters are

formed and incline in the field direction, a larger heat production performance is achieved.

In the case of ξ=5, the value of W_{cycl}^{*} slightly increases until $\lambda \simeq 5$ and then turns to significantly decrease with increased values of λ. This characteristic is evident from the behavior of the characteristics of the chain-like clusters in the alternating magnetic field. That is, chain-like clusters are formed in the field direction and their length becomes larger until $\lambda \simeq 5$ with increasing values of λ. Similar to the case of λ=10, these chain-like clusters formed in the field direction function to delay the orientation of the magnetic moments along the field direction. This tendency of the rotational motion of particles results into a hysteresis loop with a larger area, i.e., a larger heating effect is attained. In contrast, in the area larger than $\lambda \simeq 5$, since the magnetic particle-particle interaction becomes more dominant than the influence of the applied magnetic field with increasing values of λ, the chain-like clusters are not restricted to the field direction in orientation, which yields the convergence of the quantity $\langle n_X \rangle$ to $\langle n_X \rangle \simeq 0$. This implies that the hysteresis loop become significantly small and thus the heating effect approaches approximately zero. This characteristic can be recognized also for a suspension composed of small magnetic particles where the heat production is generated due to the Neel relaxation mechanism [15].

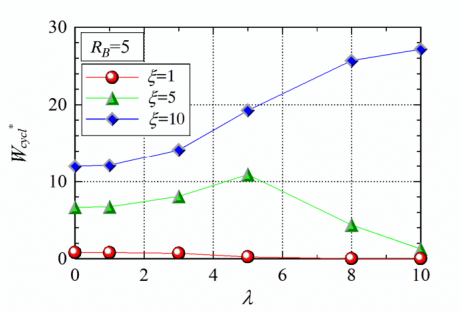

Figure 3. Dependence of the heating effect on the magnetic particle-particle interaction strength. A decrease after $\lambda \simeq$ 5 with increasing values of λ in the case of ξ=5 implies that larger clusters do not significantly respond to the change in the magnetic field strength.

CONCLUSION

We have investigated the aggregate structures in a suspension of magnetic particles in an alternating magnetic field and their influence on the heat production effect. In the present study, we address the Brownian relaxation mode that generates the heat production due to the rotational motion of magnetic particles in an ambient viscous medium with experience of the friction force (or torque). The main factors characterizing the present phenomenon are the viscous friction force arising from an alternating external magnetic field, the applied magnetic field strength and the particle-particle interaction strength. In the situation where chain-like clusters are stably formed in the magnetic field direction, the magnetic particle-particle interaction considerably delays the response of the magnetic moment reorienting in the field direction to a change in the alternating magnetic field. In the situation where particle aggregates are not significantly formed due to an insufficient magnetic interaction, the viscous friction force alone is the main factor for delaying the orientation of the magnetic moments in the field direction and therefore the response of the orientation of particles becomes more prompt in comparison with the other situations. A large heat production performance can be achieved in the situation where large chain-like clusters are formed and inclined in the applied alternating magnetic field that is more dominant than the magnetic interaction between particles. On the other hand, if these chain-like clusters are not sufficiently restricted to the field direction in orientation, a large heat production cannot be obtained.

REFERENCES

[1] U. Häfeli, W. Schütt, J. Teller, M. Zborowski, (Eds.), 1997, "Scientific and Clinical Applications of Magnetic Carriers", Springer, Berlin.

[2] A. M. Schmidt, 2007, "Thermoresponsive magnetic colloids", Colloid Polymer Sci. **285**, 953-966.

[3] C. S. S. R. Kumar, F. Mohammad, 2011, "Magnetic nanomaterials for hyperthermia-based therapy and controlled drug delivery", Advan. Drug Delivery Rev. **63**, 789-808.

[4] I. M. Obaidat, B. Issa, Y. Haik, 2015, "Magnetic properties of magnetic nanoparticles for efficient hyperthermia", Nanomaterials. **5**, 63-89.

[5] Y. I. Golovin, S. L. Gribanovsky, D. Y. Golovin, N. L. Klyachko, A. G. Majouga, A. M. Master, S. Marina, A. V. Kabanov, 2015, "Towards nanomedicines of the future: Remote magneto-mechanical actuation of nanomedicines by alternating magnetic fields", J. Controll. Release. **219**, 43-60.

[6] S. Patra, E. Roy, P. Karfa, S. Kumar, R. Madhuri, P. K. Sharma, 2015, "Dual-responsive polymer coated superparamagnetic nanoparticle for targeted drug delivery and hyperthermia treatment", ACS Appl. Mater. Inter. **7,** 9235-9246.

[7] A. Satoh, 2003, “Introduction to Molecular-Microsimulation of Colloidal Dispersions”, Elsevier, Amsterdam.
[8] A. Satoh, 2017, “Modeling of Magnetic Particle Suspensions for Simulations”, CRC Press, Boca Laton, FL.

[9] M. P. Allen, D. J. Tildesley, 1987, “Computer Simulation of Liquids”, Clarendon Press, Oxford.

[10] A. Satoh, 2010, “Introduction to Practice of Molecular Simulation: Molecular Dynamics, Monte Carlo, Brownian Dynamics”, Lattice Boltzmann and Dissipative Particle Dynamics, Elsevier, Amsterdam.

[11] A. Satoh, 2015, “Brownian dynamics simulations with spin Brownian motion on the negative magneto-rheological effect of a rod-like hematite particle suspension”, Molec. Phys. **113**, 656-670.

[12] A. Satoh, 2015, “Brownian dynamics simulation of a dispersion composed of disk-like hematite particles regarding aggregation phenomena”, Colloid Surf. A. **483**, 328-340.

[13] R. E. Rosensweig, 2002, “Heating magnetic fluid with alternating magnetic field”, J. Magn. Magn. Mater. **252**, 370-374.

[14] S. A. Gudoshnikov, B. Y. Liubimov, N. A. Usov, 2012, “Hysteresis losses in a dense superparamagnetic nanoparticle assembly”, AIP Advan. **2**, 012143.

[15] R. P. Tan, J. Carrey, M. Respaud, 2014, “Magnetic hyperthermia properties of nanoparticles inside lysosomes using kinetic Monte Carlo simulations: Influence of key parameters and dipolar interactions, and evidence for strong spatial variation of heating power”, Phys. Rev. B. **90**, 214421.

Colloid and Polymer Science (2019) 297:1265–1273
https://doi.org/10.1007/s00396-019-04546-x

ORIGINAL CONTRIBUTION

Influence of the cluster formation in a magnetic particle suspension on heat production effect in an alternating magnetic field

Seiya Suzuki [1] · Akira Satoh [2]

Received: 14 May 2019 / Revised: 9 July 2019 / Accepted: 12 July 2019 / Published online: 6 August 2019

Abstract
In the present study, we concentrate on the results of the unexpected characteristic that the stable particle cluster formation induces a decrease in the degree of heating effect in an alternating magnetic field, by means of Brownian dynamics simulations. If chain-like clusters are stably formed in the system, whether or not a large heating effect is obtained is dependent on the magnitude relationship between the magnetic particle-particle and the magnetic particle-field interaction strengths. As the magnetic particle-particle interaction strength increases and becomes more dominant than the influence of the magnetic field, the magnetic moments of stable chain-like clusters do not have a sufficient tendency to inline in the field direction. This leads to a smaller area of the hysteresis loop, and therefore the stable cluster formation induces a significant decrease in the heating effect.

Keywords Magnetic particle suspension · Aggregation phenomenon · Magnetic hyperthermia · Brownian dynamics · Heating effect · Hysteresis loop

Introduction

A magnetic particle suspension is a prospective functional fluid for numerous applications, and many researchers have been active in conducting both fundamental and application studies in a variety of fields. Recently, the interest in magnetic particle suspensions has expanded into the new application areas of biomedical engineering and environmental resource engineering. In the field of biomedical engineering, magnetic particle suspensions are finding potential application in the development of magnetically guided drug delivery systems [1] and magnetic particle hyperthermia treatments [2–5]. In the field of environmental and resource engineering, functional magnetic particles are employed to absorb precious metals or harmful substances dissolved in seawater, after which they may be gathered and removed using a non-uniform magnetic field [6, 7].

In the present study, we focus on physical phenomena in relation to the application of a magnetic particle suspension to magnetic particle hyperthermia. A magnetic particle hyperthermia treatment is a medical therapy for killing tumor or cancer cells by means of the heating effect arising from the relaxation of magnetic moments in an external alternating magnetic field [2]. There are two mechanisms for the heat production arising in an alternating magnetic field, that is, a Néel relaxation mode and a Brownian relaxation mode [8]. In the Brownian relaxation mode, the magnetic moment is fixed within the particle body, and the particle itself rotates to follow the change in a time-dependent magnetic field which gives rise to heat production due to viscous friction torques. The Brownian relaxation mechanism governs the heat generation

Highlights of the present paper
(1) We focus on the results of the unexpected characteristic that the stable particle cluster formation induces a decrease in the degree of heating effect.
(2) The degree of heating effect is dependent on the magnitude relationship between the magnetic particle-particle and the magnetic particle-field interaction strengths.
(3) With the magnetic particle-particle interaction being more dominant, the area of hysteresis loops of the field-magnetization curves becomes smaller, leading to poorer heating effect.
(4) In the opposite case, the magnetic moment of each constituent particle is able to sufficiently respond to the change in the magnetic field, leading to a better heat production.
(5) Significant heat production can be achieved in the situation where large chain-like clusters are formed and inclined in the applied alternating magnetic field.

✉ Akira Satoh
asatoh@akita-pu.ac.jp

[1] Graduate School of Akita Prefectural University, Yurihonjo, Japan

[2] Department of Mechanical Engineering, Akita Prefectural University, Yurihonjo, Japan

phenomena for larger particles. Almost all studies with respect to the application to magnetic hyperthermia address the smaller magnetic particles that produce a heating effect due to Néel relaxation mechanism [2–5]. A macroscopic theory regarding the heating of a magnetic particle suspension in an alternating magnetic field has been developed without consideration of particle aggregate formation by Rosensweig's pioneering work [8]. The dependence of the heating effect on the cluster formation was indirectly clarified in a suspension with a high volumetric fraction of particles, and therefore, large clusters are to be expected in the system, and the interaction between magnetic moments is expected to have a significant contribution to the heating effect. Therefore we understand that it may be of importance to clarify the effect of the cluster formation of magnetic particles on the degree of heat production.

Recently, Zhao and Rinaldi [9] have performed Brownian dynamics simulations in order to investigate the relationship between the aggregate structure of magnetic particles and the heat production characteristics at a microscopic level. Our Brownian dynamics approach is quite similar to that of Zhao and Rinaldi, but in the present report, we focus on the discussion of the unexpected characteristic that the stable particle cluster formation induces a decrease in the degree of heating effect, which has not sufficiently been discussed in their paper.

Model of magnetic particles and an external alternating magnetic field

We consider aggregation phenomena in a suspension composed of magnetic spherical particles in an alternating magnetic field and their influence on heat production due to a Brownian relaxation mechanism. Magnetic particles are required to perform translation and rotational Brownian motion in an applied alternating magnetic field. In order to induce Brownian motion, an appropriate simulation method has to be used, and here we employ the Brownian dynamics method [10–12]. The magnetic forces and torques acting on magnetic particles and the repulsive force due to the overlap of steric layers covering each particle are straightforwardly derived from the corresponding interaction energies. These expressions may be found from references [10, 13] and so not written here. The present physical phenomenon is characterized by the four non-dimensional parameters λ, ξ, λ_V, and R_B. The former three parameters are expressed relative to the thermal motion and imply the strength of magnetic particle-particle, particle-field, and steric repulsive interactions, respectively. These are defined as [13].

$$\lambda = \frac{\mu_0 m^2}{4\pi d^3 k_B T}, \qquad \xi = \frac{\mu_0 m H_0}{k_B T}, \qquad \lambda_V = \frac{\pi n_s d^2}{2} \tag{1}$$

The last parameter R_B describes the strength of the random force relative to the viscous force, expressed as.

$$R_B = \frac{k_B T}{3\pi\eta d^3} \cdot \frac{2\pi}{\omega_H} \tag{2}$$

In these equations, d is the particle diameter, m is the magnitude of the magnetic moment $\boldsymbol{m}_i$ ($=m\boldsymbol{n}_i$) of an arbitrary particle i, η is the viscosity of a base liquid, μ_0 is the permeability of free space, n_s is the number of surfactant molecules on the unit surface of a magnetic particle, k_B is Boltzmann's constant, and T is the absolute temperature of the system.

The time-dependent magnetic field $\boldsymbol{H}$ is applied along the x-direction and expressed as.

$$\mathbf{H}(t) = (H_0 \sin(\omega_H t))\,\mathbf{h} \tag{3}$$

in which $\boldsymbol{h}$ is the unit vector denoting the x-direction, expressed as $\boldsymbol{h} = (1,0,0)$, H_0 is the magnitude of an alternating magnetic field, and ω_H is the angular velocity.

Heating effect due to the relaxation phenomenon of magnetic moments

In a magnetic particle suspension, the work per unit volume exerted on the system, W_{cycl}^{total}, during one cycle of an alternating magnetic field in order to induce the magnetization $\boldsymbol{M}$ is expressed using the alternating magnetic field $\boldsymbol{H}$ as [8].

$$W_{cycl}^{total} = -\mu_0 \oint \mathbf{M} \cdot d\mathbf{H} = -\mu_0 m H_0 \hat{N} \oint \langle n_x \rangle d(H/H_0) \tag{4}$$

This is equivalent to the area of the hysteresis loop of the field-magnetization (H–M) curve. In this equation, $\hat{N}$ is the number density of particles, and$\langle n_x \rangle$is the mean value of the x-component n_x of the unit vector $\boldsymbol{n}$ denoting the magnetic moment orientation. We here address the work per particle, $W_{\mathrm{cycl}} = W_{cycl}^{total}/\hat{N}$.

Results and discussion

As already described in the introduction, we here restrict our discussion to the influence of the cluster formation of magnetic particles on the degree of heating effect. Unless specifically noted, we used the following values for performing the present simulations. The number of particles N is set as $N = 512$ ($=8^3$), the volumetric fraction ϕ_V ($=N(\pi/6)d^3/V$) as $\phi_V = 0.02$ where V is the volume of the simulation region, the side length l_x^*($=l_x/d$) of the cubic simulation region as $l_x^* = l_y^* = l_z^* = 23.75$. Moreover, the thickness of the steric layer, δ^* ($=\delta/d$), was taken as $\delta^* = 0.15$, and the repulsive interaction strength λ_V was taken as $\lambda_V = 150$. In order to verify the present results of having a sufficient accuracy, we show the dependence of

the heating effect W^*_{cycl} (=W_{cycl}/k_BT) on the value of the number of particles, N, for a typical case of $\lambda = 10$, $\xi = 10$, and $R_B = 5$. The dependence of the heating effect on the system size is as follows: $W_{cycl}{}^* = 27.1$, 22.9, 23.7, 23.8, and 23.7 for $N = 125$, 216, 343, 512, and 729, respectively. This characteristic exemplifies that the present simulation results for the case of $N = 512$ have a sufficient accuracy and thus may be regarded as approximately independent of this value employed for simulations. In addition, the formation of aggregate structures is strongly dependent on the magnetic interaction strength and the steric repulsive interaction strength, and therefore the characteristics of potential curves will be discuss for different values of λ and λ_V in Appendix. Moreover, in order to validate the accuracy of the results regarding the heating effect, the time change in the system energy to a steady-state situation will be addressed also in Appendix.

Figure 1 shows the dependence of the heat production $W_{cycl}{}^*$ on the magnetic particle-particle interaction strength λ for the case of a relatively weak viscous force ($R_B = 5$). Results are shown for the field strengths $\xi = 5$ and 10. It is seen that in both cases, a larger heating effect is obtained with increasing values of λ until each certain criterion value of λ. That is, the value of $W_{cycl}{}^*$ tends to increase until $\lambda \simeq 5$ and 10 for $\xi = 5$ and 10, respectively, and thereafter decreases and approaches zero with increasing values of λ. Moreover, a larger value of the magnetic field strength ξ leads to a larger effect of the heat production. This decrease tendency after each certain criterion value of the magnetic interaction strength is a significantly unexpected characteristic of the heating effect, and therefore in the following discussion, we concentrate on the mechanism for this decrease with increasing values of λ in conjunction with the formation of particle aggregates.

Figure 2 shows snapshots for two different cases of the magnetic interaction strength, (a) $\lambda = 10$ and (b) $\lambda = 16$, for the same condition of the particle-field interaction strength $\xi = 10$ and the strength of the random force relative to the viscous force, $R_B = 5$. In these figures, only the snapshot at the phase angle of $\theta_{time} = 45°$ is shown since in this case the response characteristics are more straightforwardly recognized with respect to the chain-like clusters and the orientation of the magnetic moments. Moreover, a relatively small system of $N = 125$ is intentionally addressed for a clear understanding of the structure of particle aggregates.

From Fig. 2(a), it is seen that large aggregate structures are stably formed since the magnetic particle-particle interaction $\lambda = 10$ is sufficiently strong for the cluster formation. In addition, the effect of the magnetic field strength is also sufficiently larger than thermal energy, and therefore these clusters tend to form a linear thick chain-like formation inclined along the magnetic field direction (x-direction). The strong magnetic interactions ($\lambda = 10$) between particles function to maintain the linear cluster formation without a large distortion, whereby the magnetic moments exhibit a resistance to rotate toward the magnetic field direction; even at the angle of $\theta_{time} = 45°$, the magnetic moments do not significantly incline in the field direction. This tendency does not simply lead to the characteristic that more stable chain-like clusters give rise to a better heat production, which will be clarified later. It is a noteworthy point that even if the magnetic field switches in the positive x-direction, the chain-like clusters do not collapse but remain while rotating the particle body itself in order for the magnetic moment to incline toward the magnetic field direction. The reason for exhibiting this characteristic behavior of the chain-like clusters may be explained in the following manner. As the magnetic field strength is increased after switching from the negative to the positive x-direction, the chain-like clusters gradually become unstable and tend to make the magnetic moments of the constituent particles reorient in the field

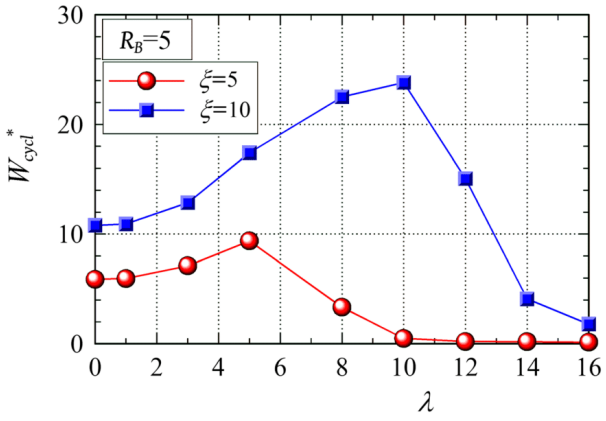

Fig. 1 Dependence of the heating effect on the magnetic particle-particle interaction strength. It is seen that the value of $W_{cycl}{}^*$ tends to increase until $\lambda \simeq 5$ and 10 for $\xi = 5$ and 10, respectively, and thereafter decreases and approaches zero with increasing values of λ

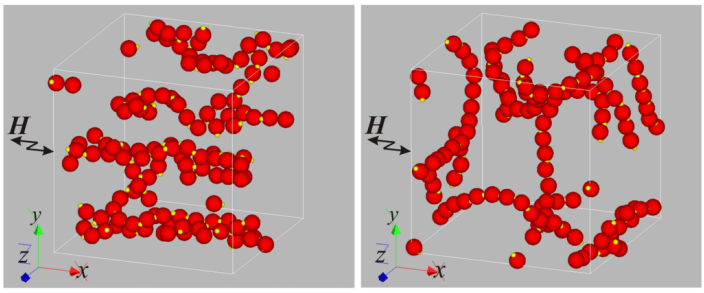

Fig. 2 Aggregate structures of magnetic particles at $\theta_{time} = 45°$ for $R_B = 5$ and $\xi = 10$: **a** $\lambda = 10$ and **b** $\lambda = 16$. A stronger magnetic interaction strength ($\lambda = 16$) leads to a weaker tendency of the reorientation of the magnetic moments toward the field direction and also a weaker tendency of the formation of chain-like clusters along the field direction. It is noted that the yellow dot implies the direction of the magnetic moment of each particle

direction. This reorientation of each magnetic moment may be accomplished by the two mechanisms, i.e., the rotation of each particle or the rotation of chain-like clusters as a whole. It may be reasonably expected that the rotational motion of each particle can be performed more quickly than the rotational motion of chain-like clusters as a whole. Hence, as shown in Fig. 2(a), chain-like clusters can be maintained to a certain degree in reorientating the magnetic moments of the constituent particles toward the field direction, although this reorientation of the magnetic moments is achieved through a temporal transition of unstable chain-like clusters during a short period.

From Fig. 2(b), it is seen that long chain-like clusters are not restricted to the field direction but orient in various directions, which is a significant contrast to the previous snapshot in Fig. 2a. Moreover, it is observed that each magnetic moment of the particles is not restricted to the field direction to a considerable level. This characteristic of not inclining in the field direction does not vary during one period of the alternating magnetic field for the case of $\lambda = 16$. Furthermore, it is recognized that the magnetic moments of the particles constituting several chain-like clusters approximately incline in each cluster direction; the direction of some clusters is roughly opposite to the magnetic field direction. We may understand that these orientational characteristics arise due to the situation where the influence of the magnetic interaction between particles is sufficiently stronger than that of the external magnetic field, which leads to a poor Brownian relaxation effect, i.e., a poor degree of heating effect. This expectation will be discussed in more detail in a quantitative manner in the following.

Figure 3 shows results of the response of the averaged quantity$\langle n_x \rangle$to a change in the alternating magnetic field $H/H_0 = |\boldsymbol{H}|/H_0 = \sin(2\pi t^*)$ for $R_B = 5$ and $\xi = 10$ where two cases of $\lambda = 10$ and $\lambda = 16$ are addressed. It is noted that the non-dimensional time of $t^* = 1$ corresponds to the phase angle of $\theta_{time} = 360°$. In the case of $\lambda = 10$, it is seen that the curve has a trapezoidal change with a maximum value of $\langle n_x \rangle \simeq 0.85$ at $t^* \simeq 0.34$ and a plateau area between $t^* \simeq 0.3$ and $t^* \simeq 0.5$. The maximum value of around unity implies that the magnetic particles can sufficiently follow a change in the magnetic field during one period, although a large delay is observed in the response. These characteristics should give rise to a larger area of the hysteresis loop of the field-magnetization curve, which will be shown later, and therefore as a result lead to a larger heating effect at $\lambda = 10$ in the curve shown in Fig. 1. The reason why the delay in the response is significant is that particles belonging to the same cluster which have not already oriented in the field direction show a resistance to change their orientation to follow the switched direction of the alternating magnetic field due to the magnetic interactions between the particles in a cluster. That is, the particles constituting a cluster are strongly bound with each other, and this gives rise to a large resistance to the rotation of the magnetic moment toward the magnetic field direction, which leads to a large delay in the response. A steep increase toward the maximum value from $t^* \simeq 0.1$ is due to the characteristic that the magnetic particles which have already oriented in the field direction accelerate other particles in the cluster to rotate in the field direction through the influence of the magnetic particle-particle interactions. The curve for $\lambda = 16$ exhibits a completely different response in comparison to the former case of $\lambda = 10$. The most different feature is that the maximum value is much lower than unity around$\langle n_x \rangle \simeq 0.3$ at $t^* \simeq 0.3$, which implies that numerous magnetic particles do not follow the field direction, as already pointed out in the discussion of the snapshots. Since the magnetic interaction is the dominant effect in the case of $\lambda = 16$, $R_B = 5$ and $\xi = 10$, the magnetic moments cannot rotate sufficiently during the period of the alternating magnetic field. It is this characteristic that is the cause for the heating effect decreasing and approaching zero with increasing values of λ after each criterion value in the curves of $\xi = 5$ and 10 shown in Fig. 1. The reason why the curve for $\lambda = 16$ does not vary around zero but is shifted toward the y-axis direction by a certain small positive value is that the system of $N = 512$ is not sufficiently large for the case of a strong magnetic interaction strength $\lambda = 16$, where stable

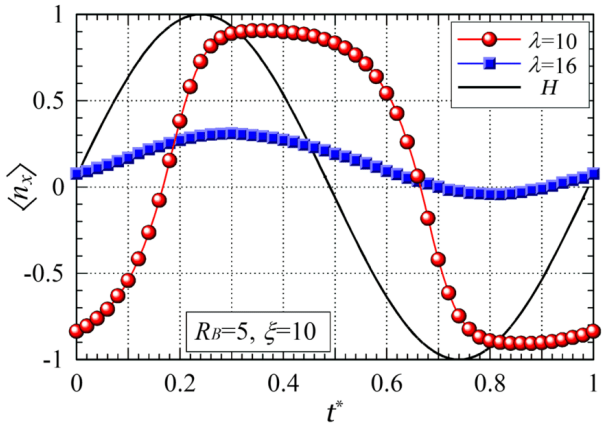

Fig. 3 Response of the reorientation of the magnetic particles to the change in the magnetic field strength for the case of $R_B = 5$ and $\xi = 10$, where two curves for $\lambda = 10$ and $\lambda = 16$ are shown. For the case of $\lambda = 10$ chain-like clusters sufficiently respond to the change in the magnetic field strength with a larger delay. In contrast, for the case of $\lambda = 16$ the magnetic moments do not significantly reorient in the magnetic field direction

chain-like clusters are significantly formed in the whole simulation region. However, from simulations for various sizes of the simulation region, we understand that the essential features regarding the response of the magnetic moments are able to be obtained even for the present system size of $N = 512$.

We show results of the hysteresis loops of the field-magnetization curves in Fig. 4, where two cases of $\lambda = 10$ and $\lambda = 16$ are addressed for the case of $R_B = 5$ and $\xi = 10$. As already mentioned, a larger area of the hysteresis loop gives rise to a larger heating effect which is produced by the Brownian relaxation of the magnetic moments. As already expected from the response curves shown in Fig. 3, the hysteresis loop is significantly larger in the case of $\lambda = 10$, which gives rise to a more significant heating effect shown in Fig. 1. That is, a strong magnetic interaction between the particles will function to delay the response of the particle rotational motion toward the magnetic field direction, and therefore, this significant delay in the orientation gives rise to a larger area of the hysteresis loop indicating a higher degree of heat production. In contrast, for the case of $\lambda = 16$, the area of the hysteresis loop is significantly smaller in comparison to the previous case of $\lambda = 10$, which leads to a significantly poor heating effect. This poor performance is mainly due to the tendency that the magnetic moment of each constituent particle in a cluster tends to resist to the reorientation toward the field direction, which cannot give rise to a larger maximum value of $\langle n_x \rangle$in the case of the magnetic particle-particle interaction being significantly more dominant. The reason why the curve for $\lambda = 16$ is shifted toward the y-axis direction by a certain small positive value has already been described in the above discussion regarding the response of the magnetic moments.

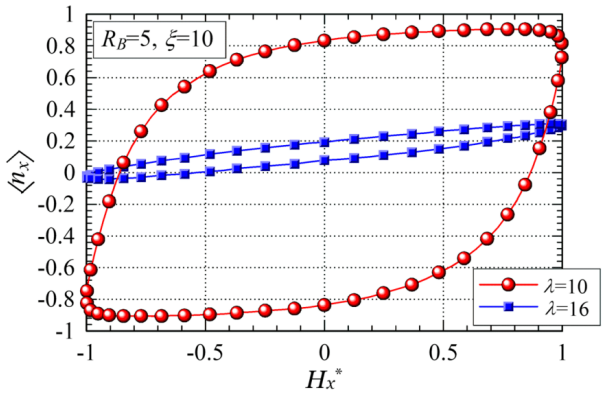

Fig. 4 Hysteresis loop of the magnetic field-magnetization curves for the case of $R_B = 5$ and $\xi = 10$, where two curves for $\lambda = 10$ and $\lambda = 16$ are shown. In the case of the magnetic interaction being dominant ($\lambda = 16$), the magnetic moments of particles do not sufficiently reorient toward the magnetic field direction, which leads to a smaller area of the hysteresis loop

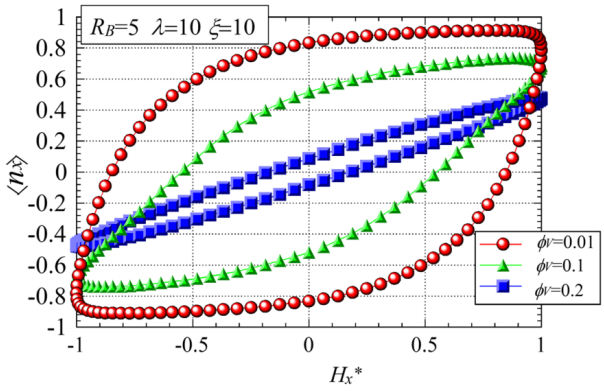

Fig. 5 Influence of the volumetric fraction of particles on the hysteresis loops of the field-magnetization curves, which was obtained for $R_B = 5$, $\lambda = 10$, and $\xi = 10$ and three cases of the volumetric fraction $\phi_V = 0.01$, 0.1, and 0.2 are addressed. It is seen that the heating effect decreases with increasing values of the volumetric fraction since much clearer network (chain-like) clusters tend to be formed for larger values of ϕ_V, which induces a larger resistance to the inclination of the magnetic moments toward the magnetic field direction

Finally, we discuss the influence of the volumetric fraction of particles on the hysteresis loops of the field-magnetization curves using in Fig. 5, which was obtained for $R_B = 5$, $\lambda = 10$, and $\xi = 10$, and three cases of the volumetric fraction $\phi_V = 0.01$, 0.1, and 0.2 are addressed. Since a strong dependence of the hysteresis loop on the volumetric fraction is recognized for $\lambda = 10$ much more significantly than for $\lambda = 16$, and therefore, we here focus on the results for this case. It is clearly seen that the heating effect more strongly decreases with increasing values of the volumetric fraction. The curve for $\phi_V = 0.2$ is quite similar to that for $\lambda = 16$ and $\phi_V = 0.02$ in Fig. 4, leading to an extraordinary decrease in the heating effect in comparison to the case of $\phi_V = 0.02$ or $\phi_V = 0.01$. This is because more stable and clearer network (chain-like) structures of particle aggregates are formed with increasing volumetric fractions, and these clusters tend to exhibit a much stronger resistance of the magnetic moments inclining toward the magnetic field direction due to the magnetic interactions in each cluster. As a result, the area of the loop for $\phi_V = 0.2$ becomes much smaller than for dilute suspensions, similar to that for the case of $\lambda = 16$ and $\phi_V = 0.02$.

Concluding remarks

We have investigated the relationship between the aggregate structures in a suspension of magnetic particles and the heating effect in an alternating magnetic field. In the present study, we address the Brownian relaxation mode that generates heat due to the rotational motion of magnetic particles that experience a frictional force or torque in an ambient viscous medium. The main factors characterizing the present phenomenon are the viscous friction force arising from an alternating external magnetic field, the applied magnetic field strength, and the particle-particle interaction strength. The magnitude correlation of these factors will govern the characteristics of the aggregate structures and the heat production effect. In the present study, we focus on the results of the unexpected characteristic that the stable particle cluster formation induces a decrease in the degree of heating effect, which has not sufficiently been discussed in other papers. That is, the heating effect tends to increase until a criterion value and thereafter decreases and approaches zero with increasing magnetic interaction strengths. From the present results, we may conclude the cause for the decrease in the degree of heating effect after criterion values in the following manner. If chain-like clusters are stably formed in the system, whether or not a large heating effect is obtained is dependent on the magnitude relationship between the magnetic particle-particle and the magnetic particle-field interaction strengths. As the magnetic particle-particle interaction strength increases and becomes more dominant than the influence of the magnetic field, the area of hysteresis loops of the field-magnetization curves become smaller and so the heating effect comes to vanish. In the opposite case where the magnetic particle-field interaction is significantly more dominant, the magnetic moment of each constituent particle is able to sufficiently respond to the change in the magnetic field, which leads to a larger area of the hysteresis loop or a better heat production performance. We therefore understand that significant heat production can be achieved in the situation where large chain-like clusters are formed and inclined in the applied alternating magnetic field. On the other hand, if these chain-like clusters are not sufficiently restricted in orientation to the field direction, a significant heat production cannot be obtained.

Compliance with ethical standards

Conflict of interest The authors declare that they have no conflict of interest.

Appendix

Figure 6 shows results of the dependence of potential curves on the magnetic particle-particle interaction strength for the two cases of $\lambda = 10$ and 16, where the common steric interaction strength of $\lambda_V = 150$ is used. In the figure, U^{m*} and U^{V*} are the non-dimensional magnetic particle-particle and steric repulsive interaction energy based on the thermal energy k_BT, respectively, and U^* is the total interaction energy as $U^* = U^{m*} + U^{V*}$. A representative snapshot of particle aggregates is also shown in the figure for each case of the magnetic interaction strength for reference. It is noted that the magnetic particle-particle interaction energy is evaluated under the assumption that the magnetic moments of the two magnetic particles of interest incline in the same direction along the line connected between the centers of the particles, and the abovementioned energies are evaluated as a function of the non-dimensional distance between the two particles, r_{ij}^* ($= r_{ij}/d$). The cluster formation is mainly governed by the depth of a potential curve, and if the depth is much deeper than thermal energy k_BT, stable clusters more strongly tend to be formed in the system. The depth of the potential curve is $U^* = -9.12$ and -14.7 at $r_{ij}^* = 1.295$ and 1.29 for $\lambda = 10$ and 16, respectively. Since these depths are much deeper than unity (i.e., thermal energy), the snapshots exhibit significantly similar network (chain-like) clusters between these cases, but slightly clearer network structures are recognized in the case of $\lambda = 16$. Moreover, it is noted that the minimum energy in each net potential energy arises in close vicinity to the contact surface of the steric layer (i.e., $r_{ij}^* = 1.3$)

Figure 7 shows results of the time change in the system energy to a steady state situation for the case of $R_B = 5$ in no applied magnetic field $\xi = 0$, where results are shown for the magnetic interaction strengths $\lambda = 10$ and 16. Two representative snapshots of particle aggregates are also shown in the figure at the cycle number of $N_{cycl} = 5$ and 25 for each case of the magnetic interaction strength in order to assess the rate of the convergence. From the results regarding the change in the system energy, it is clearly evident that the convergence to a steady-state situation is approximately accomplished in an early stage of the simulation steps, at $N_{cycl} \simeq 10$ and 5 for $\lambda = 10$ and 16, respectively. Moreover, it is seen that there is no essential difference between the snapshots at $N_{cycl} = 5$ and 25 for both the cases. The snapshots in the figures are essentially quite similar to those for thermodynamic equilibrium in no applied magnetic field in Fig. 6. However, it is recognized that slightly looser network structures are formed in the case of an alternating magnetic field (Fig. 7) since in this case, the viscous forces and torques function to decrease the stability of network clusters. These characteristics may clearly validate the accuracy of the present results in respect to the snapshots, the hysteresis loops, and so forth.

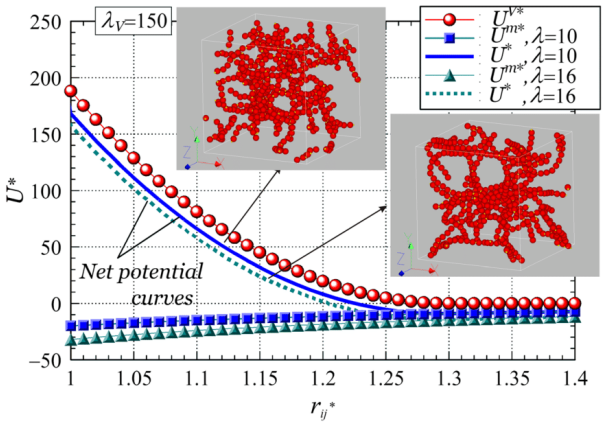

Fig. 6 Dependence of potential curves on the magnetic particle-particle interaction strength for the two cases of $\lambda = 10$ and 16, where the common steric interaction strength of $\lambda_V = 150$ is used. The distance giving rise to a minimum energy in each net potential energy is in close vicinity to the contact surface of the steric layer. Snapshots are not significantly different between these two cases, but slightly clearer network structures are observed for $\lambda = 16$ than for $\lambda = 10$

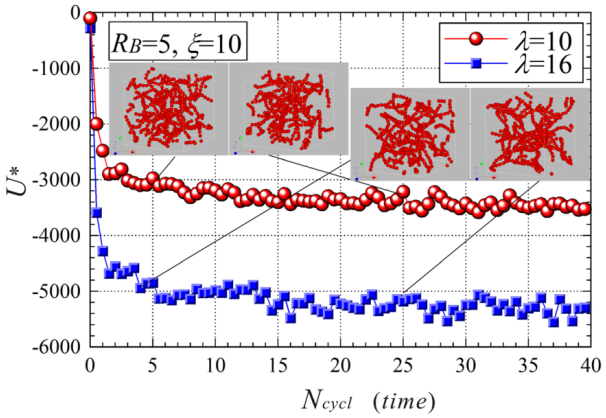

Fig. 7 Time change in the system energy to a steady-state situation for the case of $R_B = 5$ in no applied magnetic field. The convergence to a steady-state situation is accomplished in an early stage of the simulation steps, at $N_{cycl} \simeq 10$ and 5 for $\lambda = 10$ and 16, respectively. There is no essential difference between the snapshots at $N_{cycl} = 5$ and 25 for the both cases

Figure 8 shows the dependence of potential curves on the steric repulsive interaction strength for the common value of the magnetic interaction strength, where two representative cases of $\lambda_V = 100$ and $\lambda_V = 200$ are addressed: Figs. 8 a and b are results for $\lambda = 10$ and $\lambda = 16$, respectively. A representative snapshot of particle aggregates in thermodynamic equilibrium is also shown in the figure for each case of the steric repulsive interaction strength for reference. The method of evaluating the magnetic particle-particle interaction energy has already been described in Fig. 6. Although in the Brownian relaxation mode of the magnetic moments the surface roughness may be expected to have an influence on the heating performance, it seems to be reasonable to consider that the structure of network clusters is essentially the dominant factor for determining the motion of the network clusters in the situation of an alternating applied magnetic field. This is because these clusters are stably formed in the system due to magnetic interactions under the influence of the disturbance of an alternating field in the present cases of $\lambda = 10$ and $\lambda = 16$, not due to the surface roughness of magnetic particles. Hence, we here discuss the influence of the steric repulsive interaction strength λ_V on the potential curves and particle aggregates; a larger value of λ_V implies a more numerous number of surfactant molecules, i.e., a larger value of the number density n_s. The depth of the potential curve is $U^* = -9.15$ and -9.08 at $r_{ij}^* = 1.285$ and 1.295 for $\lambda_V = 100$ and 200, respectively, in the case of $\lambda = 10$, and similarly, $U^* = -14.76$ and -14.61 at $r_{ij}^* = 1.285$ and 1.295 for $\lambda_V = 100$ and 200, respectively, in the case of $\lambda = 16$. It is seen that the energy depth is not strongly dependent on the value of the steric repulsive interaction strength λ_V for both the cases of $\lambda = 10$ and 16. This characteristic clearly

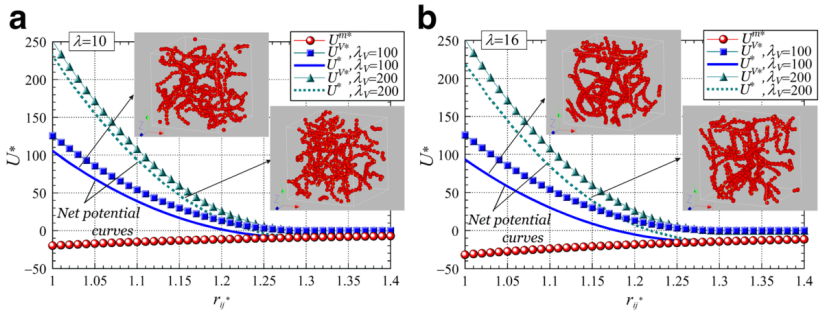

Fig. 8 Dependence of potential curves on the steric repulsive interaction strength for the common value of the magnetic interaction strength, where two representative cases of $\lambda_V = 100$ and $\lambda_V = 200$ are addressed: Figs. 8 a and b are results for $\lambda = 10$ and $\lambda = 16$, respectively. A representative snapshot of particle aggregates in thermodynamic equilibrium is also shown in the figure for each case of the steric repulsive interaction strength for reference. The energy depth is not strongly dependent on the value of the steric repulsive interaction strength λ_V for both the cases of $\lambda = 10$ and 16, which clearly exemplifies that the snapshots of particle aggregates are not significantly different among those for the three cases of $\lambda_V = 100$, 150, and 200

exemplifies that the snapshots of particle aggregates are not significantly different among those for the three cases of $\lambda_V = 100$, 150, and 200

References

1. Häfeli U, Schütt W, Teller J, Zborowski M (1997) Scientific and clinical applications of magnetic carriers. Springer Science, New York
2. Schmidt AM (2007) Thermoresponsive magnetic colloids. Colloid Polymer Sci 285:953–966
3. Kumar CSSR, Mohammad F (2011) Magnetic nanomaterials for hyperthermia-based therapy and controlled drug delivery. Advan Drug Delivery Rev 63:789–808
4. Obaidat IM, Issa B, Haik Y (2015) Magnetic properties of magnetic nanoparticles for efficient hyperthermia. Nanomaterials 5:63–89
5. Golovin YI, Gribanovsky SL, Golovin DY, Klyachko NL, Majouga AG, Master AM, Marina S, Kabanov AV (2015) Towards nanomedicines of the future: remote magneto-mechanical actuation of nanomedicines by alternating magnetic fields. J Control Release 219:43–60
6. Bruce IJ, Sen T (2005) Surface modification of magnetic nanoparticles with alkoxysilanes and their application in magnetic bioseparations. Langmuir 21:7029–7035
7. Girginova PI, Daniel-da-Silva AL, Lopes CB, Figueira P, Otero M, Amaral VS, Pereira E, Trindade T (2010) Silica coated magnetite particles for magnetic removal of Hg2+ from water. J Colloid Interface Sci 345:234–240
8. Rosensweig RE (2002) Heating magnetic fluid with alternating magnetic field. J Magn Magn Mater 252:370–374
9. Zhao Z, Rinaldi C (2018) Magnetization dynamics and energy dissipation of interacting magnetic nanoparticles in alternating magnetic fields with and without a static bias field. J Phys Chem C 122: 21018–21030
10. Satoh A (2003) Introduction to molecular-microsimulation of colloidal dispersions. Elsevier, Amsterdam
11. Allen MP, Tildesley DJ (1987) Computer simulation of liquids. Clarendon Press, Oxford
12. Satoh A (2010) Introduction to practice of molecular simulation: molecular dynamics, Monte Carlo, Brownian dynamics, lattice Boltzmann and dissipative particle dynamics. Elsevier, Amsterdam
13. Satoh A (2017) Modeling of magnetic particle suspensions for simulations. CRC Press, Boca Laton

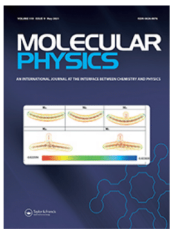

Taylor & Francis
Taylor & Francis Group

Molecular Physics

An International Journal at the Interface Between Chemistry and Physics

ISSN: (Print) (Online) Journal homepage: https://www.tandfonline.com/loi/tmph20

The behaviour of magnetic spherical particles and the heating effect in a rotating magnetic field via Brownian dynamics simulations

Seiya Suzuki, Akira Satoh & Muneo Futamura

To cite this article: Seiya Suzuki, Akira Satoh & Muneo Futamura (2021) The behaviour of magnetic spherical particles and the heating effect in a rotating magnetic field via Brownian dynamics simulations, Molecular Physics, 119:9, e1892225, DOI: 10.1080/00268976.2021.1892225

To link to this article: https://doi.org/10.1080/00268976.2021.1892225

Published online: 01 Mar 2021.

MOLECULAR PHYSICS
2021, VOL. 119, NO. 9, e1892225 (10 pages)
https://doi.org/10.1080/00268976.2021.1892225

Taylor & Francis
Taylor & Francis Group

RESEARCH ARTICLE

The behaviour of magnetic spherical particles and the heating effect in a rotating magnetic field via Brownian dynamics simulations

Seiya Suzuki[a], Akira Satoh[b] and Muneo Futamura[b]

[a]Graduate School of Akita Prefectural University, Yurihonjo, Japan; [b]Department of Mechanical Engineering, Akita Prefectural University, Yurihonjo, Japan

ABSTRACT

The present study addresses the physical phenomena of a suspension composed of magnetic spherical particles in a rotating magnetic field in order to elucidate the influence of particle aggregation phenomena on the heat production from Brownian relaxation by means of Brownian dynamics simulations. In the case of a weak magnetic particle-particle interaction, particles do not aggregate to form specific cluster configurations. In this situation, the magnetic moment of each particle quickly inclines toward the field direction, and single particles do not give rise to a sufficiently large heating effect. With an increasing magnetic interaction between particles, chain-like clusters tend to form in the system and function to offer a larger resistance to the orientation of the magnetic moments, which leads to an increase in the heating effect. In the case of a significantly strong magnetic particle-particle interaction, the particles tend to aggregate to form stable ring-like clusters where the magnetic moments of the constituent particles are not able to be so responsive to the rotating magnetic field and this leads to a decrease in the heating effect.

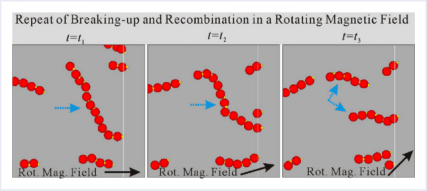

Highlights of the present paper

(1) The characteristics of particle aggregation have been clarified.
(2) The relationship between the strength of the magnetic particle-particle interaction and the frequency of the rotating magnetic field on the aggregation phenomena has been clarified.
(3) The response of the particle aggregates to an applied rotating magnetic field has been clarified.
(4) The relationship between the performance of the degree of heat production and the internal structure of magnetic particle configurations has been clarified.

ARTICLE HISTORY
Received 15 October 2020
Accepted 8 February 2021

KEYWORDS
Magnetic particle suspension; magnetic hyperthermia; heat generation; Brownian dynamics; rotating magnetic field

1. Introduction

Active research regarding a magnetic particle suspension is currently being conducted in both fundamental and application studies in a variety of fields. Typical research and application fields may be fluid engineering [1], magnetic material engineering [2] and environmental resource engineering [3]. In addition, in medical engineering field, hopeful applications are magnetically targeted drug delivery systems and magnetic particle hyperthermia treatment [4]. In order to realise these functions more effectively, rather than employ the more common uniform magnetic field, it is desirable to apply a non-uniform or a time-dependent magnetic field to a magnetic particle suspension. A representative time-dependent field would be an alternating magnetic field or a rotating magnetic field. It has been clarified by Rosensweig's pioneering study [5] that magnetic particles in an alternating magnetic field induce a heating

CONTACT Akira Satoh asatoh@akita-pu.ac.jp

effect due to the Brownian relaxation of the magnetic moment. A magnetic particle hyperthermia treatment is a medical therapy for killing tumour or cancer cells by means of this heating effect, and has been attracting attention as a new cancer treatment.

There are a variety of studies regarding the heat generation phenomena of magnetic particles in an alternating magnetic field. Yao et al. [6] have treated a suspension composed of magnetic spheroidal particles with the size larger than 100 nm and have investigated a heating effect of this suspension, whilst Lahiri et al. [7] have addressed magnetic emulsion droplets. In addition, Zhao and Rinaldi have clarified the heat production characteristics of magnetic spherical particles in an alternating magnetic field [8]. Our research group has focused on the internal structure of the particle aggregates found in a spherical particle suspension, and have elucidated the relationship between the performance of heat generation and the particle aggregate structures in an alternating magnetic field [9]. We now advance this simulation study to the aggregation phenomena and the heating effect in the situation of a rotating magnetic field.

There are several experimental studies that have been conducted in regard to the behaviour of magnetic particles in a rotating magnetic field. Cantillon-Murphy et al. [10] have elucidated the mechanism of heat generation in a magnetic fluid under a rotating magnetic field and in the study of Bekovic et al. [11], it has been experimentally clarified that the heating performance of magnetic particles in a rotating magnetic field may be more enhanced than in an oscillating magnetic field. Furthermore, Abu-Bakr and Zubarev [12] have clarified that the interaction between magnetic particles is expected to contribute to the performance of the heating effect. However, at the present time, there are no experimental or simulation studies elucidating the relationship between the internal structure of particle aggregates and the heating characteristics.

In a previous study [9], we investigated the relationship between the heating effect and the particle aggregates for the case of a spherical particle suspension in an alternating magnetic field. From this study it was suggested that the aggregation phenomena may be expected to have an effective contribution to the heating effect under the certain conditions. In other words, the cluster formation does not necessarily contribute to better performance of the heat generation.

From this background, in the present study, we address the behaviour of magnetic spherical particles in the situation of an applied rotating magnetic field. From Brownian dynamics simulations, we attempt to clarify the internal structure of the particle aggregates and the relationship between the particle aggregates and the heating effect due to the mechanism of Brownian relaxation. Moreover, we compare the heating effect in a rotating and an alternating magnetic field in order to clarify a difference in the characteristics of the heat generation for the two different applied magnetic fields.

2. Particle model and a rotating magnetic field

A spherical magnetic particle with diameter d is coated with a uniform steric layer of thickness δ and has a point magnetic moment $\boldsymbol{m}$ at the particle centre.

As described above, here we intend to discuss the heating effect of a magnetic particle suspension in a time-dependent magnetic field. Therefore, a rotating magnetic field $\boldsymbol{H}$ is applied along the xy-plane and expressed as

$$\boldsymbol{H}(t) = H_0\{\cos(\omega_H t)\boldsymbol{i}_x + \sin(\omega_H t)\boldsymbol{i}_y\} \tag{1}$$

in which, H_0 is the magnitude of the magnetic field, ω_H is the angular velocity and $\boldsymbol{i}_x$ and $\boldsymbol{i}_y$ are the unit vectors in the x- and y- direction, respectively.

The response of the magnetic particles is affected by the five factors, i.e. (1) the strength of the magnetic particle-particle interaction, (2) the magnetic particle-field interaction, (3) the repulsive force due to the overlap of steric layers, (4) the strength of the viscous force related to the frequency of the rotating field and (5) the thermal motion of magnetic particles, which are denoted by the non-dimensional parameters, λ, ξ, λ_V and R_B, respectively, relative to the effect of the thermal motion. The expressions for these quantities are shown in the previous study [9]. If the quantities of λ, ξ and λ_V are significantly larger than unity, then it is implied that each factor is much more dominant than the thermal motion. If the quantity R_B is much smaller than unity, then the frequency of the rotating magnetic field is significantly large and thus the viscous friction force is much more dominant than the thermal motion. Hence, the behaviour of magnetic particles will be determined in a complex manner by these five factors inducing the effect of the thermal motion.

3. Heating effect

The heat production in a time-dependent magnetic field arises from the relaxation of the magnetic moments of the suspended particles. In general, there are two different modes for this relaxation phenomenon [5]. The Néel relaxation mode is a mechanism for magnetic particles with a diameter smaller than approximately 10 nm, where the magnetic moment can rotate within the particle body, and there are a numerous number of studies [13–16] regarding the heat production due to this mechanism. The Brownian relaxation mode [5] is another mechanism

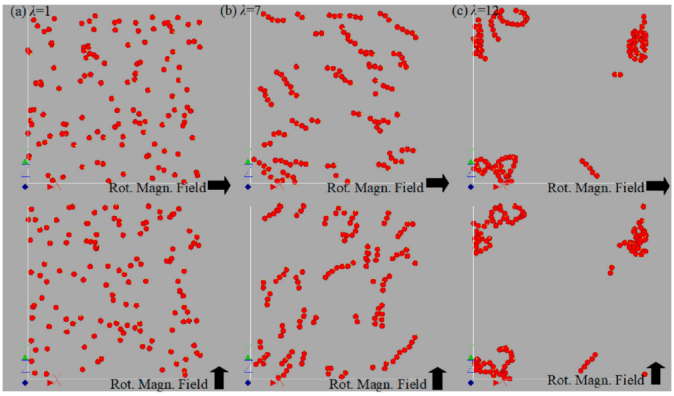

Figure 1. Aggregate structures for $\xi = 5$ and $R_B = 20$: (a) $\lambda = 1$, (b) $\lambda = 7$ and (c) $\lambda = 12$. A stronger magnetic particle-particle interaction induces the formation of larger and more stable clusters.

that is for larger particles, where the magnetic moment is locked to the particle body, and thus the particle itself rotates to incline in the field direction, which leads to the heat generation [5–8]. In the present study, we focus on heat generation based on the Brownian relaxation mode. The heating effect of a magnetic particle suspension in a rotating magnetic field is obtained from the work during one cycle of the magnetic field. As in the previous study [9], we here treat the heating effect generated by one particle, W_{cycl}, which is evaluated from the same equation shown in the previous study.

4. Parameters for simulations

Unless specifically noted, the present results were obtained by adopting the following parameter values. The number of particles $N = 125 = 5^3$, time step $\Delta t^* = \Delta t / (2\pi/\omega_H) = 0.0001$, and total simulation time $t_{total}{}^* = t_{total} / (2\pi/\omega_H) = 5000$ where data from the last 50% of the simulation time was used for the averaging procedure. The diameter of a particle is $d^* = 1.0$, the thickness of the steric layer $\delta^* = \delta/d = 0.15$, and the cutoff radius $r_{coff}{}^* = r_{coff}/d = 8.0$.

The main reason why we adopted a relatively small system of $N = 125$ is that it is more straightforward to graphically grasp a change in the formation of clusters in a rotating field, especially the breaking-up and recombination of the chain-like clusters, shown in Figure 3 in addition to Figures 1 and 4. We assessed the dependence of the results on the size of a simulation region (i.e. the number of magnetic particles in a system), and obtained a conclusion that the results for the case of $N = 125$ are not essentially dependent on the system size even in a quantitative meaning.

Moreover, in contrast to the previous study [9] where the volumetric fraction was taken as $\phi_V = 0.02$, we focus on a significantly dilute suspension such as $\phi_V = 0.001$ in the present rotating magnetic field. This is because in a dense system the rotation of magnetic particles in the situation of a rotating magnetic field is expected to have a significant tendency to induce the rotating flow field of a dispersion medium. Since the Brownian dynamics method is not able to solve the flow field together with the particle motion, it is quite reasonable that we restrict our attention to a dilute suspension system of $\phi_V = 0.001$ in the first change of the present phenomenon for a rotating magnetic field.

Furthermore, it is certainly desirable to employ the Ewald sum [17] for taking into account long-range magnetic interactions. However, since we here address a significantly dilute particle suspension of $\phi_V = 0.001$, the employment of a sufficiently longer cutoff distance such as $r_{coff} = 8d$ may be sufficient as a first approximation [18]. Other researchers [19] also have a conclusion that the minimum image convention is a reasonable technique as a first approximation even for a dipolar system. Similar treatment without the employment of the Ewald sum was sufficient for the case of a monolayer of magnetic spherical particles with the volumetric fraction $\phi_V = 0.05$ to 0.5 [20]. From this background, we have here used a sufficiently long cutoff distance of $r_{coff} = 8d$ without the employment of the Ewald sum [18]. It is noted that the present results were not substantially dependent on the value of the cutoff radius unless a small value such as $r_{coff} = 3d$ and $5d$ is used.

Using the above-mentioned parameters we evaluate the dimensions of the simulation cell as $l_x^* = l_x/d = l_y^* = l_z^* \approx 40.3$. The non-dimensional parameters λ, ξ, λ_V and R_B are set within the wide ranges of $\lambda = 1 \sim 15$, $\xi = 1 \sim 10$, $\lambda_V = 150$ and $R_B = 1 \sim 20$. In this study, one of the parameters on which we focus is the frequency of the rotating magnetic field that is represented by the non-dimensional parameter R_B. It is noted that as the frequency is decreased the value of R_B will increase. We now consider the actual values of the physical parameters in order to assess the range of the non-dimensional parameters. If we set the physical diameter of a magnetic particle as $d = 1.8 \times 10^{-8}$ m, the viscosity of liquid $\eta = 1 \times 10^{-3}$ Pa·s, the magnitude of the rotating magnetic field $H_0 = 1 \times 10^4$ A/m, the saturation magnetisation $M = 4.46 \times 10^5$ A/m, the frequency of field $\omega_H = 20 \times 10^3$ Hz and the temperature $T = 293$ K, then the non-dimensional parameters are then evaluated as $\lambda = 7.86$, $\xi = 4.23$ and $R_B = 3.68$. The ranges of the non-dimensional parameters used in the simulations are set around these typical values. The Brownian dynamics method for a spherical particle system is adequately described in textbooks [17,21].

5. Results and discussion

First, we discuss the dependence of the aggregate structures on the magnetic particle-particle interaction strength λ. Although the simulations were performed on a 3D system, it is relatively difficult to discern the characteristics of the aggregate structures from 3D snapshots, therefore in order to grasp the behaviour of the aggregates more clearly we use snapshots of an xy-plane, viewed along the z-axis. Figure 1 shows the aggregate structures for the magnetic particle-field strength $\xi = 5$, the relative viscous force $R_B = 20$ and the magnetic particle-particle interaction strengths of $\lambda = 1$, $\lambda = 7$ and $\lambda = 12$. It is noted that the yellow dot of each particle implies the direction of the magnetic moment. In the case of the weak magnetic particle-particle interaction strength $\lambda = 1$ shown in Figure 1(a), the particles do not tend to aggregate to form clusters and tend to move as single particles. The magnetic moment of each particle quickly inclines in the field direction due to the influence of the relatively strong magnetic particle-field interaction strength $\xi = 5$. In the case of the relatively large magnetic particle-particle interaction strength $\lambda = 7$ shown in Figure 1(b), it is seen that short linear chain-like clusters are formed in the system that tend to be restricted to motion in the xy-plane. This is because the magnetic moment of each particle is restricted to the magnetic field direction due to the influence of the magnetic field being more dominant. Moreover, it is seen that the short chain-like clusters tend to incline in the field direction to a greater degree than the long chain-like clusters. This is because long chain-like clusters are significantly influenced by the viscous friction force, which leads to a larger resistance when the particle motion is tending to incline them in the field direction. That is, these long chain-like clusters function to delay the magnetic moments of the constituent particles to align toward the magnetic field direction. In the case of the relatively strong magnetic particle-particle interaction strength $\lambda = 12$ shown in Figure 1(c), both chain-like and ring-like clusters are formed in the system. The direction of the magnetic moments of the particles constituting the ring-like clusters is not significantly restricted to the magnetic field direction because the influence of the magnetic particle-particle interaction tends to dominate over the effect of the magnetic field. In the situation where the frequency of the magnetic field is sufficiently low, the orientation of the magnetic moment of each particle is primarily determined by the influence of magnetic particle-particle interaction.

Figure 2 shows the radial distribution function for the three cases of the magnetic particle-particle interaction strength $\lambda = 1$, $\lambda = 7$ and $\lambda = 12$. For the case of the weak magnetic particle-particle interaction strength $\lambda = 1$, the curve exhibits a typical gas-like distribution. For the case of the relatively strong magnetic particle-particle interaction strength $\lambda = 7$, several sharp peaks are seen that clearly imply the formation of the linear chain-like clusters where the second, third and fourth neighbouring particles in a linear cluster would be located at $r^* \simeq 1.3$, $r^* \simeq 2.6$ and $r^* \simeq 3.9$. For the case of the stronger magnetic particle-particle interaction strength $\lambda = 12$, although similar peaks appear at $r^* = 1.3$, $r^* \simeq 2.6$ and $r^* \simeq 3.9$, they exhibit duller characteristics that quantitatively suggest that ring-like clusters have formed in the system. The distance between the constituent particles in a ring-like cluster is dependent on the number of constituent particles, giving rise to the duller characteristics of the radial distribution function.

We now focus on the rotational behaviour of a linear chain-like cluster. Figure 3 shows the transition of the aggregate structures for the case of the magnetic particle-particle interaction strength $\lambda = 10$, the magnetic particle-field interaction strength $\xi = 10$ and the relative viscous force $R_B = 20$. The linear chain-like cluster shown in Figure 3(a) transforms to the distorted chain-like cluster shown in Figure 3(b) since the frequency of the magnetic field is not low enough to maintain the linear chain-like configuration. The constituent particles located at both the ends of the chain-like cluster exhibit a relative freedom in their motion over the particles in the centre area of the cluster, so they are able

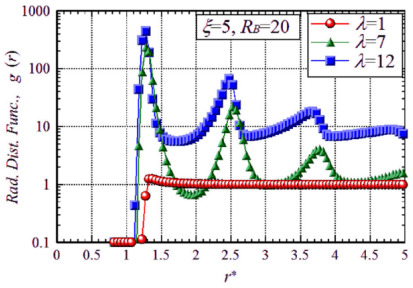

Figure 2. Radial distribution function for $\xi = 5$ and $R_B = 20$. For the case of $\lambda = 7$ and 12, the curves exhibit pronounced peaks. For the case of a relatively strong magnetic particle-particle interaction strength $\lambda = 7$, it is seen that several sharp peaks appear, which clearly implies the formation of the linear chain-like clusters.

to exhibit a significant tendency to follow the rotating magnetic field. When the distortion exceeds a certain degree, the long chain-like cluster cannot maintain the linear configuration and then dissociate into two chain-like clusters as shown in Figure 3(c). In the process of following the magnetic field, these short chain-like clusters then tend to reassemble and reform a long chain-like cluster. In this manner, the long linear chain-like clusters repeat this dissociation and association behaviour while following the applied rotational magnetic field.

Next, we discuss the dependence of the aggregate structures on the frequency of the rotating magnetic field. Figure 4 shows the aggregate structures for the case of the magnetic particle-particle interaction strength $\lambda = 12$, and the magnetic particle-field strength $\xi = 5$ for the relative frequency of a rotating field with values $R_B = 1$, $R_B = 5$ and $R_B = 10$. It is noted that a larger value of R_B implies a lower frequency of the rotating magnetic field. In the case of the relatively low frequency $R_B = 10$ shown in Figure 4(c), the more complex chain-like and ring-like clusters are formed. The orientation of the magnetic moments tends to follow the field more significantly than for the case of $R_B = 20$ shown in Figure 1(c). This is because the ring-like clusters are unstable in the case of $R_B = 10$ since the viscous force is more dominant than the magnetic particle-particle force. From a change in the internal structure of the clusters, we observe that these clusters alternate between a chain-like and a ring-like formation as the time advances. In contrast, in the case of a high frequency $R_B = 1$ shown in Figure 4(a), many single particles move without forming clusters, although several clusters composed of a configuration of two or three particles are formed. This is because, in the situation of a dilute system with a small volumetric fraction $\phi_V = 0.001$, the influence of the large viscous force of $R_B = 1$ does not provide an opportunity for particles to approach each other and therefore, only single particles and small clusters will be observed. In the case of the intermediate frequency $R_B = 5$ shown in Figure 4(b), ring-like clusters tend not to be formed and only distorted chain-like clusters and single particles are observed in the system. This is because the influence of the viscous force is of the same order as the magnetic particle-particle interaction, and thus the particles are able to form chain-like clusters but are not able to form ring-like clusters. From these results, we may understand that the frequency of the rotating magnetic field is able to control the regime of the internal configuration of the clusters.

Figure 5 shows the cluster size distribution for the three cases of the relative viscous force $R_B = 1$, $R_B = 5$ and $R_B = 10$, where N_s is the number of the clusters composed of s constituent particles. For the case of a rotating field with the relatively high frequency $R_B = 1$, the curve exhibits a high peak value at $s = 1$ that steeply decreases with increasing values of s. This characteristic quantitatively suggests that the particles predominately move as single particles as shown in Figure 4(a). For the case of the intermediate frequency $R_B = 5$, a peak still evident at $s = 1$, but the height is much lower than for the previous case and a cluster composed of around 7 particles is observed in the system. For the case of the further lower frequency $R_B = 10$, since the frequency is sufficiently low, particles are able to form longer clusters and thus a more flat region of the curve appears in the range of $s \lesssim 5$, and also a larger 9 particle cluster is evident. These characteristics quantitatively indicate that even with the influence of viscous forces, stable clusters have formed with 2–9 constituent particles.

We now proceed to the discussion regarding the characteristics of the heating effect. First, we consider the dependence of the heating effect on the magnetic particle-particle interaction strength. Figure 6 shows the dependence of the heating effect on the magnetic particle-particle interaction strength for the case of the relatively low viscous force $R_B = 20$ and the magnetic particle-field interaction strengths $\xi = 1$, $\xi = 5$ and $\xi = 10$. In the figure, W_{cycl}^* is the quantity non-dimensionalized by the thermal energy kT, where k is Boltzmann's constant and T is the absolute temperature of the system. For the case of the relatively weak magnetic particle-field strength $\xi = 1$, as is to be expected, the heating effect is significantly small. This is simply because the applied magnetic field strength is too weak for generating a heat production by means of magnetic particle-field interactions. In contrast, for the case of the

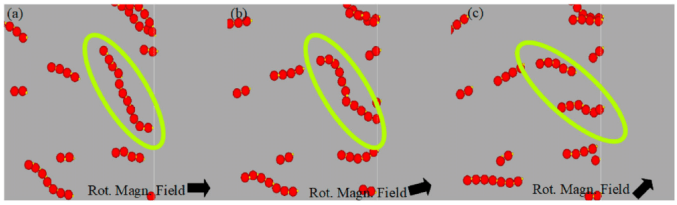

Figure 3. Transition of the aggregate structures for $R_B = 20$, $\lambda = 10$ and $\xi = 10$. When the distortion exceeds allowance, the long chain-like cluster cannot keep the linear formation. Then, the cluster dissociates into two chain-like clusters shown in Figure 3(c).

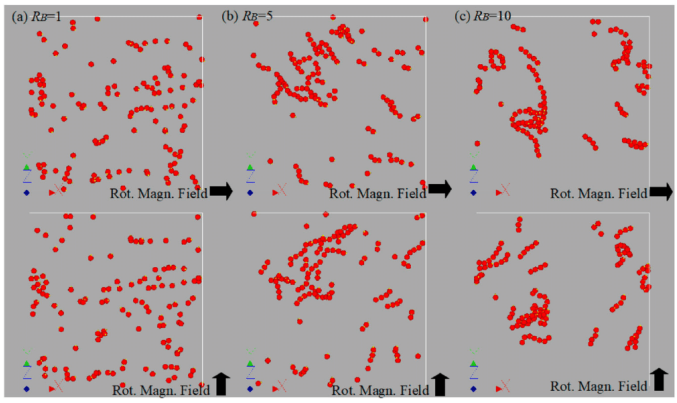

Figure 4. Aggregate structures in a rotating field with the relative frequency (a) $R_B = 1$, (b) $R_B = 5$ and (c) $R_B = 10$ for a system with parameter values $\lambda = 12$ and $\xi = 5$. In the case of a low frequency $R_B = 10$ shown in Figure 4(c), the complex chain-like and ring-like clusters are formed. The orientation of the magnetic moments tends to follow more significantly than for the case of $R_B = 20$ shown in Figure 1(c).

higher magnetic field strength $\xi = 10$, the heating effect exhibits a monotonic increase with increasing values of λ. This is because chain-like clusters that offer a larger resistance to the particle rotation are formed in the system, which leads to a larger value of the heating effect. Therefore in this situation, there is no significant formation of ring-like clusters in the system. In contrast, the curve for $\xi = 5$ exhibits a pronounced change in the heating effect as a function of the magnetic particle-particle interaction strength. That is, the heating effect increases in a similar way to the case of $\xi = 10$ in the region below $\lambda \simeq 6$ but then deviates and attains to a maximum value at $\lambda \simeq 10$ and then finally with increasing values of λ monotonically decreases to zero. In the range of $3 \lesssim \lambda \lesssim 10$, the chain-like clusters are predominately formed in the system and these increase in length with increasing values of λ. Within this range the magnetic moments of the particles are able to sufficiently follow the changing magnetic field direction by the motion of a delayed rotation of the whole chain-like cluster. The rotational motion of a longer chain-like cluster exhibits a larger viscous resistance, which leads to a more significant heating effect. The decrease in the heating effect in the region with a magnetic particle-particle interaction strength greater than $\lambda = 10$ is due to an increase in the formation of ring-like clusters together with a decrease in the number of chain-like clusters. Ring-like clusters tend to be much more stable than chain-like clusters in the situation of the magnetic particle-particle interaction of $\lambda \gtrapprox 10$ being more dominant than the magnetic particle-field interaction of $\xi = 5$. Hence, the magnetic moment of each constituent particle in a ring-like cluster does not respond sufficiently to the rotating magnetic field, and therefore the more stable ring-like cluster gives rise to a smaller heating effect with increasing values of λ.

Next, we discuss the influence of the frequency of the rotating magnetic field on the heating characteristics, where the average size of clusters is shown for

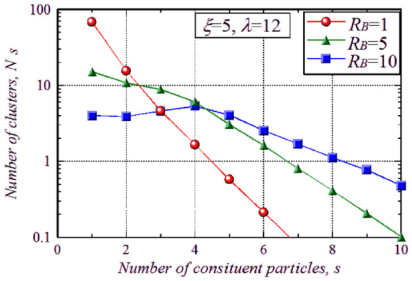

Figure 5. Cluster size distribution for $\lambda = 12$ and $\xi = 5$. For the case of $R_B = 10$, since the frequency is sufficiently low, particles are able to form longer clusters and thus a more flat region of the curve appears in the range of $s \lesssim 5$, and a larger cluster composed of 9 particles is evident in the system.

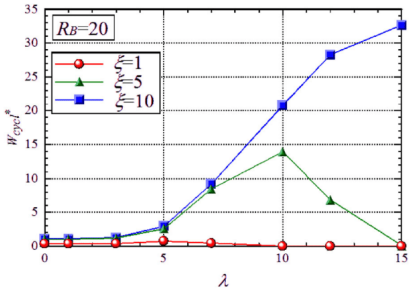

Figure 6. Dependence of the heating effect on the magnetic particle-particle interaction strength. Since ring-like clusters are much more stable than chain-like clusters in the situation of the magnetic particle-particle interaction being more dominant than the magnetic particle-field interaction, thus giving rise to a smaller heating effect in the *range of* $\lambda \gtrapprox 10$ for $\xi = 5$.

references. Figure 7 shows this influence to the heating effect and the average size of the aggregate structures for the case of the magnetic particle-particle interaction strength $\lambda = 1$, $\lambda = 5$ and $\lambda = 10$ and the magnetic particle-field strength $\xi = 5$. For the cases of a weak $\lambda = 1$ and a relatively weak $\lambda = 5$ magnetic particle-particle interaction strength, the heating effect decreases with increasing values of R_B or with decreasing values of the relative frequency. Since a larger value of R_B also implies a lower viscous friction force, the magnetic moment of single particles and the shorter clusters can easily follow a change in the orientation of the rotating magnetic field, which gives rise to the monotonic decrease in the heating effect with decreasing values of the frequency. On the other hand, for the case of $\lambda = 5$, it is seen that a deviation from the curve of $\lambda = 1$ becomes evident around $R_B \simeq 10$ and shows a slight increases with increasing values of R_B that may be explained in the following. For the case of $\lambda = 5$, many short clusters are expected to be formed if the viscous friction force is not a dominant factor in relation to the magnetic particle-particle interaction, or, if R_B has a sufficiently large value such as $R_B = 20$. However, short clusters are not formed in the region of a large viscous force such as $R_B = 5$, and this accounts for the monotonic decrease in the range of $R_B \lesssim 10$. For values greater than $R_B \simeq 10$, the effect of the magnetic interaction gradually surpasses the viscous force and thus with increasing values of $R_B$an increasing number of short clusters are formed. Short chain-like clusters give rise to a larger resistance to their orientation than the single particles following a change in the frequency of the rotating magnetic field. This yields a slight increase in the heating effect in the range of $R_B \gtrapprox 10$. The curve for $\lambda = 10$ exhibits a significantly different characteristic in contrast to the former two curves. That is, the heating effect decreases until around $R_B = 3$, then exhibits a significant increase that finally approaches a constant value in the region of $R_B \simeq 14$. The decrease in the region before $R_B = 3$ can be explained by the same reasoning as for the previous two cases. As the value of R_B exceeds a value around $R_B \simeq 3$, the effect of the magnetic particle-particle interaction surpasses the effect of the viscous friction forces and so particles are able to approach each other. This results in the formation of chain-like clusters that induce a larger resistance to the rotational motion, leading to a larger heating effect. The reason for the asymptotic approach of $R_B$to the value around $R_B \gtrapprox 14$ is that the chain-like clusters have tended to maximum growth and therefore a larger resistance cannot be obtained even if the frequency of the rotating magnetic field decreases.

Finally, we make a comparison of the present results with those for the previous alternating magnetic field [9], which were obtained by re-performing the simulations for the same condition of the present prescribed parameters. Figure 8 shows the dependence of the heating effect on the magnetic particle-particle interaction strength λ for the case of $R_B = 20$ and $\xi = 10$. In the region of weak magnetic particle-particle interaction strengths, $\lambda \lesssim 7$, the alternating magnetic field gives rise to a higher heating effect than the rotating magnetic field. This is because magnetic particles rotate with larger angular velocities in order to follow the change in the direction of an alternating magnetic field, whereas in the rotating magnetic field magnetic particles almost constantly rotate with smaller angular velocities. A larger angular velocity yields a larger friction force, and therefore a more significant heating effect is obtained for an alternating magnetic field. As the magnetic particle-particle interaction strength is

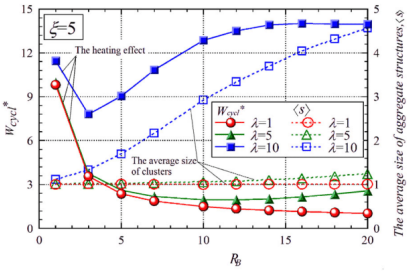

Figure 7. Dependence of the heating effect and the average size of clusters on the frequency of the magnetic field. The solid line and the broken line indicate the degree of the heating effect W_{cycl}^* and the average size of the aggregate structures, respectively. The curve for $\lambda = 10$ exhibits a steep increase since around $R_B = 3$ in contrast to the other cases. As the value of R_B exceeds around $R_B \simeq 3$, the magnetic particle-particle interaction surpasses the viscous friction forces for particles to approach each other and to form chain-like clusters, which induces a larger heating effect.

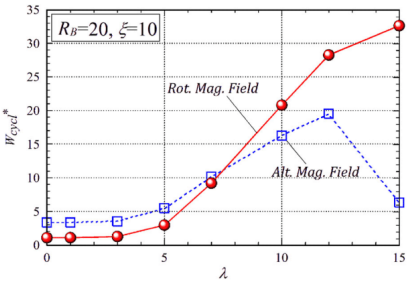

Figure 8. Comparison of the results for a roating and an alternating magnetic field with respect to the dependence of the heating effect on the magnetic particle-particle interaction strength. A characteristic difference in the heating effect in the region of $\lambda \gtrapprox 12$ is due to the completely different behaviours of chain-like clusters in a rotating and an alternating magnetic field.

increased from $\lambda \simeq 4$, both the magnetic fields more significantly enhance the heat production and afterwards exhibit characteristic differences in the dependence on the magnetic particle-particle interaction strength. That is, the heating effect continuously increases with values of λ for the rotating magnetic field, whereas the curve arrives at a maximum value at $\lambda \simeq 12$ and then significantly decreases for the case of the alternating magnetic field. These different heating characteristics are evidently due to the completely different behaviours of the chain-like clusters in a rotating and an alternating magnetic field. As sufficiently clarified in the previous study [9], longer chain-like clusters have a stronger tendency to maintain their configuration without rotation as the magnetic particle-particle ingeneration becomes more dominant than the magnetic particle-filed interaction, i.e. in the region of $\lambda \gtrapprox \xi$, giving rise to a sharp decrease after the value of $\lambda \simeq 12$. In significant contrast, for the case of a rotating magnetic field, linear chain-like clusters are able to rotate to a certain degree without a large resistance to the rotation in order to follow the change in the orientation of an rotating magnetic field, which gives rise to a constant increase in the range of $\lambda \gtrapprox 5$, although there is a repeat of breaking-up and recombination of linear chain-like clusters, as already pointed out in Figure 3. From these characteristics, we understand that a rotating magnetic filed is more superior in order to obtain a more significant heating effect if we make use of a magnetic particle suspension where chain-like clusters are significantly expected to be formed.

Figure 9 shows the comparison of the results of a rotating and an alternating magnetic field with respect to the dependence of the heating effect on the frequency of the applied magnetic field, where a relatively weak magnetic field of $\xi = 5$ is addressed. In the case of $\lambda = 1$, magnetic particles solely move or rotate without the formation of clusters, and thus similar characteristics are exhibited for these two different applied magnetic fields. Since long linear chain-like clusters are expected to be formed for the case of $\lambda = 10$, a rotating and an alternating magnetic field certainly yield completely different characteristics regarding the dependence on the value of R_B, i.e. on the frequency of the magnetic field. That is, the heating effect monotonically increases after $R_B \simeq 3$ with increased values of R_B for a rotating magnetic field, whereas in the case of an alternating magnetic field the heating effect comes to decrease after the attainment to an maximum value at $R_B \simeq 10$. Moreover, it is a noticeable point that the former field gives rise to a significantly larger heat performance than the latter magnetic field. A much poorer heat generation performance for an alternating magnetic field is due to the characteristic feature of chain-like clusters that the magnetic interactions of the magnetic particles constituting a chain-like cluster play a governing role to maintain the configuration of linear chain-like clusters without the rotation as a whole of clusters. This feature becomes more significant as the value of R_B is increased, i.e. as the frequency of the magnetic field is decreased. In contrast, for the case of a rotating field, chain-like clusters are able to rotate as a whole without a significant resistance resulting from the magnetic interactions among the particles forming a cluster,

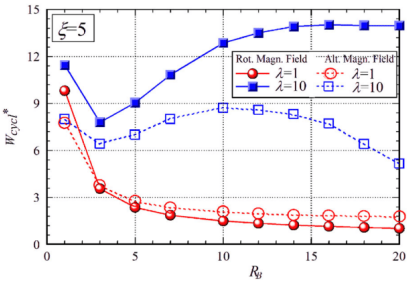

Figure 9. Comparison of the results for a rotating and an alternating magnetic field with respect to the dependence of the heating effect on the frequency of the magnetic field for the case of the magnetic field strength $\xi = 5$. For the case of a rotating field, chain-like clusters are able to rotate as a whole without a significant resistance resulting from the magnetic interactions among the particles forming a cluster, which leads to a large and monotonic increase after $R_B \simeq 3$.

as already pointed out in Figure 8, which leads to a monotonic increase after $R_B \simeq 3$. The reason why the heating effect is decreased for the both cases with increased values of R_B in the region of $R_B \lesssim 3$ is that the frequency of the magnetic field is too large for chain-like clusters to follow the change in the direction of the magnetic field, where large viscous resistances arise for the chain-like clusters to rotate in this situation, giving rise to less active rotational motion of chain-like clusters. From these characteristics, as in Figure 8, we also make a conclusion that a rotating magnetic field is significantly more suitable for producing the heat generation in a strongly interaction system of magnetic particles.

6. Conclusion

In the present study, we have investigated the relationship between the aggregate structures and the heating effect in a rotating magnetic field by means of Brownian dynamics simulations. The main factors characterising the present phenomenon are the viscous friction force arising from the strength of a rotating magnetic field, the strength of the magnetic particle-particle interaction and the random Brownian force. The main results obtained are summarised in the following. In the situation of a weak magnetic particle-particle interaction, magnetic particles do not aggregate to form significant clusters, and the single particles do not give rise to a sufficiently large heating effect. In the situation where chain-like clusters are predominantly formed in the system and where the aggregates exhibit a larger viscous resistance during their rotation, a significantly large heating effect may be obtained as a result. If the magnetic particle-particle interaction is sufficiently strong then particles may form ring-like clusters. The magnetic moments of the constituent particles in a ring-like cluster are not able to respond sufficiently to a change in the field direction due to the strong attractive forces between the constituent particles. This implies that stable ring-like clusters are not able to provide a large heating effect in a rotating magnetic field. From these characteristics, we may conclude that if the effect of the applied magnetic field is relatively more dominant than the magnetic particle-particle interaction in the situation where the magnetic interaction surpasses the effect of the thermal motion, then linear chain-like clusters are predominately formed in the system that give rise to a significantly larger heating effect than single particles. From the comparison of the present results with the previous ones for an alternating magnetic field, we have obtained a significant difference in the heat generation performance. In the case of a rotating magnetic field, chain-like clusters are able to rotate as a whole without a significant resistance resulting from the magnetic interactions among the particles forming a cluster, which yields a sufficiently large heating effect even in the situation of the magnetic particle-particle interaction being more dominant than the magnetic particle-field interaction. We therefore make a conclusion that a rotating magnetic field is significantly more suitable for producing the heat generation in a strongly interaction system of magnetic particles than an alternating magnetic field.

Disclosure statement

No potential conflict of interest was reported by the authors.

Funding

SS would like to acknowledge the financial support from Grant-in-Aid for Japan Society for the Promotion of Science Fellows [grant number 20J22468].

References

[1] N.M. Wereley, editor, *Magnetorheology: Advances and Applications* (Royal Society of Chemistry, London, 2013).
[2] J.W. Harrell, S. Kang, Z. Jia, D.E. Nikles, R.W. Chantrell and A. Satoh, Appl. Phys. Lett. **87**, 202–208 (2005). doi:10.1063/1.2132539
[3] S.H. Sajjadi and E.K. Goharshadi, J. Environ. Chem. Eng. **5**, 1096–1106 (2017). doi:10.1016/j.jece.2017.01.035
[4] U. Häfeli, W. Schütt, J. Teller and M. Zborowski, editors, *Scientific and Clinical Applications of Magnetic Carriers* (Springer, Berlin, 1997).
[5] R.E. Rosensweig, J. Magn. Magn. Mater. **252**, 370–374 (2002). doi:10.1016/S0304-8853(02)00706-0

[6] X. Yao, K. Sabyrov, T. Klein, R.L. Penn and T.S. Wiedmann, J. Magn. Magn. Mater. **381**, 21–27 (2015). doi:10.1016/j.jmmm.2014.12.035
[7] B.B. Lahiri, S. Ranoo, A.W. Zaibudeen and J. Philip, J. Magn. Magn. Mater. **441**, 310–327 (2017). doi:10.1016/j.jmmm.2017.05.076
[8] Z. Zhao and C. Rinaldi, J. Phys. Chem. C. **122**, 21018–22130 (2018). doi:10.1021/acs.jpcc.8b04071
[9] S. Suzuki and A. Satoh, Colloid Poly. Sci. **297**, 1265–1273 (2019). doi:10.1007/s00396-019-04546-x
[10] P. Cantillon-Murphy, L.L. Wald, E. Adalsteinsson and M. Zahn, J. Magn. Magn. Mater. **322**, 727–733 (2010). doi:10.1016/j.jmmm.2009.10.050
[11] M. Bekovic, M. Trbusic, M. Trlep, M. Jesenik and A. Malter, Adv. Mater. Sci. Eng (2018). doi:10.1155/2018/6143607.
[12] A.F. Abu-Bakr and A. Yu, J. Magn. Magn. Mater. **477**, 404–407 (2019). doi:10.1016/j.jmmm.2018.07.010
[13] I.M. Obaidat, B. Issa and Y. Haik, Nanomaterials. **5**, 63–89 (2015). doi:10.3390/nano5010063
[14] C.S.S.R. Kumar and F. Mohammad, Advan. Drug Delivery Rev. **63**, 789–808 (2011). doi:10.1016/j.addr.2011.03.008
[15] C. Guibert, V. Dupuis, V. Peyre and J. Fresnais, J. Phys. Chem. C. **119**, 28148–28154 (2015). doi:10.1021/acs.jpcc.5b07796
[16] D. Serantes, D. Baldomir, C. Martinez-Boubeta, K. Simeonidis, M. Angelakeris, E. Natividad, M. Castro, A. Mediano, D.-X. Chen, A. Sanchez, L.I. Balcells and B. Martínez, J. Appl. Phys. **108**, 073918 (2010). doi:10.1063/1.3488881
[17] M.P. Allen and D.J. Tildesley, *Computer Simulation of Liquids* (Clarendon Press, Oxford, 1987).
[18] A. Satoh, A. R, W. Chantrell, S. Kamiyama and G.N. Coverdale, J. Magn. Magn. Mater. **154**, 183–192 (1996). doi:10.1016/0304-8853(95)00588-9
[19] D.J. Adams, E.M. Adams and G.J. Hills, Molec. Phys. **38**, 387–400 (1979). doi:10.1080/00268977900101751
[20] P.D. Duncan and P.J. Camp, J. Chem. Phys. **121**, 11322–11331 (2004). doi:10.1063/1.1812744
[21] A. Satoh, *Modeling of Magnetic Particle Suspensions for Simulations* (CRC Press, Boca Raton, 2017).

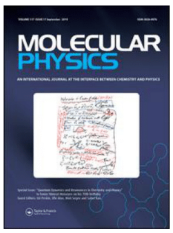

Taylor & Francis
Taylor & Francis Group

Molecular Physics

An International Journal at the Interface Between Chemistry and Physics

ISSN: (Print) (Online) Journal homepage: https://www.tandfonline.com/loi/tmph20

The behavior and heat generation effect of a magnetic rod-like particle suspension in an alternating and a rotating magnetic field

Seiya Suzuki & Akira Satoh

To cite this article: Seiya Suzuki & Akira Satoh (2022): The behavior and heat generation effect of a magnetic rod-like particle suspension in an alternating and a rotating magnetic field, Molecular Physics, DOI: 10.1080/00268976.2022.2151523

To link to this article: https://doi.org/10.1080/00268976.2022.2151523

MOLECULAR PHYSICS e2151523
https://doi.org/10.1080/00268976.2022.2151523

Taylor & Francis
Taylor & Francis Group

RESEARCH ARTICLE

The behavior and heat generation effect of a magnetic rod-like particle suspension in an alternating and a rotating magnetic field

Seiya Suzuki[a] and Akira Satoh[b]

[a]Graduate School of Akita Prefectural University, Yurihonjo, Japan; [b]Department of Mechanical Engineering, Akita Prefectural University, Yurihonjo, Japan

ABSTRACT

We have investigated the behavior of magnetic rod-like particles and their relationship with the heat generation effect for both alternating and rotating magnetic fields, by means of Brownian dynamics simulations. As a common feature for both type of magnetic field variations, in the case of significantly strong particle-particle interaction strengths, densely-packed clusters are formed, which do not contribute to the heat generation. For the case of the alternating magnetic field, in the intermediate frequency range, linear thick chain-like clusters are formed and the constituent rod-like particles themselves tend to rotate to follow the change in the field. In contrast, for the case of the rotating field, linear clusters rotate as a whole body to respond to the magnetic field rotation. In both type of magnetic field variations, the magnetic interactions between the constituent particles in a cluster tend to function to suppress the relaxational motion of the rod-like particles, which, as a result, leads to increase in the heat generation effect in certain situations. In a relatively large frequency region, the rotating applied magnetic field gives rise to a larger heat generation effect, whereas in contrast, in the lower frequency region the alternating magnetic field yields the larger heating effect.

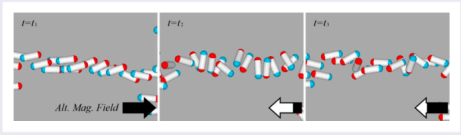

Highlights

- The behavior of magnetic rod-like magnetic particles has been elucidated in the case of an alternating and a rotating magnetic field.
- The magnetic interactions between the constituent particles in a cluster tend to suppress the relaxation motion of the rod-like particles.
- The frequency and strength of a time-dependent magnetic field have complex influences on the heating effect.
- In a relatively large frequency region, the rotating applied magnetic field gives rise to a larger heat generation effect.
- In a relatively lower frequency region, the alternating magnetic field is superior to the rotating field.

ARTICLE HISTORY
Received 31 August 2022
Accepted 17 November 2022

KEYWORDS
Magnetic rod-like particle; heat generation effect; magnetic hyperthermia; alternating magnetic field; rotating magnetic field

1. Introduction

A magnetic particle suspension is a functional fluid for potential application in a variety of fields, such as fluid engineering [1], magnetic material engineering [2,3], environmental resource engineering [4,5], and so forth. Recently, the interest in magnetic particle suspensions has been expanded to the biomedical engineering field, where the typical applications are in magnetically-guided drug delivery system and magnetic hyperthermia treatment [6–9]. Magnetic hyperthermia is one of the medical therapies for killing tumor or cancer cells by means of a heating effect that is generated by the interactions between magnetic particles and an applied magnetic field [10–12]. To this end, an alternating or a rotating applied

CONTACT Akira Satoh asatoh@akita-pu.ac.jp Department of Mechanical Engineering, Akita Prefectural University, Yurihonjo, Japan

magnetic field is ordinarily employed instead of a typical uniform time-independent magnetic field.

Our research group has an interest in the behavior of magnetic particles with size relatively larger than ten nanometers, where heat generation arises due to the Brownian relaxation mechanism in a time-dependent applied magnetic field [13]. Although there are a large number of studies for magnetic particles of around ten nm, where the Néel relaxation mechanism is governing factor for the heat generation, there are limited studies with respect to the heat generation phenomenon for a suspension of these larger magnetic particles [14–16]. For example, Yao et al. [14] have addressed magnetic spheroidal particles with the size larger than 100nm, and Lahiri et al. [16] have treated magnetic emulsion droplets. In addition to the ordinary alternating magnetic field, there are several experimental studies regarding the heat generation effect in the case of a rotating magnetic field [17,18]. Bekovic et al. have experimentally showed that a rotating magnetic field gives rise to a significantly larger heat generation performance than an alternating magnetic field [18].

In a previous study [19], we have addressed the behavior of a magnetic spherical particle suspension in response to an alternating magnetic field, and clarified that chain-like clusters effectively function to give rise to a significant heat generation effect under certain situations. Subsequently we expanded this study to the case of a rotating magnetic field in order to clarify the dependence of the aggregate structure and the heat generation effect on the type of a time-dependent applied magnetic field [20]. From this study, we clearly understand that a higher heating effect is obtained by means of a rotating magnetic field rather than an alternating magnetic field in the situation where stable aggregate structures are formed in the system.

In the Brownian relaxation mode, a larger viscous friction may be expected to give rise to a larger heat generation performance, and thus as a simulation study at the next stage it is naturally required to address a suspension of magnetic particles with a more general geometrical shape such as rod-like, disk-like and cube-like shape. Modern synthesis technology enables the generation of these magnetic particles, for example, rod-like particles [21–23], disk-like particles [24,25] and cubic particles [26–29].

From this background, in the present study we address a suspension composed of magnetic rod-like particles in order to elucidate the behavior of the aggregate structure and the heat generation effect in the two cases of an applied magnetic field, an alternating and a rotating applied magnetic field. To this end, as in the previous studies, we have employed the Brownian dynamics method as a particle-based simulation technique, which enables us to discuss the influence of the dynamic behavior of the aggregate structure of the particles on the heat generation effect.

2. Modelling of magnetic rod-like particles and time-dependent applied magnetic fields

We employ a spherocylinder particle shown in Figure 1 as a model of rod-like particles. The rod-like particle has a magnetic moment $\boldsymbol{m}$ oriented in the major axis direction at the particle centre. The diameter and length of the rod-like particle are denoted by d and l, which give rise to the particle aspect ratio $r_p (= l/d)$. In order to recognise the magnetic moment direction in snapshots, the hemisphere in the magnetic moment direction is colored by red (dark) and the opposite hemisphere is colored by blue (light), as shown in Figure 1. Moreover, it is assumed that the surface of each particle is covered by a uniform steric layer with thickness δ for generating a steric repulsion in order to prevent them from a physically unreasonable overlap.

As already mentioned, in the present study we employ two types of time-dependent applied magnetic fields, specifically, an alternating magnetic field and a rotating magnetic field. An alternating magnetic field $\boldsymbol{H}_{alt}(t)$ is applied in the x-direction, expressed as.

$$\boldsymbol{H}_{alt}(t) = H_0 \sin(\omega_H t)\ \boldsymbol{i}_x \tag{1}$$

Similarly, a rotating magnetic field $\boldsymbol{H}_{rot}(t)$ is applied in the xy-plane, expressed as

$$\boldsymbol{H}_{rot}(t) = H_0 \{ \cos(\omega_H t)\ \boldsymbol{i}_x + \sin(\omega_H t)\ \boldsymbol{i}_y \} \tag{2}$$

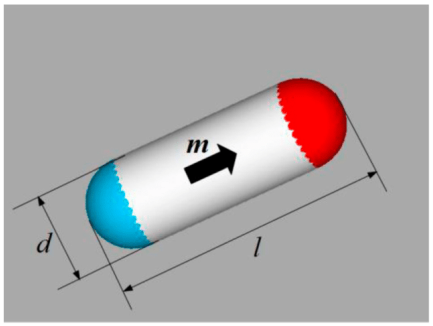

Figure 1. Particle model of a magnetic rod-like particle. It is idealised as a spherocylinder with a magnetic dipole moment in the major axis direction at the particle centre.

In these expressions, H_0 and ω_H are the magnitude and the angular velocity of the applied magnetic field, respectively, and $\boldsymbol{i}_x$ and $\boldsymbol{i}_y$ are the unit vectors in the x- and y-direction, respectively.

3. Brownian dynamics

The Brownian dynamics simulation method for axisymmetric particles such as rod-like and disk-like particles has already been described sufficiently in previous papers and textbook [30–32], and therefore we here merely describe only the key expressions relevant for the current investigation.

In the case of the axisymmetric particle, the equation of motion can be decomposed into the translational motion in the particle axis direction and in the direction normal to the particle axis. The particle position $\boldsymbol{r}(t)$ at time t is described as

$$\boldsymbol{r}_{||}(t+\Delta t) = \boldsymbol{r}_{||}(t) + \frac{1}{k_B T} D_{||}^T \boldsymbol{F}_{||}^P(t)\Delta t + \Delta r_{||}^B \boldsymbol{e}(t) \quad (3)$$

$$\boldsymbol{r}_{\perp}(t+\Delta t) = \boldsymbol{r}_{\perp}(t) + \frac{1}{k_B T} D_{\perp}^T \boldsymbol{F}_{\perp}^P(t)\Delta t + \Delta r_{\perp 1}^B \boldsymbol{e}_{\perp 1}(t) + \Delta r_{\perp 2}^B \boldsymbol{e}_{\perp 2}(t) \quad (4)$$

The particle direction $\boldsymbol{n}$ ($= \boldsymbol{m}/m = \boldsymbol{m}/|\boldsymbol{m}|$) obeys the following equation of motion

$$\boldsymbol{n}(t+\Delta t) = \boldsymbol{n}(t) + \frac{1}{k_B T} D_{\perp}^R \boldsymbol{T}_{\perp}^p(t) \times \boldsymbol{n}\Delta t + \Delta\phi_{\perp 1}^B \boldsymbol{e}_{\perp 1}(t) + \Delta\phi_{\perp 2}^B \boldsymbol{e}_{\perp 2}(t) \quad (5)$$

In these equations the notations have the following meanings. The quantities with subscripts $\perp$ and $||$ represent components normal and parallel to the particle axis, respectively, $\boldsymbol{F}^P$ and $\boldsymbol{T}^P$ are the forces and torques acting on the particle of interest, Δt is the time interval, D^T and D^R are the diffusion coefficients of the spherocylinder particle for the translational and rotational motion [31,32], respectively, $\boldsymbol{e}_{\perp 1}$ and $\boldsymbol{e}_{\perp 2}$ are the unit vectors normal to each other in the plane normal to the particle axis, T is the liquid temperature, and k_B is Boltzmann's constant. It is noted that the force $\boldsymbol{F}^P$ and torque $\boldsymbol{T}^P$ are evaluated from sum of the magnetic and steric repulsive forces and torques exerted by the other particles and an applied magnetic field. Moreover, $\Delta r_{||}^B$, $\Delta r_{\perp 1}^B$ and $\Delta r_{\perp 2}^B$ are the random displacements inducing the translational Brownian motion and have the stochastic characteristics that imply a relationship with the translational diffusion coefficients [31,32]. Similarly, $\Delta\phi_{\perp 1}^B$ and $\Delta\phi_{\perp 2}^B$ are the random displacements inducing the rotational Brownian motion and have the stochastic characteristics that imply a relationship with the rotational diffusion coefficients [31,32]. For reference, the diffusion coefficients will be expressed in Appendix, where the non-dimensional expressions are shown to be dependent on the particle aspect ratio r_p.

4. Heating effect

As already mentioned, magnetic particles sufficiently larger than around 10 nm tend to give rise to a heat generation due to the Brownian relaxation mechanism. From the thermodynamic theory, it is seen that the work dW done on the system by an increase in the magnetic flux density, $d\boldsymbol{B}$, in a magnetic field $\boldsymbol{H}$ gives rise to an increase in the internal energy of the system, dU, that is, $dW = \boldsymbol{H}\cdot d\boldsymbol{B} = dU$, where an adiabatic process has been assumed. By taking into account the expression of $\boldsymbol{B} = \mu_0(\boldsymbol{H}+\boldsymbol{M})$, where $\boldsymbol{M}$ is the magnetization and μ_0 is the permeability of free space, the work per period of an applied magnetic field is expressed as

$$\begin{aligned} W_{cycl}^{total} &= \oint \boldsymbol{H}\cdot d\boldsymbol{B} = \mu_0 \oint \boldsymbol{H}\cdot d(\boldsymbol{H}+\boldsymbol{M}) \\ &= [\mu_0 \boldsymbol{H}\cdot(\boldsymbol{H}+\boldsymbol{M})]_{cycl} - \mu_0 \oint (\boldsymbol{H}+\boldsymbol{M})\cdot d\boldsymbol{H} \\ &= -\mu_0[(1/2)\boldsymbol{H}\cdot\boldsymbol{H}]_{cycl} - \mu_0 \oint \boldsymbol{M}\cdot d\boldsymbol{H} \\ &= -\mu_0 \oint \boldsymbol{M}\cdot d\boldsymbol{H} \end{aligned} \quad (6)$$

This relationship has already been shown and formalised in a pioneer work by R. E. Rosensweig [13]. In Eq. (6) the magnetic field $\boldsymbol{H}$ is the time-dependent magnetic field, $\boldsymbol{H} = \boldsymbol{H}_{alt}$ or $\boldsymbol{H} = \boldsymbol{H}_{rot}$ in the present study. The magnetization $\boldsymbol{M}$ is a quantity per unit volume and therefore this quantity corresponds to $\boldsymbol{m} = m\boldsymbol{n}$ per particle. Hence, the heat generation per particle in one cycle is expressed as

$$W_{cycl} = -\mu_0 m H_0 \oint (\langle\boldsymbol{n}\rangle \cdot d(\boldsymbol{H}/H_0)) \quad (7)$$

Equation (7) is normalised by thermal energy $k_B T$, expressed as

$$W_{cycl}{}^* = -\xi \oint (\langle\boldsymbol{n}\rangle \cdot d(\boldsymbol{H}/H_0)) \quad (8)$$

In Eqs. (7) and (8), H_0 is the maximum value of a time dependent magnetic field $\boldsymbol{H}$, as already defined, and ξ is a non-dimensional parameter that implies the strength of the magnetic particle-field interaction, which will be shown in Eq. (9).

5. Parameters for simulations

Unless specifically noted, the present results were obtained by adoption of the following parameter values. The number of particles $N = 216 = 6^3$, the volumetric function $\phi_V = 0.001$, the time step $\Delta t^* (= \Delta t / (2\pi/\omega_H)) = 0.00001$, and the total simulation time $t_{total}{}^* (= t_{total}/(2\pi/\omega_H)) = 3000$, where data from the last 30% of the simulation time were used for the averaging procedure. The diameter of the particles $d^* = 1.0$, the thickness of the steric layer $\delta^* (= \delta/d) = 0.15$, the particle aspect ratio $r_p = 3$, and the cutoff radius $r_{coff}{}^* (= r_{coff}/d) = 8.0$ for evaluation of magnetic forces and torques. Using these parameters, we evaluate the dimensions of the simulation cell as $l_x{}^* = l_y{}^* = l_z{}^* = 76.77$, where $l_x{}^* = l_x/d$, and so forth.

The present phenomenon is characterised by the four non-dimensional parameters, λ, ξ, λ_V and R_B as [31,32]

$$\lambda = \frac{\mu_0 m^2}{4\pi d^3 k_B T}, \qquad \xi = \frac{\mu_0 m H_0}{k_B T}, \qquad \lambda_V = \frac{\pi n_s d^2}{2},$$
$$R_B = \frac{k_B T}{3\pi\eta d^3} \cdot \frac{2\pi}{\omega_H} \tag{9}$$

in which λ is the strength of the magnetic particle-particle interaction, ξ is the strength of the magnetic particle-field interaction and λ_V is the strength of the repulsive force due to the overlap of the steric layers relative to thermal motion. Moreover, R_B is the strength of the random force relative to the viscous force. In these expressions, η is the viscosity of the base liquid, and n_s is the number of surfactant molecules per unit surface of magnetic particles.

If R_B is much smaller than unity, i.e. if the frequency is significantly high, then viscous friction forces become the dominant factor for governing the particle motion, and therefore the magnetic rod-like particles may not be able to follow a change in the magnetic field direction due to large viscous forces. On the other hand, if R_B is much smaller than unity, the random force, i.e. Brownian motion, becomes dominant over the viscous forces, and thus the magnetic rod-like particles may change their direction in response to the applied magnetic field in the case of sufficiently strong interactions between the magnetic moment and the applied magnetic field. In the latter case, the relationship between the magnitudes of λ and ξ determines the behavior of the magnetic rod-like particles in a time-dependent applied magnetic field. In the present study, these non-dimensional parameters λ, ξ, R_B and λ_V are set within the wide range of $\lambda = 1 \sim 100$, $\xi = 0 \sim 100$, $R_B = 0.1 \sim 3$ and $\lambda_V = 150$.

6. Results and discussion

6.1. For the case of the alternating magnetic field

6.1.1. Time variation change in aggregate structures of particles

In Section 6.1 we discuss results for the case of an alternating magnetic field and firstly consider the characteristics of aggregate structures of rod-like particles. It is noted that, although the present simulations were performed for a 3D system, snapshots that are viewed from the z-axis direction will be shown in order to illustrate aggregate structures more straightforwardly.

Before proceeding to a discussion regarding the time change in aggregate structures, we show the influence of magnetic particle-particle interactions on the cluster formation for the case of a low frequency region of $R_B = 3$, where an alternating magnetic field is applied along the x-axis direction. Figure 2 shows snapshots for three different cases of the magnetic particle-particle interaction strength, $\lambda = 1$, 60 and 100, which were obtained at the time of maximum field strength in the x-axis direction, i.e. $|\boldsymbol{H}| = H_0$ with the particle-field interaction strength $\xi = 80$.

In the case of a weak magnetic particle-particle interaction strength $\lambda = 1$, shown in Figure 2(a), the particles do not aggregate to form clusters and thus move as single particles. This is because the magnetic interaction strength is not sufficient for the formation of clusters for $\lambda = 1$. Moreover, since viscous forces are sufficiently low for the rotational motion of the particles in the low frequency $R_B = 3$, the rod-like particles are able to respond to a change in the field direction. This is clearly shown in the snapshot where all the rod-like particles strongly tend to incline in the magnetic field direction (or x-axis direction). In the case of $\lambda = 60$, it is evidently seen that relatively thick chain-like clusters are formed along the magnetic field direction and each constituent particle of the rod-like clusters inclines along the field direction. In contrast, in the case of a further increase in interaction strength $\lambda = 100$, the rod-like particles exhibit completely different clusters, that is, densely-packed clusters are formed, rather than chain-like clusters, and the neighboring rod-like particles constituting a cluster orient in the opposite directions to each other, which gives rise to a lower magnetic interaction energy. Although the values of $\lambda = 60$ and $\lambda = 100$ are sufficiently strong for the cluster formation, why do these completely different aggregate structures appear? It is the magnetic field strength that mainly governs the behavior of the rod-like particles, that is, these different structures arise due to the relative magnitudes between the magnetic particle-particle (λ) and particle-field (ξ) interaction strengths.

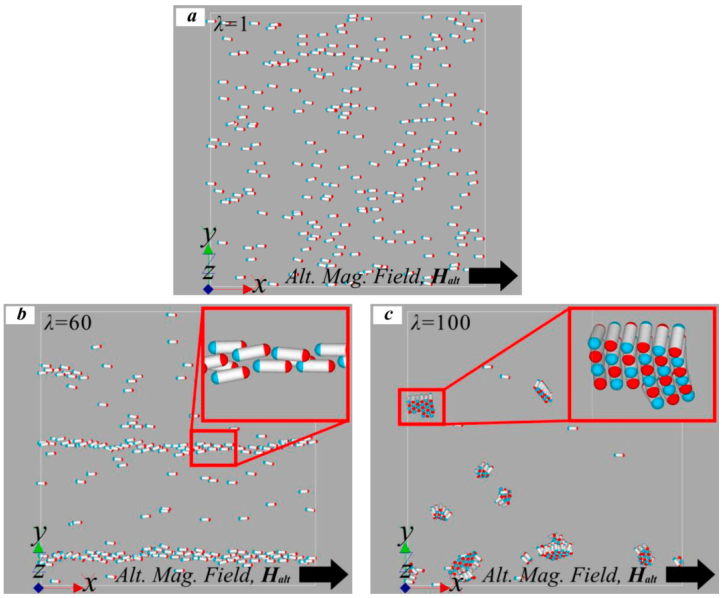

Figure 2. Aggregate structures for $\xi = 80$ and $R_B = 3$: (a) for $\lambda = 1$, (b) for $\lambda = 60$ and (c) for $\lambda = 100$. In the case of an intermediate magnetic particle-particle interaction strength $\lambda = 60$, relatively thick chain-like clusters are formed along the magnetic field direction and each rod-like particle inclines along the field direction.

In the case of $\lambda = 60$, the field strength is still one of the governing factors for the particle motion in the situation of $\xi = 80$, and therefore the rod-like particles are able to form clusters and each particle strongly tends to incline in the field direction, which leads to linear thick chain-like clusters with the constituting particles aligning to the field direction, shown in Figure 2(b). In contrast, in the case of $\lambda = 100$, the magnetic particle-particle interaction is significantly stronger than the magnetic particle-field interaction, and thus in this situation the former factor has a main influence on the cluster formation. If the rod-like particles have a dipole moment along the major axis direction at the particle centre, in the case of a sufficiently strong interaction, two particles aggregate to form a raft-like cluster along the minor axis direction. This cluster unit is repeated and expanded in the 3D system to form the densely-compacted aggregate structures shown in Figure 2(c). From now on, we focus on results for the case of $\lambda = 60$ unless specifically noted.

Figure 3 shows the time variation in the chain-like clusters for the case of a strong magnetic field $\xi = 80$ with a low frequency of $R_B = 3$, where three different snapshots are shown at the phase angles, (a) $\theta = \pi$, (b) $\theta = 6\pi/5$ and (c) $\theta = 4\pi/3$. The snapshot in Figure 2(b) should be referred to for the case of $\theta = \pi/2$. As already shown above, since rod-like particles form relatively thick chain-like clusters, as shown in Figure 2(b), we here focus on the behavior of the thick chain-like clusters mainly at the phase angle around $\theta = \pi$, where the alternating magnetic field switches direction from the positive towards the negative x-axis direction. At the phase angle of $\theta = \pi/2$, shown Figure 2(b), the magnetic field strength attains the maximum value, and thus the thick chain-like clusters strongly tend to align to the field direction (x-direction). At the larger phase angle of $\theta = \pi$, the thick chain-like cluster starts to become unstable since the mechanism for keeping linear chain-like cluster formation disappears in the absence of an external magnetic field. At a later phase of $\theta = 6\pi/5$, it seems that the raft-like cluster is largely formed and at the phase angle of $\theta = 4\pi/3$ each particle has completed the reversal motion to align to the field direction (the negative x-direction). It is reasonable that raft-like clusters shown in Figure 3(b) are preferred as intermediate cluster formation from an energy point of view. Since viscous friction forces are not sufficiently strong in the case of $R_B = 3$,

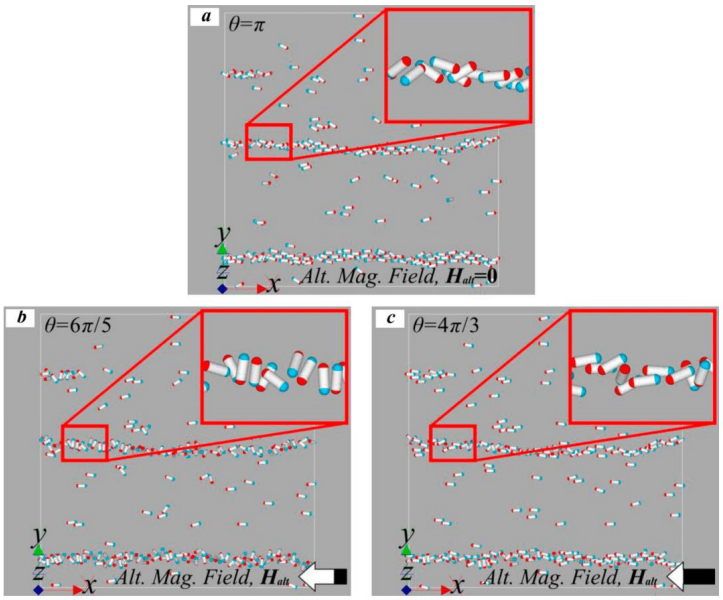

Figure 3. variation in the aggregate structures for $\xi = 80$, $R_B = 3$ and $\lambda = 60$: (a) at $\theta = \pi$, (b) at $\theta = 6\pi/5$ and (c) at $\theta = 4\pi/3$. The snapshot in Figure 2(b) should be referred to for the case of $\theta = \pi/2$. Since the viscous friction forces are not sufficiently strong in the case of $R_B = 3$, each particle promptly changes the orientation in order to follow the change in the magnetic field direction, through the intermediate formation of raft-like clusters.

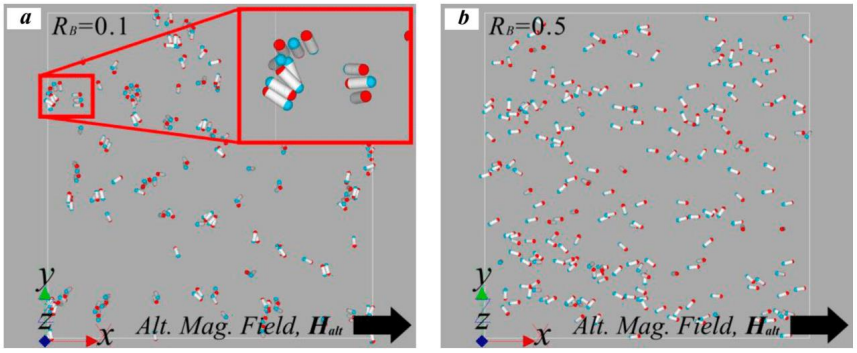

Figure 4. Influence of the frequency of the magnetic field, R_B, on the aggregate structures for the case of $\lambda = 60$ and $\xi = 80$: (a) $R_B = 0.1$ and (b) $R_B = 0.5$. Magnetic rod-like particles tend to aggregate to form linear thick chain-like clusters from short raft-like clusters with increasing values of R_B or with smaller values of the frequency of the alternating magnetic field.

each particle promptly changes the orientation in order to follow the change in the magnetic field direction, which leads to the reformation of stable thick chain-like cluster inclining in the reverse direction, shown in Figure 3(c).

Figure 4 shows the influence of the frequency of the magnetic field, R_B, on the behavior of the rod-like particles for the case of $\lambda = 60$ and $\xi = 80$, where two different snapshots are shown for $R_B = 0.1$ and $R_B = 0.5$. The

snapshot in Figure 2(b) should be referred to for the case of $R_B = 3$. It is noted that all the snapshots were obtained at the phase angle of $\theta = \pi/2$ and also that a smaller value of R_B corresponds to a larger frequency of the alternating magnetic field. In the case of a larger frequency of $R_B = 0.1$, shown in Figure 4(a), many short raft-like clusters are observed to be formed and these clusters do not follow the change in the magnetic field direction, rather tend to incline in various directions. The reason why only short raft-like clusters are formed but do not grow to form densely-packed clusters as in Figure 2(c) is that the viscous friction forces are significantly large for the translational and rotational motion of rod-like particles, and therefore they are not able to perform the translational motion to join the other raft-like clusters: a requirement for significant growth of structures, which results in the formation of many small raft-like clusters located separately from each other. Moreover, in the case of large viscous friction forces, they are not restricted to the field direction and exhibit a preference for the formation of small raft-like clusters, where the neighboring particles internal to a cluster incline in the opposite directions to each other, giving rise to a lower magnetic interaction energy. In contrast, for the case of an intermediate frequency of $R_B = 0.5$, short raft-like cluster are not formed, but instead rod-like particles tend to individually rotate in order to follow the change in the magnetic field direction. This may be explained as follows. In the case of $R_B = 0.5$, viscous friction forces are small enough that the particles are able to follow the change in the field direction, but sufficiently large to inhibit the translational motion required to join the other clusters. Hence, the rod-like particles tend to rotate due to the interaction with the applied magnetic field while remaining essentially fixed at their original position. Since the rod-like particles orientate in the field direction, in this situation, the neighboring particles are exerted by a repulsive magnetic interaction, which leads to the independent rotational motion of the rod-like particles, as shown in Figure 4(b). For the case of a lower frequency of $R_B = 3$, shown in Figure 2(b), rod-like particles have sufficient time for the translational motion and thus aggregate to form linear thick chain-like clusters. As already pointed out, in this situation, the constituent particles are able to respond to the change in the field direction while remaining at their specific site within a cluster, with the linear chain-like cluster formation maintained during the process.

6.1.2. Hysteresis loops

In the previous section we have qualitatively discussed the behavior of the rod-like particles in the alternating magnetic field, including the different regimes of the aggregate structures. In this section, we focus on hysteresis loops that arise from a delay of the magnetic moment (rod-like particle) relative to the change in the strength and direction of the applied magnetic field. The hysteresis loops are directly used for discussing a heat generation effect.

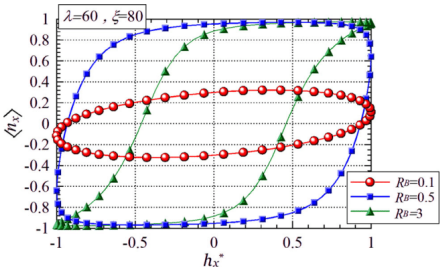

Figure 5. Dependence of hysteresis loops on the frequency of the magnetic field for the case of $\lambda = 60$ and $\xi = 80$, where results for three cases of the frequency, $R_B = 0.1$, 0.5 and 3 are shown for comparison. In the case of $R_B = 0.5$, the hysteresis loop becomes significantly larger than that for the other cases of $R_B = 0.1$ and $R_B = 3$. This is because relatively large viscous friction forces act on the rod-like particles, and therefore a sufficiently large magnetic field strength is required in order to trigger the rotational motion of rod-like particles.

Figure 5 shows the dependence of hysteresis curves (or loops) on the frequency of the magnetic field for the case of $\lambda = 60$ and $\xi = 80$, where results for three cases of the frequency, $R_B = 0.1$, 0.5 and 3 are shown for comparison. The ordinate is the mean value of the x-components of the magnetic moments which were obtained by averaging the magnetic moments of the particle in the system at each phase angle. It is noted that a larger area enclosed by a loop gives rise to a more significant heat generation effect, which will be discussed in Section 6.3.

In the case of $R_B = 0.1$, the hysteresis loop is significantly different from those for the cases of $R_B = 0.5$ and $R_B = 3$. That is, the maximum value of $\langle n_x \rangle$ does not reach unity, which implies that the rod-like particles are not able to significantly follow the change in the magnetic field strength and direction. This is quite understandable because in this case, as shown in Figure 4(a), short raft-like clusters incline in various directions and do not incline in the magnetic field direction. The appearance of the maximum value $\langle n_x \rangle \simeq 0.33$ at around $h_x^* \simeq 0.4$ during the path from $h_x^* = 1$ to $h_x^* = 0$ is due to a large delay of the relaxation of the magnetic moment (rod-like particle) under a significant influence of large viscous friction forces.

In the case of $R_B = 0.5$, the hysteresis loop becomes significantly larger than that for the previous case of $R_B = 0.1$. One characteristic point is that the rod-like particles remain inclining in the opposite direction even at the time when the applied magnetic field changes direction towards the positive x-axis direction and they promptly start to rotate since around $h_x^* = 0.7$, approaching $\langle n_x \rangle = 1$ at $h_x^* = 1$. This may be explained as follows. In this case, relatively large viscous friction forces act on the rod-like particles, and therefore a sufficiently large magnetic field strength is required in order to trigger the rotational motion of rod-like particles. In other words, we understand that this threshold magnetic field strength is around $h_x^* \simeq 0.7$. Another characteristic point is that the maximum value $\langle n_x \rangle = 1$ appears at around $h_x^* \simeq 0.6$ during the path from $h_x^* = 1$ to $h_x^* = 0$. This delay is due to the same mechanism that has already been described for the previous case of $R_B = 0.1$.

In contrast, for the case of $R_B = 3$, the hysteresis loop gives rise to a significantly smaller enclosed area in comparison with that for $R_B = 0.5$, although we initially expected that a large hysteresis area could be obtained due to the linear chain-like cluster formation, which may lead to a large delay in the response to the time-varying applied magnetic field. The reason for this smaller enclosed area may be explained as follows. The formation of linear chain-like clusters certainly tends to delay the reorientation of the constituent particles in the alternating magnetic field, which should provide a large hysteresis loop. However, the value of $R_B = 3$ corresponds to a low frequency region of the alternating magnetic field, and therefore the constituting particles are able to follow the change in the magnetic field more promptly in the case of lower viscous friction forces, even in the case where the magnetic interactions acting between constituent particles function to suppress the reorientation of each particle. This consideration may be reinforced by the characteristic of the hysteresis loop that the curve starts to steeply increase since $h_x^* \simeq 0$ when the magnetic field is switched to the positive x-direction, which is significantly in contrast to the curve for $R_B = 0.5$.

We next discuss the dependence of the hysteresis loops on the magnetic particle-particle interaction strength λ. Figure 6 show results for the hysteresis loops for the case of $R_B = 3$ and $\xi = 80$, where the two cases of $\lambda = 1$ and 60 are shown for comparison. It is noted that the value of $\lambda = 60$ is sufficient for cluster formation, as shown in Figure 2(b), whereas no clusters appear for the case of $\lambda = 1$, as shown in Figure 2(a). It is seen that the cluster formation in the case of $\lambda = 60$ gives rise to a larger loop than the weakly interacting case of $\lambda = 1$ where no

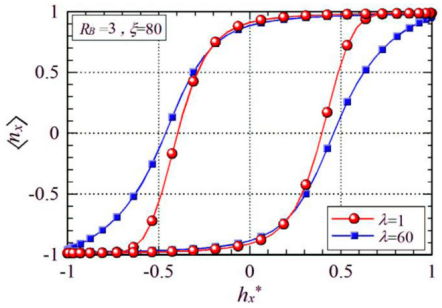

Figure 6. Hysteresis loops for the case of $R_B = 3$ and $\xi = 80$, where the two cases of $\lambda = 1$ and 60 are shown for comparison. It is seen that the cluster formation in the case of $\lambda = 60$ gives rise to a larger loop than no cluster formation in the case of $\lambda = 1$.

clusters are formed. As already pointed out above, the rod-like particles can rapidly respond to the change in the alternating magnetic field in the case of smaller viscous friction forces for $R_B = 3$. A significant differently characteristic between these two loops appears in the relaxation motion of the rod-like particles in the path from $h_x^* = 0$ to 1 (or from $h_x^* = 0$ to -1). That is, the curve for $\lambda = 1$ increases more steeply than that for $\lambda = 60$, in other words, the rod-like particles reorient more rapidly to follow the change in the magnetic field in the case of $\lambda = 1$. This may be explained as follows. After the magnetic field moves into the positive x-direction at $h_x^* = 0$, the rod-like particles rapidly start to incline in the field direction, which leads to a steep increase since $h_x^* = 0$ in the path towards $h_x^* = 1$ for both the cases of $\lambda = 1$ and 60. However, the magnetic interactions between the constituent particles forming a chain-like cluster significantly inhibits the rotation of each constituent particle following the magnetic field change, which leads to a gentler slope than for $\lambda = 1$ as shown in Figure 6.

From the results shown in Figures 5 and 6, we understand that the rapid rotational motion of rod-like particles is mainly dependent on the frequency of the alternating applied magnetic field, and the second governing factors are the magnetic particle-particle interaction strength and the magnetic field strength.

6.2. Time variation in aggregate structures for the case of the rotating magnetic field

In this section, we investigate the effects of a rotating magnetic field on the behavior of magnetic rod-like particles. As already described, a magnetic field is rotated about the z-axis in the anticlockwise direction.

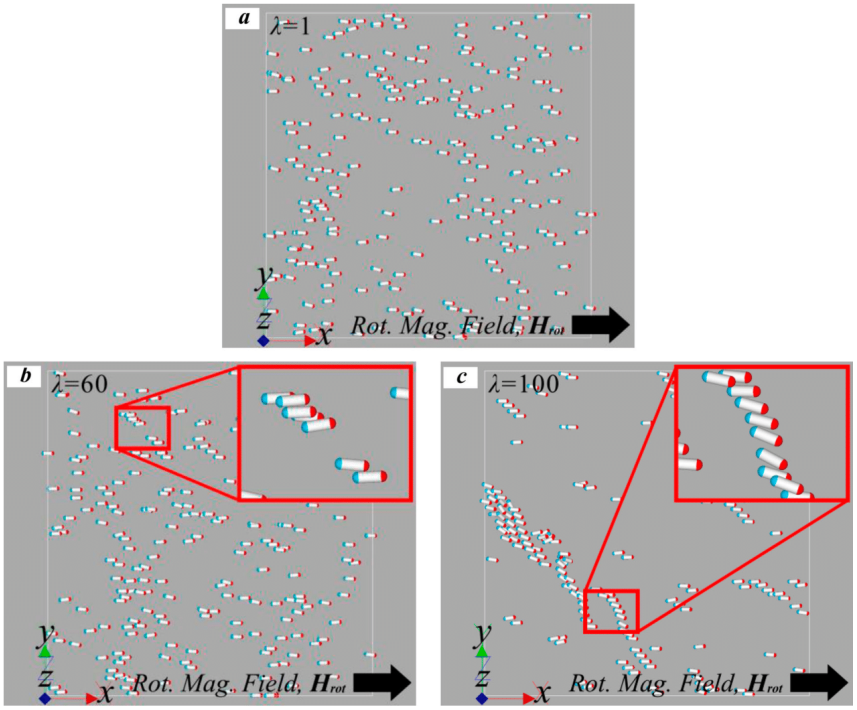

Figure 7. Dependence of magnetic particle-particle interactions on the cluster formation for the case of a low frequency region of $R_B = 3$ and a strong applied magnetic field of $\xi = 80$, where three cases of the magnetic interactions $\lambda = 1$, 60 and 100 are shown for comparison. As recognised in Figure 7(c), linear and large clusters rotate as a whole body with a large delay to the rotating magnetic field.

Figure 7 shows the effect of magnetic particle-particle interactions on the cluster formation for the case of a low frequency of $R_B = 3$ and a strong applied magnetic field of $\xi = 80$, where three cases of the magnetic interactions $\lambda = 1, 60$ and 100 are shown for comparison. These snapshots were obtained at the phase angle of $\theta = 0$, when the rotating magnetic field aligns to the x-axis direction. In the case of $\lambda = 1$, since the magnetic particle-particle interaction strength is sufficiently weak, the rod-like particles perform rotational motion individually without the cluster formation and are able to follow the change in the field direction, thus inclining in the x-axis direction (or the magnetic field direction). In the case of $\lambda = 60$, only several small clusters comprising three or four particles are observed to be formed, which is significantly in contrast to the case of the alternating magnetic field, where linear thick chain-like clusters are formed along the field direction and keep these linear formation during the change in the direction and strength of the alternating magnetic field. The above-mentioned small clusters have the following characteristics regarding the aggregate internal structure. If the two magnetic rod-like particles or the two magnetic moments approximately incline in the same direction, a staggered configuration is preferred as a cluster, where the neighboring particle is located at an off-set position by around half the particle length along the major axis direction, leading to a lower magnetic interaction energy or an attractive force between the two particles. This cluster unit is repeated and expanded to form the linear thick chain-like clusters in Figure 2(b). However, in the case of the rotating magnetic field, the rotational motion of the constituent particles functions to prevent this linear cluster formation following the field direction. We describe this situation in more detail in the following. As recognised in Figure 7(b), the upper rod-like particle is necessarily located at an offset position

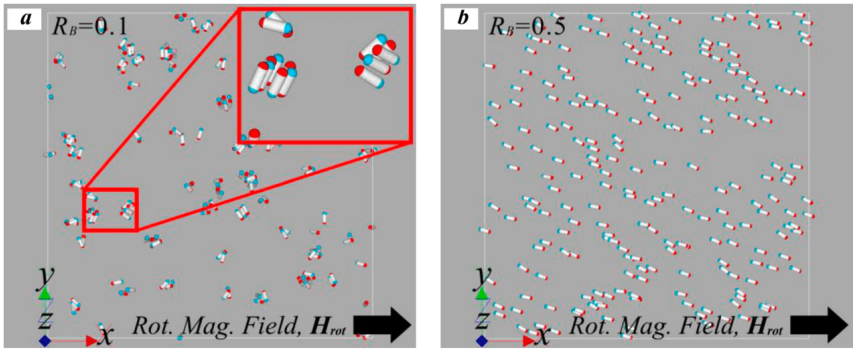

Figure 8. Influence of the frequency of the magnetic field, R_m, on the aggregate structures for the case of $\lambda = 100$ and $\xi = 80$: (a) for $R_B = 0.1$ and for (b) $R_B = 0.5$. The snapshot shown in Figure 7(c) should be referred to for the case of $R_B = 3$. In the case of an intermediate frequency of $R_B = 0.5$, shown in Figure 8(b), viscous friction forces are still large with respect to the rotational motion, but the single particles are able to rotate to follow the rotation of the magnetic field with a large delay.

along the major axis in the direction opposite to the magnetic field direction. In this configuration, even if the two rod-like particles rotate in the anticlockwise direction (the direction of rotation), the integrity of this cluster unit is maintained without dissociation during the rotational motion of each constituent particle. In the case of an increased magnetic interaction strength $\lambda = 100$, shown in Figure 7(c), this cluster unit is repeated and expanded in an oblique direction (or in the upper-left direction in Figure 7(c)). This large linear cluster formation is expected to be maintained and will rotate to follow the rotation of the applied magnetic field in the low frequency region. Hence these linear clusters with offset internal structure will rotate as a whole body with a large phase delay to the rotating magnetic field, which can be clearly seen in Figure 7(c). At relatively large frequencies, these linear clusters might be expected to repeatedly dissociate into several long clusters and re-associate into longer clusters, as shown in the previous study [32] for a magnetic spherical particle suspension. Another characteristic point recognised from Figure 7(c) is that the constituent rod-like particles exhibit a larger rotational delay for a longer cluster. The reason for this delay may be similar to that of the observed slow increase of the hysteresis loop for $\lambda = 60$ in Figure 6. That is, a longer and larger cluster is more significantly influenced by viscous friction forces in the rotational motion, which leads to a larger phase delay to the magnetic field in comparison with the rotational motion of single rod-like particles. Hence, the magnetic particle-particle interactions function to delay the rotational motion of each constituent particle in a linear cluster. Moreover, a noticeable point is that a larger magnetic field strength is required for the formation of stable larger clusters in a rotating magnetic field than in the alternating magnetic field, which becomes clearer by comparing Figure 7(b) with Figure 2(b) for the same case of $\lambda = 60$. This may be due to the difference in the strength of steric repulsive forces; that is, in the rotational field case, steric repulsive forces more significantly appear through the overlap of the steric layer arising from the rotational motion of the constituent rod-like particles in a long cluster. In contrast, in the alternating magnetic field situation, significant steric repulsive forces appear only in a short period during the change in their direction from the negative to the positive x-direction or in the reverse case, which leads to the stability of the thick chain-like clusters for a smaller magnetic particle-particle interaction strength in comparison with the case of a rotating magnetic field.

We next discuss the dependence of the behavior of rod-like particles on the frequency of the rotating magnetic field, shown in Figure 8 for the case of $\lambda = 100$ and $\xi = 80$, where two different snapshots are shown for $R_B = 0.1$ and $R_B = 0.5$. The snapshot shown in Figure 7(c) should be referred to for the case of $R_B = 3$. It is noted that all the snapshots were obtained at the phase angle of $\theta = 0$.

In the case of a high frequency region of $R_B = 0.1$, shown in Figure 8(a), several short raft-like clusters are formed and these clusters do not significantly respond to the rotation of the magnetic field, as in Figure 4(a). This is because significantly larger viscous friction forces will act on the particles during the rotational motion, and therefore these short raft-like clusters are unable to

rotate sufficiently rapidly to follow the rotation of the applied magnetic field. Even single particles incline in various directions and, do not align to the field direction. In the case of an intermediate frequency of $R_B = 0.5$, shown in Figure 8(b), viscous friction forces are still large with respect to the rotational motion, and thus the single particles are able to rotate to follow the rotation of the magnetic field with a large delay, that is, the rod-like particles incline in the bottom-right direction. In the case of a low frequency of $R_B = 3$, as already described above, viscous friction forces are not large for the rotational motion, and also magnetic particle-particle interaction forces are sufficiently strong for the cluster formation. Hence, the particles aggregate to form long clusters and these clusters rotate as a whole body to follow the rotation of the field with a large delay.

6.3. Comparison of results between the alternating and rotating magnetic fields

Finally we discuss the characteristics of the heat generation effect by comparing results between the alternating and rotating magnetic fields.

We first address the influence of the frequency of the magnetic field on the characteristics of the heating effect. Figure 9 shows these characteristics for the case of a weak magnetic interaction strength $\lambda = 1$, where the results for both the magnetic fields are shown for $\xi = 40$ and 80. It is noted that the value of $\lambda = 1$ is too small for the formation of clusters and this is common for the alternating and the rotating applied magnetic field, that is, linear and raft-like clusters are not formed in the system. Moreover, a smaller value of R_B corresponds to a lower frequency of the time-dependent applied magnetic fields. The ordinate $W_{cycl}{}^*$ in Figure 9 is a quantity that is evaluated by integrating over one cycle of the alternating and the rotating magnetic field.

Several common characteristics of both the applied magnetic fields are recognised and are described as follows. In the limits of large and small of R_B, the heating effect tends to decrease and eventually disappear for both cases of the applied magnetic field. This is because large viscous forces act on rod-like particles and thus they cannot rotate for small R_B. For large R_B, rod-like particles can perform rotational motion with a slower rotational velocity for the case of significantly lower viscous friction forces. This slower rotational motion of rod-like particle gives a smaller contribution to the heat generation effect. We summarise the dependence of the heat generation effect on the frequency as follows. As the value of R_B increases from zero, i.e. as the frequency of the applied magnetic fields is decreased, rod-like particles begin to perform rotational motion to follow the

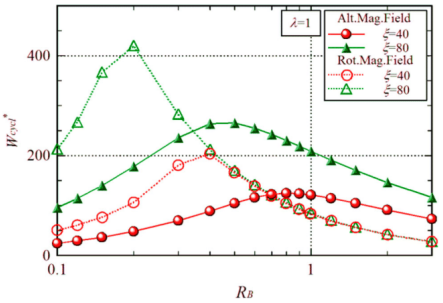

Figure 9. Influence of the frequency of the magnetic field on the characteristics of the heating effect for the case of a weak magnetic interaction strength $\lambda = 1$, where the results for two cases of the field strength are shown for $\xi = 40$ and 80. As the value of R_B increases form zero, i.e. as the frequency of the applied magnetic fields is decreased, rod-like particles starts to perform the rotational motion to follow the change in the magnetic fields, and this tendency becomes more significant with decreasing values of the frequency (or, increasing R_B values), giving rise to a larger heating effect.

magnetic fields, and this tendency becomes more significant with decreasing values of frequency (or increasing R_B values), giving rise to a larger heating effect. As the value of R_B further increases, the rod-like particles are able to follow the change in the magnetic field with slower speeds due to lower viscous friction forces, which leads to a decrease in the heating effect. The contrasting relationship between the magnetic torques and the viscous friction torques gives rise to maximum values of the heating effect in the intermediate region of the values of R_B for all the curves in Figure 9.

For both alternating and rotational magnetic fields, the peak position yielding a maximum value is shifted towards to a larger value of R_B, with decreasing field, specifically, the peak position is shifted from $R_B \simeq 0.2$ for $\xi = 80$ to $R_B \simeq 0.4$ for $\xi = 40$ in the case of the rotating field and from $R_B \simeq 0.5$ for $\xi = 80$ to $R_B \simeq 0.8$ for $\xi = 40$ in the case of the alternating magnetic field. The reason for the shifting of the peak position may be explained as follows, for example, by focusing on the results for the alternating magnetic field. The threshold value of R_B, after which the rod-like particles can respond to a more slowly rotating magnetic field for smaller viscous friction forces, should determine the position yielding the maximum value. If the magnetic torque is larger or if the magnetic field is stronger, the rod-like particles can respond to the magnetic field from a larger frequency in the intermediate region. This characteristic is certainly

the reason for the shifting of the peak position. A similar argument is also valid for the rotating magnetic field case.

From Eq. (8), it is seen to be quite reasonable that a larger magnetic field gives rise to a larger heat generation effect for both the magnetic field variations, since the heat generation effect arises from the relaxation phenomenon through the magnetic interactions between rod-like particles and a time-dependent external magnetic field. An interesting observation is that the dependence on the frequency after $R_B = 0.4$ is approximately the same for $\xi = 40$ and 80 in the case of the rotating magnetic field, whereas it is completely different in the case of the alternating field. This is certainly due to the different characteristics in the motion of the rod-like particle in a time-varying applied magnetic field. In the region of $R_B \gtrapprox 0.4$ for the rotating field, rod-like particles are able to follow the rotation of the magnetic field, albeit with a delay. Even if the applied magnetic field strength is different, the rod-like particles rotate with the approximately same rotational velocity with a different phase delay for the case of the same frequency, which gives rise to essentially the same heating as the case without cluster formation. In contrast, for the case of the alternating magnetic field, large viscous friction forces arise only during the short time when the rod-like particles switch their direction to follow the change in the magnetic field direction (i.e. at the phase angle $\theta = 0$ and π). In this switching motion, the rotational speed of rod-like particles is larger for a larger magnetic field strength. Moreover, continuous rotational motion of rod-like particles under the friction forces (torques) in the rotating field in the early stage of the intermediate region, $R_B \lesssim 0.2$, is able to contribute to the heat generation performance more significantly during a longer period than in the alternating field where heat generation arises during a much shorter period when rod-like particles switch their direction.

From these characteristics, we may understand that for the case of rod-like particles capable of responding rapidly to the field changes, a rotating magnetic field is significantly superior to an alternating field for obtaining a larger heat generation effect, whereas in the situation of rod-like particles rotating with a slower speed, which corresponds to a low frequency region, the alternating magnetic field is desirable for heat generation. The critical value of R_B for decision regarding which magnetic field should be employed is of course dependent on the magnetic field strength, as suggested in Figure 9 as one example.

We next discuss how the cluster formation influences the heat generation effect. To this end, the case of a large applied magnetic field strength $\xi = 80$ is focused on for investigating the characteristics of the heat generation. Figure 10 shows the influence of the magnetic particle-particle interaction strength λ on the heat generation, where results for the three different cases of magnetic interaction strengths are shown for $\lambda = 1$, $\lambda = 60$ and $\lambda = 100$ for each applied magnetic field. The results for $\lambda = 1$ are just for reference, since this value is not sufficient for the formation of clusters.

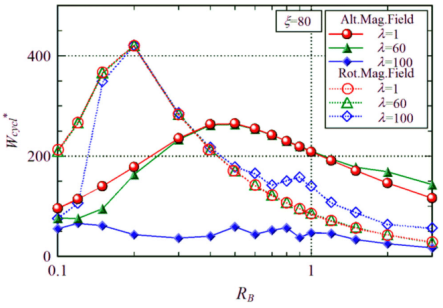

Figure 10. Influence of the magnetic particle-particle interaction strength λ on the heat generation effect, where results for three different cases of magnetic interaction strengths are shown for $\lambda = 1$, $\lambda = 60$ and $\lambda = 100$ for each applied magnetic field. Larger magnetic interaction $\lambda = 100$ yields larger values of the heat generation effect in the region of $R_B \gtrapprox 0.5$ for the case of the rotating field, whereas a rather weak heating effect is predicted for $\lambda = 100$ in the case of the alternating field.

We first consider the results for the alternating magnetic field. It is seen that the curves for $\lambda = 1$ and $\lambda = 60$ exhibit the almost same characteristics but the curve for $\lambda = 100$ is significantly different from those for the former two cases. As shown in Figure 2(c), this is due to the formation of densely-packed clusters that are notably stable even in the situation of the time-changing applied magnetic field. These clusters do not respond to the varying magnetic field, and tend to orient in various directions rather than that of the magnetic field. Hence this limited motion of each constituent particle in a densely-packed cluster cannot yield a significant relaxation effect, resulting in a weak heating effect as shown in Figure 10. A slight improvement of the heat generation in the region of $R_B \gtrapprox 1$ for the case of $\lambda = 60$ is due to the magnetic particle-particle interactions that function to suppress the rotational motion of the consituent particles in a cluster, which results in faster rotational motion of the rod-like particles, giving a response to the alternating magnetic field. This consideration has already been made with respect to the hysteresis loop shown in Figure 6. On the other hand, in the range of $R_B \lesssim 0.3$, the heat generation effect for $\lambda = 60$ is slightly smaller than for

$\lambda = 1$. This is simply because the constituent particles in the stable short clusters shown in Figure 4(a) cannot sufficiently rotate in the alternating magnetic field with a larger frequency. That is, the magnetic interactions between rod-like particles function to add a more significant restriction to the rotational motion than single particles.,

Next we consider the results for the rotating magnetic field. The most different characteristic between the two applied magnetic fields appears in the result for the case of $\lambda = 100$. The heat generation effect for the rotating field exhibits characteristics similar to those for $\lambda = 1$ and $\lambda = 60$, not shows significantly smaller values. This is simply because the rod-like particles rotate to follow the rotation of the field irrespective of whether particles aggregate to form linear clusters. This characteristic regarding the relaxation motion of rod-like particles will give rise to approximately similar characteristics of the heat generation effect, which is clearly shown in Figure 10. Smaller values for $\lambda = 100$ than those for $\lambda = 1$ and $\lambda = 60$ in the range of $R_B \lesssim 0.15$ is due to the same reason for the characteristics of the curve for $\lambda = 100$ in the range of $R_B \lesssim 0.3$ for the case of the alternating field, as described above. Another characteristic feature is observed in the region of $R_B \gtrapprox 0.5$ in the curve for $\lambda = 100$. That is, the larger magnetic interaction strength $\lambda = 100$ yields larger values of the heat generation effect, which can be understood by considering the characteristics of the cluster formation, shown in Figure 7(c). Similar to thick chain-like clusters shown in Figure 2(b) for the case of the alternating field, the long linear clusters, observed in Figure 7(c), function to suppress the rotational motion of the constituent particles through the magnetic particle-particle interactions, although in the range of sufficiently low frequencies, these particles will finally rotate to follow the rotation of the field. Hence, the constituent particles of a long linear cluster will rotate with a larger rotational velocity than single particles, which results in larger friction forces (torques) and therefore leads to a larger heating effect.

Finally we discuss the influence of the magnetic particle-particle interaction strength on the heat generation effect. Figure 11 shows the heat generation effect as a function of the magnetic particle-particle interaction strength for the intermediate frequency $R_B = 1$. From these results we observe a common feature that the variation with interaction strength changes dramatically at the threshold it which clusters are formed. This is valid for both the applied magnetic field variation types. Specifically, this threshold can be seen to occur at $\lambda \simeq 50$ and $\lambda \simeq 65$ for $\xi = 40$ and $\xi = 80$, respectively, in the case of the alternating field, and $\lambda \simeq 75$ for both the cases of

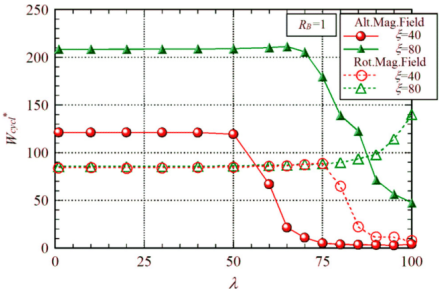

Figure 11. Heat generation effect as a function of the magnetic particle-particle interaction strength for the intermediate frequency $R_B = 1$. The magnetic interactions between constituent particles in a cluster tend to function to suppress the rotational motion of the particles. As a result, the rod-like particles finally rotate with a larger speed, which leads to a larger heating effect in the region of $\lambda \gtrapprox 75$ for $\xi = 80$ in the case of the rotating magnetic field.

$\xi = 40$ and $\xi = 80$ in the case of the rotating field. Prior to reaching these threshold values, the heat generation effect is due to the motion of single particles and is thus approximately constant, that is independent of the values of λ. In the following, we discuss the dependence on the magnetic interaction strength for the two types of magnetic field variations separately in more detail.

In the case of the alternating magnetic field, the heat generation steeply decreases to approach zero above each threshold value of $\xi = 40$ and 80. Above these threshold values, the densely-packed aggregates shown in Figure 2(c) are formed in increasing numbers and density. As a result, the constituent particles are not able to change their orientation due to the stronger magnetic interactions between neighboring particles. This is quite understandable because the densely-packed aggregates shown in Figure 2(c) are extremely stable from an interaction energy point of view. The reason why the threshold value for $\xi = 80$ is much larger than for $\xi = 40$ is that, for a larger applied field strength, a larger magnetic interaction strength is required in order for the magnetic interaction to overcome the influence of the applied magnetic field.

In the case of the rotating magnetic field, the dependence on the magnetic interaction strength exhibits divergent behavior for the two applied field values. Specifically, in the case of $\xi = 40$, the situation of $\lambda = 75$ ensures that the magnetic interaction is the dominant factor for the behavior of the constituent particles, and therefore these particles cannot respond to the change in the rotating field due to strong magnetic interactions.

Table 1. Summary of the situation and results in the alternating magnetic field.

Situations		Results	
Magnetic particle-particle interaciton strength λ	Magnetic field strength ξ	Aggregate structure	Heating effect
(1) $\lambda \ll 60$ (weak)	$\xi \ll \lambda$	No cluster formation (any R_B)	Significantly Low for any R_B
(2) $\lambda \ll 60$ (weak)	$\xi \gg \lambda$	No cluster formation (any R_B)	Significantly High for $0.3 \lesssim R_B \lesssim 1.0$ Higher with increasing ξ
(3) $\lambda \ll 60$ (weak)	$\xi \gg \lambda$	No cluster formation (any R_B)	High for $1.0 \lesssim R_B \lesssim 3.0$ Higher with increasing ξ
(4) $\lambda \gg 60$ (strong)	$\xi \ll \lambda$	Densely-packed clusters ($R_B \gtrapprox 1$)	Significantly Low for any R_B
(5) $\lambda \gg 60$ (strong)	$\xi \simeq \lambda$	Chain-like and raft-like clusters ($R_B \gtrapprox 1$)	Low for $R_B \gtrapprox 1$
(6) $\lambda \gg 60$ (strong)	$\xi \gg \lambda$	No cluster formation ($R_B \lesssim 1$)	Significantly Low for $R_B \lesssim 1$

Table 2. Summary of the situation and results in the rotating magnetic field.

Situations		Results	
Magnetic particle-particle interaciton strength λ	Magnetic field strength ξ	Aggregate structure	Heating effect
(1) $\lambda \ll 75$ (weak)	$\xi \ll \lambda$	No cluster formation (any R_B)	Significantly Low for any R_B
(2) $\lambda \ll 75$ (weak)	$\xi \gg \lambda$	No cluster formation (any R_B)	Significantly High for $0.1 \lesssim R_B \lesssim 0.5$ Higher with increasing ξ
(3) $\lambda \ll 75$ (weak)	$\xi \gg \lambda$	No cluster formation (any R_B)	High for $0.5 \lesssim R_B \lesssim 3.0$
(4) $\lambda \gg 75$ (strong)	$\xi \ll \lambda$	Densely-packed clusters ($R_B \gtrapprox 1$)	Significantly Low for any R_B
(5) $\lambda \gg 75$ (strong)	$\xi \gg \lambda$	Chain-like clusters ($R_B \gtrapprox 1$)	Significantly High for $0.1 \lesssim R_B \lesssim 0.5$ Significanlty Higher with increasing ξ
(6) $\lambda \gg 75$ (strong)	$\xi \gg \lambda$	No cluster formation ($R_B \lesssim 1$)	Significantly Low for $R_B \lesssim 1$

This leads to a diminishing effect with increasing magnetic interaction strength. In contrast, for the case of $\xi = 80$, in the region of $75 \lesssim \lambda \lesssim 100$, the magnetic field retains significant influence on the particle behavior, and consequently the constituent particles are able to rotate to follow the rotation of the field, albeit with a phase lag. As already described before with respect to the hysteresis loops for the alternating field in Figure 6, the magnetic interaction between the constituent particles tend to suppress the rotational motion of the individual particles. As a result, the rod-like particles finally rotate with a larger speed, which leads to a larger heating effect, as shown in Figure 11.

Finally, we summarise the characteristic features with respect to the aggregate structure and the heat generation effect using tables by focusing on several typical situations of the magnetic particle-particle and particle field interaction strengths. It is noted that in each situation these features are dependent on the frequency of the time-dependent applied magnetic field, that is, on the inverse of the non-dimensional parameter R_B. The cluster formation is mainly governed by the magnetic interaction strength λ and the internal structure is influenced by both the magnetic field strength ξ and the frequency of the applied magnetic field, $1/R_B$. Hence, the criterion value of the magnetic interaction strength for the formation of clusters is employed for specifying typical cases or situations in order to describe the characteristic features regarding the aggregate structure and the heating effect.

Tables 1 and 2 show the characteristic features regarding the aggregate structure and the heat generation effect for the cases of alternating and rotating magnetic fields, respectively. A noticeable point is that in Situation (5) the rotational magnetic field gives rise to a significantly high heating effect, whereas the alternating field yields a simply low heating effect. This is mainly due to the difference in the behavior of chain-like clusters in these two time-dependent magnetic fields. In the rotating magnetic field, if the chain-like clusters stably formed in the system are able to follow the rotation of the field, this motion induces a significantly larger viscous friction force, which leads to a larger heat generation effect. In contrast, for the case of the alternating magnetic field, each constituting particle of a chain-like cluster strongly tends to rotate to follow the alternating magnetic field, which clearly gives rise to a significantly smaller viscous friction force, resulting in a much smaller heat generation effect in comparison with the former applied magnetic field.

7. Conclusions

In the present study, we have investigated the behavior of rod-like magnetic particles and their relationship with the heat generation effect for two kinds of applied magnetic field variations, i.e. alternating and rotating magnetic fields, by means of Brownian dynamics simulations. The governing factors for characterising the present phenomenon are viscous friction forces

(torques), the strength and directional characteristics of each applied magnetic field variations and magnetic particle-particle interactions. The relative magnitudes of these factors govern the characteristics of the aggregate structures and the heating effect. The main results obtained here are summarised as follows. As a common feature for both the magnetic field variations, in the case of significantly strong particle-particle interaction strengths, rod-like particles exhibit densely-packed clusters are formed, rather than chain-like clusters, and the neighboring rod-like particles constituting a cluster incline in opposite directions to each other. For the case of an alternating magnetic field, in the intermediate frequency range, linear thick chain-like clusters are formed along the field direction and the constituent rod-like particles themselves tend to rotate to follow the change in the alternating magnetic field during a short period. In contrast, for the case of the rotating field, linear clusters rotate as a whole body to respond to the rotation of the magnetic field. In both the applied magnetic field variations, the magnetic interactions between the constituent particles in a cluster tend to function to suppress the relaxation motion of the rod-like particles, which, as a result, leads to improvement in the heat generation effect in certain situations. In a relatively large frequency region, the rotating applied magnetic field gives rise to a larger heat generation effect, whereas in a relatively lower frequency region the alternating magnetic field is superior to the former applied magnetic field for a heat generation point of view.

Disclosure statement

No potential conflict of interest was reported by the author(s).

Funding

S.S. would like to acknowledge the financial support from Grant-in-Aid for JSPS Fellows (20J22468).

References

[1] N.M. Wereley, editors, *Magnetorheology: Advances and Applications* (Royal Society of Chemistry, London, 2013).
[2] F. Jorgensen, *The Complete Handbook of Magnetic Recording*, 4th ed. (McGraw-Hill, New York, 1996).
[3] J.W. Harrell, S. Kang, Z. Jia, D.E. Nikles, R.W. Chantrell and A. Satoh, Appl. Phys. Lett. **87**, 202508–202208 (2005). doi:10.1063/1.2132539
[4] P.I. Girginova, A.L. Daniel-da-Silva, C.B. Lopes, P. Figueira, M. Otero, V.S. Amaral, E. Pereira and T. Trindade, J. Colloid Interface Sci. **345**, 234–240 (2010). doi:10.1016/j.jcis.2010.01.087
[5] S.H. Sajjadi and E.K. Goharshadi, J. Environ. Chem. Eng. **5**, 1096–1106 (2017).
[6] U. Häfeli, W. Schütt, J. Teller and M. Zborowski, editors, *Scientific and Clinical Applications of Magnetic Carriers* (Springer, Berlin, 1997).
[7] Y.I. Golovin, S.L. Gribanovsky, D.Y. Golovin, N.L. Klyachko, A.G. Majouga, A.M. Master, S. Marina and A.V. Kabanov, J. Controlled Release. **219**, 43–60 (2015). doi:10.1016/j.jconrel.2015.09.038
[8] A.M. Schmidt, Colloid Polym. Sci. **285**, 953–966 (2007). doi:10.1007/s00396-007-1667-z
[9] Q.A. Pankhurst, J. Connolly, S.K. Jones and J. Dobson, J. Phys. D: Appl. Phys. **36**, R167 (2003). doi:10.1088/0022-3727/36/13/201
[10] A.E. Deatsch and B.A. Evans, J. Magn. Magn. Mater. **354**, 163–172 (2014).
[11] I.M. Obaidat, B. Issa and Y. Haik, Nanomaterials. **5**, 63–89 (2015). doi:10.3390/nano5010063
[12] C.S.S.R. Kumar and F. Mohammad. Adv. Drug Delivery Rev. **63**, 789–808 (2011). doi:10.1016/j.addr.2011.03.008
[13] R.E. Rosensweig, J. Magn. Magn. Mater. **252**, 370–374 (2002).
[14] X. Yao, K. Sabyrov, T. Klein, R.L. Penn and T.S. Wiedmann, J. Magn. Magn. Mater. **381**, 21–27 (2015). doi:10.1103/PhysRevE.95.062611
[15] M. Abbas and G. Bossis, Phys. Rev. E. **95**, 062611 (2017).
[16] B.B. Lahiri, S. Ranoo, A.W. Zaibudeen and J. Philip, J. Magn. Magn. Mater. **441**, 310–327 (2017).
[17] P. Cantillon-Murphy, L.L. Wald, E. Adalsteinsson and M. Zahn, J. Magn. Magn, Mater. **322**, 727–733 (2010).
[18] M. Bekovic, M. Trbusic, M. Trlep, M. Jesenik and A. Malter, Adv. Mater. Sci. Eng. **2018** (2018).
[19] S. Suzuki and A. Satoh, Colloid Poly. Sci. **297**, 1265–1273 (2019).
[20] S. Suzuki, A. Satoh and M. Futamura, Mol. Phys. **119**, e1892225 (2021). doi:10.1080/00268976.2021.1892225
[21] L.C. Varanda, M. Jafelicci, Jr. and G.F. Goya, J. Magn. Magn. Mater. **226-230**, 1933–1935 (2001).
[22] T.P. Raming, A.J.A. Winnubst, C.M. Van Kats and A.P. Philipse, J. Colloid Interface Sci. **249**, 346–350 (2002). doi:10.1006/jcis.2001.8194
[23] K. Slyusarenko, D. Constantin and P. Davidson, J. Chem. Phys. **140**, 104904 (2014). doi:10.1063/1.4867790
[24] K. Kandori, Y. Yamotoa and T. Ishikawa, J. Colloid Interface Sci. **283**, 432–439 (2005). doi:10.1016/j.jcis.2004.09.006
[25] D. Van der Beek, H. Reich, P. Van der Schoot, M. Dijkstra, T. Schilling, R. Vink, M. Schmidt, R. Van Roij and H. Lekkerkerker, Phys. Rev. Lett. **97**, 087801 (2006). doi:10.1103/PhysRevLett.97.087801
[26] J.M. Meijer, F. Hagemans, L. Rossi, D. Byelov, S.I.R. Castillo, I. Snigireva, A.P. Philipse and A.V. Petukhov, Langmuir. **28**, 7631–7638 (2012). doi:10.1021/la3007052
[27] J.M. Meijer, D. Byelov, L. Rossi, A. Snigirev, I. Snigireva, A.P. Philipse and A.V. Petukhov, Soft Matter. **9**, 10729–10738 (2013). doi:10.1039/c3sm51553b
[28] M. Aoshima, M. Ozaki and A. Satoh, J. Phys. Chem. C. **116**, 17862–17871 (2012).
[29] E. Wetterskog, M. Agthe, A. Mayence, J. Grins, D. Wang, S. Rana, A. Ahniyaz, G. Salazar-Alvarez and L. Bergström, Sci. Technol. Adv. Mater. **15**, 055010 (2014).
[30] A. Satoh, *Introduction to Practice of Molecular Simulation: Molecular Dynamics, Monte Carlo, Brownian Dynamics, Lattice Boltzmann and Dissipative Particle Dynamics* (Elsevier, Amsterdam, 2010).

[31] A. Satoh, Mol. Phys. **112**, 1002–1011 (2014).
[32] A. Satoh, Mol. Phys. **112**, 2122–2137 (2014).
[33] H. Brenner, Int. J. Multiphase Flow. **1**, 195–341 (1974). doi:10.1016/0301-9322(74)90018-4

Appendix

A1. Diffusion coefficients

As the diffusion coefficients of the present spherocylinder, we here use the expressions for the circular cylinder with diameter d and length l [33]:

$$D_{||}^{T} = \frac{kT}{2\pi\, l\eta}\{\ln 2r_p + \ln 2 - 3/2\},$$
$$D_{\perp}^{T} = \frac{kT}{4\pi\, l\eta}\{\ln 2r_p + \ln 2 - 1/2\} \tag{A1}$$
$$D_{||}^{R} = \frac{kT}{\pi\, l^3\eta} r_p^2,$$
$$D_{\perp}^{R} = \frac{3kT}{\pi\, l^3\eta}\left\{\frac{1}{\ln r_p}\left(1 + \frac{\ln 2 - 1}{\ln r_p}\right) + \frac{3\times 5.45}{8\pi}\cdot\frac{1}{r_p^2}\right\}^{-1} \tag{A2}$$

Since the translational and rotational diffusion coefficients for a sphere with diameter d are expressed as

$$D^{T(sphere)} = \frac{kT}{3\pi\, d\eta}, \qquad D^{R(sphere)} = \frac{kT}{\pi\, d^3\eta} \tag{A3}$$

and therefore the diffusion coefficients shown in Eqs. (A1) and (A2) are normalised by these quantities for a sphere as

$$D_{||}^{T*} = \frac{3}{2r_p}\{\ln 2r_p + \ln 2 - 3/2\},$$
$$D_{\perp}^{T*} = \frac{3}{4r_p}\{\ln 2r_p + \ln 2 - 1/2\} \tag{A4}$$
$$D_{||}^{R*} = \frac{1}{r_p},$$
$$D_{\perp}^{R*} = \frac{3}{r_p^3}\left\{\frac{1}{\ln r_p}\left(1 + \frac{\ln 2 - 1}{\ln r_p}\right) + \frac{3\times 5.45}{8\pi}\cdot\frac{1}{r_p^2}\right\}^{-1} \tag{A5}$$

As described in Section 5, we have focused on the case of the aspect ratio $r_p = 3$ for performing the present simulations.